GEOLOGY, GEOCHEMISTRY, GEOCHRONOLOGY AND GENESIS OF GRANITOID CLASTS IN BRECCIA-CONGLOMERATES, MacLEAN EXTENSION OREBODY, BUCHANS, NEWFOUNDLAND

PETER WILLIAM STEWART

Maps (3) included

CANADIAN THESES

THÈSES CANADIENNES

NOTICE

The quality of this microfiche is heavily dependent upon the quality of the original thesis submitted for microfilming. Every effort has been made to ensure the highest quality of reproduction possible.

If pages are missing, contact the university which granted the degree.

Some pages may have indistinct print especially if the original pages were typed with a poor typewriter ribbon or if the university sent us an inferior photocopy.

Previously copyrighted materials (journal articles, published tests, etc.) are not filmed.

Reproduction in full or in part of this film is governed by the Canadian Copyright Act, R.S.C. 1970, c. C-30. Please read the authorization forms which accompany this thesis.

AVIS

La qualité de cette microfiche dépend grandement de la qualité de la thèse soumise au microfilmage. Nous avons tout fait pour assurer une qualité supérieure de reproduction.

S'il manque des pages, veuillez communiquer avec l'université qui a conféré le grade.

La qualité d'impression de certaines pages peut laisser à désirer, surtout si les pages originales ont été dactylographiées à l'aide d'un ruban usé ou si l'université nous a fait parvenir une photocopie de qualité inférieure.

Les documents qui font déjà l'objet d'un droit d'auteur (articles de revue, examens publiés, etc.) ne sont pas microfilmés.

La reproduction, même partielle, de ce microfilm est soumise à la Loi canadienne sur le droit d'auteur, SRC 1970, c. C-30. Veuillez prendre connaissance des formules d'autorisation qui accompagnent cette thèse.

THIS DISSERTATION HAS BEEN MICROFILMED EXACTLY AS RECEIVED

LA THÈSE A ÉTÉ MICROFILMÉE TELLE QUE NOUS L'AVONS REÇUE

GEOLOGY, GEOCHEMISTRY, GEOCHRONOLOGY AND GENESIS OF GRANITOID CLASTS IN BRECCIA-CONGLOMERATES, MacLEAN EXTENSION OREBODY, BUCHANS, NEWFOUNDLAND

by

© PETER WILLIAM STEWART, B.SC.

A thesis submitted to the School of Graduate Studies in partial fulfillment of the requirements for the degree of Master of Science (Geology)

Department of Earth Sciences
MEMORIAL UNIVERSITY OF NEWFOUNDLAND

OCTOBER, 1985

St. John's Newfoundland

ABSTRACT

Granitoid clasts found in association with the transported orebodies at Buchans are largest, and occupy the greatest volume of the host polylithic breccia-conglomerate subunit when proximal to the greatest sulphide accumulation in the sequence of debris flow deposits. The granitoid clasts are typically the most rounded clast lithology present in the debris flow deposits. They decrease in size and volume with increasing distance from the lowermost sulphide-rich sections of the debris flow sequence. They show igneous textures and compositions ranging from trondhjemite (rare) to quartz porphyritic microtrondhjemite to aplite to granophyric aplite. All granitoid clasts have been classified into six 'types' based on these textural and grain size differences. The five most abundant 'types' are reduced to 'granitic' and 'aplitic' groups based on textural similarities.

Hydrothermal fluids deposited calcite, barite and quartz, sericitized plagioclase grains, and chloritized all mafic phases present. Despite this alteration, and variable alkali metasomatism (loss of K) that is presumed due to late-stage volatile loss, all granitoid clasts appear to have a common magmatic source based on similar trace element abundances.

The 'granitic' group clasts are typically larger, occupy more volume and are more altered than 'aplitic' group clasts. The proportion of 'aplitic' group clasts to 'granitic' group clasts increases with decreasing sulphide concentration in the debris flow sequence. Similarly, the average size and volume occupied by granitoid clasts in debris flow subunits decreases with increasing distance from the sulphide-rich sections of the debris flow deposits.

All granitoid clasts appear to represent fragments of the same magma system that produced the felsic volcanic rocks of the Buchans Group. This conclusion is based on similar mineralogical and petrographic features, and similar major and trace element abundances (especially TiO_2, Zr, Y, V, Nb, Ga and REE) between granitoid clast types and the Buchans Group felsic flows. U/Pb isotopic data for an 'aplitic' group clast, although imprecise, overlaps within analytical uncertainty the isochron produced from a Buchans River Formation rhyolite. The calculated ages, 464 ± 40 Ma

and 489±20 Ma respectively, overlap within the estimated age uncertainties.

The granitoid clasts were altered, rounded and transported to the surface in breccia pipes by explosive volatile activity that is probably due (at least in part) to the exsolution of an aqueous phase from the source magma chamber. The explosive hydrothermal events that transported the granitoid clasts (and fragments of previously deposited lithologies) to the surface may have initiated the movement of the debris flows when the breccia pipe breached the surface, disrupted the *in situ* sulphide mineralization process and resulted in the eventual cessation of massive sulphide deposition at Buchans.

The change in character of the granitoid clasts during the period of production of the debris flows from highly altered 'granitic' group clasts to a finer grained, smaller, and volumetrically less abundant 'aplitic' group clasts suggests that the latter originated from shallower depths and had a more rapid transportation history (i.e. less exposure to the hydrothermal fluids) than the 'granitic' group clasts.

The Feeder Granodiorite as exposed at Wiley's River is considered a high level plutonic facies of the Buchans Group, and evidence of a slightly more differentiated magma

than that which produced the Buchans Group felsic volcanic rocks and granitoid clasts. The textural, mineralogical and geochemical similarities between these populations suggested by Thurlow (1981a,b) are verified. The Little Sandy Lake intrusion appears to be from the same magma system as the Wiley's River Intrusion, Buchans Group felsic flows and the granitoid clasts on the basis of textural and mineralogical similarities and major and trace element geochemistry.

The geochronological study, although relatively imprecise, suggests that the Buchans Group is Middle Ordovician (Llanvirn-Llandeilo?) in age rather than post-Caradocian as suggested by earlier workers. If true, this requires a reappraisal of the position of the Buchans Group in central Newfoundland volcanic stratigraphy.

Table of Contents

ABSTRACT..... ii

LIST OF TABLES..... x

LIST OF FIGURES..... xi

LIST OF PLATES..... xvii

CHAPTER ONE

INTRODUCTION

1.1 Location, access and topography..... 1

1.2 Previous work in the Buchans area..... 5

1.3 Previous work on plutonic inclusions in volcanic terranes..... 8

1.4 Objectives of present study..... 13

1.5 Methods of investigation..... 13

1.6 Acknowledgements..... 15

CHAPTER TWO

REGIONAL GEOLOGY

2.1 Introduction..... 18

2.2 The Central Volcanic Belt of Newfoundland..... 19
2.2.1 Introduction..... 19
2.2.2 Oceanic crust..... 22
2.2.3 The island-arc sequence..... 24
2.2.4 The Late Ordovician sedimentary interval... 25
2.2.5 The Buchans-Robert's Arm Belt..... 27
2.2.6 Post-Silurian rocks..... 27
2.2.7 Intrusive rocks..... 27

2.3 Geological setting of the Buchans Group..... 29

2.4 Metamorphism and deformation of the Buchans Group.. 34

2.5 Ore deposits at Buchans..... 35

2.6 Stratigraphy of the Buchans Group..... 39
2.6.1 Introduction..... 39
2.6.2 Lundberg Hill Formation..... 42
2.6.3 Ski Hill Formation..... 42
2.6.4 Buchans River Formation..... 43
2.6.5 Sandy Lake Formation..... 45
2.6.6 Unnamed Formation..... 47

CHAPTER THREE

FEEDER GRANODIORITE

3.1 Introduction..... 48

3.2 Little Sandy Lake field area..... 48
3.2.1 Field relationships..... 48
3.2.2 Petrography..... 49

3.3 Wiley's River field area..... 53
3.3.1 Field relationships..... 53
3.3.2 Petrography..... 54

3.4 Classification of Feeder Granodiorite..... 57

3.5 Comparison of field and petrographic observations.. 59

CHAPTER FOUR

OBSERVATIONS IN THE MacLEAN MINE

4.1 Introduction..... 62

4.2 Geological setting of the MacLean Extension orebody 63

4.3 Morphological observations..... 77
4.3.1 Introduction..... 77
4.3.2 Size, shape, and volume occupied by granitoid clasts..... 78
4.3.3 Roundness..... 84

4.4 Petrography and classification of granitoid clasts. 85
4.4.1 Introduction and methods of classification. 85
4.4.2 General petrography of the granitoid clasts 90
4.4.3 Classification of the granitoid clasts..... 96

4.5 Granitoid clast type descriptions..... 101
4.5.1 Type 1 Clasts..... 101
4.5.2 Type 2 Clasts..... 104
4.5.3 Type 3 Clasts..... 107
4.5.4 Type 4 Clasts..... 107
4.5.5 Type 5 Clasts..... 112
4.5.6 Type 6 Clasts..... 112

4.6 Interpretation of the petrography of the granitoid clasts..... 115

4.7 Distribution of granitoid clasts in MacLean Extension..... 122
4.7.1 Formation of 'granitic' and 'aplitic' groups..... 122
4.7.2 Distribution of granitoid groups..... 123

4.8 Summary of underground observations..... 130

CHAPTER FIVE

GEOCHEMISTRY

5.1 Introduction..... 133
5.1.1 Statement of purpose..... 133
5.1.2 Methods used to establish comagmatism..... 134

5.2 Chemical effects of alteration..... 147
5.2.1 Alteration of the granitoid clasts..... 147
5.2.2 Alteration of the Feeder Granodiorite..... 157
5.2.3 Summary of alteration effects..... 162

5.3 Composition of the granitoid clasts..... 164
5.3.1 Trace elements..... 164
5.3.2 Rare earth elements..... 173

5.4 Comagmatism of the granitoid clasts, the Feeder Granodiorite and Buchans Group felsic flows..... 179
5.4.1 Introduction..... 179
5.4.2 Major elements..... 180
5.4.3 Trace elements..... 182
5.4.4 Rare earth elements..... 192
5.4.5 Tectonic setting..... 196

5.5 Summary..... 199

CHAPTER SIX

Geochronology

6.1 Introduction..... 202

6.2 New data..... 206
6.2.1 Granitoid clast (KQS-82-095)..... 206
6.2.2 Rhyolite (KQS-82-210)..... 214

6.3 Discussion of the analytical results..... 223
6.3.1 Source of the granitoid clasts..... 223
6.3.2 Age of the Buchans Group..... 225

6.4 Conclusions..... 229

CHAPTER SEVEN

Discussion and conclusions

7.1 Introduction..... 231

7.2 General discussion of events at Buchans..... 232

7.3 Discussion of observed features of granitoid clasts in MacLean Extension area..... 239

7.4 A model for the occurrence of the granitoid clasts. 249

7.5 Summary and conclusions..... 262

Bibliography..... 266

APPENDICES

Appendix 1. Major element analytical procedures..... 290

Appendix 2. Trace element analytical procedures..... 292

Appendix 3. Rare earth element analytical procedures.. 294

Appendix 4. Geochronology analytical procedures..... 298

Appendix 5. Tables of geochemical analyses..... 303

Appendix 6. Previous related publications..... 318

LIST OF TABLES

Table 4.1 Average dimensions of granitoid clasts, estimated volume percent of lithologic subunit occupied by granitoid clasts and proportion of roundness classes for granitoid clasts at main study locations in MacLean Extension. North and south in brackets under location refer to rock face observed, 'both' indicates that both faces have been calculated together. Sub = Sublevel, Dr = Drive. 83

Table 4.2 Abundances of the 'granitic', 'aplitic' and 'other' groups of granitoid clast types at the main study locations in MacLean Extension based on the macroscopic classification of Stewart (1983). 129

Table 5.1 Range of major and trace element contents found in granitoid clast types. Zero indicates the measured abundance is below the analytical detection limit. 148

Table 5.2 Mean abundance and standard deviation of major and trace element contents found in granitoid clast types. 149

Table 5.3 Mean abundance and standard deviation of major and trace element contents in granitoid clasts, Feeder Granodiorite (Wiley's River intrusion, and Little Sandy Lake intrusion), felsic flows from the Lundberg Hill, Ski Hill and Buchans River Formations (undivided; data from Thurlow, 1981a) and felsic flows in the Little Sandy Lake area. 181

Table 5.4 Rare earth element contents (in ppm) in granitoid clast types 1, 2, 3 and 4, and the Wiley's River intrusion as determined at Memorial University using the thin-film XRF technique of Fryer and Edgar (1977). 195

Table 6.1 Uranium-lead isotopic data. 213

Table 6.2 Comparison of estimates for the absolute ages (Ma) for the base of the Silurian epoch and the base of the British paleontological stages of the Ordovician epoch. 226

Table 7.1 Comparison of observed features of granitoid clasts in MacLean Extension with the proposed source (right-hand column) and alternative sources (first three columns). Yes indicates that the source can explain the observed feature; possible indicates that the source can possibly explain the feature but not as conclusively as a 'yes' response; doubtful indicates that the source may explain the feature and cannot be dismissed entirely but is considered to be geologically unlikely; no indicates that the potential source can not possibly explain the observed feature. 260

Appendix Table 1.1 Examples of replicate major element analysis to estimate precision of analyses (Mrs. G. Andrews, analyst). 291

Appendix Table 2.1 Arithmetic means, standard deviations and range of trace elements determined at Memorial University by X-ray fluoresence spectroscopy for five replicate analyses of granite standard (MUN-1). 293

Appendix Table 4.1 Flow chart outlining the steps followed in the extraction and separation of zircons used in U-Pb isotopic analysis of granitoid clast sample KQS-82-095. 299

Appendix Table 4.2 Flow chart outlining the steps followed in the extraction and separation of zircons used in U-Pb isotopic analysis of rhyolite sample KQS-82-210. 300

LIST OF FIGURES

Figure 1.1 The island of Newfoundland showing the location of the town of Buchans in relation to the tectono-lithofacies zones of Williams (1978, 1979) and the Central Volcanic Belt of Newfoundland (CVB) of Kean et al. (1981). 2

Red Indian Lake is shown to the south of Buchans.

Figure 1.2 Simplified geological map of the Buchans area with locations of Figures 2.1, 3.1 and 3.2 (after Thurlow and Swanson, 1985). 3

Figure 2.1 Schematic geological map of the Buchans Group in the immediate vicinity of the massive sulphide orebodies showing the most economically important thrust blocks and projections of the orebodies to the surface (after Thurlow and Swanson, 1985). 38

Figure 3.1 Geological map of the Little Sandy Lake field area, with sample locations. in pocket

Figure 3.2 Geological map of the Wiley's River field area, with sample locations. in pocket

Figure 4.1 Schematic cross-section of the detailed stratigraphy of the Buchans River Formation in the MacLean Extension area (after Thurlow and Swanson, 1985). 64

Figure 4.2 Plan of MacLean Extension transported orebody showing extreme outlines of the upper and lower ore units, main study locations and sample numbers collected at these locations including the locations of the geochronology samples (KQS-82-095 and -210) (modified from Binney et al., 1983). in pocket

Figure 4.3 Schematic representation of changes in matrix composition, dominant composition of clasts, size of clasts, relative angularity of clasts and abundance of granitoid clasts that describe the lithologic continuum of sedimentological units comprising the transported orebodies and genetically related strata in MacLean Extension. 69

Figure 4.4 Schematic cross-section through the MacLean Extension orebody showing the idealized distribution of the debris flow lithologic subunits including the main granitoid-rich zone (modified from Binney et al., 1983). 72

Figure 4.5 Graphical representation of phenocryst and groundmass grain size and textural criteria used to classify granitoid clast types in 88

MacLean Extension.

Figure 4.6a Histograms of the estimated volume percent occupied by granitoid clasts in debris flows at the four main study locations (see Figure 4.2). Average size (in centimeters) of granitoid clasts at each location is shown within each histogram. 126

Figure 4.6b Relative frequency histograms of granitoid clast groups at the four major study locations. Macroscopic classification after Stewart (1983); 'granitic' group consists of clast types 1, 4 and 6, 'aplitic' group consists of clast types 2, 5 and 7. Microscopic classification after Stewart (1984); 'granitic' group consists of clast types 1 and 3, 'aplitic' group consists of clast types 2, 4 and 5. Numbers in brackets below histograms indicate the number of clasts classified at each location by each method. 126

Figure 5.1 Igneous spectrum diagram of Hughes (1973) for granitoid clast types. Crosses (+) represent type 1 clasts, symbol (X) represent type 2 clasts, asterisks (*) represent type 3 clasts, circles (0) represent type 4 clasts, a star (★) represents the type 5 clast and the symbol (H) represent type 6 clasts. 152

Figure 5.2 Na/K/Ca diagram for granitoid clast types. Symbols as defined in Figure 5.1. Fields of type 2 and 4 (aplitic group) granitoid clasts are shown. 154

Figure 5.3 Loss-on-ignition (LOI, weight %) vs. Ba and CaO (CaO, in weight %, Ba in ppm) variation diagrams for granitoid clast types. Symbols as defined in Figure 5.1. 156

Figure 5.4 CaO (weight %) vs. Sr (in ppm) variation diagram. Crosses (+) represent Topsails granite (TS) samples, circles (0) represent the Wiley' River intrusion (WR) samples, asterisks (*) represent Little Sandy Lake intrusion (LS), the symbol (H) represent rhyolites from the Little Sandy Lake area, the symbol (X) represent granitoid clasts and the star (★) is the rhyolite from the Buchans River Formation in MacLean Extension used in 159

the geochronology study.

Figure 5.5 SiO2 (weight %) vs. Agpaiitic Index (Na2O+K2O/Al2O3) variation diagram. Symbols as defined in Figure 5.4. 160

Figure 5.6 Igneous spectrum diagram of Hughes (1973). Symbols as defined in Figure 5.4. 161

Figure 5.7 Na/K/Ca diagram. Symbols as defined in Figure 5.4. The field of granitoid clasts is shown. 163

Figure 5.8 TiO2 (weight %) vs. trace elements (V, Y and Zr, in ppm) variation diagrams for granitoid clast types. Fields of granitoid clast type 2, 4 and 6 are shown. Symbols as defined in Figure 5.1. 166

Figure 5.9 Zr vs. Y (both in ppm) variation diagram for granitoid clast types. Symbols as defined in Figure 5.1. 168

Figure 5.10 Zr/Y/Nb diagram for granitoid clast types. Symbols as defined in Figure 5.1. Fields of type 2 and 4 (aplitic group) granitoid clasts are shown. 170

Figure 5.11 Zr/Y/Sr diagram for granitoid clast types. Symbols as defined in Figure 5.1. Fields of type 2 and 4 (aplitic group) granitoid clasts are shown. 172

Figure 5.12a Abundances of rare earth elements in granitoid clast types 1, 3 and 6 normalized to chondritic values of Taylor and Gorton (1977). Symbols and accompanying numbers designate the sample analysed (all numbers are KQS-82-xyz). 177

Figure 5.12b Abundances of rare earth elements in granitoid clast types 2 and 4 normalized to chondritic values of Taylor and Gorton (1977). Symbols and accompanying numbers designate the sample analysed (all numbers are KQS-82-xyz). 178

Figure 5.13 SiO2 (weight %) vs. Y and Zr (in ppm) variation diagrams. Fields of Buchans Group felsic flows (BV) (from Thurlow, 1981a) and granitoid clasts (GC) are shown. Symbols as 184

defined in Figure 5.4.

Figure 5.14 SiO2 (weight %) vs. trace elements (V and Rb, in ppm) diagrams. Fields of Buchans Group felsic flows (BV) (from Thurlow, 1981a) and granitoid clasts (GC) are shown. Symbols as defined in Figure 5.4. 186

Figure 5.15a Zr vs. Y (both in ppm) variation diagram. Symbols as defined in Figure 5.4. 189

Figure 5.15b TiO2 (weight %) vs. trace elements (Y and Zr, in ppm) variation diagrams. Field of Buchans Group felsic flows (BV) (data from Thurlow, 1981a) is shown. Symbols as defined in Figure 5.4. 189

Figure 5.16 Triangular plots of trace elements (Zr, Y, Nb, Ga and Sr, in ppm). Field of granitoid clasts (GC) is shown. Symbols as defined in Figure 5.4. 191

Figure 5.17 Abundances of rare earth elements in Lundberg Hill Formation rhyolites of the Buchans Group (BGR) (data from Strong, 1984), Wiley's River intrusion (WRI) and Buchans Group rhyolites (unnamed formation in the Little Sandy Lake area east of Buchans River, formerly in the Little Sandy Lake sequence (LSLR) (data from Strong, 1984) normalized to the chondritic values of Taylor and Gorton (1977). Symbols and accompanying numbers designate the sample analysed. Wiley's River Formation samples are all KQS-82-xyz. 194

Figure 5.18 Tectonic discrimination diagram of Pearce et al. (1984) for the granitoid clast types. Symbols as defined in Figure 5.1. Fields for volcanic arc granites (VAG), ocean ridge granites (ORG), within plate granites (WPG) and syn-collosion granites (syn-COL) are shown. 197

Figure 5.19 Tectonic discrimination diagram of Pearce et al. (1984). Symbols as defined in Figure 5.4. Fields for volcanic arc granites (VAG), ocean ridge granites (ORG), within plate granites (WPG) and syn-collosion granites (syn-COL) are shown. 198

Figure 6.1 U/Pb concordia diagram. 215

Figure 7.1 Idealized cross-sectional model for the genesis of the granitoid clasts associated with transported sulphide orebodies at Buchans: a) hiatus in felsic volcanism permitting; deposition of sulphide muds and siltstone unit, partial crystallization of underlying magma chamber with accompanying release of a volatile phase that fractures the intruded rock and possibly contributes fluid and metals to the hydrothermal fluids depositing the sulphide muds: b) period of felsic pyroclastic volcanism, propagation of a breccia pipe containing granitoid clasts toward the surface; c) either accompanying or preceeding another period of felsic pyroclastic activity, the breccia pipe breaches the surface in the vicinity of the sulphide mud pond, probably explosively; as a result of this explosion, accompanying volcanism or related earthquakes, debris flows are initiated that transport portions of the sulphide mud pond, ejected granitoid clasts and other entrained material downslope as subaqueous debris flows. Subsequent debris flows are increasingly less sulphide- and granitoid-rich and are presumed to indicate a waning of sulphide mineralization and the explosiveness of the associated hydrothermal activity. 252

Appendix Figure 3.1 Comparison of chondrite-normalized rare earth element abundances in granite standard MUN-1 as determined by XRF techniques and instrumental neutron activation (INAA) techniques. Top figure shows the range of four replicate XRF analyses of MUN-1 at Memorial University in 1983. Bottom figure shows four independent INAA results for MUN-1 (McM1 and McM2 data produced at McMaster University, McM1 data courtesy of P. O'Neil; McM2 data courtesy of D.F. Strong; JH data produced by Jan Hoertgen, courtesy of D.F. Strong; RPT data produced by R.P. Taylor, courtesy of D.F. Strong). 297

LIST OF PLATES

Plate 3.1 Representative photomicrographs of Little Sandy Lake intrusion. 52

Plate 3.2 Representative photomicrographs of Wiley's River intrusion. 56

Plate 4.1 Photograph of typical arenaceous conglomerate in MacLean Extension area. 70

Plate 4.2 Photograph of two large 'granitic' group granitoid clasts with large clast of black ore in granitoid-bearing pplylithic breccia-conglomerate within 30 m of sulphide matrix ore. 73

Plate 4.3 Photograph of variably coloured, quartz-porphyritic 'granitic' group granitoid clast with yellow ore clast in granitoid-bearing polylithic breccia-conglomerate overlying sulphide matrix ore. 74

Plate 4.4 Photograph of two 'granitic' group granitoid clasts with large clast of black ore that shows evidence of plastic deformation. 75

Plate 4.5 Photograph of well rounded, brick-red, 'aplitic' group granitoid clast in granitoid-bearing polylithic breccia-conglomerate. 80

Plate 4.6 Photograph showing rounded nature of 'granitic' group granitoid clasts in contrast to angular to subangular form of other clast lithologies in granitoid-bearing polylithic breccia-conglomerate within 60 m of sulphide matrix ore. 81

Plate 4.7 Photograph of rounded granitoid and other lithic clasts typical in granitoid-bearing polylithic breccia-conglomerate without associated sulphide matrix ore. 86

Plate 4.8 Photograph of two large type 6 granitoid clasts in siltstone breccia. 91

Plate 4.9 Photograph showing colour differences due to variable hydrothermal alteration of 'granitic' group granitoid clasts. 97

Plate 4.10 Photograph of white, rounded and subrounded, 'aplitic' group granitoid clasts in granitoid-bearing polylithic breccia-conglomerate without associated sulphide matrix ore. 98

Plate 4.11 Photograph of partially altered, spindle shaped, 'aplitic' group granitoid clast. 99

Plate 4.12 Representative photomicrographs of granitoid clast type 1. 103

Plate 4.13 Representative photomicrographs of granitoid clast type 2. 106

Plate 4.14 Representative photomicrographs of granitoid clast type 3. 109

Plate 4.15 Representative photomicrographs of granitoid clast type 4. 111

Plate 4.16 Representative photomicrographs of granitoid clast type 5. 114

Plate 4.17 Representative photomicrographs of granitoid clast type 6. 117

Plate 4.18 Photomicrographs comparing a typical granitoid clast (type 3) and quartz porphyritic volcanic rock from the Lundberg Hill Formation (formerly the Prominent Quartz Sequence). 120

Plate 6.1 Photograph of granitoid clast (KQS-82-095) used in geochronology study prior to its extraction from the rock face. 207

Plate 6.2 Photomicrographs comparing non-magnetic, heavy mineral concentrate produced by 211

conventional geochronological separation methods from granitoid clast (top) and rhyolite sample (bottom).

Plate 6.3a (Top) Photomicrograph of example of inclusion-bearing, cracked zircon from granitoid clast with attached gangue material excluded from zircon population selected for isotopic analysis. 218

Plate 6.3b (Bottom) Photomicrograph of zircon population selected from granitoid clast for isotopic analysis after abrasion and hand-picking. 218

Plate 6.4a (Top) Photomicrograph of typical euhedral, clear, inclusion-free zircon selected for isotopic analysis from rhyolite. 220

Plate 6.4b (Bottom) Photomicrograph of euhedral, clear zircon from rhyolite with a small amount of attached gangue material prior to abrasion. 220

Plate 7.1 Photograph of elongate granitoid clast with irregular outer surface. 246

Plate 7.2 Photograph of polylithic breccia-conglomerate showing irregular outer surface of granitoid clast in contrast to smooth, rounded surface of rhyolite clast. 247

CHAPTER ONE

INTRODUCTION

1.1 LOCATION, ACCESS AND TOPOGRAPHY

The thesis area consists of three main study locations at Buchans, Newfoundland. These are the 20 Level of the MacLean mine, the Wiley's River field area and the Little Sandy Lake field area.

Buchans is situated in central Newfoundland at approximately 48° 49' N latitude and 56°52' W longitude (Fig. 1.1). The Wiley's River area is centered 12.5 km southwest of Buchans and the Little Sandy Lake area is centered 14 km due east of Buchans (Fig. 1.2). The town of Buchans is accessible by provincial highway 370 and located 77 km from the town of Badger on the Trans-Canada Highway.

The Little Sandy Lake field area (Fig. 1.2, 3.1) is situated within 4 km of Highway 370 and is accessible by traverse. The Wiley's River field area (Fig. 1.2, 3.2) was reached by helicopter from Buchans in 1982. In 1983, a bush vehicle provided access to an Abitibi-Price field

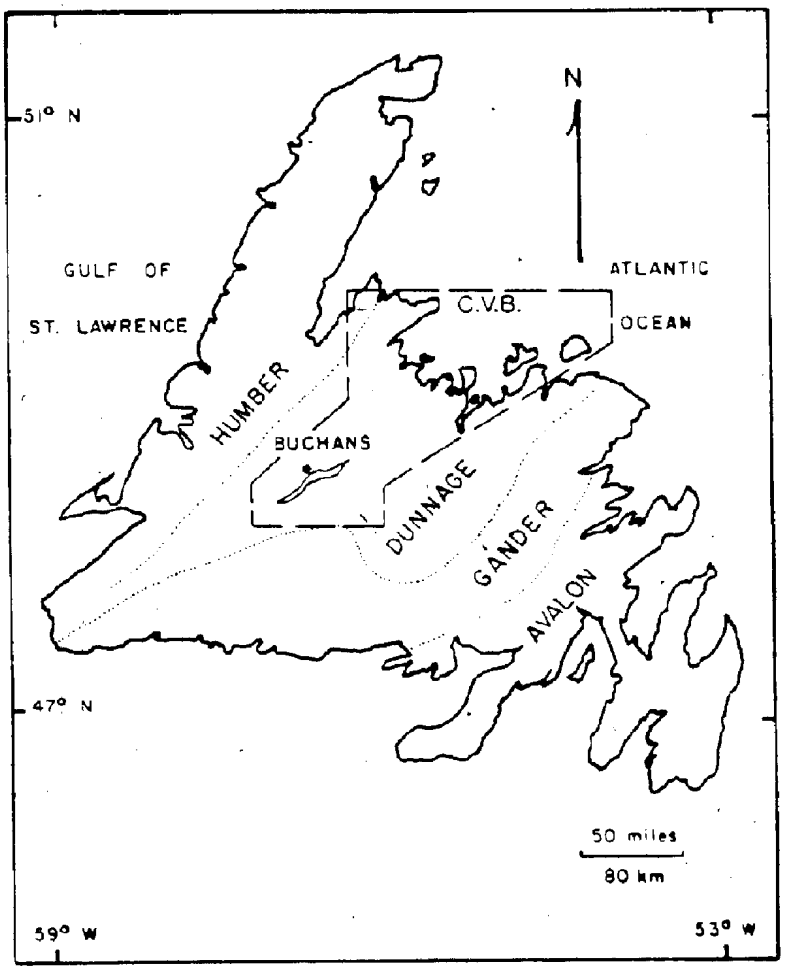

FIGURE 1.1 The island of Newfoundland showing the location of the town of Buchans in relation to the tectono-lithofacies zones of Williams (1978, 1979) and the Central Volcanic Belt (CVB) of Kean et al. (1981). Red Indian Lake is shown to the south of Buchans.

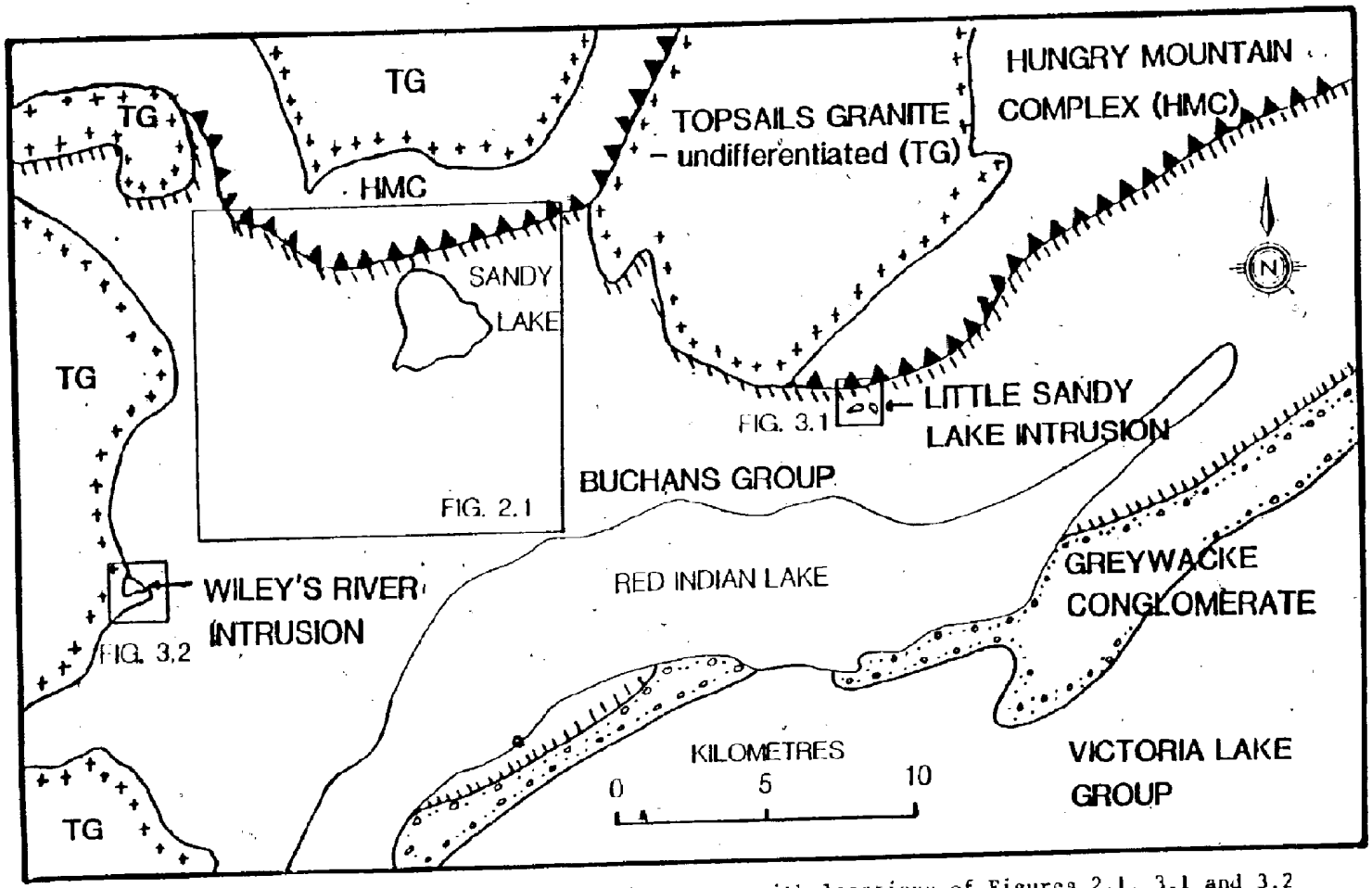

FIGURE 1.2 Simplified geological map of the Buchans area with locations of Figures 2.1, 3.1 and 3.2 (modified from Thurlow and Swanson, 1985).

exploration camp located within foot traverse of Wiley's River. The MacLean Extension orebody (Fig. 2.1) is reached via the MacLean mine headframe located 2 km northwest of the Lucky Strike mine and the town of Buchans.

Buchans is located in the gently rolling upland area of central Newfoundland. To the north and west lie the bog-covered and otherwise barren plateaus of the Topsails Highlands. Red Indian Lake and Mary March River bound the area to the south and east.

Outcrop exposure of the Buchans Group volcanic rocks is generally poor, about 1% (Thurlow, 1981a). Bogs and heavily forested knolls occupy most of the area. Intrusive rocks, i.e., diabase and gabbro, form most of the elevated areas and outcrops in the Buchans area.

The mines at Buchans have operated since 1928 under a series of Co-Tenancy Agreements between the owners, originally the Anglo-Newfoundland Development Co. Ltd. (A.N.D.), then the Price (Nfld.) Co. Ltd., a subsidiary of Abitibi-Price Co. Ltd, and the operators, American Smelting and Refining Co. Ltd. (ASARCO). With the expiration of the existing agreement in 1976 Abitibi-Price took a more active role in the operations at Buchans and presently functions there as the exploration manager under the name Abitibi-Price Co. Ltd.

In addition to field studies, diamond drill core stored in Buchans was examined and sampled, thereby permitting sampling of the otherwise inaccessible Lucky Strike, Oriental and Rothermere mines. The Old Buchans Conglomerate Orebody open pit on the bank of the Buchans River was briefly examined (Fig. 2.1).

1.2 PREVIOUS WORK IN THE BUCHANS AREA

Previous work in the Buchans area was summarized by Thurlow (1981a). Brief mention of the more significant work is given below.

Murray (1877) was the first to describe rocks in the Red Indian Lake vicinity. He considered these rocks to be correlative with the 'Silurian' rocks of the Exploits River Valley. The granitic rocks were considered to be 'Laurentian' (Archean) in age.

Although the first sulphides were discovered in the Buchans area in 1905, milling and smelting difficulties with the fine grained and polymetalic Pb-Zn-Cu-Ag-Au ores delayed development until 1926 with the first production in 1928 (Neary, 1981). Snelgrove (1928), Newhouse (1931) and George (1937) provided the first detailed descriptions of the

regional geology and geological setting of the orebodies. George (1937) produced a valuable record of the earliest ores mined, i.e. the Lucky Strike and Oriental orebodies. Buchans Staff (1955) published the first description of the Rothermere orebody.

Relly (1960) provided large amounts of descriptive data and the first petrochemical analyses aimed at understanding the alteration related to sulphide mineralization. Although accurately describing features now generally recognized as indicative of a syngenetic origin for most massive sulphide orebodies, Relly followed the prevalent theory of the day and concluded that the ore was of epigenetic, hydrothermal replacement origin.

Swanson and Brown (1962) reduced Relly's voluminous work and provided concise descriptions of the ores mined at that time, including the MacLean orebody. This paper was deemed "Paper of the Year" by the Canadian Institute of Mining and Metallurgy. The ores were still presented as having formed epigenetically.

Anger (1963) concluded from the published descriptions that the Buchans ores were similar to the Rammelsberg and Meggan deposits of Germany and were probably of a similar syngenetic origin. An examination of the relationship between lithogeochemistry and mineralization (Thurlow, 1973,

1981a) and comparison of the Buchans ores and the Kuroko deposits of Japan (Thurlow et al., 1975; Thurlow, 1981a,b) demonstrated that the formation of the orebodies was syngenetic with deposition of the volcanic host rocks, and documented many similarities between the Buchans and Kuroko deposits.

The expiration of the Co-tenancy Agreement between ASARCO and A.N.D. (now Abitibi-Price) in 1976 marked the end of fifty years of continuous mining operations. Commemorating this event, the Buchans Volume (Swanson et al., 1981) was commissioned by the two companies to provide an historical, operational and geological account of the Buchans operation, and to conduct some original geological research on the deposits prior to the cessation of mining operations (projected to be 1979 at that time). The resulting volume, published by the Geological Association of Canada, contains not only a review of the history of development of the mines and the town of Buchans but also the results of previous as well as recently commissioned scientific research on various aspects of the Buchans Group and its contained orebodies.

Studies by Thurlow (1973, 1981a) greatly advanced the understanding of the genesis of the ores and the stratigraphy and structural setting of the Buchans Group. In the process of demonstrating a syngenetic origin for the

in situ orebodies, Thurlow recognized the transported nature of several massive sulphide orebodies at Buchans (Thurlow, 1977).

Swanson and Brown (1962) mentioned the presence of granitoid clasts associated with sulphide accumulations, i.e., "granite conglomerates". Thurlow (1981a,b) also showed an apparent spatial relationship between the occurrences of granitoid clasts and transported sulphide orebodies.

The continuing search for ore at Buchans resulted in a reappraisal of the structure and stratigraphy of the Buchans Group (Thurlow, 1984). The newly revised stratigraphy will be the first formal stratigraphic subdivision (under the North American Stratigraphic Code) of the Buchans Group (Thurlow and Swanson, 1985). This interpretation and reports of other recent research conducted at Buchans under the auspices of the Canada-Newfoundland Cooperative Mineral Program 1982-1984, including the results of this study, are presently being prepared for publication (Kirkham, 1985).

1.3 PREVIOUS WORK ON PLUTONIC ROCKS IN VOLCANIC TERRANES

The presence of plutonic (or coarse grained igneous) rocks in volcanic terranes is not uncommon. Various interpretions of their origin and significance have been presented in the literature. They have been interpreted to be coeval with the volcanic host rocks in many locations, e.g. Hawaii (Kuno, 1969), Kamchatka (Erlich et al., 1979; Volynets and Bogoyavlenskaya, 1979), the Carpathians (Hovork and Fejdi, 1980), southern British Columbia (Fujii and Scarfe, 1982), Ascension Island (Roedder and Coombs, 1967; Harris, 1983), Kenya (Jones, 1979), Papua New Guinea (Arculus et al., 1983), the Aleutians (Conrad et al., 1983; Conrad and Kay, 1984) and the Lesser Antilles (Lewis, 1973; Arculus and Wills, 1980). The latter paper contains many references which document the occurrence of plutonic material associated with volcanic rocks in the Lesser Antilles. Although most plutonic material reported in the literature is ultra-mafic to mafic in composition (e.g., Erlich et al., 1979; Fujii and Scarfe, 1982; Conrad and Kay, 1984), plutonic material of granitic composition is not uncommon (Roedder and Coombs, 1967; Volynets and Bogoyavlenskaya, 1979).

Plutonic rocks have also been reported to be found in volcanic strata associated with massive sulphide deposits, e.g. the Tertiary Kuroko deposits of Japan (Osada et al., 1974; Takanouchi, 1978; Urabe et al., 1983) and the

Siluro-Devonian Harbourside, Maine deposit (Bouley, 1978; Bouley and Hodder, 1984).

Thurlow (1981a,b) and Walker and Barbour (1981) described the occurrence of granitoid clasts in strata at Buchans. The presence of granitoid clasts in polylithic breccia-conglomerates associated with the ore grade breccias and breccia-conglomerates (transported ore) was considered enigmatic by Thurlow (1981a,b). Despite the large variety of lithic clast types in these rudaceous rocks, all lithic types could be ascribed to known underlying units with the exception of the granitoid and rare carbonate clasts (see Nowlan and Thurlow (1984) for a discussion of the carbonate clasts found at Buchans, their age and possible origin). In addition, the granitoid clasts appeared to be anomalously rounded relative to all other clast lithologies present in these rudaceous units (Thurlow and Swanson, 1981).

Two small bodies of granodiorite, that are texturally similar to the granitoid clasts, occur near the margins of the Buchans Group (Thurlow, 1981a,b; Thurlow and Swanson, 1981). Geochemical similarities between the granodiorite, the granitoid clasts and some felsic volcanic rocks in the Buchans area were also outlined. Thurlow (1981a,b) suggested that the granodiorite is a plutonic facies of the Buchans felsic volcanic rocks and may also be the source of the granitoid clasts. For these reasons, and in an attempt

to provoke further work that would determine the source of these granitoid clasts, Thurlow (1981a,b) named these plutonic bodies the Feeder Granodiorite (Thurlow, pers. comm., 1982).

The mechanism for transport of these clasts to the surface proposed by Thurlow and Swanson (1981) was in 'pebble dykes' or breccia pipes and dykes (Bryner, 1961; Bryant, 1968) such as those seen in association with the Japanese Kuroko deposits (Takahashi and Suga, 1974, p.102; Takanouchi, 1978; Urabe et al., 1983, p.355), some porphyry deposits of the North and South American Cordillera (Sillitoe and Sawkins, 1971; Norton and Cathles, 1973; Carlson and Sawkins, 1980) and some high-level felsic intrusive bodies (e.g. Allman-Ward et al., 1982). Sulphide mineralized breccia pipes in the Canadian Shield are reported to contain rounded trondhjemitic clasts (Armbrust, 1969).

Many theories to explain the genesis of breccia pipes have been made in the literature (e.g., Reynolds, 1954; Kents, 1964; Bryant, 1968; Norton and Cathles, 1973; Mitcham, 1974; Williams and McBirney, 1979; Wolfe, 1980). These pipes are most commonly considered to be the product of the explosive expulsion of fluids, from mantle depths in the case of kimberlite or carbonatite bearing breccia pipes, or within the upper crust in most other cases (e.g.,

Bryant, 1968; Norton and Cathles, 1973; Wolfe, 1980). The ultimate source of the fluids is, however, often difficult or impossible to establish (Williams and McBirney, 1979). The mechanism by which rock fragments are transported upwards is also unequivocal (Mitcham, 1974; Wolfe, 1980). The 'fluidization' model of Reynolds (1954) is commonly invoked to explain the transportation of rock material from depth (e.g., Kents, 1964; Bryant, 1968; Allman-Ward et al., 1982). However, the relative density differences between the fluid and any transported rock material requires very high velocity fluid streaming to suspend or transport rock material (Wolfe, 1980). For this reason Wolfe favours explosions rather than a constant high velocity fluid flow to provide the required velocities for transport of subsurface matetial upward, i.e., they are moved ballistically.

An alternative mechanism (Thurlow and Swanson, 1981) to explain the presence of granitoid clasts in strata at Buchans was as debris shed by a block of crystallized magma up-faulted within or flanking the volcanic edifice due to magmatic pressure (Cobbing and Pitcher, 1972). They could also, theoretically, be eroded remnants of nearby older crystalline terranes.

Neither 'pebble dykes' nor a plutonic body suitably located within the volcanic rocks have been found in the Buchans area (Thurlow, 1981a,b). For this reason, Thurlow (1981a,b) considered their presence enigmatic.

1.4 OBJECTIVES OF PRESENT STUDY

The purpose of this study was to research the morphology, petrology, lithogeochemistry and geochronology of granitoid clasts associated with transported sulphide orebodies and other related rudaceous strata of the MacLean Extension area at Buchans, Newfoundland and to determine the provenance of the granitoid clasts, especially with regard to the proposed comagmatism of the Feeder Granodiorite and Buchans Group felsic volcanic rocks.

1.5. METHODS OF INVESTIGATION

This study integrates data from several sources in order to establish the best logical source for the granitoid clasts and the relationship between the clasts, the Feeder Granodiorite and Buchans Group felsic volcanic rocks. The data sources used for this investigation were:

(1) field mapping at 1":1000' (1:12000) of the two exposures of the Feeder Granodiorite in the Wiley's River and the Little Sandy Lake field areas (Fig. 1.2; Chapter Three);

(2) underground mapping (typically at 1":10' (1:120)) and sampling of all accessible occurrences of pebble sized or larger granitic detritus in volcanic or volcaniclastic strata associated with the MacLean Extension orebody (Fig. 2.1). Mapping and sampling were conducted predominantly on the 20 Level of the MacLean Mine, and were concentrated on exposures of granitoid-rich polylithic breccia-conglomerate subunits of the transported orebodies (Chapter Four);

(3) petrographic examination of the granitoid clasts, Wiley's River intrusion, Little Sandy Lake Intrusion, and Buchans Group volcanic rocks (Chapter Three and Four);

(4) lithogeochemical analyses for major, trace and rare earth element abundances in samples of the rock units listed in (3) above (Chapter Five);

(5) geochronological investigation by the uranium-lead (zircon) method of a granitoid clast from an ore-grade granitoid-bearing polylithic breccia-conglomerate on 20 Level, MacLean Extension mine and a nearby underlying quartz- and feldspar-phyric rhyolite of the Buchans River

Formation (Chapter Six);

(6) examination and sampling of diamond drill core intersections of granitoid-bearing strata from the Lucky Strike, Oriental, Rothermere, MacLean and MacLean Extension orebodies;

(7) examination and sampling of "granite conglomerate" exposed in the Old Buchans Conglomerate Orebody open pit (Fig. 2.1)(Thurlow and Swanson, 1981);

1.6 Acknowledgements

Financial support for field work, the geochronological study and incidental expenses from July 1982 until April 1984 was provided by a Canada Department of Energy, Mines and Resources personal research contract (Contract No. 1583327) with the author. The administration of this contract was overseen by Dr.W.H. Poole.

ASARCO and Abitibi-Price Co. Ltd. co-operated completely with the author during his stay in Buchans. Permission to go underground, access to drill core and to company files, maps and other material in their offices at Buchans was essential for the success of this study. The occasional use of company equipment, including vehicles and contracted helicopter services, greatly assisted the

logistics of conducting the study and is greatly appreciated.

The period of residency at Memorial University was provided in the form of a Natural Sciences and Engineering Research Council Post-graduate Scholarship, which is gratefully acknowledged. Some financial assistance was also provided from NSERC Operating Grant No. A7975 to D.F. Strong.

The number of people who provided assistance, advice and encouragement to the author is large. Acknowledgement and thanks are offered to:

(1) E.A. Swanson (ASARCO), Dr. J.G. Thurlow (Abitibi-Price), D.B. Barbour (Abitibi-Price), W.P. Binney (private geological contractor), Dr. R.V. Kirkham (Geological Survey of Canada) and Dr. D.F. Strong (Memorial University) for their insights into Buchans geology;

(2) Dr. O. van Breeman provided access to the facilities of the Geochronological Laboratory of the G.S.C., Ottawa and the assistance of members of the staff of the Geochronology Lab, notably: Dave Smith, who assisted in hand-picking zircons under the binocular microscope; R.K. Stevens, who took the zircon photomicrographs; W.D. Loveridge, who conducted the isotopic analyses, made the

necessary corrections to the raw data and calculated the age parameters quoted in this report. Special thanks are extended to R.W. Sullivan who supervised the chemistry and assisted in a myriad of other ways;

(3) the staff at Memorial University- Mrs. G. Andrews conducted the major element analyses, D. Press and Dr. D.H.C. Wilton assisted in data storage, manipulation and graphical presentations of the geochemical data;

(4) Pius Brennan, miner, assisted in the extraction of the granitoid clast from the rock face by explosives and in the collection of the rhyolite sample used for the geochronology study;

(5) Lucille Gagnon of St. Boniface Community College provided access to computing facilities after the authors' departure from Newfoundland.

The constructive comments by Drs. D.F. Strong, J.G. Thurlow, R.V. Kirkham, M.A.F. Fedikow and G.H. Gale and Mr. G. Ostry on earlier drafts of some or all of this report are greatly appreciated. The final conclusions and interpretations remain the responsibility of the author.

The assistance and support of my supervisor Dr. D.F. Strong during the course of this research, especially in the final preparation of this report, is greatly appreciated.

CHAPTER TWO

REGIONAL GEOLOGY

2.1 INTRODUCTION

The Buchans Group forms part of the Dunnage Zone of Williams (1978, 1979), one of five tectono-stratigraphic subdivisions of the Canadian Appalachians in Newfoundland (Fig. 1.1). The Dunnage Zone is considered to represent vestiges of Iapetus, the paleo-Atlantic ocean that existed during the Lower Paleozoic (Wilson, 1966). The Dunnage zone or terrane contains rocks which are interpreted to record the evolution and destruction of this oceanic domain (Williams, 1979, 1984).

The Buchans volume (Swanson et al., 1981) contains a comprehensive description and correlation of the regional geological setting of the volcanic and associated rocks of the Central Volcanic Belt (Kean et al.,1981), as well as the stratigraphic and structural setting of the Buchans Group (Thurlow, 1981b). However, the Buchans Group stratigraphy has undergone substantial re-interpretation recently (Thurlow, 1984; Thurlow and Swanson, 1985) resulting in a simplification of the Buchans stratigraphy with a

corresponding increase in complexity of the structural history of the Buchans Group. The massive sulphide Pb-Zn-Cu-Ag-Au deposits at Buchans have been described as occurring in three types: stockwork ore, in situ ore and transported ore (Thurlow and Swanson, 1981). The in situ and transported orebodies occur in a restricted stratigraphic interval within the Buchans River Formation of the Buchans Group (Thurlow and Swanson, 1985).

2.2 THE CENTRAL VOLCANIC BELT OF NEWFOUNDLAND

2.2.1 Introduction

To avoid the tectonic implications of William's (1979) zonal terminology, the volcanic and related rocks of the Dunnage zone have been termed the Central Volcanic Belt of Newfoundland (Figure 1.1) (Kean et al., 1981) or the Central Mobile Belt (Swinden and Kean, 1984; Swinden and Thorpe, 1984). Regional geological models emphasize the importance of island arc processes in forming many of the rocks of the Central Volcanic Belt during the early and middle Paleozoic (Strong, 1977; Dean, 1978; Kean et al., 1981; Swinden and Kean, 1984; Swinden and Thorpe, 1984). The recent overviews of Ordovician volcanism in the British Caledonides (Stillman, 1984) and throughout the entire

Appalachian-Caledonian orogen (Stephens et al., 1984) also emphasized subduction-related volcanic activity.

The Central Volcanic Belt is considered to be underlain by Cambro-Ordovician oceanic crust (Miller and Deutsch, 1976; Strong, 1977; Haworth et al., 1978). It has recently been suggested that the Dunnage zone is entirely allochthonous, and although largely composed of oceanic crust, is possibly underlain by continental crust (Karlstrom, 1983). Recent work by Whalen and Currie (1985) indicates that some units of the Topsails Igneous terrane were derived, at least in part, from continental crust. Continental crust is, therefore, presumed to underlie at least some parts of this terrane. The nature of the crust under the Buchans Group is not known at the present.

The composite stratigraphic section of the Central Mobile Belt presented by Swinden and Kean (1984) is the model adhered to in this study. Three main geologic settings are recognized: 1) ophiolitic sequences, which are considered to represent oceanic crust, e.g., Betts Cove Complex (Upadhyay et al., 1971), and are the lowestmost stratigraphic units where stratigraphic contacts are preserved; 2) thick sequences (to 8km) of tholeiitic and calc-alkaline, dominantly submarine volcanic, subvolcanic and related volcaniclastic rocks that conformably overlie the oceanic crustal volcanic rocks and have been interpreted

to be the remains of island arc complexes (Strong and Payne, 1973; Kean and Strong, 1975; Strong, 1977); and 3) a post-island arc sedimentary sequence of flysch, argillite and conglomerate of Middle Ordovician (Caradoc) to Early Silurian age that conformably overlies some of the island arc volcanic rocks (Dean, 1978), and was succeeded by younger Silurian subaerial volcanic and sedimentary rocks (e.g., the Springdale Group (Coyle et al., 1985)). Small outliers of terrestial Carboniferous strata are preserved locally within the Central Volcanic Belt (Kean et al., 1981).

This model permits the assignment of Buchans Group and Robert's Arm Group volcanic rocks (Section 2.2.5) to either a pre- or post-Caradocian age. In an earlier model (Dean, 1978; Kean et al., 1981), there were two phases of volcanism ('early' and 'late' or 'post' island arc sequences) that were separated by a period of quiessence marked by the Caradocian argillites and younger flysch and other related sedimentary rocks. The Buchans and Robert's Arm Groups were previously assigned to the 'late' or post-Caradocian island arc volcanic phase (Strong, 1977; Dean, 1978; Kean et al., 1981). There is clear evidence that some volcanic rocks conformably overlie Caradocian or younger sedimentary rocks in Notre Dame Bay, e.g., Long Island (Dean, 1978), and Oil Island (McHale and McHale, 1984). However, the observable

contacts between most volcanic rocks and underlying sedimentary sequences in the Central Volcanic Belt are structural in origin or controversial as to their nature (see Nelson and Kidd, 1979). The base of the Buchans Group is not exposed, and although the Buchans Group structurally overlies the pre-Caradocian Victoria Lake Group (Kean, 1977; Thurlow and Swanson, 1985) its age relative to the Victoria Lake Group is uncertain.

Radiometric ages for the Buchans Group of 447±18 Ma (Bell and Blenkinsop, 1981) and the Robert's Arm Group of 447±7 Ma (Bostock et al., 1979) do not conclusively resolve this matter, especially when the absolute ages assigned to the paleontologically defined epochs are not well established or agreed upon. Discussions of the age interpretations of the Robert's Arm Group (Bostock et al., 1979) by Nelson and Kidd (1979) and especially Dean and Kean (1980) and Currie and Bostock (1980) exemplify this problem. The differences in the absolute ages assigned to the paleontological stages of the Ordovician epoch are discussed in Chapter Six.

2.2.2 Oceanic Crust

Partly and well preserved oceanic crustal material is found in the Notre Dame Bay area. A complete ophiolitic sequence (Penrose Field Conference Participants, 1972), i.e., layered ultramafic and gabbroic rocks, sheeted diabase dyke swarms, mafic pillow lavas and overlying sediment, is exposed in the Betts Cove Group or Complex (Church and Stevens, 1971; Upadhyay et al., 1971).

Several other fragments of presumed ophiolitic material occur within the Central Volcanic Belt. The ultramafic and related rocks of the Baie Verte peninsula (Williams et al., 1977; Hibbard, 1983), of the Annieopsquotch Mountains (Dunning and Herd, 1980; Dunning, 1981; Dunning, 1984), of the South Lake Igneous Complex (Dean, 1978; Lorenz and Fountain, 1982), on Glover Island (Knapp, 1984) and in the Topsails Highlands (Igneous terrane) (Whalen and Currie, 1982, 1983, 1985) are considered to be remnants of oceanic crust near the western margin of the Dunnage Zone. A discontinuous belt of altered ultramafic and related rocks known as the Gander River Ultrabasic Belt (Jenness, 1954, 1958) probably marks the eastern margin of the Dunnage Zone (Dean, 1978).

The formation of the preserved remnants of the oceanic crustal domain in the Annieopsquotch Mountains occurred entirely in the Early Ordovician between 477 Ma and 489 Ma (Dunning and Krogh, 1983; Dunning, 1984). All oceanic crust

in Newfoundland formed in the interval between 463±6 Ma (Betts Cove Complex) and 505±10 Ma (Bay of Islands Complex) (Dunning, 1984).

2.2.3 The Island-Arc Sequence

The base of island arc volcanic sequences in the Central Volcanic Belt is usually a structural contact or not exposed (Swinden and Kean, 1984). However, volcanic sequences in the Snook's Arm and Western Arm areas of Notre Dame Bay conformably overlie ophiolitic rocks of the Betts Cove Complex and the Lushs Bight Group (Dean, 1978). On the basis of structural and stratigraphic correlations, other volcanic sequences with undefined bases are presumed to overlie ophiolitic rocks, e.g. Catcher's Pond Group (Dean, 1978)

The volcanism of the island arc sequences changes in character from the Notre Dame Bay area in the north through the central Victoria Lake area to the Hermitage Flexure area in the south (Swinden and Kean, 1984; Swinden and Thorpe, 1984). In the north, thick intercalated units of mafic pillow lavas and submarine volcaniclastic-sedimentary units dominate. Felsic volcanic rocks are minor in volume and typically form small plugs and domes, e.g. the Wild Bight Group of Notre Dame Bay (Dean, 1978). The centrally located Victoria Lake Group generally lacks pillow lavas, and

contains a greater volume of felsic pyroclastic rocks that tend to occur in linear belts. In the Hermitage Flexure area, mafic volcanism was typically minor in volume and this area is characterized by widespread, dominantly felsic volcanism followed by a period of extensive sedimentation, e.g. La Poile Group (Swinden and Kean, 1984).

2.2.4 The Late Ordovician sedimentary interval

In the eastern and central sections of the Central Volcanic Belt, island arc sequences are conformably overlain by an extensive graptolitic argillite-shale (±chert) sequence of Caradocian age, e.g. Shoal Arm Formation (Dean, 1978). This sedimentary sequence is absent in the western section, north of the Lobster Cove Fault (Dean and Strong, 1975), except on Oil Island and Long Island (McHale and McHale, 1984; Dean, 1978) where upper volcanic units of the Cutwell Group conformably overlie a sequence of Caradocian shales. Pre-Silurian unconformities usually record the erosion or the non-deposition of the shale units in the west (DeGrace et al., 1976). In western Notre Dame Bay, greywacke with an apparent western source transgressed eastward across the shales (Dean, 1978).

Conformably overlying the shales are Upper Ordovician to Lower Silurian greywacke and conglomerate sequences that show characteristics of flysch-turbidite sedimentation (Dean, 1978; Kean et al., 1981). Greywacke deposition dominated in the Upper Ordovician, e.g. the Sansom greywacke (Dean, 1978), with a general coarsening upward until conglomerate deposition predominated in the Lower Silurian, e.g. Goldson conglomerate (Dean, 1978). The progradation of the greywackes toward the east and sedimentary structures indicating transport direction from the north and northwest (Helwig and Sarpi, 1969) imply that the northwestern section was emergent and the probable source area for these flysch sequences (Dean, 1978; Nelson, 1981). Unnamed, but similar sedimentary rocks overlie the Victoria Lake Group and are considered correlative with those to the north (Dean, 1978).

The dominantly subaerial volcanic and sedimentary rocks of the Springdale Group rest unconformably upon Ordovician volcanic and intrusive rocks in the west (Dean, 1978). In the eastern part of the Central Volcanic Belt the products of volcanism have been assigned to the Botwood Group and are represented by the subaerial flows and pyroclastics of the Lower Silurian Lawrencetown Formation and the volcanic interbeds of the overlying Wigwam Formation (Dean, 1978).

2.2.5 The Buchans-Robert's Arm Belt

The Buchans-Robert's Arm Belt consists of the dominantly submarine volcanic, volcaniclastic and sedimentary rocks of the Buchans, Robert's Arm, Cottrell's Cove and Chanceport Groups (Dean, 1978; Swinden and Kean, 1984). Each group comprises a regionally extensive submarine volcanic (and related rock) sequence of chemically similar calc-alkaline suites (Strong, 1977). These volcanic rocks display weakly to distinctly bimodal (basalt-rhyolite) assemblages (Strong, 1977; Dean, 1978). Base metal deposits, e.g. the Buchans ores and the Bull Road Pb-Zn-Cu-Ag-Au showing on Pilley's Island, are found in each Group and show remarkable similarities (Thurlow, 1981a,b), that include the mechanical transportation of parts of each deposit (Tuach, 1984).

2.2.6 Post-Silurian rocks

Thin outliers of Carboniferous rocks, chiefly red sandstones and conglomerates, are preserved in several areas of the Central Volcanic Belt including the Red Indian Lake area. These units rest with angular unconformity on the underlying rocks and the conglomerates contain clasts of apparently local derivation (Kean et al., 1981).

2.2.7 Intrusive rocks

Many intrusive rocks in the Central Volcanic Belt appear to be genetically related to the various evolutionary phases of the volcanic stratigraphy (Kean et al., 1981). The intrusive rocks have been considered comagmatic with associated volcanic rocks in several areas, e.g., the Topsails Igneous Complex (Taylor et al., 1980; Whelan and Currie, 1982, 1983) and the Cape Brule Porphyry in the Springdale Belt (DeGrace et al., 1976).

Predominantly gabbroic, diabasic and sodic granodioritic plutonic bodies are associated with ophiolitic and early island arc sequences (Payne and Strong, 1979; Kean et al., 1981; Dunning, 1981, 1984). Small tonalite and granitic masses often occur close to extruded felsic volcanic rocks of the 'early' arc sequence (Kean et al., 1981).

Gabbros and diabase sills commonly intrude the post-Caradocian flysch and late island arc sequences, especially in the Robert's Arm Belt. Fine grained granitic bodies and quartz-feldspar porphyritic bodies are often associated with centers of silicic volcanism in the west (DeGrace et al., 1976).

Devonian and later intrusive rocks range in composition from gabbro to syenite (Dean, 1978). These intrusive bodies are usually large (of batholithic dimensions), discordant,

and often show a compositional evolution from an earlier gabbroic phase that is subsequently intruded by intermediate and felsic phases. These plutons are probably related to the suturing of the island arc complexes to the North American continental mass during the Acadian orogeny (Strong, 1980; Taylor et al., 1980). The bimodal character of Buchans Group volcanism and the peralkaline nature of most of the intrusive rocks in the Topsails Igneous Complex has been interpreted to indicate a period of extensional tectonics with subsidence and basin formation at the margin of the Topsails terrane (Whelan and Currie; 1985).

2.3 GEOLOGICAL SETTING OF THE BUCHANS GROUP

The base of the Robert's Arm Group appears to conformably overlie a post-Caradocian flysch sequence on Burton's Harbour peninsula (Dean, 1978). The relationship between the Buchans Group and the structurally underlying strata south and east of Red Indian Lake is not known with certainty (Thurlow, 1981a,b). Overlying the pre-Caradocian Victoria Lake Group is an unnamed greywacke-conglomerate sequence, lithologically similar to the post-Caradocian Sansom Greywacke and Goldson Conglomerate of Notre Dame Bay area (Anderson, 1972; Kean, 1977). Although the Buchans

Group structurally overlies this sequence, the original nature of this unexposed contact has been controversial. Williams (1970) considered it to be a faulted contact, whereas Anderson (1972) mapped the Buchans Group to conformably overlie these flysch units. Dean (1978), from Anderson's observations and for regional correlative reasons, also considered this contact to be conformable. Kean (1977, 1980) interpreted the contact to be a fault but considered the Buchans Group to be younger than the greywacke-conglomerate units overlying the Victoria Lake Group. The significance of a major structural lineament which traverses Red Indian Lake, and the presence of red sandstones (non-fossiliferous) south of Red Indian Lake are not presently understood. It has been suggested (Thurlow, 1981a,b; Nowlan and Thurlow, 1984) that the Victoria Lake Group may be a time stratigraphic equivalent to the Buchans Group and represents a deeper water and more distal facies of the Buchans Group.

Both the Robert's Arm and Buchans Group rocks are virtually devoid of fossils. Lower Ordovician (latest Arenig-early Llanvirnian) conodonts in carbonate clasts within Buchans Group debris flows have recently been reported (Nowlan and Thurlow, 1984). Rb-Sr whole rock radiometric dating methods for volcanic rocks from each group give similar ages of formation as dates of 447±7 Ma

from Robert's Arm Group volcanic rocks (Bostock et al., 1979) and 447±18 Ma from Buchans Group volcanic rocks (Bell and Blenkinsop, 1981) have been obtained. The assignment of these rocks to a post-Caradocian time of formation depends on the time scale used to assign absolute ages to the Ordovician fossil stages. The Ordovician absolute time scale is discussed in Chapter Six.

The Buchans Group is bounded to the north, east and west by the Topsails Igneous Terrane (Whelan and Currie, 1982, 1983, 1985). The Topsails are a mosaic of igneous rocks of great diversity both in composition and age and appear to be separated from juxtaposed terranes by major tectonic breaks (Whelan and Currie, 1985). Within the Topsail Igneous Complex, rafts of ultramafic and mafic rocks that may represent ophiolitic material and are probably the oldest rocks present are found in a 'sea' of younger plutonic bodies. Younger intrusive bodies of diorite, tonalite, granodiorite, syenite and peralkaline granites are also present (Whelan and Currie, 1982, 1983, 1985).

Deformed units of ultramafic, gabbroic, tonalitic and granodioritic compositions within the Topsails terrane are heterogenous in nature, of diverse ages and have complex contact relationships. These units are poorly understood and collectively form the Hungry Mountain Complex (Thurlow, 1981a,b; Whelan and Currie, 1982, 1983, 1985). This unit

is of uncertain age but appears to be older than either the associated intermediate and felsic volcanic, subvolcanic or intrusive rocks (Bell and Blenkinsop, 1981; Whalen and Currie, 1983, 1985). Rubidium-strontium age-dates of 400±60 Ma and 660±70 Ma from the Hungry Mountain Complex have been obtained by Bell and Blenkinsop (1981). An early Middle Ordovician zircon age-date from a younger tonalitic phase of this complex is in contrast with an Early Silurian age-date from a lithologically similar phase of the Rainy Lake Complex to the south (Whelan and Currie, 1985). U-Pb (zircon) dates from the ophiolitic (trondhjemite) rocks of the Annieopsquotch Ranges to the southeast of the Central Mobile Belt and south of the Topsails Highlands are between 477 and 481 Ma, i.e., Early Ordovician (Arenigian?) (Dunning and Krogh, 1983; Dunning, 1984).

Peralkaline granitic and syenitic bodies (Topsails-type granite) form the most important volumetric phase of the terrane. These bodies apparently formed in the Early Silurian between 420 and 430 Ma (Whelan and Currie, 1985). These dates contrast with previous Rb-Sr whole rock isochrons of 387±16 Ma and 421±7 Ma for alkali-feldspar and peralkaline granites, respectively, of the Topsails Igneous Complex (Bell and Blenkinsop, 1981).

Granitic rocks that are cut by the Topsails-type granites but younger than intermediate phases of the Hungry Mountain Complex cut the mafic to felsic volcanic and sedimentary rocks of the Glover Formation on the western flank of the Topsails Highlands. This formation has not been dated radiometrically but has recently yielded middle-late Arengian conodonts (G.S. Nowlan, referenced in Whelan and Currie, 1985). One such plutonic body within the Topsails Igneous Complex yielded an early Middle Ordovician age (zircon), similar to the date obtained from a granitoid clast in this study (Chapter Six).

The Hungry Mountain Complex is considered to have been thrust southeastward over the Buchans Group (Thurlow, 1981a,b). Dykes, which are believed to be related to the Topsails alkali feldspar granite, cut both the Hungry Mountain Complex and the Buchans Group (Thurlow, 1981a,b); this evidence suggests that thrusting occurred before or during the Early Silurian. Thus, the Buchans Group/Topsails Complex contact, although not exposed, is considered to be intrusive. Topsails-type granite and related dykes are seen to intrude and to be chilled against the Wiley's River Intrusion of the Feeder Granodiorite (Stewart, 1983; Chapter Three).

2.4 METAMORPHISM AND DEFORMATION OF THE BUCHANS GROUP

Henley and Thornley (1981) estimated Buchans volcanic rocks to have mineral assemblages characteristic of sub-greenschist (prehnite-pumpellyite) metamorphism produced in whole or in part by hydrothermal alteration penecontemporaneous with volcanism. Thurlow (1981a,b) reported occurrences of greenschist and higher grade metamorphic facies near the contact with the Hungry Mountain Complex; he interpreted these to have resulted from thrusting of the Hungry Mountain Complex southeastward over the Buchans Group.

The Buchans Group has been subjected to small and large scale thrusting toward the southeast (Thurlow and Swanson, 1985). Current interpretation of these fault structures is that they form a thrust duplex (terminology after Dahlstrom, 1970), i.e., a suite of steeply dipping imbricate thrust blocks and slices bounded by more shallow dipping roof and floor thrusts. Movement was often localized on bedding planes and thus hinders stratigraphic interpretation of the Buchans Group (Thurlow and Swanson, 1985). Despite this proposed thrusting, textures in the Buchans Group volcanic rocks are remarkably well preserved and there is no evidence of penetrative deformation or rotation of clasts or mineral grains in any reports or observations made at Buchans.

2.5 ORE DEPOSITS AT BUCHANS

The mines at Buchans produced over 17.8 million tons of ore from 1928 to May 1984 (Thurlow, 1984). After a brief interruption in 1982 production resumed in 1983, but the mine closed permanently in September, 1984. Ore grades averaged 14.5% Zn, 7.60% Pb, 1.33% Cu, 3.68 oz/ton Ag (128 g/ton) and 0.043 oz/ton Au (1.5 g/ton) (Thurlow, 1984). Barite is a common constituent of the ore and has recently been recovered from the waste piles at Buchans.

The deposits consist of three genetically related types of ore: stockwork, in situ and transported ore (Thurlow and Swanson, 1981). Stockwork ore consists of base metal sulphides (primarily pyrite) epigenetically disseminated and emplaced as veinlets within highly silicified and locally chloritized and/or sericitized host rocks. In situ ore consists of fine-grained sphalerite, galena, chalcopyrite, pyrite and barite in conformable, massive to weakly bedded lenses overlying stockwork ore and the associated alteration zone. According to George (1937), the Lucky Strike in situ orebody consisted of 90% sphalerite and galena mineralization and 10% chalcopyrite, pyrite and sphalerite mineralization. It occurs as conformable lenses overlying altered felsic pyroclastic rocks. Well developed compositional banding is uncommon but thin, discontinuous

wispy streaks of fine grained yellow ore occurred in very fine to fine grained aggregates of black ore. This "streaky ore" may have been produced by lateral flow in an unconsolidated, watery, plastic sulphide mud (Thurlow and Swanson, 1981).

The in situ orebodies were formed on or near the seawater/sediment interface by the precipitation of sulphides from hydrothermal fluids (Thurlow et al., 1975; Thurlow, 1981a,b; Henley and Thornley, 1981). This hydrothermal fluid system altered and mineralized the volcanic rocks underlying the discharge site to form the stockwork orebodies. The transported orebodies were formed as a result of the disruption and fragmentation of a pond of sulphide mud by explosive volcanic, phreato-magmatic or earthquake activity, and subsequent transportation of this and other entrained material as subaqueous sediment debris flows (Thurlow, 1977; Thurlow and Swanson, 1981; Calhoun and Hutchinson, 1981; Walker and Barbour, 1981; Binney et al., 1983).

These debris flows were apparently contained and directed by linear, north-west trending paleo-depressions (Thurlow, 1981a,b; Walker and Barbour, 1981; Thurlow and Swanson, 1985). The largest of these channels in the Buchans area contains the Rothermere, MacLean and MacLean Extension orebodies (Figure 2.1). The transported orebodies

are capped by a series of barite-rich debris flows, e.g., MacLean Extension (Binney et al., 1983). This is considered to reflect an original zonation of the sulphide mud ponds. A similar zonation can be seen in the Lucky Strike *in situ* orebody (Thurlow, 1981a). The geology of the MacLean Extension transported orebody is discussed in more detail in Section 4.2.

Whether the source of the sulphide-rich debris flows was the Lucky Strike *in situ* orebody or not is uncertain, however, they both occur within the same stratigraphic horizon in the Buchans River Formation (Thurlow and Swanson, 1985). Comparisons of metal ratios between transported ores and *in situ* ores, and the similar zonations seen in the *in situ* and transported orebodies suggest that the Lucky Strike is the most logical source presently known for the transported orebodies of the Rothermere/MacLean channel (Hutchinson, 1981).

The Buchans deposits have been described (Thurlow, 1977, 1981a; Thurlow and Swanson, 1981) as being similar to the volcanogenic massive sulphide deposits of the Kuroko district of Japan (Ishihara, 1974; Ohmoto and Skinner, 1983). Features of Kuroko ore deposits recognized at Buchans (Thurlow, 1981a; Thurlow and Swanson, 1981) include: the stratabound nature of the orebodies; sedimentary structures and textures in the sulphide masses including

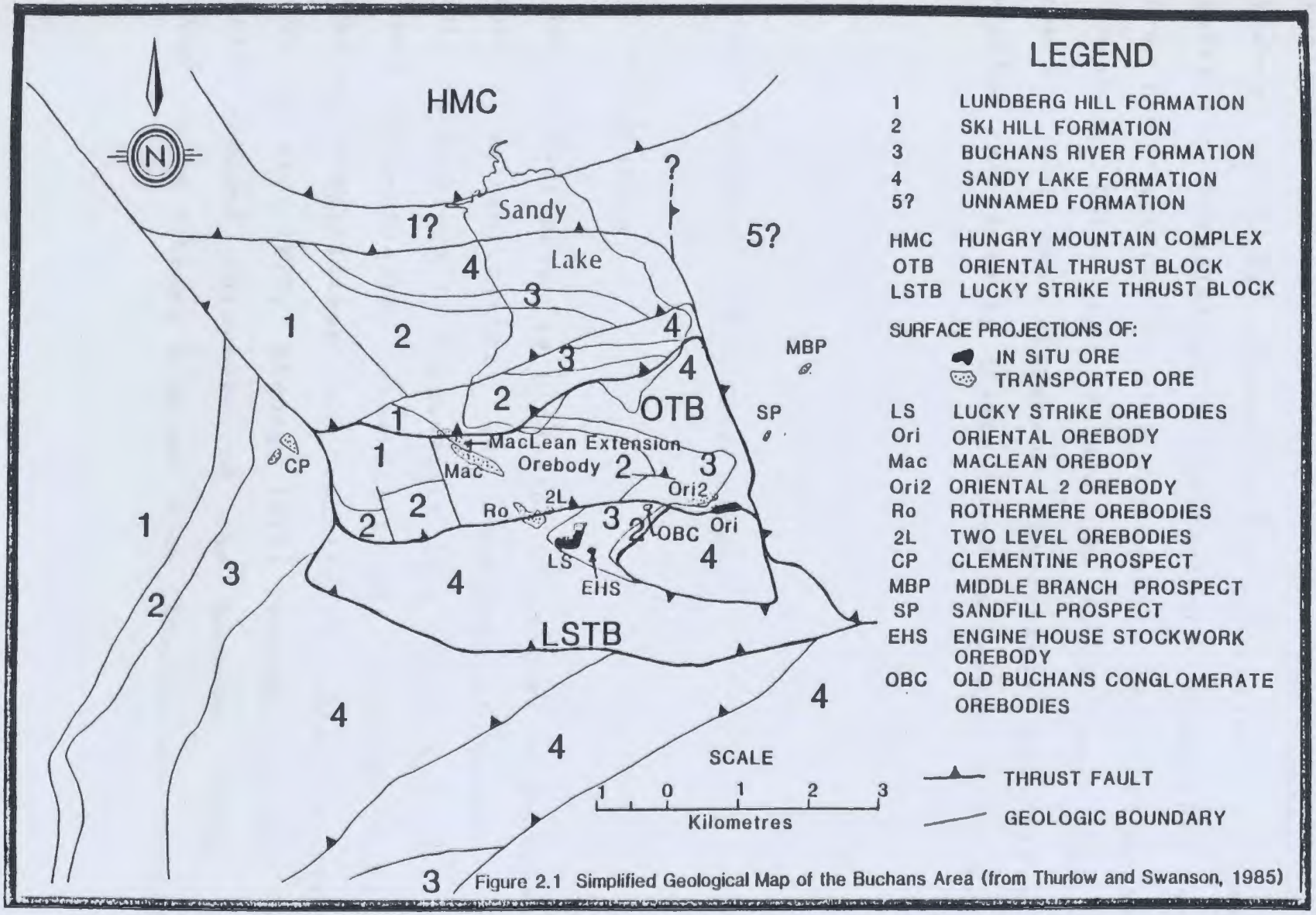

Figure 2.1 Simplified Geological Map of the Buchans Area (from Thurlow and Swanson, 1985)

mechanically transported orebodies; the presence of siliceous stockwork alteration and mineralization (similar to Keiko ore) underlying the strata-bound orebodies; metal zoning from pyritic Cu-rich sections in the lower parts of the orebody (Oko) to Pb and Zn -rich upper sections (Kuroko); and the different expressions and types of alteration exhibited by clasts found in transported ore.

2.6 STRATIGRAPHY OF THE BUCHANS GROUP

2.6.1 Introduction

The Buchans Group is a complex assemblage of subaqueous volcanic, volcaniclastic and sedimentary rocks. The volcanic rocks range in composition from basalt to rhyolite and show calc-alkaline chemical trends, although rocks of intermediate compositions are relatively underrepresented (Thurlow et al., 1975; Strong, 1977; Thurlow, 1981a). The presently exposed thickness of the Buchans Group is estimated to be between 3 km and 6 km (Thurlow and Swanson, 1985).

The stratigraphy of the Buchans Group has never been completely elucidated. There are several factors that hinder stratigraphic correlations. Exposure of the volcanic and sedimentary rocks is poor. Abrupt lateral facies and thickness changes, especially in the felsic volcanic assemblages, are common. These abrupt changes are a common aspect of felsic volcanic rocks (Williams and McBirney, 1979) and are probably due to the rugged topography during volcanism. No basin-wide lithologically distinctive marker beds occur in the succession. The absence of fossiliferous strata further hampers stratigraphic correlation within the Buchans Group. The topography may have been periodically modified by faulting concurrent with deposition (Thurlow and Swanson, 1985).

Probably the greatest handicap in unravelling the true story of Buchans geology, however are the several episodes of faulting including a period of significant thrust movement (Thurlow and Swanson, 1985). Thrust movement often occurred on bedding planes and is recorded as zones of brittle shear from a few centimeters to several meters in thickness, depending on the amount of movement. The resulting fault gouge is normally lithified by secondary quartz and epidote, although occurrences of unlithified clayey gouge suggests very late movement. Diabase dykes have often intruded these fault zones before and after

re-activation of movement in these zones.

The current interpretation of structures evident at Buchans as a thrust duplex (Dahlstrom, 1970) has allowed for simplification of the stratigraphy, albeit with a corresponding increase in the complexity of the structural history (Thurlow and Swanson, 1985). In the vicinity of the orebodies, the Buchans Group is now recognized as a series of roughly east-west trending imbricate thrust blocks. Two such blocks, the Oriental and Lucky Strike thrust blocks contain all known economically important orebodies (Fig. 2.1). The presented stratigraphic relationships are primarily based on observable conformable contacts within the Oriental block where original relations are best preserved (op cit.). Recognition of the geometry of the thrust duplex has permitted the correlation of lithologically similar sequences between thrust blocks. These lithological similarities had been recognized for some time at Buchans but, in the absence of observed conformable contacts between certain stratigraphic units, stratigraphic correlations were not made (Thurlow and Swanson, 1981). For the first time in the history of the Buchans Group formal stratigraphic names have been proposed (Thurlow and Swanson, 1985). Because the stratigraphy is best understood in the vicinity of the orebodies, the possibility of changes or additions to the stratigraphy of the Buchans Group increases

with increasing distance from the orebodies.

It is outside the scope of this thesis to resolve the complexities of Buchans Group stratigraphy or its structures.

2.6.2 Lundberg Hill Formation

This is the lowest recognized mappable unit in the Buchans Group and was formerly called the Prominent Quartz Sequence (Thurlow and Swanson, 1981). It is a sequence of dominantly rhyolitic pyroclastic rocks. In other thrust blocks, similar felsic pyroclastic rocks are interbedded with subaqueous debris flows, tuffaceous wackes, siltstone and cherty mudstone. The base of this sequence is either not exposed or it bottoms on a major thrust fault. It has an estimated thickness of approximately 1000 m. The volcanic rocks are characterized by rounded to subhedral quartz phenocrysts which commonly exceed 10 mm in diameter and smaller plagioclase phenocrysts (Plate 4.18) (Thurlow and Swanson, 1985).

2.6.3 Ski Hill Formation

This sequence of basaltic to andesitic pillow lavas, breccias and pyroclastic rocks was formerly called the Ski Hill Sequence (Thurlow and Swanson, 1981). The lavas are usually amygdaloidal and contain augite and plagioclase phenocrysts. It conformably overlies the Lundberg Hill Formation and has a maximum thickness of approximately 1000 m (Thurlow and Swanson, 1985).

2.6.4 Buchans River Formation

All major volcanogenic massive sulphide orebodies are hosted by this formation. It is a complex assemblage of felsic pyroclastic rocks, breccias, flows and clastic sediments which conformably overlies the Ski Hill sequence. It has an estimated maximum thickness of 200 m in the Oriental thrust block.

This formation is characterized by the products of dominantly explosive felsic volcanism. The most common lithologies are felsic crystal-lithic pyroclastic rocks and breccias. Typical felsic tuff consists of 20-40% 1-2 mm quartz and plagioclase crystals in a fine grained to glassy, variably altered matrix (Thurlow, 1981a).

Beneath the Oriental and Lucky Strike *in situ* orebodies, hydrothermal alteration obscures the contact between the mafic volcanic rocks of the Ski Hill Formation and the felsic pyroclastic rocks of the Buchans River Formation. Where the original composition is recognizable, altered, felsic, quartz-poor lithologies are assigned to the Buchans River Formation (Thurlow and Swanson, 1985). Underlying altered rocks of recognizable mafic composition are assigned to the Ski Hill Formation. These altered lithologies were previously assigned to the Intermediate Footwall (Thurlow and Swanson, 1981,1985).

In addition to the felsic pyroclastic rocks, quartz and feldspar-phyric rhyolitic bodies, lenses of distinctive pyritic siltstones, wackes, siltstone breccias, the *in situ* and transported orebodies, and other debris flow deposits occur locally within this Formation.

Although not as heterolithic as overlying debris flow deposited breccias and breccia-conglomerates, the siltstone breccias in the MacLean Extension contain several large (>30cm) boulders of granitoids that are texturally and chemically distinctive from the granitoid clasts contained in the overlying sulphidic breccia-conglomerates (see Chapters 4 and 5). The siltstone breccia and its contained granitoid clasts are thought to be related to syn-depositional faulting, but this cannot be proven with

any certainty at present.

The narrow, linear distribution of the debris flow deposits, the siltstone and siltstone breccia suggests a paleo-topographic control on their deposition (Thurlow and Swanson, 1985). The troughs or depressions may have been fault-bounded. Alteration underlying the in situ orebodies appears to have been controlled by structures that existed at the time of ore deposition. These fault planes, altered and weakened by this earlier movement were preferentially re-activated during the later period of major thrusting (Thurlow and Swanson, 1985). The formation of the sulphide orebodies and structural complexities in the vicinity of these orebodies therefore appears to be genetic and not coincidental (Thurlow and Swanson, 1985).

Ore deposition, including the transported orebodies, was succeeded by felsic pyroclastic activity. The initiation and deposition of the transported orebodies appears to have resulted in the cessation of significant sulphide mineralizing activity (Chapter Four). Deposition of arkosic conglomerate of the overlying Sandy Lake Formation appears to have leveled the paleo-topography after the final period of explosive felsic volcanism (Thurlow and Swanson, 1985).

2.6.5 Sandy Lake Formation

In the Oriental block, the Buchans River Formation is conformably overlain by basaltic pillow lavas and pillow breccias, with arkose and arkosic conglomerate interbeds. Pillows are well preserved, variable in size and weakly to strongly amygdaloidal.

The arkose and arkosic conglomerate is usually massive and coarse grained with sparsely dispersed outsized pebbles, cobbles and boulders of primarily quartz-phyric rhyolitic material. The presence of relict glass shards, a lack of obvious paleo-weathering of the plagioclase feldspar grains and the paucity of granitic clasts or detritus suggests that a felsic volcanic center in the area was the source of the arkose and arkosic conglomerate rather than an older exposed intrusive terrane (Thurlow and Swanson, 1981). The basalt and arkose intertongue extensively, but with very little mixing. Basaltic cobbles in arkose, or arkose in intrapillow depressions are very rare. This indicates that two compositionally distinct volcanic centres were active simultaneously (Thurlow and Swanson, 1985).

This formation contains units previously assigned to the Footwall Basalt, Footwall Arkose, Lake Seven Basalt, and Upper Arkose (Thurlow and Swanson, 1981). The original relationship of this formation to the informal Skidder Basalt unit, which was recently subdivided from the Footwall Basalt (Pickett and Barbour, 1984) is not known.

2.6.6 Unnamed Formation

To the east and north-east of Sandy Lake and the Buchans River, intermediate to felsic flows, breccias and pyroclastic rocks overly arkose of the Sandy Lake Formation. Mafic tuff, pillow lavas, and volcaniclastic sedimentary rocks may be important locally. The relative stratigraphic position of these rocks is not known. Although widely distributed northeast of the Oriental block, this formation is little studied and not well understood. These rocks were formerly assigned to the Upper Buchans Subgroup by Thurlow and Swanson (1981).

Volcanic rocks of this unnamed formation are seen intruded by the Little Sandy Lake Intrusion of the Feeder Granodiorite in the Little Sandy Lake area (Chapter Three). These rocks are hereafter informally referred to as the Little Sandy Lake sequence.

Chapter Three

FEEDER GRANODIORITE

3.1 INTRODUCTION

The primary intent of the field work was to map the two Feeder Granodiorite bodies to determine the nature of their contacts with the Buchans Group volcanic rocks. The Little Sandy Lake Intrusion and the Wiley's River Intrusion are described separately and then classified and compared.

3.2 LITTLE SANDY LAKE FIELD AREA

3.2.1 Field relations

The Little Sandy Lake Intrusion of the Feeder Granodiorite outcrops as two small oval bodies which underlie an area of 0.15 km2 within the Little Sandy Lake sequence of the Buchans Group (Section 2.6.6) in the Little Sandy Lake area (Fig. 3.1). These two bodies are characterized by prominent (up to 15mm across) quartz phenocrysts and medium grained feldspar phenocrysts in a fine grained groundmass (Plate 3.1). Colour variations (green, white and brown on weathered surfaces) are due to

varying quantities of epidote and chlorite in the rock.

Exposed contacts of the Little Sandy Lake Intrusion with the associated volcanic rocks are rare and small. No effects of contact metamorphism on the intruded volcanics have been observed. The quartz and feldspar phyric center of the intrusion grades to a fine grained aplitic textured rock toward the western margin. Towards the eastern margin, the rock becomes equigranular, finer grained and highly granophyric. These features suggest chilling and support the proposed intrusive nature of these bodies into the Buchans Group.

In the Little Sandy Lake area, the Little Sandy Lake sequence (Section 2.6.6) consists of a series of interfingered and interbedded mafic, intermediate and felsic volcanic rocks with the latter predominent (Thurlow and Swanson, 1981). Most of the study area is underlain by dacitic to rhyolitic breccias and lapillistones. Several lensoidal bodies of both aphyric and quartz and feldspar phyric rhyolitic flows, similar to many clasts seen in the breccias, occur in the area (Fig. 3.1).

3.2.2 Petrography

The Little Sandy Lake Intrusion is a seriate porphyritic (allotriomorphic inequigranular) intrusive rock. In the central areas of the intrusion where the groundmass grain size is medium grained, the feldspar crystals occur as subhedral plagioclase laths with anhedral, irregularly formed quartz crystals. In the extremities of the intrusion, a fine grained groundmass is more common and quartz and plagioclase phenocrysts occur in a mosaic of anhedral, ragged quartz and plagioclase feldspar with irregular intergrowths and interdigitations. Whether fine or medium grained, the groundmass usually comprises over 80% of the rock (Plate 3.1a).

The rounded quartz phenocrysts are composite, show embayments, and have cavities and fractures that contain very fine grained material similar to the groundmass (Plate 3.1). Quartz phenocrysts commonly show undulous extinction, unlike the feldspar phenocrysts and groundmass quartz crystals. Feldspar phenocrysts are typically glomerocrystic and composed of anhedral to subhedral components which though rounded, are rarely corroded. Feldspar phenocrysts are partially replaced by sericite, epidote and calcite (Plate 3.1b). All feldspars appear to be sodic plagioclase based on staining techniques (Friedman, 1971), the absence of petrographic features indicative of potassium feldspar and the major element chemistry (Chapter Five).

Plate 3.1a (Top) Representative photomicrograph of Little Sandy Lake intrusion (KQS-83-141) showing the porphyritic texture, fine grain size of groundmass and composite nature of quartz and feldspar phenocrysts; polarized light; bar length = 10 mm.

Plate 3.1b (Bottom) Representative photomicrograph of Litle Sandy Lake intrusion (KQS-82-066) showing large difference in grain size between phenocrysts and groundmass, anhedral nature of groundmass crystals and alteration of plagioclase grains; polarized light; low power (x2.5)

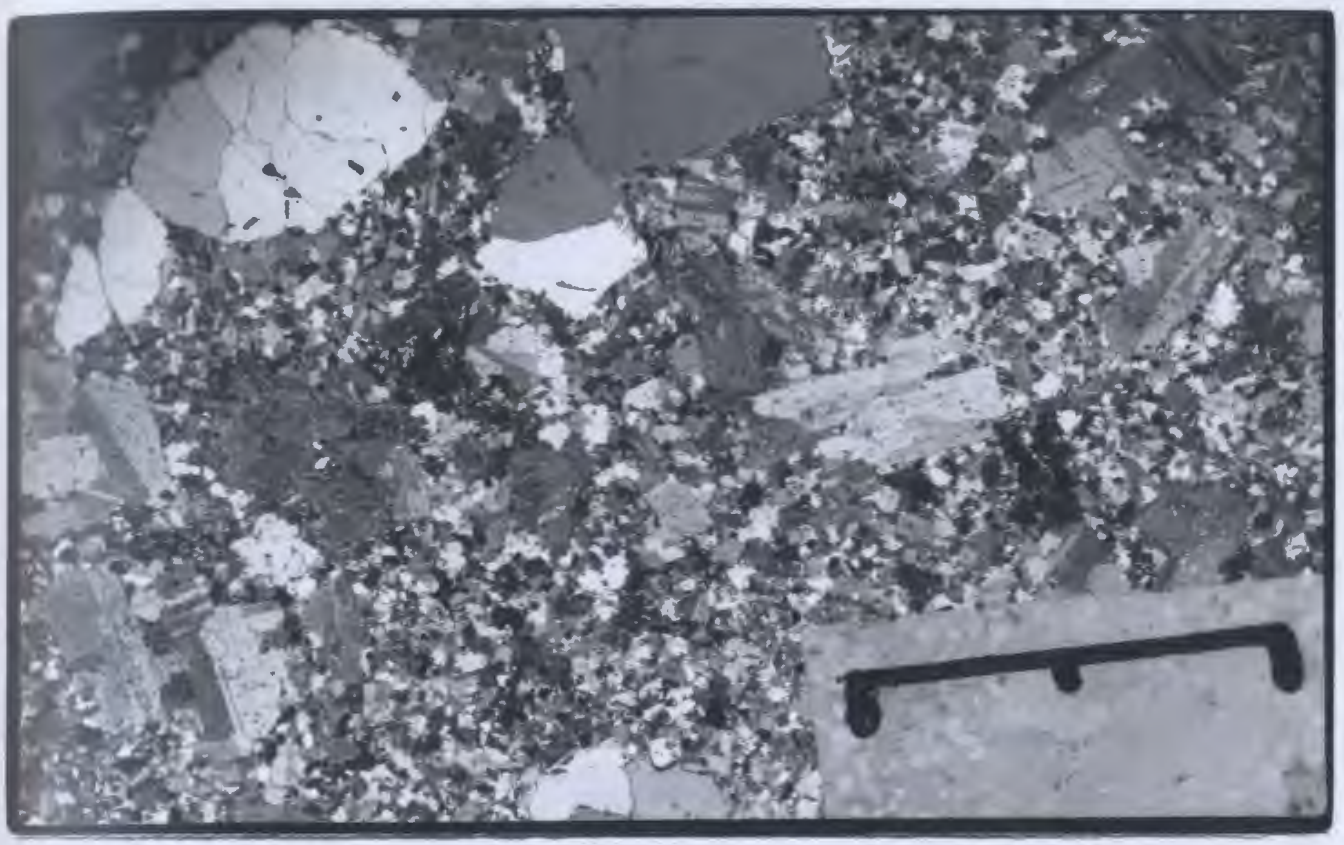

Biotite, magnetite and possibly ilmenite occur in trace amounts. Biotite is partially to completely altered to chlorite. Epidote occurs in local concentrations.

3.3 WILEY'S RIVER FIELD AREA

3.3.1 Field relations

The Wiley's River Intrusion of the Feeder Granodiorite outcrops in the Wiley's River area and underlies a roughly triangular area of 1.1 km2 (Fig. 3.2). The Wiley's River Intrusion contains large (up to 15mm), rounded composite quartz phenocrysts (20-30%) and smaller (up to 8mm), white, subhedral tabular laths of plagioclase feldspar crystals (30-40%). These occur in a fine grained to very fine grained groundmass of quartz, pink-brown potassium feldspar, biotite (and chlorite after biotite) and magnetite. The Wiley's River Intrusion is a white-brown massive rock that is increasingly reddened toward the contact with the Topsails granite in Wiley's River. No colour change is observed in the Wiley's River Intrusion at the contact with the Topsails granite on the hill to the southwest (Figure 3.2).

The volcanic rocks in this area are poorly exposed. The contact with the Buchans Group is covered by a large bog (Fig. 3.2). A low magnetic anomaly (Geological Survey of Canada, 1968) coincides with the limited outcrop distribution of the Wiley's River Intrusion. The Topsails alkali feldspar granite (Taylor et al., 1980; Whelan and Currie, 1983, 1985) is seen in chilled contact with the Wiley's River Intrusion. Dykes macroscopically similar to the alkali feldspar granite, i.e. brick-red, fine grained and equigranular, are also seen cutting the Wiley's River Intrusion (Stewart, 1983). Mafic dykes of similar appearance and composition to fine grained mafic intrusive bodies in the area cut the Wiley's River Intrusion. These mafic bodies are considered to be related to the Topsails igneous complex (Taylor et al., 1980). No contacts between the large diabasic body and the Wiley's River Intrusion are exposed (Figure 3.2).

3.3.2 Petrography

The Wiley's River Intrusion is a medium to coarse grained. It is hypidiomorphic to allotriomorphic inequigranular with quartz and plagioclase phenocrysts (Plate 3.2). Potassium feldspar is often seen to rim the larger plagioclase crystals and is an essential component of the groundmass.

Plate 3.2a (Top) Representative photomicrograph of Wiley's River intrusion (KQS-82-196) showing inequigranular texture, relative proportion of phenocrysts to groundmass which is greater than in Little Sandy Lake intrusion; note the rounded, anhedral and composite nature of the quartz phenocrysts; polarized light; bar length = 10 mm.

Plate 3.2b (Bottom) Representative photomicrograph of Wiley's River intrusion (KQS-82-198) showing extremely fine grain size of groundmass relative to size of phenocrysts, and alteration of plagioclase to sericite; polarized light; low power (x2.5).

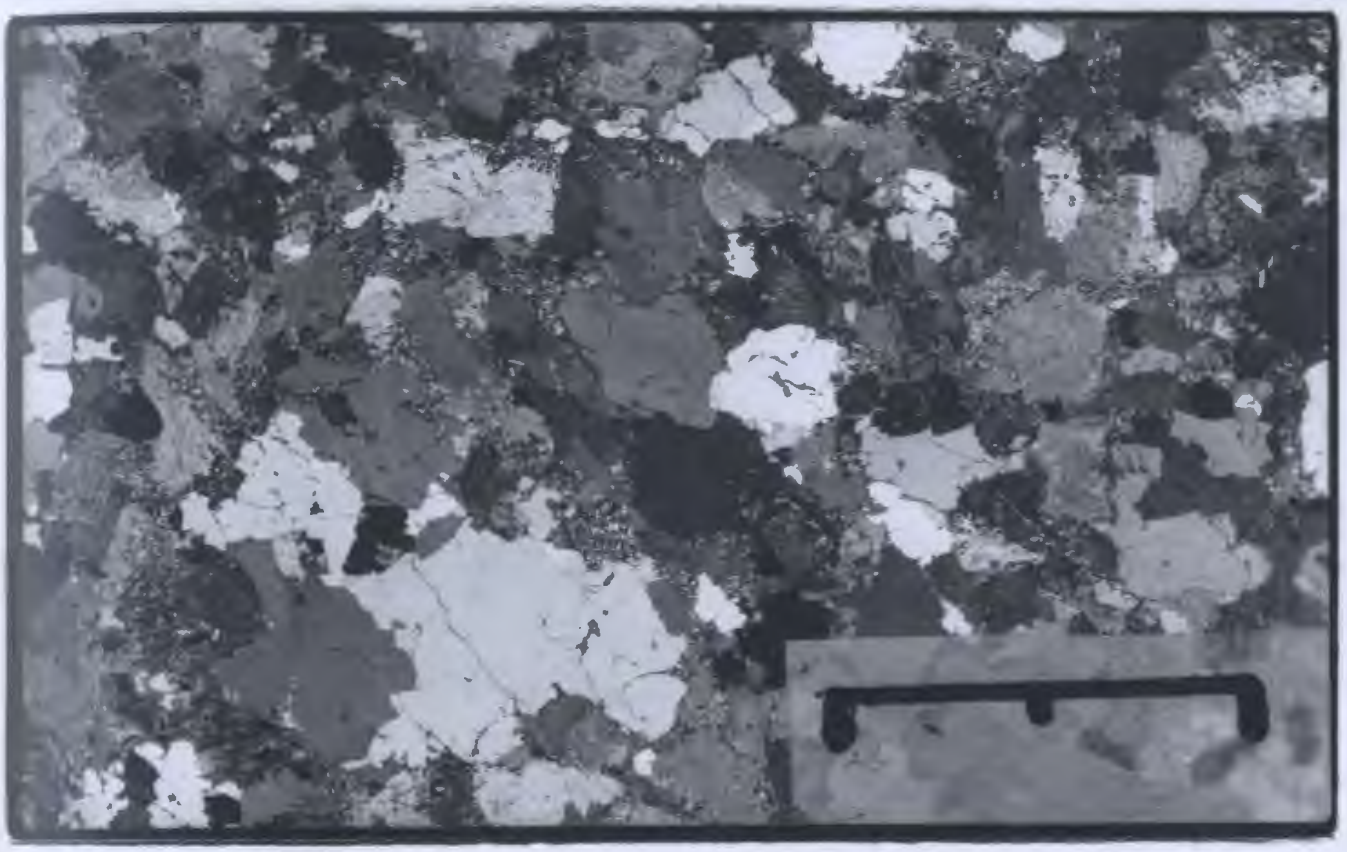

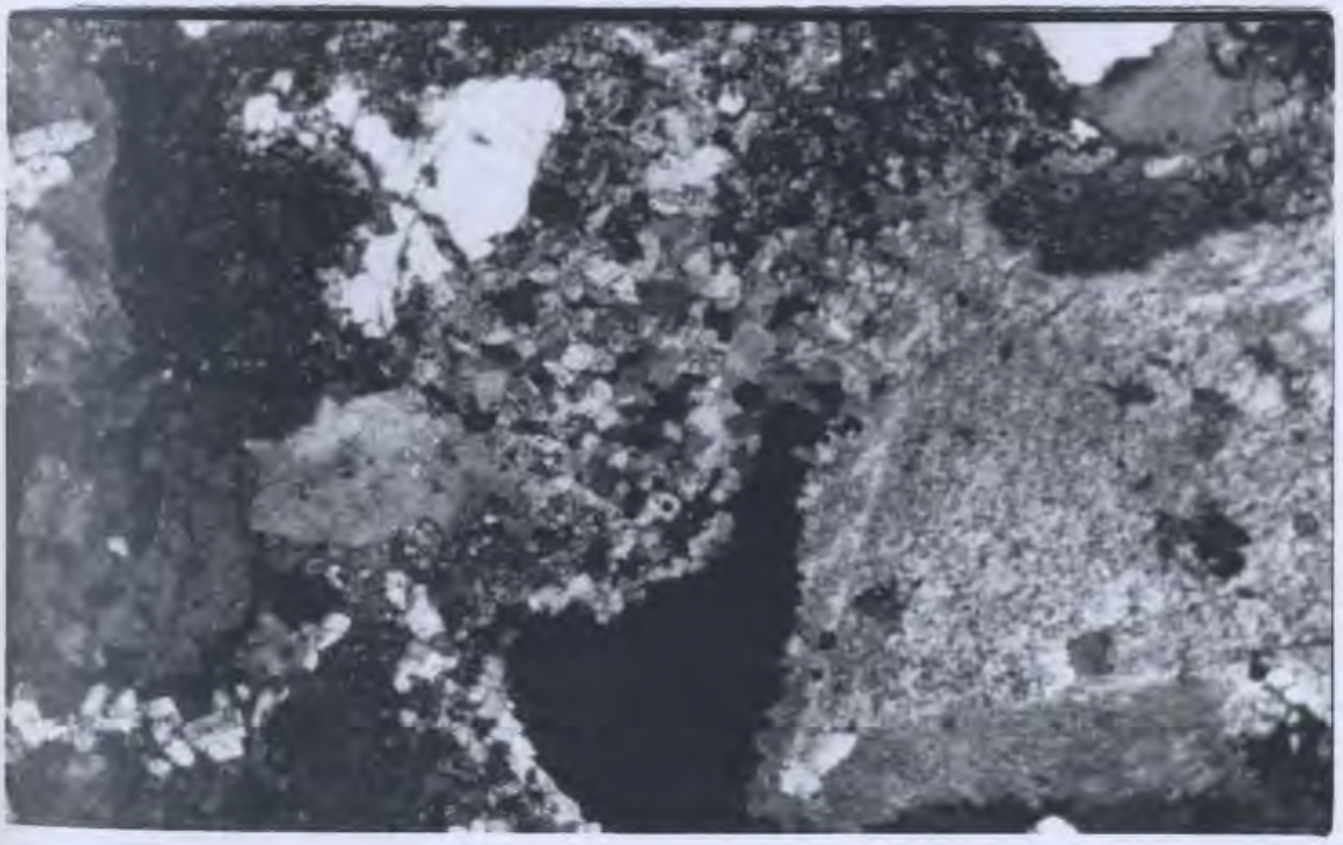

Biotite occurs interstitial to the quartz and plagioclase phenocrysts as either clusters of fine grained anhedral sheaths or as medium grained books. Biotite appears to have crystallized before, and with, fine grained potassium feldspar and quartz in the groundmass. Rare subhedral amphibole crystals are observed. Both amphibole and biotite are partially to completely chloritized. Granophyric rims on plagioclase phenocrysts are seen rarely. The groundmass comprises from 5% to 20% (vol) of the rock (Plate 3.2).

3.4 CLASSIFICATION OF FEEDER GRANODIORITE

The classification of plutonic and volcanic rocks is commonly based on modal analyses (Streickeisen, 1967, 1976) or normative compositions (Streickeisen and LeMaitre, 1979). Recent classifications of granitic rocks that incorporate geological constraints on the source regions (continental vs. oceanic) and the tectonic setting (orogenic vs. anorogenic) has been used for classification purposes in this study (Lemeyre and Bowden, 1982; Bowden et al., 1984).

Modal analyses have not been determined for these two bodies. The absence of potassium feldspar from the Little Sandy Lake Intrusion and its subordinate volumetric abundance in the Wiley's River Intrusion limits the

usefulness of methodical modal determinations. However, the approximate position of these rocks on the QAP modal classication triangle may still be estimated. Quartz clearly occupies between 20% and 60% of each body (Plates 3.1, 3.2) and each will therefore fall within the "granitoid parallelogram" of Bowden et al. (1984). The absence of potassium feldspar in the Little Sandy Lake Intrusion requires this body to plot within the T-granitoid (T = tholeiitic, tonalitic or trondhjemitic) field, near the Q-P join. Although present as a late crystallizing phase in the Wiley's River intrusion, potassium feldspar is clearly subordinate to plagioclase feldspar because of its fine grain size and its restriction to the groundmass and as rims on earlier formed plagioclase grains. The Wiley's River intrusion will therefore plot within the T-granitoid field, or possibly within the granodiorite field. Since greater than one third of the feldspar present is not potassium feldspar, this body cannot plot within the granite field.

Their occurrence with the dominantly calc-alkaline volcanic rocks of the Buchans Group (Strong, 1977; Thurlow, 1981a) instead of ophiolitic or tholeiitic igneous rocks negates their classification as tholeiitic granitoids (Lemeyre and Bowden, 1982; Bowden et al., 1984). The absence of pyroxene or evidence that amphibole was the dominant crystallizing mafic phase demonstrates that they

are unlike the oceanic plagiogranites of Coleman and Donato (1979).

There has been some mobility of the alkalis in the Little Sandy Lake Intrusion but not in the Wiley's River Intrusion (Chapter Five). The low K2O content and low K2O/Na2O ratios of the Wiley's River Intrusion are therefore probably primary characteristics of these rocks. In combination with the generally low abundance of mafic minerals (10%) and low iron and calcium contents (Chapter Five), the Wiley's River Intrusion is a trondhjemite rather than a tonalite (Barker, 1979). In view of the finer grain size of the Little Sandy Lake Intrusion, it is termed a micro-trondhjemite (terminology after Hatch et al., 1972). The two bodies are similar to the calc-alkaline trondhjemite series granitoids of Bowden et al. (1984).

3.5 COMPARISON OF FIELD AND PETROGRAPHIC OBSERVATIONS

The Little Sandy Lake Intrusion is clearly seen to intrude the Buchans Group. The Wiley's River Intrusion is seen to have been intruded by the Topsails granite and related mafic intrusive rocks. Contacts between the Wiley's River Intrusion and the Buchans Group volcanic rocks are not seen.

Each plutonic body is characterized by prominent (up to 10-15mm), rounded quartz phenocrysts and smaller (to 8mm) subhedral plagioclase phenocrysts in a fine to very fine grained groundmass. Plagioclase phenocrysts are partially sericitized unlike the groundmass feldspar grains. The groundmass of the Little Sandy Lake Intrusion constitutes a greater average volume than the groundmass of the Wiley's River Intrusion.

Biotite appears to have been the primary mafic component in each body and to have crystallized later than the quartz and plagioclase phenocrysts. Alteration of biotite to chlorite is common in each, but is more pervasive in the Little Sandy Lake intrusion, as is the development of epidote. Hornblende has not been recognized in the Little Sandy Lake Intrusion, but evidence of it may have been destroyed during chloritization. Amphibole (hornblende) is present in the Wiley's River Intrusion as a very minor phase only.

Differences between the two bodies are the presence of amphibole, the greater average grain size and the greater proportion of phenocryst phases in the Wiley's River Intrusion. Potassium feldspar is seen in the groundmass of the Wiley's River intrusion, but is not present in the Little Sandy Lake Intrusion. In the Little Sandy Lake Intrusion, the phenocrysts are subordinate (volumetrically)

to the groundmass, while in the Wiley's River Intrusion, groundmass material is subordinate to phenocrysts.

The porphyritic textures, small grain size of the groundmass and the presence of granophyric intergrowths and aplitic textures suggest that each body was intruded at a high level. The anhedral, 'ragged' appearance and interdigitating nature of the quartz and feldspar crystals, the presence of inclusions of feldspar in quartz and vice versa, and the occurrence of biotite as a late crystallizing phase of interstitial clusters of small books suggest the relatively rapid crystallization of a magma. Resorption features on the phenocrysts, their composite nature and the presence of groundmass material between crystals in the quartz glomerocrysts suggest movement of the earlier crystallized phases within each magma chamber. Strain features, such as the preferential development of undulous extinction in the phenocryst phases, and rarely, bent plagioclase twin planes, may indicate movement of a phenocryst-rich magma prior to its final consolidation.

Chapter Four

OBSERVATIONS IN THE MacLEAN MINE

4.1 INTRODUCTION

All intersections of levels, drives, drifts and sublevels with granitoid-bearing strata on 20 Level, MacLean Mine were studied. These locations are shown in Figure 4.2. The geological setting of the MacLean Extension orebody will be described first, then observations pertaining to the morphology, petrography and occurrence of the granitoid clasts in MacLean Extension will be presented.

Much of the following description of the MacLean Extension orebody is based on Binney et al. (1983) and Thurlow and Swanson (1985). For descriptions of other transported orebodies in the Buchans area, see Thurlow and Swanson (1981), Walker and Barbour (1981) and Calhoun and Hutchinson (1981).

4.2 GEOLOGICAL SETTING OF THE MacLEAN EXTENSION OREBODY

The MacLean Extension orebody is hosted by the the Buchans River Formation. The Buchans River Formation in the MacLean Extension area consists of lenses of mineralized and non-mineralized breccias and breccia-conglomerates, barren arenaceous conglomerates and rhyolitic flows within a sequence of felsic pyroclastic rocks (Figs. 4.1,4.4). The MacLean Extension orebody occurs at the same stratigraphic interval in the Buchans River Formation as the Rothermere and MacLean transported orebodies and the Lucky Strike *in situ* orebody. It occurs down paleo-slope from the Rothermere and MacLean transported bodies in a linear arrangement extending northwest from the Lucky Strike *in situ* orebodies (Fig. 2.1) (Thurlow and Swanson, 1981). In the Lucky Strike and Rothermere area, the *in situ* and transported orebodies conformably overlie altered and mineralized Ski Hill and Buchans River Formation lithologies. The MacLean and MacLean Extension orebodies typically overlie less altered Buchans River Formation lithologies (Thurlow and Swanson, 1981, 1985).

These lenses of rudaceous rocks were deposited as subaqueous sediment gravity flows, probably initiated by explosive volcanic activity or local earthquake disturbances (Thurlow, 1977; Walker and Barbour, 1981) or

FIGURE 4.1 DETAIL OF BUCHANS RIVER FORMATION IN THE MACLEAN EXTENSION AREA (from THURLOW and SWANSON, 1985).

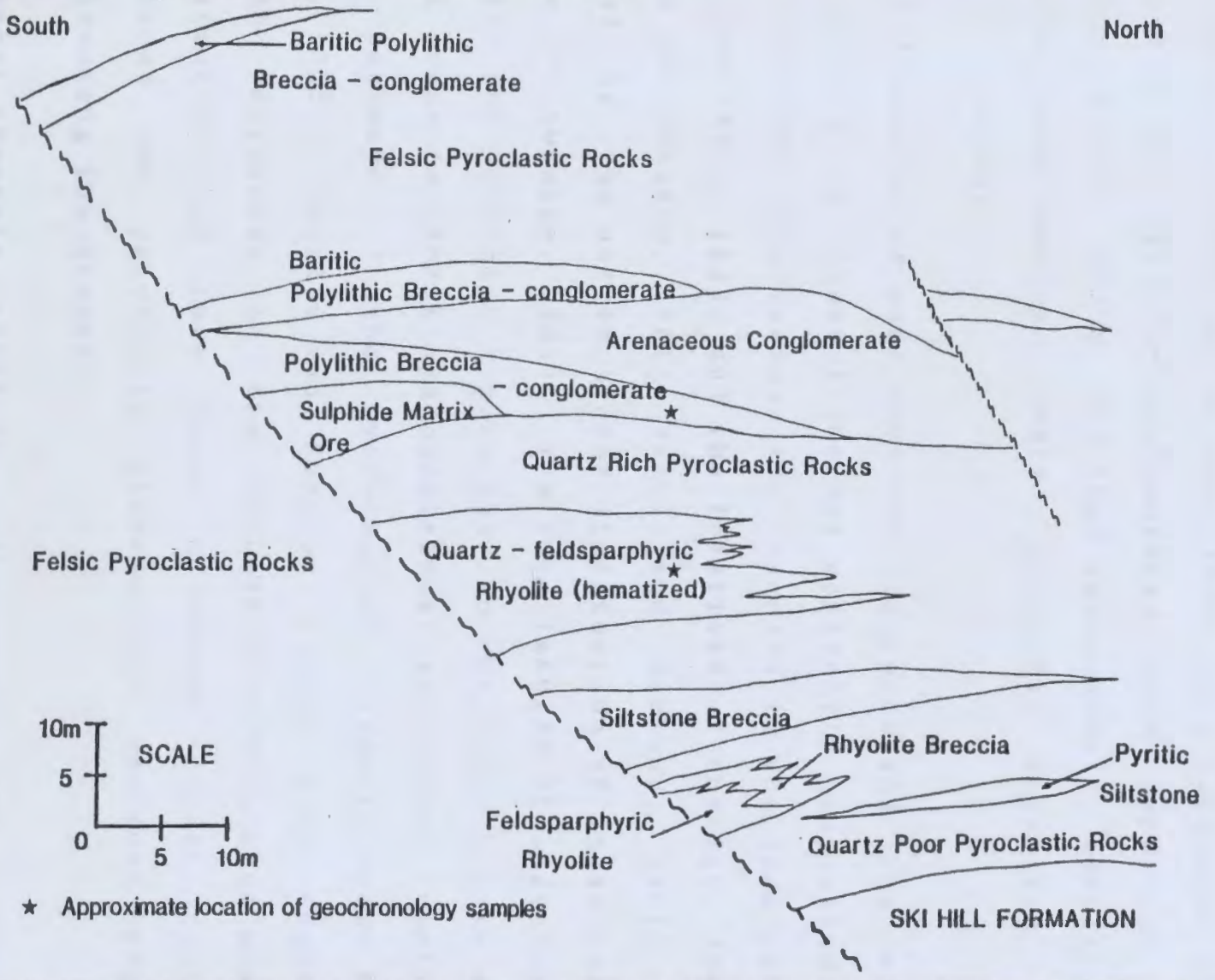

phreatomagmatic explosions (Henley and Thornley, 1981). Binney et al. (1983) and Binney (1984) also concluded that the breccias and breccia-conglomerates were deposited by subaqueous debris flows and that the spatially associated arenaceous conglomerates were probably deposited by turbidity currents.

The direction of mass sediment transport and the site of deposition of these flows was apparently controlled by paleo-topographic depressions and channels in the underlying felsic pyroclastic rocks and the locations of rhyolite domes (Thurlow and Swanson, 1981; Walker and Barbour, 1981) as indicated by the narrow linear distribution of these units (Thurlow and Swanson, 1985). The localization of sericitic, chloritic and silicic alteration in the Lucky Strike and Oriental areas implies a syndepositional structural control of the pathways of the hydrothermal fluids (Thurlow and Swanson, 1985). Thurlow and Swanson (1985) also suggest that the depression in the MacLean Extension area was a graben structure and that later thrusting preferentially re-activated the previously altered and weakened fault planes bounding the graben.

Several channels containing subeconomic and economic accumulations of sulphides have been recognized in the Buchans area (Walker and Barbour, 1981). The most important channel from an economic viewpoint is the MacLean-Rothermere

channel (Walker and Barbour, 1981), which has yielded over 7 million tons of ore (Thurlow and Swanson, 1981). The source of the sulphides in the Rothermere, MacLean and MacLean Extension transported orebodies is considered to be in the vicinity of the *in situ* Lucky Strike orebody (Thurlow and Swanson, 1981; Henley and Thornley, 1981; Hutchinson, 1981). The different transported orebodies in this channel were possibly deposited originally as one continuous series of debris flow deposits (Thurlow and Swanson, 1985; R.V. Kirkham, pers. comm., 1985). The syn- and especially post-depositional faulting, plus the intrusion of felsic and mafic dykes have considered to have disrupted and sectioned the once continuous debris flow deposit.

Debris flows in the MacLean Extension area of the Rothermere-MacLean channel were intermittent (Binney et al., 1983). The MacLean Extension orebody consists of upper and lower ore units (Fig. 4.2) (Stewart, 1983; Binney et al., 1983) that are separated by and hosted within a sequence of felsic pyroclastic rocks (Fig. 4.1). Even within each ore unit there appears to have been more than one episode of debris flow deposition as evidenced by thin tuffaceous or greywacke beds separating individual debris flow units (Binney et al., 1983).

The lower ore unit may be visualized as a continuum of lithological subunits based on varying proportions of sulphidic and lithic material and decreasing size and increasing roundness of lithic fragments (Fig. 4.3). One end member consists of breccia-conglomerates dominantly composed of sulphide clasts (both black and yellow ore) and sporadic lithic clasts in a dominantly sulphidic (sphalerite and galena) matrix and is called sulphide matrix ore (Binney et al., 1983). The other end member of this continuum is arenaceous conglomerate. This subunit consists of predominantly sub to well rounded lithic clasts and rare sulphide fragments and grains in a lithic-rich coarse sand sized matrix (Binney et al., 1983) (Plate 4.1).

Polylithic breccia-conglomerate forms the broad central portion of this continuum of debris flow units (Fig. 4.3). Rounded to angular clasts are present in the polylithic breccia-conglomerate with angular to sub-rounded clasts most prevalent (Fig. 4.3). Clasts range from several metres in diameter to pebble and sand sizes (Binney et al., 1983). The abundance and size of sulphide clasts and the sulphide component in the matrix decreases and lithic material (clasts and matrix) increases in the continuum from sulphide matrix ore to arenaceous conglomerate (Fig. 4.3). There is a corresponding decrease in average clast size and increase in the degree of rounding of all clast lithologies (Fig.

Figure 4.3 Schematic representation of changes in matrix composition, dominant composition of clasts, size of clasts, relative angularity of clasts and abundance of granitoid clasts that describe the lithologic continuum of sedimentological units comprising the transported orebodies and genetically related strata in MacLean Extension.

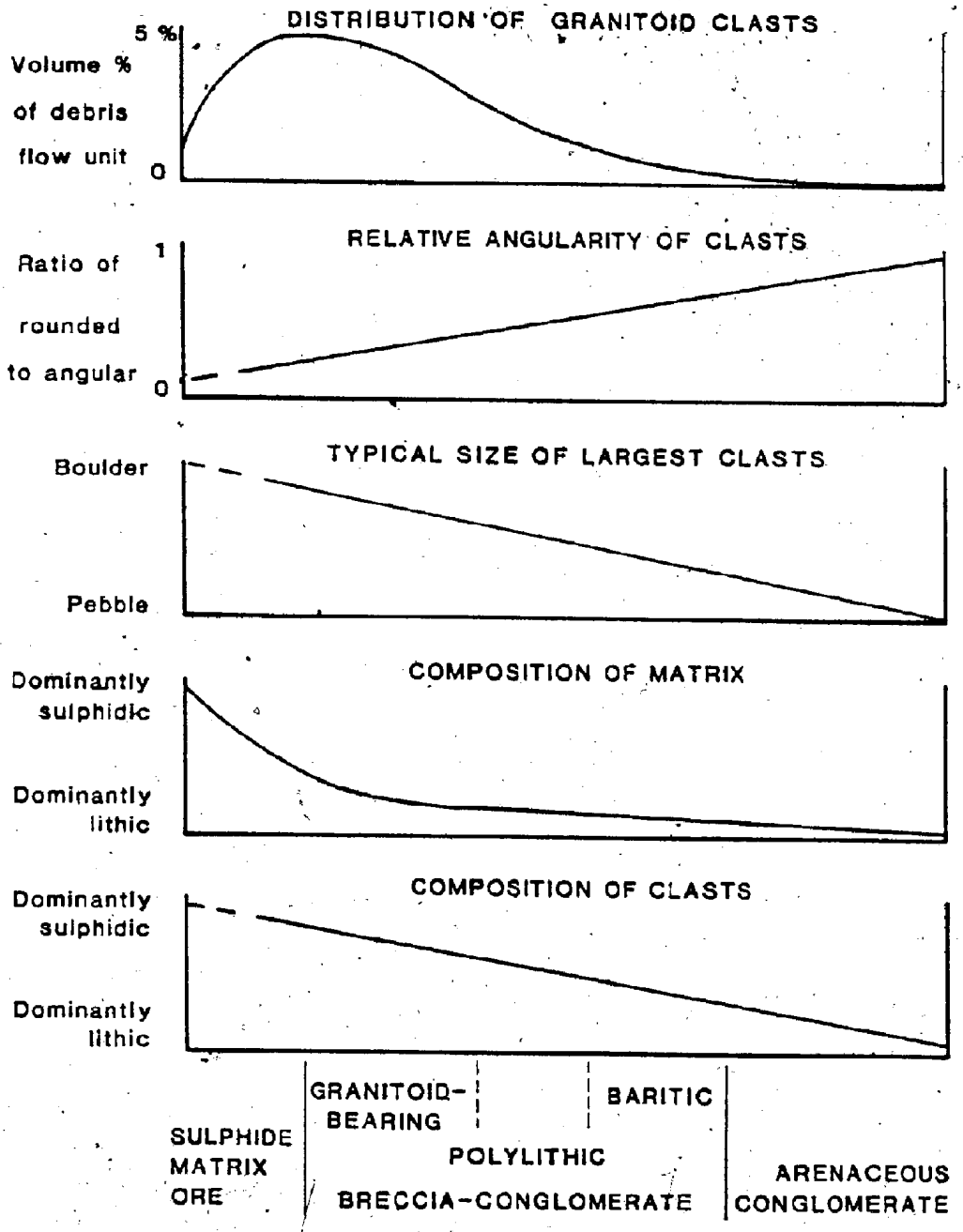

CONTINUUM OF LITHOLOGICAL UNITS COMPRISING DEBRIS FLOW SEQUENCES

Plate 4.1 Photograph of typical arenaceous conglomerate in MacLean Extension area showing the rounded nature and small size of granitoid and other lithic clasts; 20-4 Drive, MacLean mine; lens cap for scale.

4.3). With the use of modifiers, such as 'ore grade', 'granitoid-bearing' and 'baritic', discrete sections of polylithic breccia-conglomerate beds with concentrations of a particular clast lithology may be more accurately designated (Binney et al., 1983) (Fig. 4.3).

These lithological subunits are usually found in a consistent stratigraphic arrangement that is shown schematically in Fig. 4.4. Sulphide matrix ore usually occupies the base of the flow unit. This subunit generally grades upward and outward laterally into granitoid-bearing polylithic breccia-conglomerate with large black ore (Plate 4.2), or less commonly yellow ore (Plate 4.3), sulphide clasts. Some sulphide clasts show evidence of plastic deformation indicatve of their unlithified state when incorporated into the debris flow (Plate 4.4) (Thurlow and Swanson, 1981). Where present, granitoid-bearing polylithic breccia-conglomerate is found proximal to sulphide matrix ore (Fig 4.4) (Stewart, 1983). Other debris flow and/or turbidity current subunits that overlie the main sulphide-bearing sections of debris flow sequence were increasingly lithic-rich to produce low grade, baritic and subeconomic polylithic breccia-conglomerates and arenaceous conglomerate deposits. Most of the lower ore unit was subsequently capped by baritic polylithic breccia-conglomerate flows (Fig 4.4). Although the

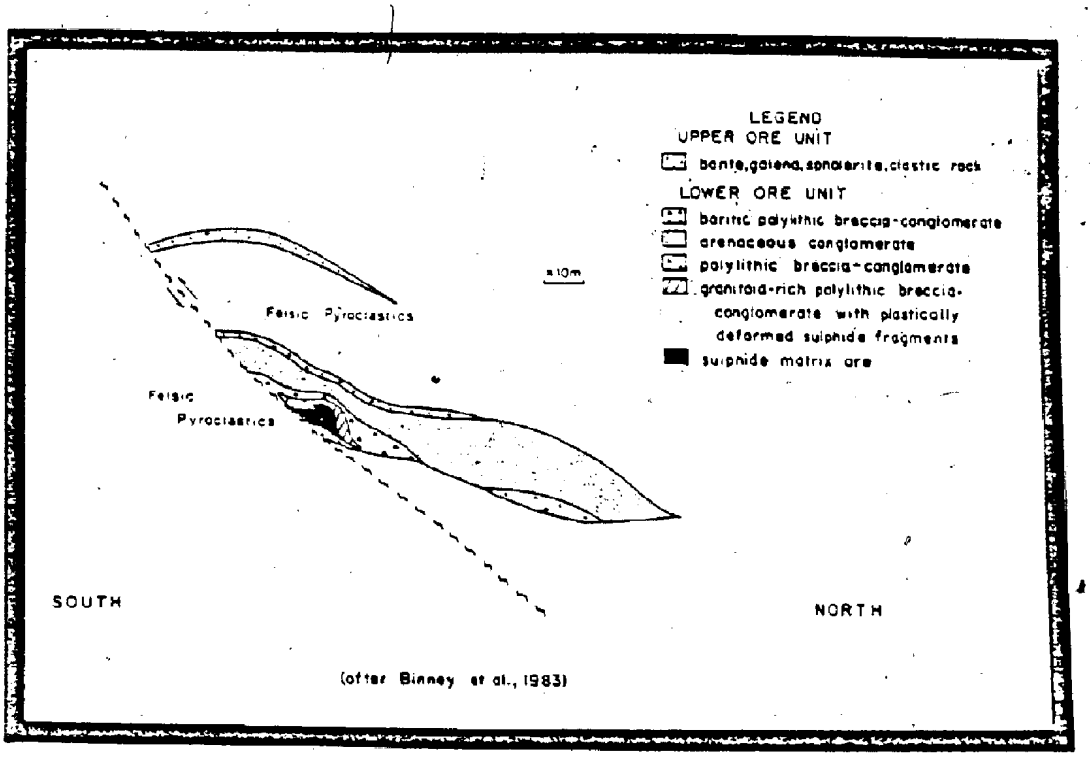

FIGURE 4.4 Schematic cross-section through the MacLean Extension transported orebody showing the idealized distribution of the debris flow lithologic subunits including the main granitoid-rich zone (modified from Binney et al., 1983). View is toward the northwest from the western edge of the MacLean transported orebody. It is an idealized composite of several short (roughly north-south) cross-sections of the MacLean Extension orebody.

Plate 4.4 Photograph of two 'granitic' group granitoid clasts with large clast of black ore showing evidence of plastic deformation, in granitoid-bearing polylithic breccia-conglomerate within 2 m of Plate 4.2; 20-5 Sublevel, MacLean mine; lens cap for scale; yellow numbers are drawn with chalk on the rock face.

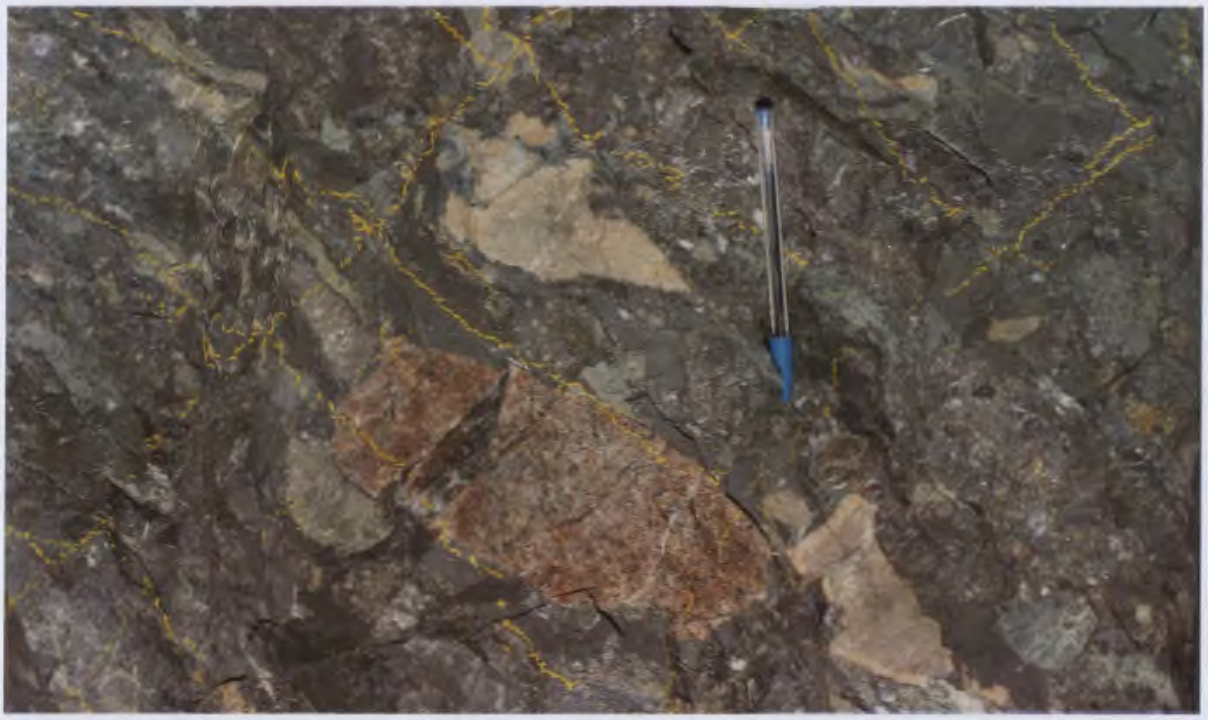

Plate 4.5 Photograph of well rounded, brick-red, 'aplitic' group granitoid clast in granitoid-bearing polylithic breccia-conglomerate, within 3 m of Plate 4.6; 20-7 Drive, MacLean mine; ball-point pen for scale; yellow lines are drawn with chalk on rock face.

Plate 4.6 Photograph showing rounded nature of 'granitic' group granitoid clasts in contrast to angular to subangular form of other clast lithologies in granitoid-bearing polylithic breccia-conglomerate within 60 m of sulphide matrix ore; 20-7 Drive, MacLean mine; granitoid clast in centre is approximately 30 cm long.

arenaceous conglomerate is volumetrically important in the northwestern MacLean Extension area (Fig. 4.4), it is absent in the vicinity of the MacLean and Rothermere orebodies (Binney, pers. comm., 1983).

The upper ore unit conformably overlies 30 to 50 m of felsic pyroclastic rocks (Binney et al., 1983) that form the hangingwall to the lower ore unit (Fig. 4.1, 4.4). The upper ore unit consists of baritic polylithic breccia-conglomerate with sub-economic sulphide accumulations (Thurlow and Swanson, pers. comm., 1982, 1983). Unlike the lower ore unit, no granitoid clasts are observed in the upper ore unit. The upper ore unit is overlain by more felsic pyroclastic rocks (Fig. 4.1, 4.4).

The main study locations as shown on the plan of the MacLean Extension orebodies (Fig. 4.2) can be related to the schematic cross-section (Fig. 4.4). At 20-13 Drift and 20-5 Sublevel study locations, sulphide matrix ore, granitoid-rich polylithic breccia-conglomerate and polylithic breccia-conglomerate are exposed. At the 20-7 Drive study location, granitoid-rich polylithic breccia-conglomerate, baritic polylithic breccia-conglomerate, and arenaceous conglomerate are exposed. This reflects the increasing distance away from the sulphide-rich core (sulphide matrix ore) into the polylithic breccia-conglomerate and arenaceous conglomerate

deposits. The debris flow subunits exposed at 20-6 Sublevel (Fig. 4.2) appear to be a different debris flow package from that seen in 20-13 drift and 20-5 Sublevel (P. Binney, pers. comm., 1983). It is represented by the lens of polylithic breccia-conglomerate shown to the north of the sulphide-rich core (Fig. 4.4). Although the sulphide matrix ore unit is absent in 20-6 Sublevel, it contains economic accumulations of sulphides in baritic and granitoid-rich polylithic breccia-conglomerate subunits.

4.3 MORPHOLOGICAL OBSERVATIONS

4.3.1 Introduction

Lithologies other than granitoids present as clasts in MacLean Extension polylithic breccia-conglomerate include; siltstone, rhyolite, altered volcanic rocks of the Ski Hill and Buchans River Formations, mafic volcanic rocks, felsic tuffs and other pyroclastic rocks, jasper, stockwork pyrite, massive crystalline barite, massive sphalerite-galena-chalcopyrite and sphalerite-galena. This clast diversity is similar to that seen in other transported orebodies at Buchans (Walker and Barbour, 1981; Galhoun and Hutchinson, 1981). The diversity of clast lithologies and the variety of igneous textures evident in clasts present in

debris flows at Buchans necessitate the definition of criteria to clearly distinguish granitoids from the other clast types. Crystallization products of volcanic, hypabyssal (sub-volcanic) and plutonic environments appear to be present and the macroscopic distinction between the subvolcanic and plutonic products is not always possible.

To ensure that all clasts of possible plutonic origin were included, the following working definition of 'granitoid clast' was employed: any clast with observable crystals (phenocrysts or groundmass) that cannot be safely ascribed to a volcanic origin.

Every granitoid clast greater than 1 cm in length in the granitoid-bearing sedimentological subunit exposed at each study location (Fig. 4.2) was described, classified (Section 4.4), the physical dimensions measured, and roundness estimates made.

4.3.2 Size, shape, and volume occupied by granitoid clasts

The length has been defined as the longest observable dimension. The width is taken to be the maximum distance perpendicular to the length. Average dimensions of all granitoid clasts at each study location are given in Table 4.1.

The largest (average size) granitoid clasts occur in exposures of polylithic breccia-conglomerate near sulphide matrix ore such as seen in 20-13 Drift and 20-5 Sublevel (Figure 4.2; Table 4.1). Although sulphide clasts larger than the granitoids (Plates 4.2, 4.4) are present and very large clasts of other lithologies may be observed, granitoid clasts are generally the largest clast type present in MacLean Extension (Binney et al., 1983). There is a general decrease in average granitoid clast size with increasing distance vertically and laterally from sulphide matrix ore (Table 4.1).

On average, granitoid clasts present at all locations were found to have unequal dimensions (Table 4.1) with many being oval or elongate in form (Plate 4.5, 4.6, 7.1). Some granitoid clasts display a spindle-shaped form (Plates 4.3, 4.11) similar to that shown by some volcanic bombs (Williams and McBirney, 1979).

The area of each study location has been calculated in order to provide estimates of the volume occupied by granitoid clasts in the debris flow lithological subunit or subunits exposed at each location. The area of a study location was usually defined vertically by the floor and ceiling of the underground working. Horizontal limits were typically determined by the presence of a diabase dyke or where there was an obvious decrease in the size and

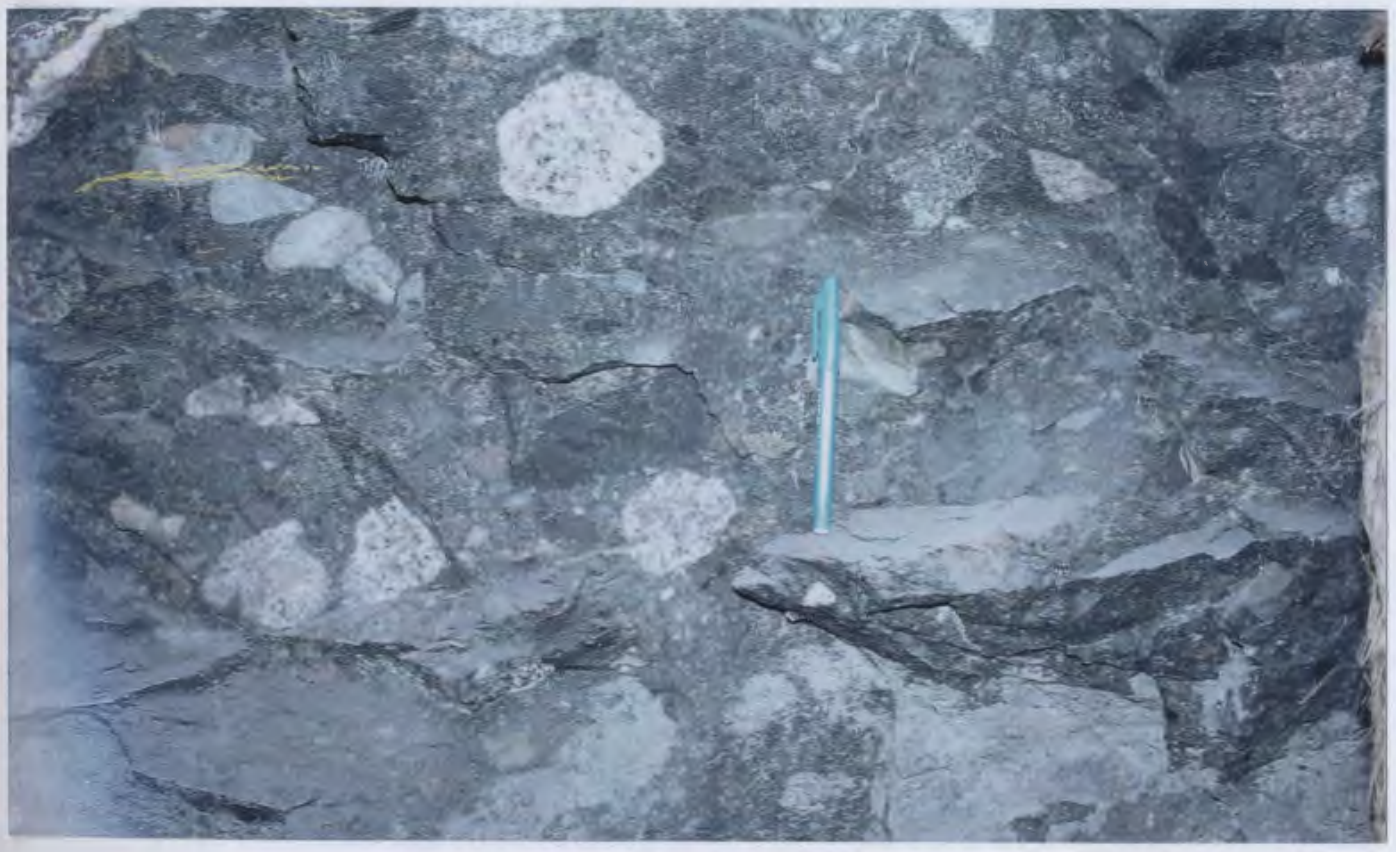

Plate 4.7 Photograph of rounded granitoid and other lithic clasts typical in granitoid-bearing polylithic breccia-conglomerate without associated sulphide matrix ore, in 20-6 Sublevel, MacLean mine; ball-point pen for scale.

Plate 4.8 Photograph of two large type 6 granitoid clasts in siltstone breccia unit that underlies the felsic pyroclastic and debris flow sequences of the Buchans River Formation; near at western end (W3000) of 20-1 Drive, MacLean mine; rock bolt plates are 14 cm wide.

abundance of granitoid clasts. Since study was focused on areas of maximum granitoid concentrations, the resulting area and volume estimates are considered maxima. The area occupied by each granitoid clast was estimated using the formula for the area of an ellipse to reflect the inequal average dimensions (Table 4.1). The total area occupied by granitoid clasts at each locality was compared to the total area of the study location to determine the percentage of the study location area occupied by granitoid clasts.

By extrapolation from the areal percent, an estimate of the volume of a debris flow occupied by granitoid clasts is made (Table 4.1). The extrapolation of areal percent to volume percent has been made because the third dimension of each clast (i.e. the dimension extending into the rock face) is not observable. This extrapolation is based on the assumption that the unobserved third dimension is not significantly and consistently longer or shorter than the two observed dimensions. This assumption is considered valid for the following reasons. No evidence of preferred orientation in any clast type within these debris flows has been recorded or was observed, including after removal of clasts from the rock face. Nor is there any evidence to indicate that there has been any tectonically produced flattening or stretching of clasts within the Buchans Group. The study locations include exposures that are parallel,

TABLE 4.1 Average dimensions of granitoid clasts, volume of lithologic subunit occupied by granitoid clasts and estimated roundness of granitoid clasts at main study locations in MacLean Extension (see Figure 4.2 for study locations).

LOCATION	UNIT	Average Dimensions			Volume	Roundness Classes					
		n	Length (cm)	Width (cm)	%	1	2	3	4	5	6
★[1] 20-5 Sub (south)	granitoid-bearing ore breccia-conglomerate	37	16.1	9.4	3.62			8	18	11	
★[2] 20-13 Drift (north)	granitoid-bearing ore breccia-conglomerate	70	17.1	10.6	4.58			1	34	34	1
20-13 Dr (both)	polylithic breccia-conglomerate	34	nd	nd	nd			1	13	17	3
★[4] 20-6 Sub (south)	granitoid-bearing ore breccia-conglomerate, minor baritic polylithic breccia-conglomerate and arenaceous conglomerate (undivided)	158	6.0	4.0	1.16			1	43	74	40
" (north)		262	4.7	3.2	.55				26	154	82
★[3] 20-7 Dr (north)	polylithic arenaceous breccia-conglomerate, granitoid-bearing polylithic breccia-conglomerate and baritic polylithic breccia-conglomerate (undivided)	171	6.8	3.6	2.90			1	43	97	30
☆[5] 20-1 Dr (both)	baritic low grade polylithic breccia-conglomerate	22	nd	nd	nd				3	12	7
☆[5] 20-4 Dr (south)	baritic polylithic breccia-conglomerate and granitoid-bearing arenaceous breccia-conglomerate (undivided)	150	3.7	2.5	1.16			2	23	79	46
" (north)		100	4.6	3.3	1.02				16	64	20
	TOTALS	1004						14	219	542	229
☆[6] 20-1 Dr	siltstone breccia	30	nd	nd	nd				16	14	
★[3] 20-7 Dr (north)	ore horizon dacitic pyroclastics	9	7.8	3.5	.10					6	3
★[1] 20-5 Sub	footwall dacitic pyroclastics	36	6.8	5.6	.58			1	17	17	1
☆[7] 20-1 Dr	hangingwall dacitic pyroclastics	3	nd	nd	nd					2	1
	nd = not determined (<0.1%)										

North and south refer to rock face of underground workings studied, both indicates that the data from each face has been calculated together. Sub = sublevel, Dr = drive.

perpendicular and oblique to the presumed debris flow direction. Therefore, the measured cross section through each clast is considered to be nonpreferential and there is no apparent reason for there to be a consistent bias toward either over- or under-estimating the unobserved dimension. The study locations were the most obvious concentrations of granitoid clasts within all debris flow units exposed, thus these estimates of volume percent are considered maxima.

Estimates of the volume occupied by granitoid clasts at the main study locations are shown in Table 4.1. The maximum volume occupied by granitoid clasts occurs in granitoid-bearing polylithic breccia-conglomerate associated with sulphide matrix ore as in 20-13 Drift and 20-5 Sublevel (Table 4.1; Figs. 4.2, 4.4). Although a greater number of granitoid clasts may be present, the estimated volume occupied by granitoid clasts decreases in granitoid-bearing polylithic breccia-conglomerate with increasing distance from the sulphide matrix ore as seen in 20-7 and 20-4 Drives (Table 4.1). A similar slight decrease in the volume occupied by them is seen in ore grade granitoid-bearing polylithic breccia-conglomerate without associated sulphide matrix ore (20-6 Sublevel, Table 4.1; Fig. 4.4).

4.3.3 Roundness

The roundness of each granitoid clast was estimated by assigning a value between one and six to each. These values correspond to the six degrees of roundness shown in the 'comparison chart of visual estimation of roundness' (Jackson, 1970, Fig. 6-1, p.329). On this scale, one indicates a very angular clast or grain and six represents a well-rounded clast or grain. The overwhelming majority of granitoid clasts (99%) were assigned roundness values of 4, 5 or 6, i.e., sub-rounded, rounded and well-rounded classes (Table 4.1).

The generally heightened rounding of granitoid clasts relative to other clast lithologies was previously noted (Thurlow, 1981; Walker and Barbour, 1981; Binney et al., 1983). These workers also observed that the granitoid clasts exhibit the highest degree of rounding of all clast lithologies present (Plates 4.1, 4.5, 4.6, 4.7).

4.4 PETROGRAPHY AND CLASSIFICATION OF GRANITOID CLASTS

4.4.1 Introduction and methods of classification

The granitoid clasts in MacLean Extension were initially classified into twelve types using macroscopic characteristics (Stewart, 1983). The macroscopic criteria used in approximate decreasing order of emphasis were: the

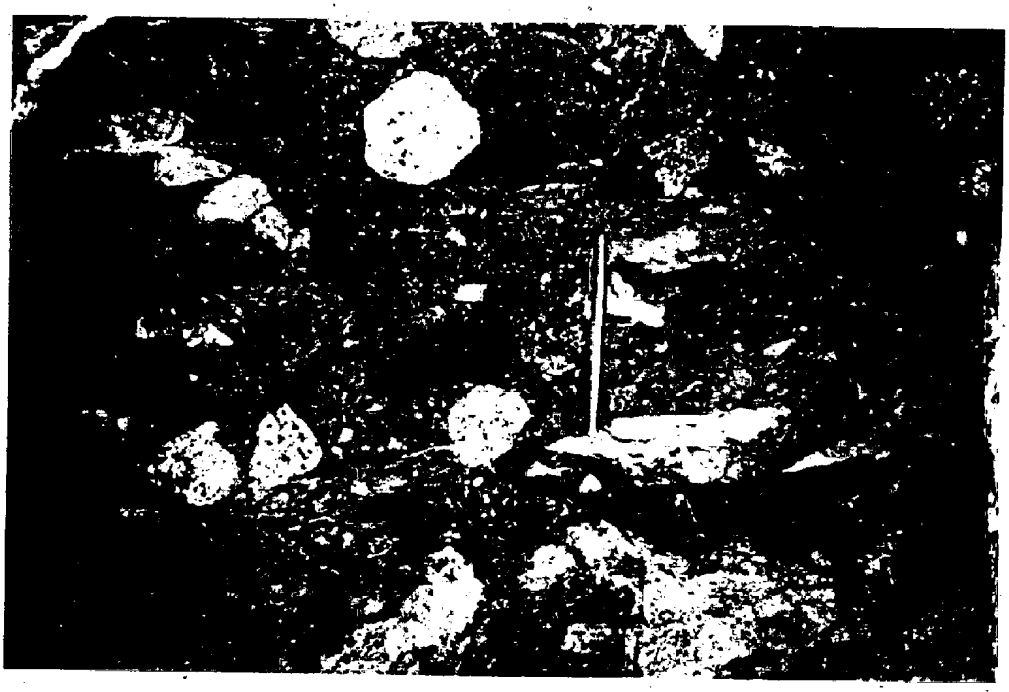

Plate 4.7 Photograph of rounded granitoid and other lithic clasts typical in granitoid-bearing polylithic breccia-conglomerate without associated sulphide matrix ore, in 20-6 Sublevel, MacLean mine; ball-point pen for scale.

dominant colour of the groundmass (i.e. the overall colour of the clast), average grain size, of the groundmass, presence or absence of phenocrysts, average size and type of phenocrysts, the amount of mafic minerals present and whether the mafic minerals are fresh or altered. The large number of clast types reflects the diversity in texture and especially colour (Plates 4.1 to 4.11) displayed by the granitoid clasts. Colour proved to be unsuitable for classification since it was greatly influenced by hydrothermal alteration (Sections 4.4.2; 5.2).

Petrographic examination indicated that subvolcanic rocks were present. Microscopically observed textural differences were considered to more adequately classify the clasts present and permitted a reduction in the number of 'types' necessary for an adequate classification. The resulting classification scheme was originally presented in Stewart (1984) and is employed here with only minor modifications.

Emphasis in classification has been placed on igneous textures and relative grain sizes because differences in primary mineralogy and their relative proportions are generally slight. Clast types 1 through to 5 are arranged and enumerated to reflect the observed textural differences. The coarsest grained clasts with the best developed phaneritic texture, i.e., most truly plutonic, have been

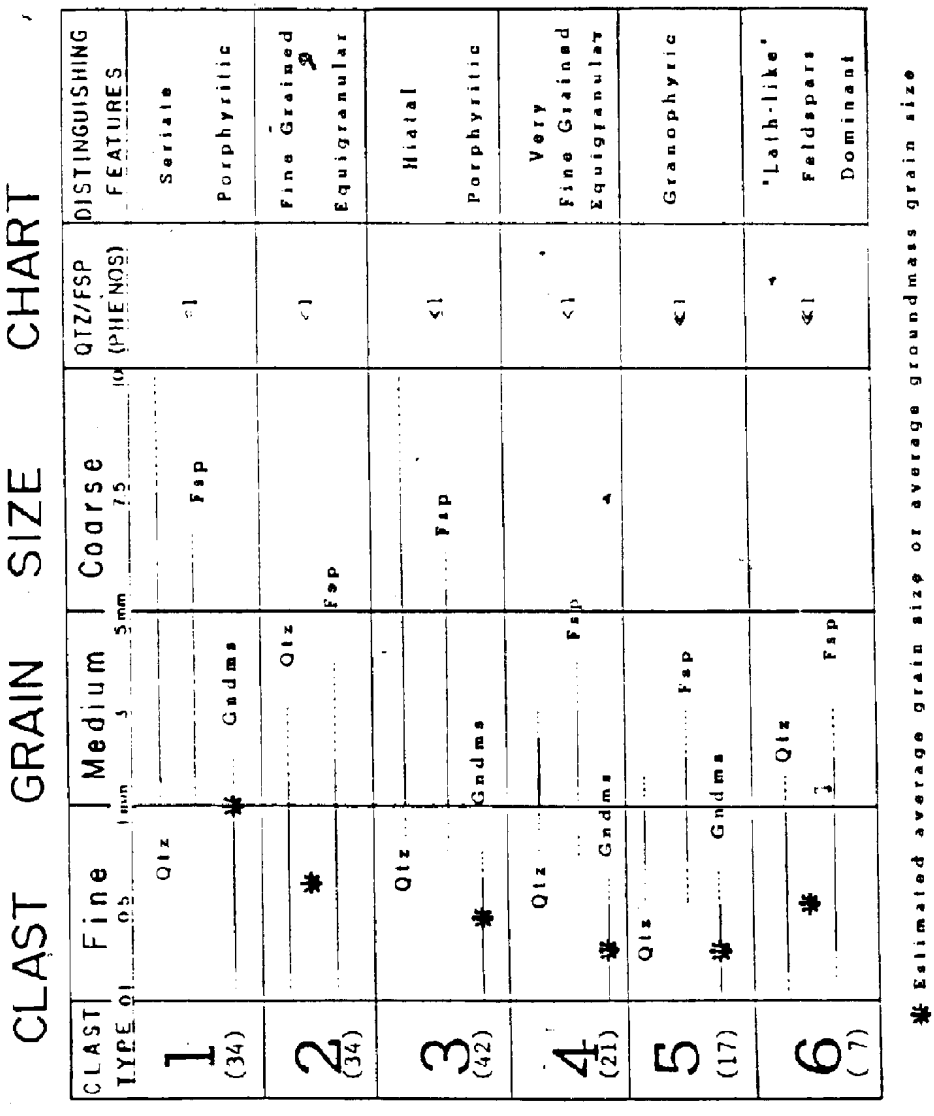

FIGURE 4.5 Graphical representation of phenocryst and groundmass grain size and textural criteria used to classify granitoid clast types in MacLeam Extension. The number of clasts examined petrographically is shown in brackets below each clast type.

assigned to type 1. The finest grained, weakly to non-porphyritic and most granophyric clasts have been assigned to type 5. Clasts types 2, 3 and 4 fill a textural continuum between these two end members. Clasts are assigned to a particular type on the basis of the abundance, mineralogy and size of phenocrysts present, average groundmass grain size and the degree of equigranularity. The characteristics of each granitoid clast type are graphically presented in Figure 4.5. In general, groundmass grain size decreases, phenocrysts decrease in size and relative abundance and the texture becomes increasingly aplitic and granophyric with the change from type 1 through to type 5 clasts. The features are interpreted to reflect different crustal levels and amount of time of crystallization in a single magma. Geochemical evidence for a common magmatic origin of the granitoid clasts is presented in Chapter Five.

Clast type 6 is texturally distinct from the other granitoid clast types as it does not contain any quartz phenocrysts or granophyric patches and contains a greater proportion of plagioclase grains relative to the other types (Stewart, 1984). The subhedral to euhedral form of the plagioclase grains results in a 'lath-like' texture in clasts of this type. Type 6 clasts are restricted within the MacLean Extension area to the siltstone breccia

underlying the MacLean Extension ore horizon (Fig. 4.1, 4.2-study location 6). No other granitoid clast types are present in the siltstone breccia. Less than twenty type 6 clasts have been observed in MacLean Extension and 75% of those were seen in the siltstone breccia. Four or five type 6 clasts are disproportionately larger than all other clast lithologies present in the siltstone breccia and dominate this exposure (Plate 4.8). A small number of type 6 clasts occur in MacLean Extension debris flows. Rare magmatic inclusions that texturally resemble type 6 clasts have been observed within other granitoid clast types. Type 6 clasts are thought to be a less differentiated product of the same magma system as the other granitoid types. Geochemical evidence for this is presented in Chapter Five.

4.4.2 General petrography of granitoid clasts in MacLean Extension

The following petrographic features are common to granitoid clast types 1 to 5. Characteristic features of these clast types and granitoid clast type 6 are described separately in Section 4.5.

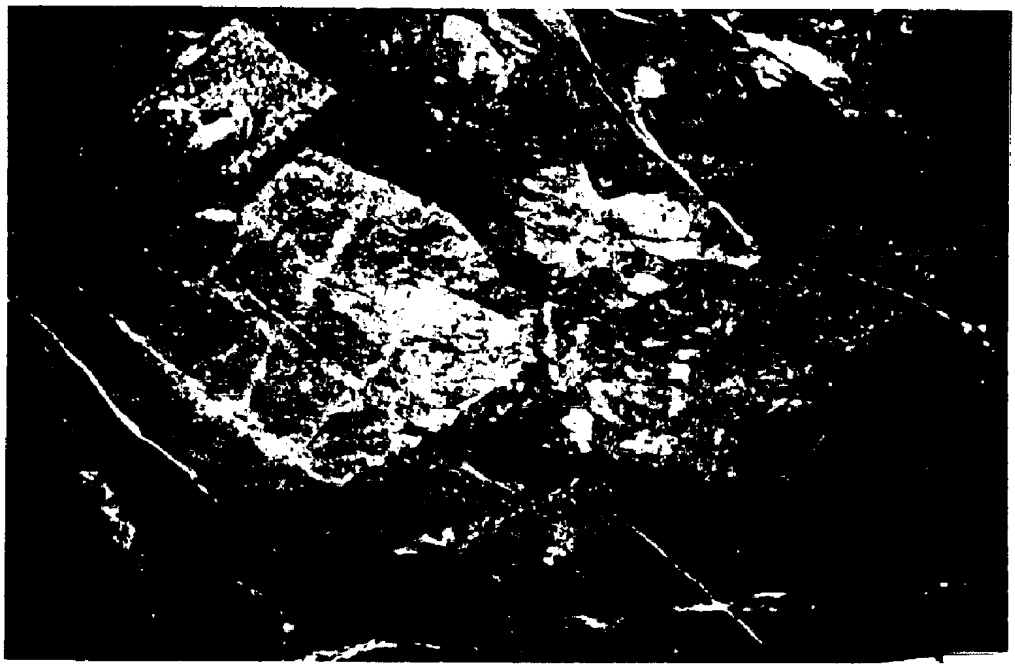

Plate 4.8 Photograph of two large type 6 granitoid clasts in siltstone breccia unit that underlies the felsic pyroclastic and debris flow sequences of the Buchans River Formation; near at western end (W3000) of 20-1 Drive, MacLean mine; rock bolt plates are 14 cm wide.

The primary mineralogy of all clast types is simple and relatively consistent. Quartz and plagioclase typically comprise 97% or more of the primary mineralogy in any clast examined. The predominant crystallizing mafic phase was biotite which is partially to completely altered to chlorite ± opaques. Biotite and its by-products typically occupy 3% or less of the clasts. Amphibole crystals have been observed in less than 5% of the samples, and clinopyroxene in only five clasts. Amphibole and pyroxene crystals are typically found in only the less altered examples of the more coarsely crystalline clasts (types 1 and 2) and are very subordinate in proportion to biotite. Accessory minerals are magnetite, apatite, zircon and rarely sphene.

Quartz comprises 30-50% of the granitoid clasts, feldspar occupies 45-65%. Frequently they are seen in subequal proportions. Potassium feldspar has not been recognized petrographically despite attempts with staining techniques (Friedman, 1971). Therefore, all feldspar grains are considered to be plagioclase.

Alteration of feldspar grains is ubiquitous, but variable in relative intensity and has two different petrographic expressions. These are; 1) the development of very fine grained, red-brown dust (hematite) clouding the plagioclase grains, and 2) the partial to complete replacement of plagioclase crystals by very fine to fine

grained calcite and sericite. Locally, barite partially replaces plagioclase. Chlorite and rarely epidote are also occasionally seen to have formed on or within feldspar grains.

All granitoid clasts display one or both of these alteration effects. In the most highly altered clasts, the plagioclase phenocrysts are partially replaced by fine grained aggregates of sericite and calcite, whereas the groundmass feldspar grains are almost completely replaced by these minerals. Hematite dust, if preserved in these intensely altered clasts, is restricted to the plagioclase phenocrysts. Quartz, both as phenocrysts and in the groundmass, appears to have been unaffected by this alteration, and stands out in a "sea" of fine grained sericite, calcite and barite (and possibly crytocrystalline quartz). This pervasive alteration is most common in clast types 1, and 3, is occasionaly seen in type 2 clasts and is absent in types 4 and 5. In less pervasively altered type 1, 2 and 3 clasts, plagioclase grains invariably show weak to strong hematite dusting. Plagioclase phenocrysts in types 4 and 5 clasts commonly have partially to strongly replaced cores with the groundmass feldspar grains typically strongly dusted without evidence of calcite or sericite replacement. Type 2 clasts generally display a relatively intermediate degree of alteration between the strongly

hematized type 4 and 5 clasts and the pervasively altered type 1 and 3 clasts.

Biotite (and amphibole when rarely recognizable) are partially to completely replaced by chlorite and opaques, or less commonly by sericite and/or epidote. Chloritization appears to correlate with the degree of alteration of feldspar grains. In the pervasively altered clasts, biotite is entirely replaced by chlorite. In very highly altered examples, only rare opaques are present, with chlorite absent or minimal. Types 4 and 5 appear to have a slightly lower abundance of primary mafic phases (1% or so), that is typically partially chloritized, but biotite is commonly better preserved than in types 1, 2 or 3. As mentioned above, amphibole is typically only recognized in the least altered coarser grained clasts.

Quartz phenocrysts are rounded and usually glomerocrystic. The quartz phenocrysts (up to 10mm) are slightly larger than the feldspar phenocrysts (up to 7mm across), and typically show evidence of simultaneous growth with plagioclase. The interpenetration of crystals or inclusion of one phase as anhedral grains within a larger grain of the other phase is common. Such intergrowths are common in both phenocryst and groundmass crystals. Cavities and embayments in quartz phenocrysts are usually filled with very fine grained groundmass material or alteration

products. The larger phenocrysts typically show sets of fine fractures. These fractures are parallel within one phenocryst but show different orientations for different phenocrysts within one thin section. Larger fractures may occur as well and are filled with groundmass material and/or alteration products. Both fractured and unfractured quartz phenocrysts show undulous extinction. The only expression of alteration of quartz grains is the occurrence of what appear to be fluid trails across the grain. Sometimes these trails are not as well expressed in plagioclase grains as in quartz grains, although they appear to be continuous and reappear in the next quartz grain. In other cases, hematite dust is removed from plagioclase grains displaying the location of these trails that may then pass through quartz grains without any apparent effect. These fluid trails are often sub-parallel within one thin section.

Plagioclase feldspar phenocrysts are subhedral, and most commonly form glomerocrysts up to 7mm across. They show variable degrees of replacement by sericite and/or calcite, but are often better preserved than the groundmass in highly altered samples. Rims and overgrowths can be recognized by differences in extinction or most commonly by differences in the degree of alteration between the cores and rims. Cores are generally more altered than the rims. Examples of preserved magmatic zoning are rare with albite

twins most common, Carlsbad and pericline twins less so. Twinning is often obscured or destroyed by the alteration.

The many different colours shown by granitoid clasts are best considered an expression of alteration. For example, light brown (Plates 4.4, 4.9), medium brown (Plate 4.6), brown-green (Plates 4.3, 4.9), brick-red (Plate 4.5), white (Plates 4.1, 4.7, 4.10), pink-red (6.1) and bleached pink-grey (Plate 4.11) coloured granitoid clasts are present in MacLean Extension. The light brown quartz-porphyritic clasts in Plate 4.9 are less altered than the larger brown-green clast nearby. Similarly, the white clasts in Plate 4.10 are more altered than the brick-red clast in Plate 4.5. Despite these differences in colour, similar textures are recognized in these clasts. The change in colour within one clast (Plate 4.11) clearly demonstrates the secondary nature of many observed colours. Quartz±calcite±barite veins that have bleached the host rock and terminate at clast boundaries clearly demonstrate the origin of the colour differences in granitoid clasts prior to their incorporation in the debris flow (Plate 6.1).

4.4.3 Petrologic classification of the granitoid clasts

Plate 4.9 Photograph of two large, rounded, cream-coloured, quartz-porphyritic 'granitic' group granitoid clasts with a larger, quartz-porphyritic, dark green, more altered granitoid clast (top centre) in granitoid-bearing polylithic breccia-conglomerate overlying sulphide matrix ore; large clast of black ore to immediate right of pen; light coloured clast of barite at bottom centre; 20-13 Drift, MacLean mine; ball-point pen for scale; number is drawn with chalk on rock face.

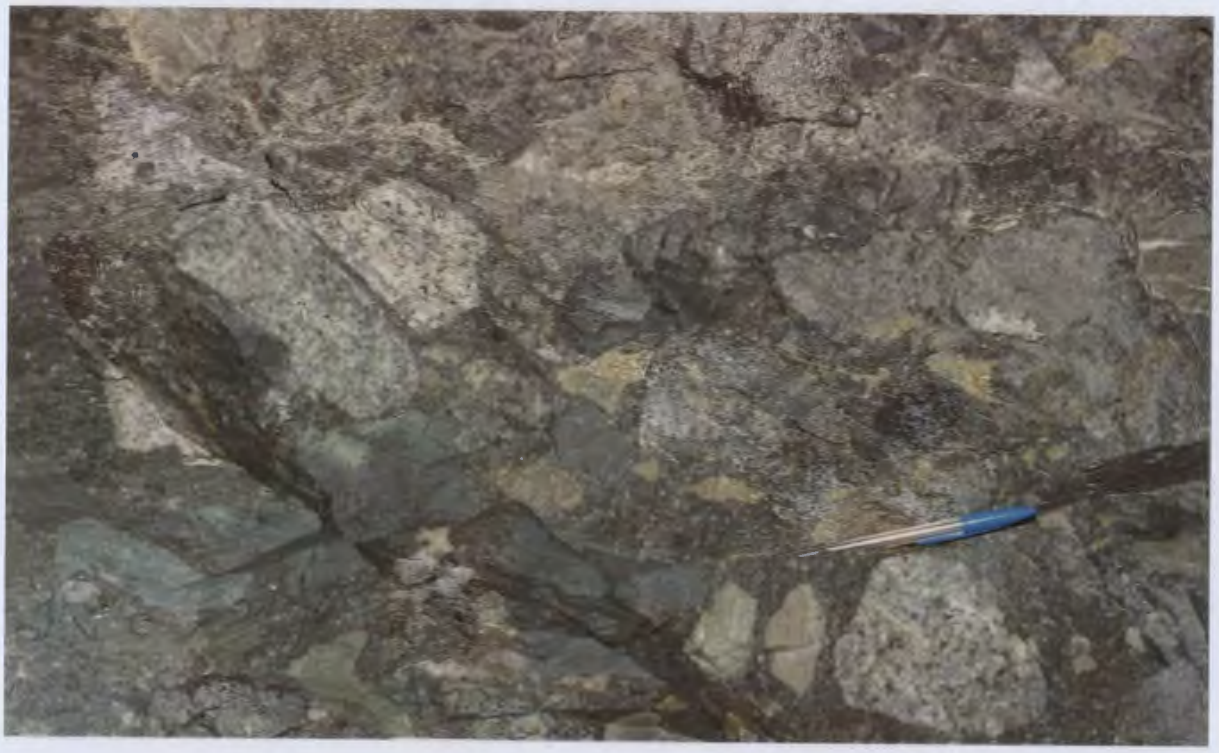

Plate 4.10 Photograph of white, rounded and subrounded, 'aplitic' group granitoid clasts in granitoid-bearing polylithic breccia-conglomerate without associated sulphide matrix ore; 20-6 Sublevel, MacLean mine; ball-point pen for scale.

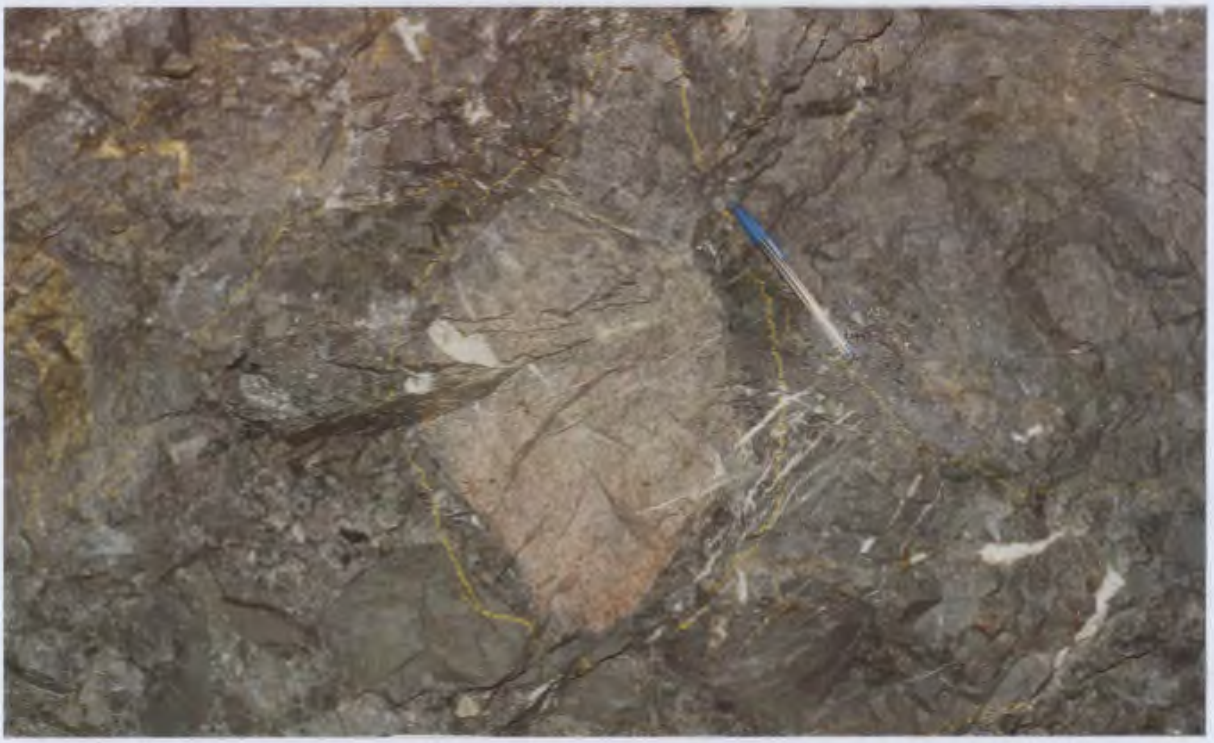

Plate 4.11 Photograph of partially altered, spindle shaped, 'aplitic' group granitoid clast and black ore clast with discontinuous bands of yellow ore (upper left), in granitoid-bearing polylithic breccia-conglomerate; 20-6 Sublevel, MacLean mine; ball-point pen for scale; yellow lines are drawn with chalk on rock face.

The classification scheme of Bowden et al. (1984) uses a slightly modified Quartz-Alkali feldspar-Plagioclase feldspar (QAP) plot from Streckeisen (1967, 1976) and is employed for classification purposes in this study. The simple mineralogy of the granitoid clasts, especially the apparent absence of potassium feldspar diminishes the importance of rigorous modal analysis and the hydrothermal alteration negates the use of normative compositions (see Chapter Five for chemical effects of alteration) for classification (Streckeisen and LeMaitre, 1979).

No plagioclase grains suitable for petrographic estimates of the An content were observed. This, combined with the hydrothermal alteration of all plagioclase grains making electron microprobe analysis tenuous, leaves the An content of these grains unknown. It is assumed that pure albite (An $<$ 05) is not the predominant plagioclase phase present, or if present, is due to metasomatism. Therefore, since all feldspars are plagioclase (as suggested by staining), and quartz is obviously greater than 20% by volume, all granitoid clasts plot within the the "granite parallelogram" on the QP join or in the T-granitoid field of the QAP plot (Bowden et al., 1984).

The low iron content of these clasts (as indicated by the low volume of primary mafic minerals), the dominance of biotite as the primary mafic phase during crystallization, the lack of evidence to indicate a genetic association with ophiolites and the high Na/K ratio in the granitoid clasts (Chapter Five) suggest that the granitoid clasts are best classified as trondhjemites (Barker, 1979) rather than tonalitic or tholeiitic granitoids (Bowden et al., 1984). Many granitoid clasts are microtrondhjemites using the terminology of Hatch et al. (1972) because of their generally fine grain size and porphyritic nature.

4.5 GRANITOID CLAST TYPE DESCRIPTIONS

4.5.1 Type 1 Clasts

These granitoid clasts are medium grained, hypidio- to allotriomorphic inequigranular with a continuous gradation in grain size from the finest grained groundmass to the largest phenocryst, i.e. they are seriate porphyritic (Plate 4.12). Included in this type are medium grained, slightly more equigranular examples, but all clasts show a wide and continuous range in grain sizes from fine to coarse. These are the coarsest grained clasts overall.

Plate 4.12a (Top) Representative photomicrograph of granitoid clast type 1 (KQS-82-044) showing the seriate porphyritic texture, large rounded, composite quartz phenocrysts, fine grained groundmass, and contact with debris flow matrix which contains an angular black ore fragment (upper right); polarized light; bar length = 10 mm.

Plate 4.12b (Bottom) Representative photomicrograph of granitoid clast type 1 (KQS-83-010) showing extreme difference in grain size between groundmass and quartz phenocrysts, and the presence of very fine grained groundmass material within phenocryst; polarized light; low power (x2.5).

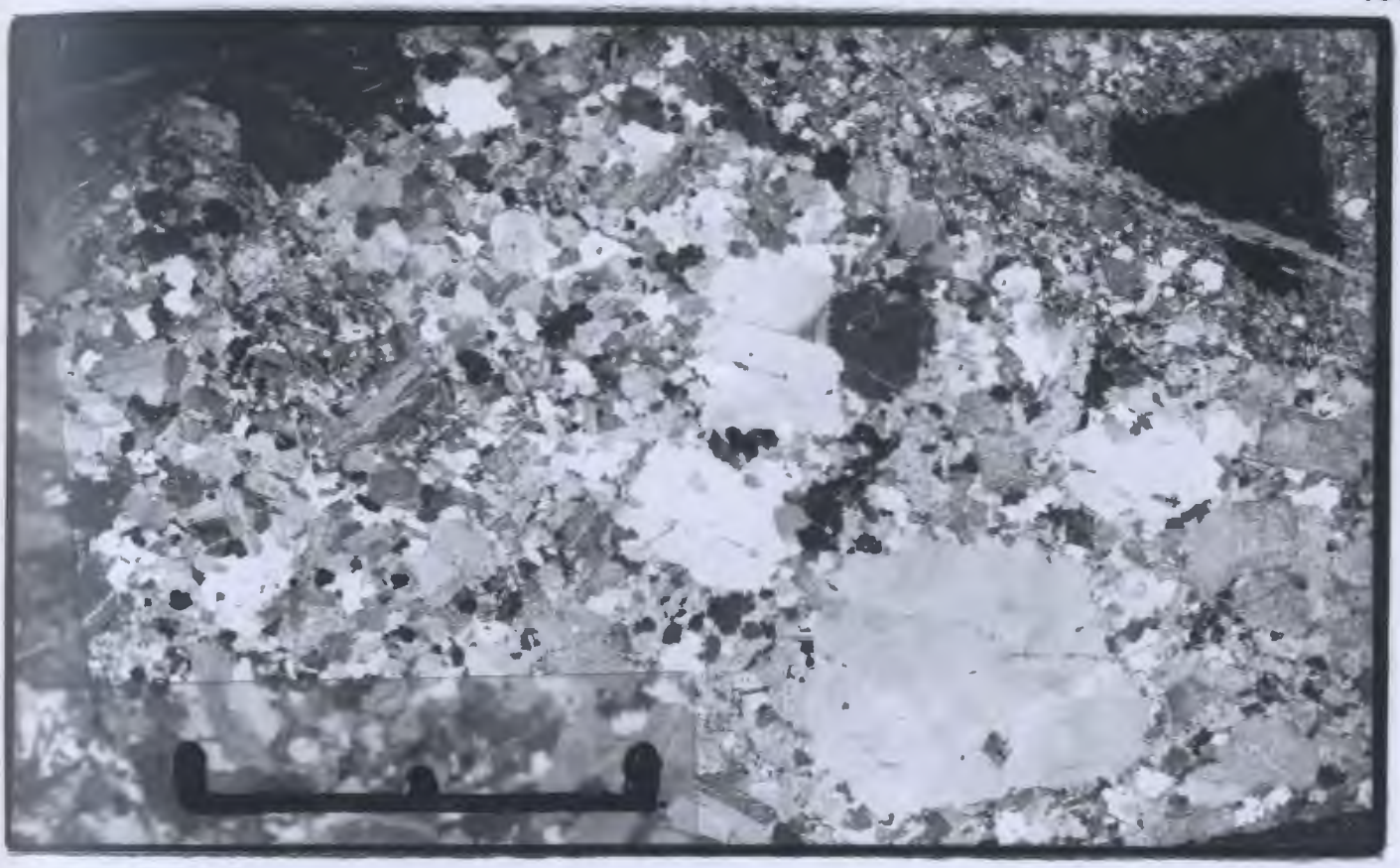

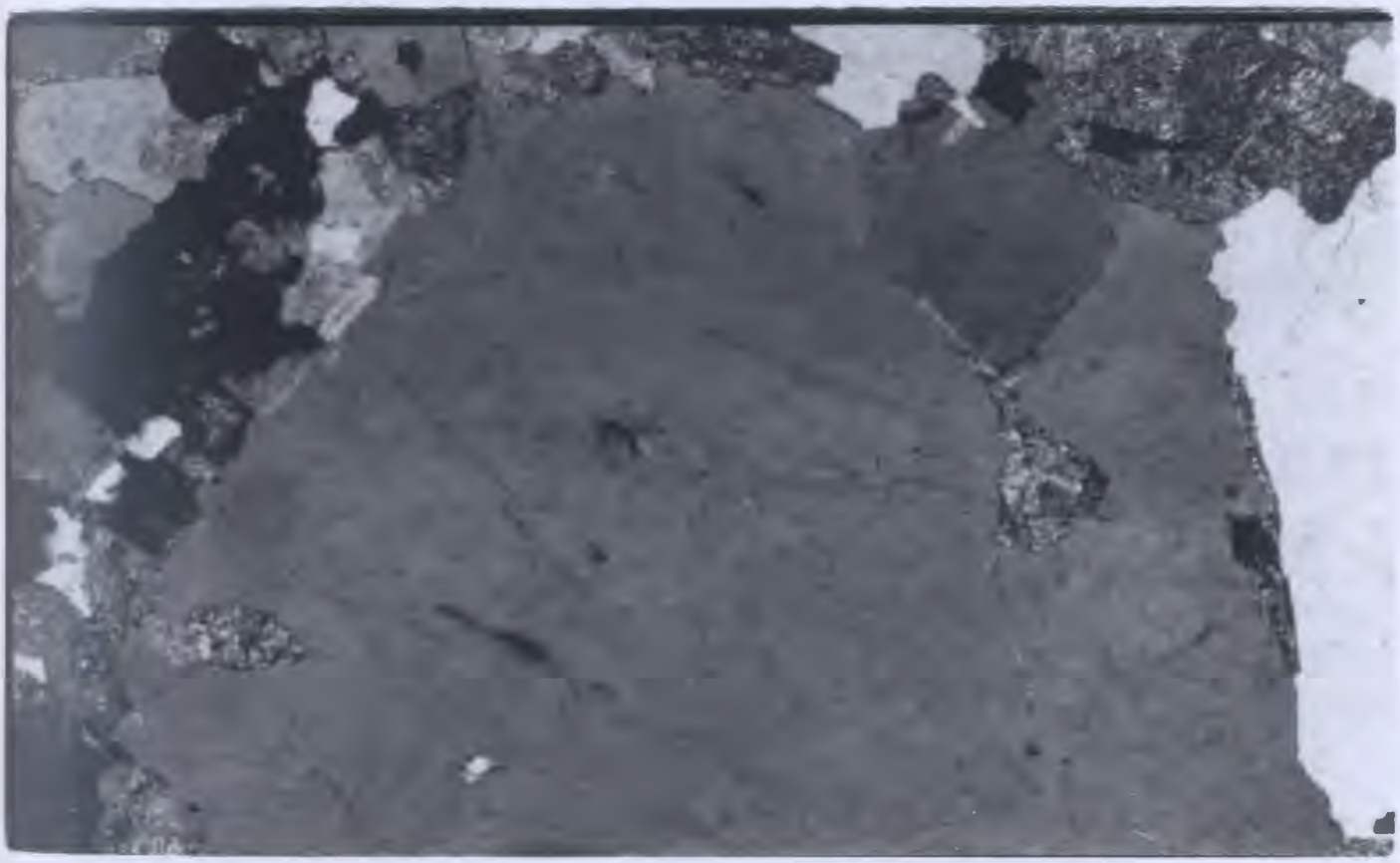

Quartz phenocrysts up to 10mm and plagioclase phenocrysts up to 6mm occur in a groundmass of fine grained anhedral quartz and feldspar crystals. The average grain size of the groundmass is approximately 1mm (Fig. 4.5). Crystal boundaries are interdigitating and very irregular. The porphyritic examples are usually more altered than the equigranular clasts but there are exceptions. Quartz phenocrysts are often embayed with very fine grained groundmass or alteration minerals in the embayments and fractures (Plate 4.12b). Most of the highly altered examples are brecciated, i.e. fractured and veined with sericite, calcite, barite and crypto-crystalline quartz. The brecciation is apparently associated with the alteration process.

4.5.2 Type 2 Clasts

These clasts are fine grained and relatively equigranular lacking a distinct phenocryst population (Plate 4.13). Relative to other clast types, they are intermediate in grain size. Grains are typically allotriomorphic, with quartz and feldspar grains ranging from 0.1mm to 3mm. The average grain size is between 0.5mm and 0.75mm (Fig. 4.5). These clasts are usually slightly less altered than either type 1 or 3. These clasts may show either a granitic or aplitic texture, but aplitic examples are more common.

Plate 4.13a (Top) Representative photomicrograph of granitoid clast type 2 (KQS-82-084) showing relatively equigranular texture, anhedral and highly intergrown nature of the grains, and the smooth rounded contact of the granitoid clast with the debris flow matrix; polarized light; bar length = 10 mm.

Plate 4.13b (Bottom) Representative photomicrograph of granitoid clast type 2 (KQS-82-084) showing equigranular texture, sub- to anhedral and intergrown crystals; partial alteration of plagioclase grains; chloritized biotite grain with opaques (left centre); polarized light; low power (x2.5).

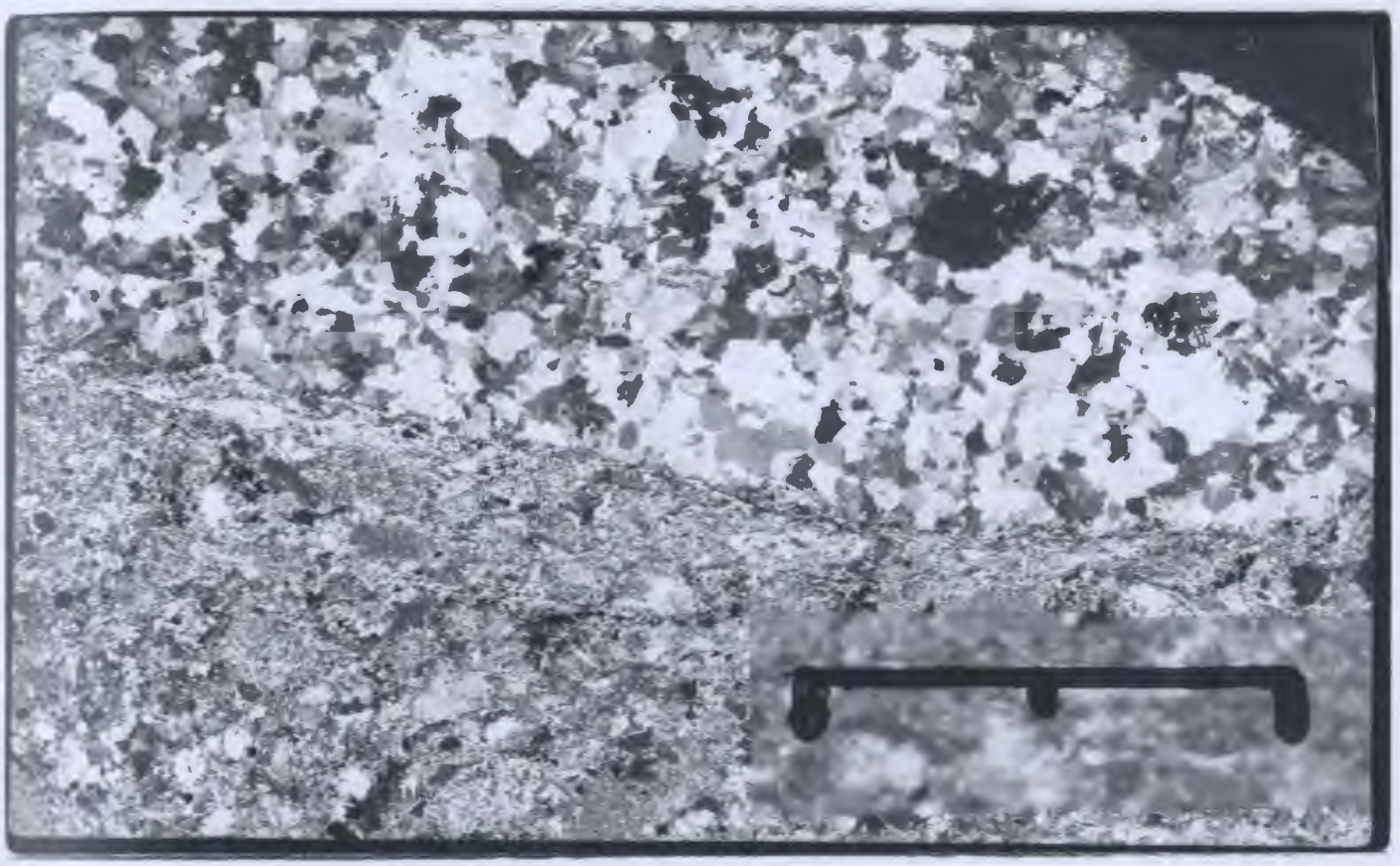

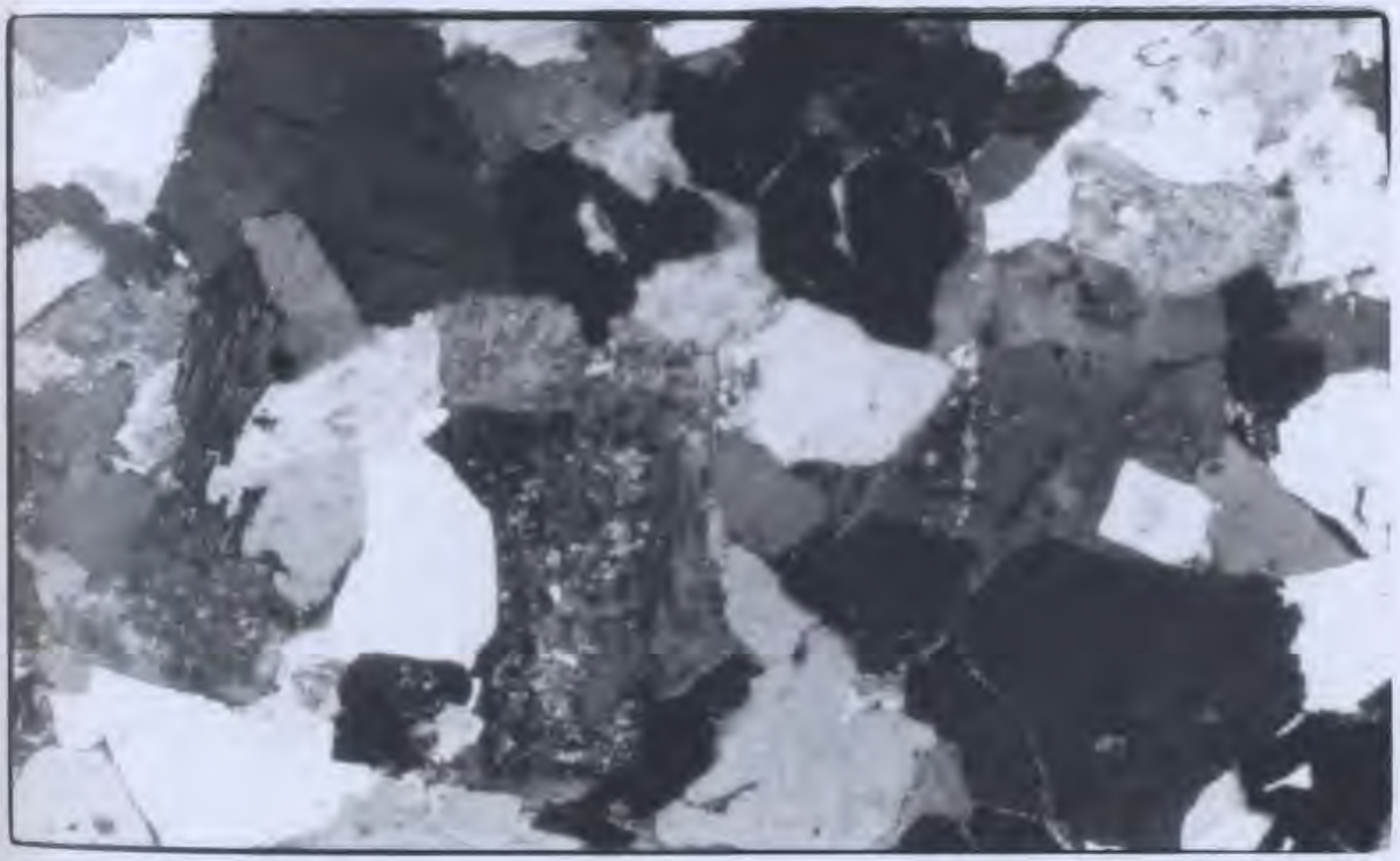

4.5.3 Type 3 Clasts

These clasts are hypidio- to allotriomorphic inequigranular with a large difference in grain size between phenocrysts and groundmass, i.e., hiatal porphyritic (Plate 4.14). The main textural difference between types 1 and 3 is between seriate and hiatal porphyritic (Fig. 4.5). Quartz phenocrysts up to 10mm and feldspar phenocrysts to 6mm in size occur in a groundmass which ranges from 0.1mm to 0.8mm, with an average grain size of approximately 0.3mm (Plate 4.5). Quartz phenocrysts are similar to those in type 1, i.e., rounded and composite, commonly with embayments and cavities, and often fractured and/or show undulous extinction. Feldspar phenocrysts are sub- to anhedral, zoned and are invariably altered to varying degrees. Some clasts contain granophyric patches, typically seen as rims around plagioclase phenocrysts.

4.5.4 Type 4 Clasts

These clasts are very fine to fine grained equigranular, with rare feldspar phenocrysts and even rarer quartz phenocrysts (each to 3mm) (Plate 4.15). Plagioclase phenocrysts are subhedral and quartz phenocrysts rounded and embayed. Other grains form an aplitic texture of tightly interlocking anhedral grains of similar grain size (approximately 0.3mm) (Fig. 4.5). Ferromagnesian minerals

Plate 4.14a (Top) Representative photomicrograph of granitoid clast type 3 (KQS-83-019) showing hiatal porphyritic texture, very fine grain size of groundmass, the large, rounded composite quartz phenocrysts, the fracturing and partial bracciation of the clast; groundmass is unaltered quartz plus calcite, sericite and/or barite; polarized light; bar length = 10 mm.

Plate 4.14b (Bottom) Representative photomicrograph of granitoid clast type 3 (KQS-83-019) showing a partially resorbed quartz phenocryst (in extinction), the fine grain size and high degree of alteration of the groundmass; polarized light; low power (x2.5).

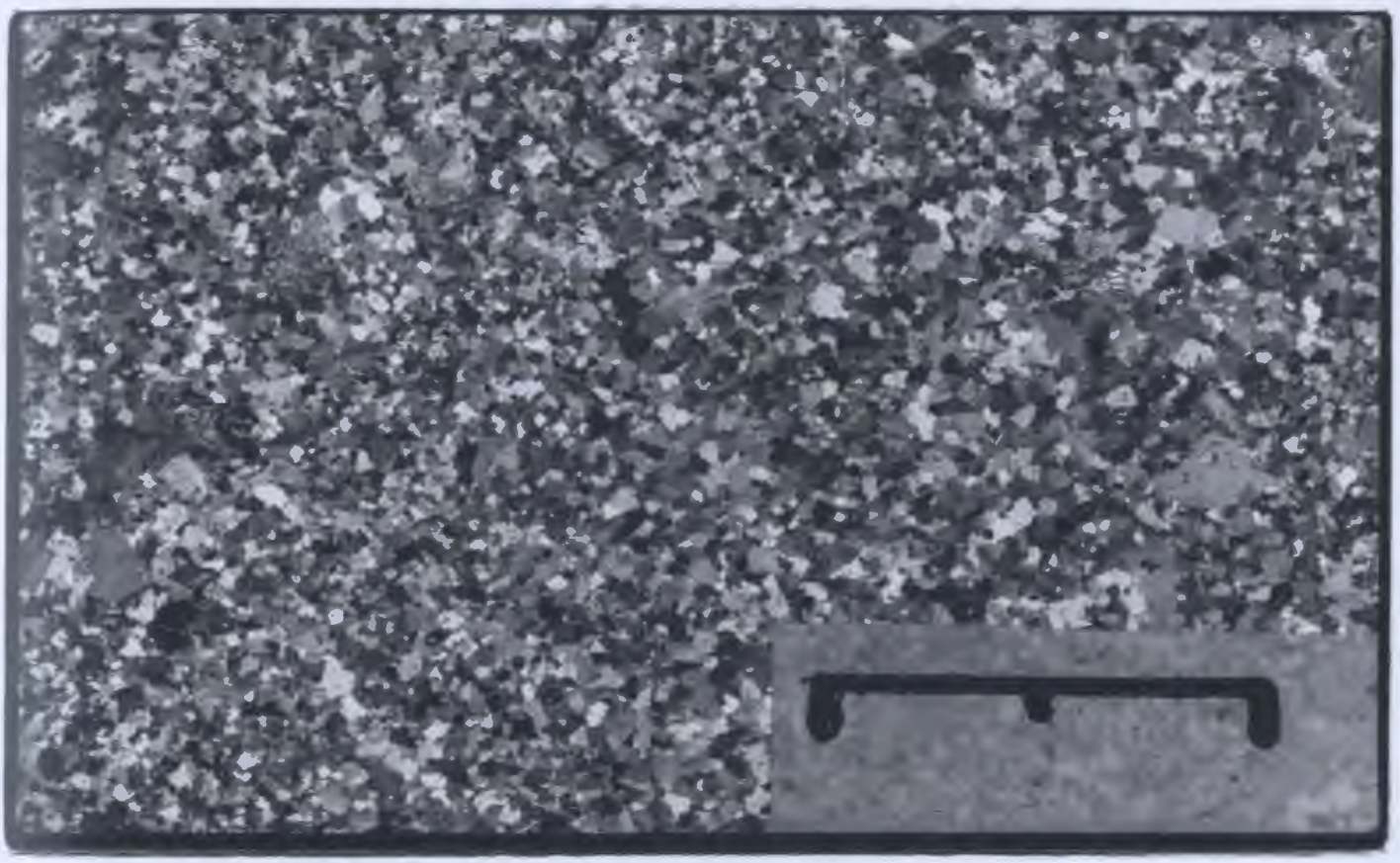

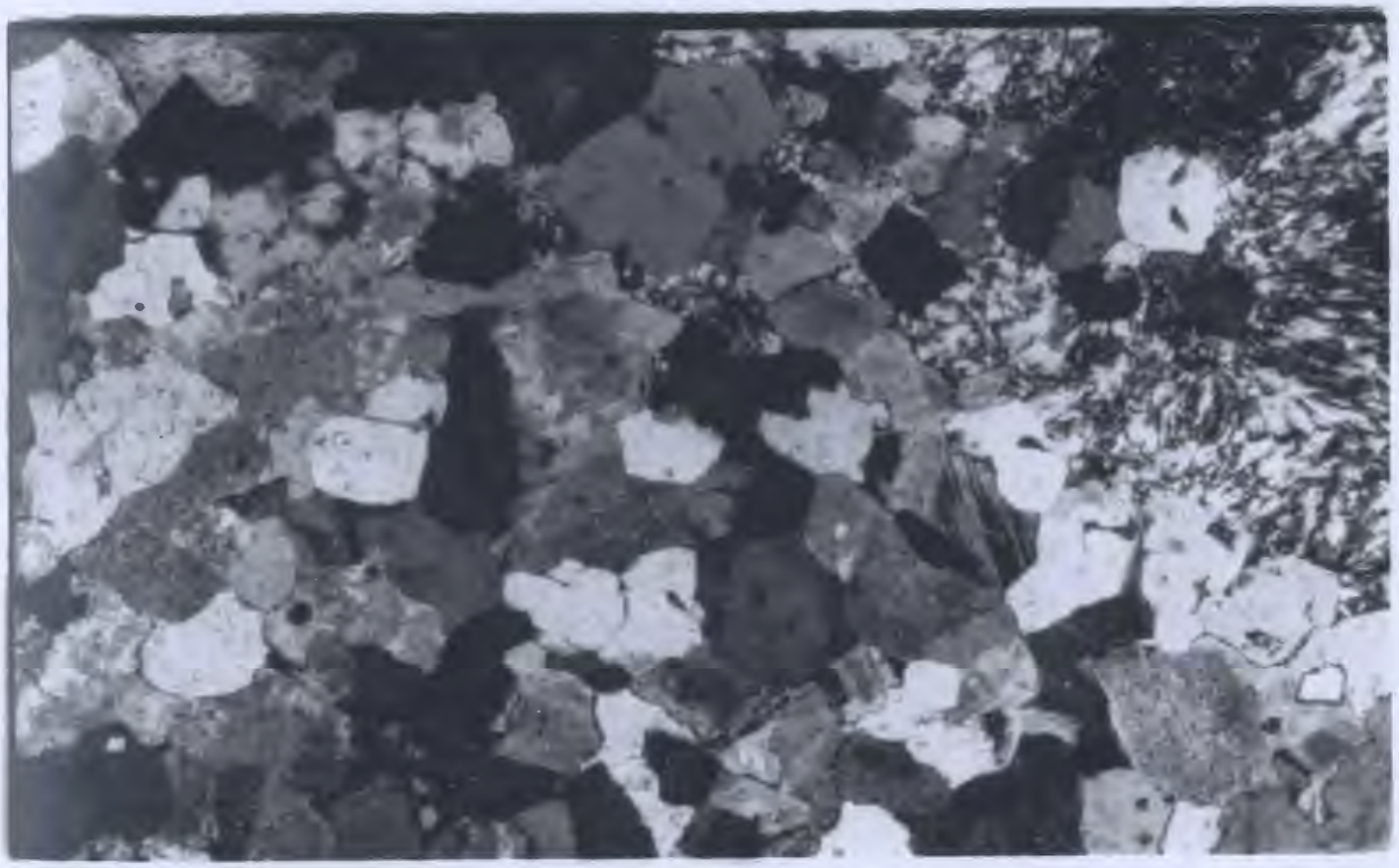

Plate 4.15a (Top) Representative photomicrograph of granitoid clast type 4 (KQS-82-095) showing the equigranular, fine grained aplitic texture, relatively unaltered, non-brecciated nature; polarized light; bar length = 10 mm.

Plate 4.15b (Bottom) Representative photomicrograph of granitoid clast type 4 (KQS-82-095) showing anhedral, equigranular quartz and plagioclase grains, hematite dust on plagioclase grains (lower right), the apparent introduction of secondary quartz (tridymite?) (upper right); polarized light; low power (x2.5).

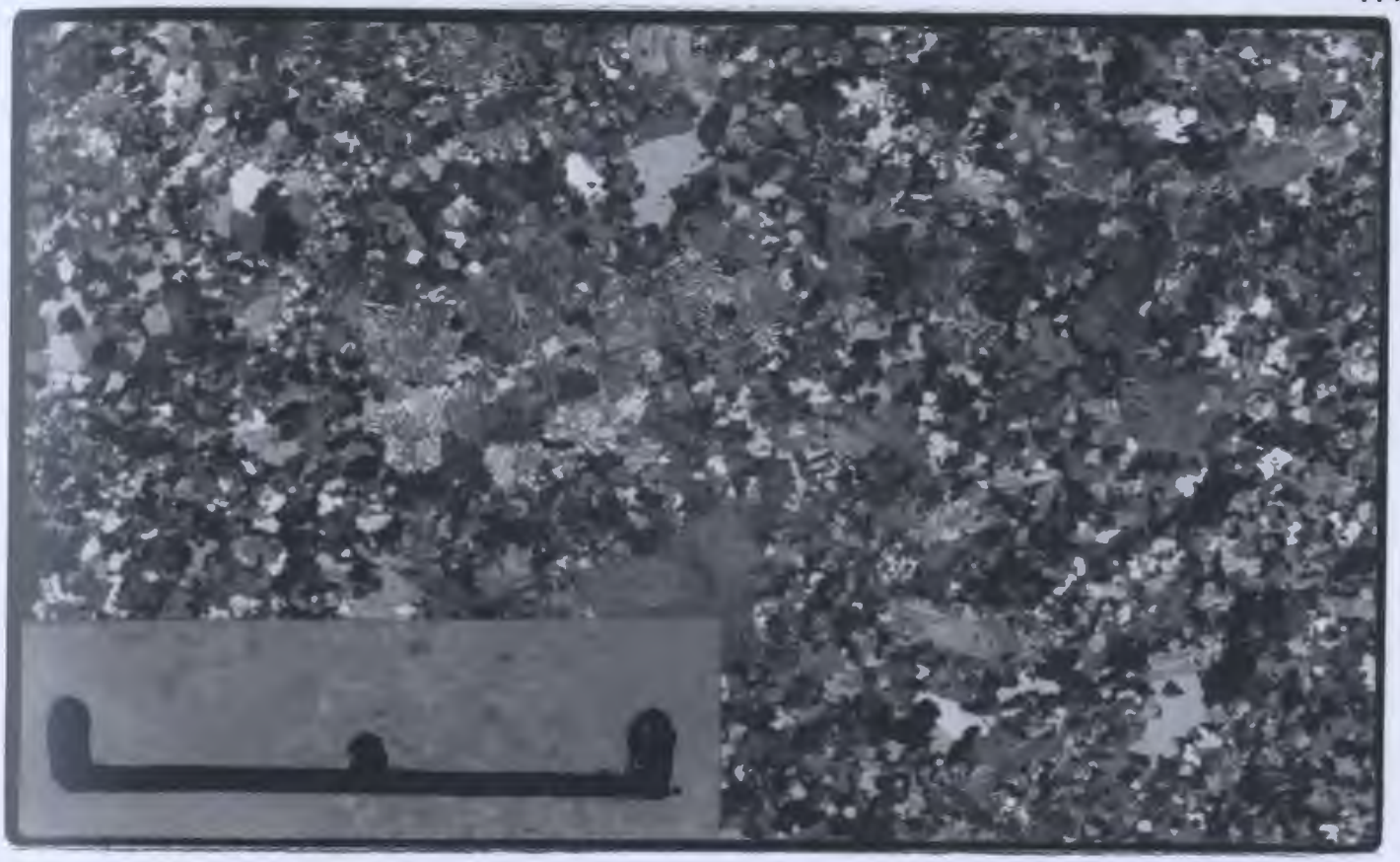

are slightly less abundant than in most weaky altered examples of the previous types. Granophyric textures similar to those described by Barker (1970) are common in clasts of this type, both as rims on earlier formed crystals and as subspherical patches in the groundmass. Plagioclase crystals are not as extensively replaced by calcite and sericite as in type 1, 2 and 3 clasts, but display hematite dusting of variable intensity. Calcite and barite occur as veins filling fractures, locally accompanied by cryptocrystalline quartz (Plate 4.15b).

4.5.5 Type 5 Clasts

These clasts are fine grained equigranular and characterized by abundant granophyric areas (Plate 4.16). They are slightly finer grained and feldspar phenocrysts are less common than in type 4 clasts but the main difference is the amount of granophyre present (Fig. 4.5). Plagioclase grains are less altered to calcite and sericite than in types 1, 2 and 3, but similar to type 4 clasts in that they are invariably dusted with hematite. Crystals are usually anhedral with irregular and interdigitating crystal boundaries except for occasional subhedral plagioclase phenocrysts.

4.5.6 Type 6

Plate 4.16a (Top) Representative photomicrograph of granitoid clast type 5 (KQS-93-091) showing the fine to very fine grain size, highly granophyric texture, relative lack of alteration and brecciation; polarized light; bar length = 10 mm.

Plate 4.16b (Bottom) Representative photomicrograph of granitoid clast type 5 (KQS-83-091) showing an example of the highly granophyric nature of some areas within the clast, granophyre occurs as rims on earlier crystallized grains and as phenocryst-like patches; note lack of alteration; polarized light; low power (x2.5).

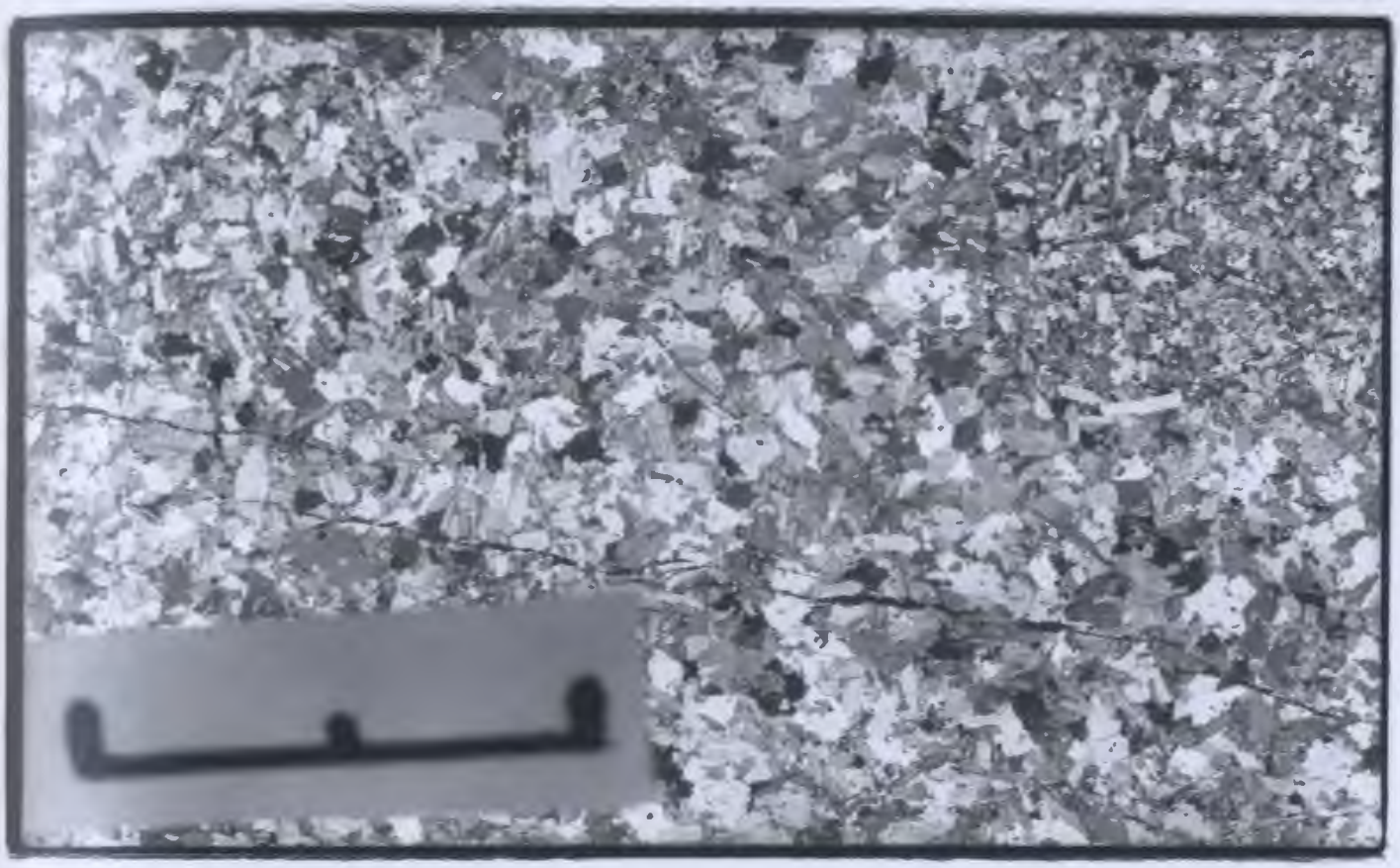

These clasts are texturally and mineralogically distinct from the earlier described types (Plate 4.17). Magnetite, biotite and especially plagioclase are more abundant than in types 1-5. Relict amphibole crystals occur as rare small anhedral crystals. Plagioclase crystals are almost invariably subhedral, form a randomly oriented lath-like texture and are more strongly dusted with hematite than in any other clast type. Anhedral quartz fills the interstitial areas and is clearly a later crystallizing phase than plagioclase. Clasts with this mineralogy and texture but different average grain sizes have been observed. Some have an average grain size of approximately 1mm, while others have an average grain size of approximately 0.5mm, with the latter more common (Fig. 4.5). Globular inclusions of the finer grained material have been observed in the coarser grained examples (Plate 4.17). Rare inclusions of type 6 material in other clast types have been observed.

4.6 INTERPRETATION OF THE PETROGRAPHY OF GRANITOID CLASTS

There appears to be little difference in the relative proportions in types 1 to 5 of the main crystallizing phases, i.e., plagioclase, quartz and biotite., The

Plate 4.17a (Top) Representative photomicrograph of granitoid clast type 6 (KQS-82-067) showing the fine grained, relatively equigranular texture, greater proportion of plagioclase crystals relative to the other granitoid clast types, subhedral 'lath-like' plagioclase forms, and the presence of finer grained, but similar material as a 'globule' within the clast (upper right); polarized light; bar length = 10 mm.

Plate 4.17b (Bottom) Representative photomicrograph of granitoid clast type 6 (KQS-82-067) showing occurrence of anhedral quartz (white, in centre of view) interstitial to the subhedral, highly dusted and partially altered laths of plagioclase; polarized light; low power (x2.5).

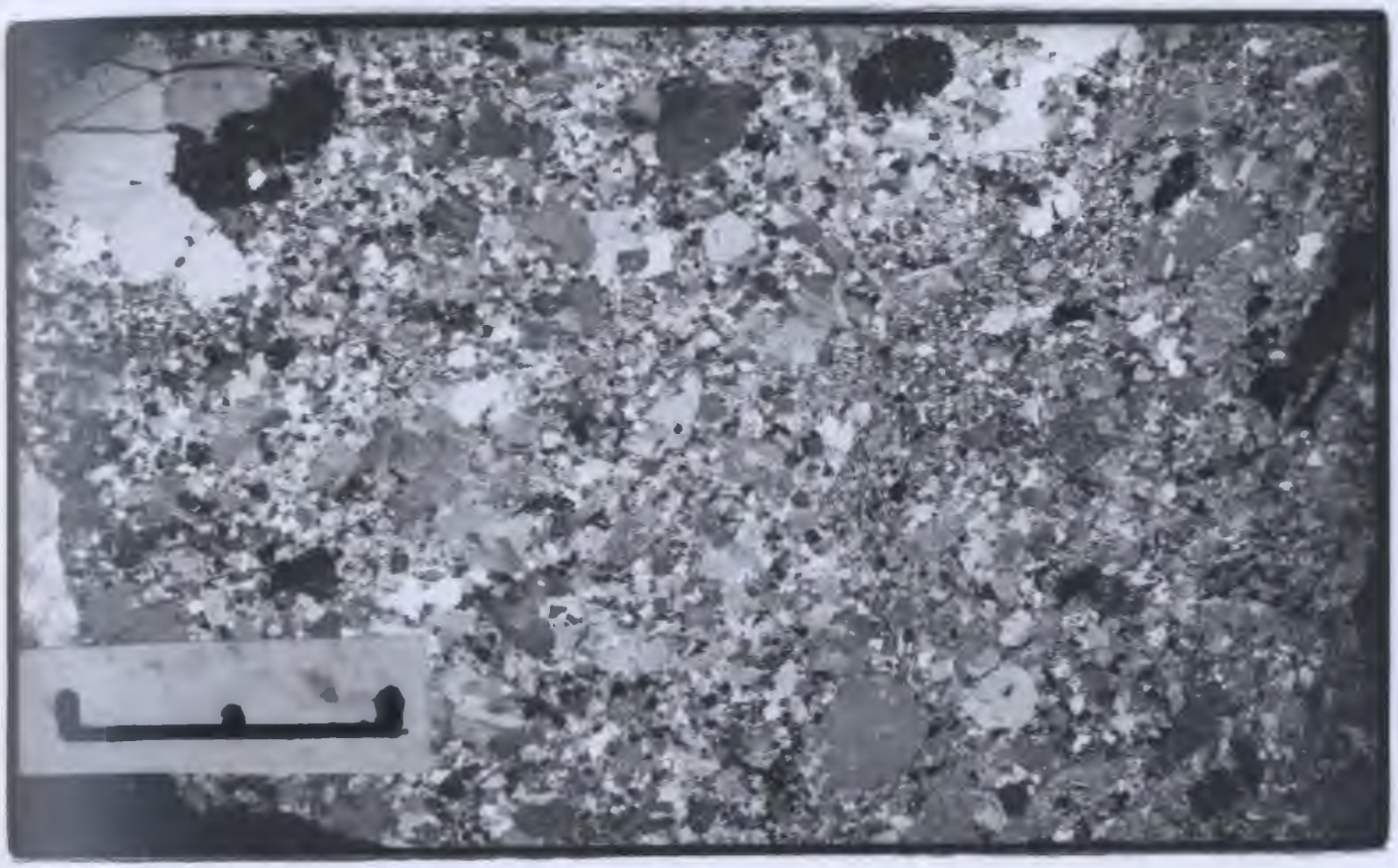

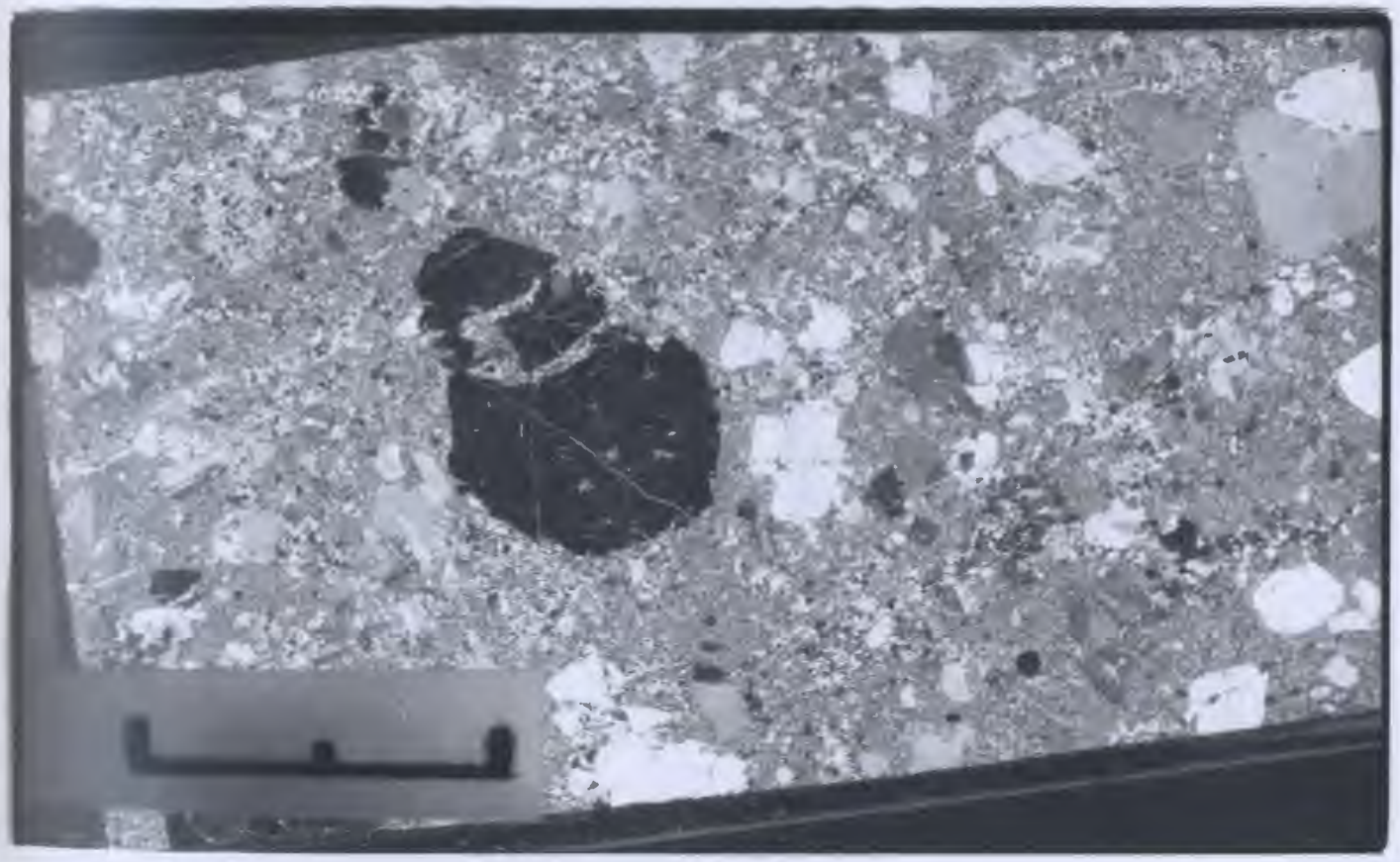

proportion of phenocrysts to groundmass and average size of phenocrysts decreases gradationally from types 1 through to 5. The average groundmass grain size also decreases gradationally between clast types 1 and 5 accompanied by an increase in the amount of granophyric intergrowths.

The igneous textures appear to range from intrusive to subvolcanic. These textural differences, the similar mineralogy and relatively consistant mineral proportions in each clast type are interpreted to reflect differences in the depth and crystallization history of a magma. The highly porphyritic nature of most of the clasts and the abundance of granophyric textures suggests a rapid crystallization history for the clasts. In combination with the generally fine grain size seen in most clasts, this suggests that all granitoid clasts crystallized at a high crustal level.

The porphyritic and coarsest grained clasts typically show the most fracturing, veining and alteration (Plate 4.14a). Quartz phenocrysts commonly have embayments and fractures filled with groundmass material (or alteration products) (Plate 4.12b) and often show a strongly developed undulous extinction. Some quartz phenocrysts are fractured and slightly pulled apart similar to quartz phenocrysts in volcanic rocks of the underlying Lundberg Hill Formation (Plate 4.18a,b). There is a lack of common orientation to

Plate 4.18a (Top) Photomicrograph of granitoid clast type 3 (KQS-83-016) showing well developed hiatal porphyritc texture, the composite and fractured quartz phenocryst (upper left), the similar grain size and composition of debris flow matrix (right of centre) and clast, and the smooth nature of the contact between the clast and the debris flow matrix; polarized light; bar length = 10 mm.

Plate 4.18b (Bottom) Representative photomicrograph of typical quartz porphyritic volcanic rock from the Lundberg Hill Formation (formerly the Prominent Quartz Sequence) showing the large size of the rounded, partially resorbed and fractured quartz phenocrysts, and groundmass material filling fractures within the phenocryst; polarized light; low power (x2.5).

these fractures within any one sample negating their origin to a later deformational event. These features indicate phenocryst deformation prior to final crystallization, i.e. a typical protoclastic texture.

Cryptocrystalline quartz (possibly intergrown with feldspar) occurs filling open spaces as veins (Plate 4.15b) and as a cement for mineral grains in highly fractured and brecciated clasts. In clasts with plagioclase completely to partially replaced by fine grained aggregates of calcite, sericite and lesser barite, secondary quartz is commonly present. These features implie that brecciation, alteration and silicification in the clasts are related and are probably due to hot fluid and/or vapor activity.

Although type 6 clasts are similar mineralogically to the other types, they contain more plagioclase, biotite and magnetite and less quartz. The larger grain size and subhedral nature of the plagioclase indicates that it probably began to crystallize earlier than the other phases. Quartz phenocrysts are absent and quartz only occurs interstitial to the larger plagioclase laths and the biotite grains, indicating it probably was a late crystallizing phase.

Type 6 clasts appear to represent an earlier, slightly less differentiated magma product than the other clast types (see Chapter Five). The occasional occurrence of type 6 globules in other clast types and its restriction to the siltstone breccia underlying the MacLean Extension debris flow sequence support this interpretation.

4.7. DISTRIBUTION OF GRANITOID CLASTS

4.7.1 Formation of 'granitic' and 'aplitic' groups

Two groupings may be made from the five main granitoid clast types based on grain size and textural similarities. Types 1 and 3 are highly porphyritic, show the best developed overall 'granitic' texture and together form the 'granitic' group. Types 4 and 5 are finer grained and relatively equigranular with only rare quartz and feldspar phenocrysts, commonly contain granophyric patches and have an overall 'aplitic' texture. Type 2 clasts, because of their relative equigranularity and predominantly aplitic texture are grouped together with types 4 and 5 into the 'aplitic' group. Some type 2 clasts show the granitic texture characteristic of the 'granitic' group but lack a clear phenocryst population and display a gradation in textures between the two groups.

Members of the 'aplitic' group often are white-grey, pink or red in colour (Plates 4.5, 4.7, 4.11) in contrast to the green and brown colours of most 'granitic' group clasts (Plates 4.2, 4.3, 4.4). Differences in colour within each group appear to be due to the effects of hydrothermal alteration rather than differences in primary compositions.

Similar groups were derived from the original macroscopically defined granitoid clast types of Stewart (1983) (Section 4.4.1). Groupings were based on characteristics similar to those used in the microscopic classification, i.e., quartz porphyritic, average grain size, etc. Clast types 1, 4 and 6 together form a 'granitic' group, while types 2, 5 and 7 constitute an 'aplitic' group based on groundmass textural similarities and the absence of phenocrysts (Stewart, 1983). The 'other' group consists of all clast types not assigned to the 'granitic' or 'aplitic' groups. The distribution of the macroscopically defined 'granitic', 'aplitic' and 'other' granitoid clast groups at the different study locations is shown in Table 4.2.

4.7.2 Distribution of granitoid groups

Study locations 20-13 Drift, 20-5 Sublevel and 20-6 Sublevel are exposures of the highest ore-grade breccia-conglomerates in MacLean mine (Section 4.2). Sulphide matrix ore is present at the first two locations, which are probably exposures of the same debris flow (Binney, pers. comm., 1983). The 20-6 Sublevel is over 150m east of the other two locations (Fig. 4.2) and although lacking sulphide matrix ore does attain economic ore grades due to the presence of abundant blocks of sulphide. It is probably a separate debris flow (Binney, pers. comm., 1983) as shown schematically in Figure 4.4. The 20-7 Drive study location occurs east of 20-13 Drift and slightly east of and below 20-5 Sublevel (Fig. 4.2). It is probably an exposure of the flank of the flow containing sulphide matrix ore.

Figure 4.6a shows the average grain size and volume percent occupied by all granitoid clasts at these four main study locations. There is a decrease in the size and volume of granitoid clasts between study locations 20-13 Drift, 20-5 Sublevel, 20-7 Drive and 20-6 Sublevel (Fig. 4.6a; Table 4.1).

The relative percent distribution of the 'granitic', 'aplitic' and 'other' clast groups at these locations based on both microscopic and macroscopic classification methods is shown in Figure 4.6b. The 'other' clast group consists

Figure 4.6a Histograms of the estimated volume percent occupied by granitoid clasts in debris flows at the four main study locations (see Figure 4.2). Average size (in centimeters) of granitoid clasts at each location is shown within each histogram.

Figure 4.6b Relative frequency histograms of granitoid clast groups at the four major study locations. Macroscopic classification after Stewart (1983); 'granitic' group consists of clast types 1, 4 and 6, 'aplitic' group consists of clast types 2, 5 and 7. Microscopic classification after Stewart (1984); 'granitic' group consists of clast types 1 and 3, 'aplitic' group consists of clast types 2, 4 and 5. Numbers in brackets below histograms indicate the number of clasts classified at each location by each method.

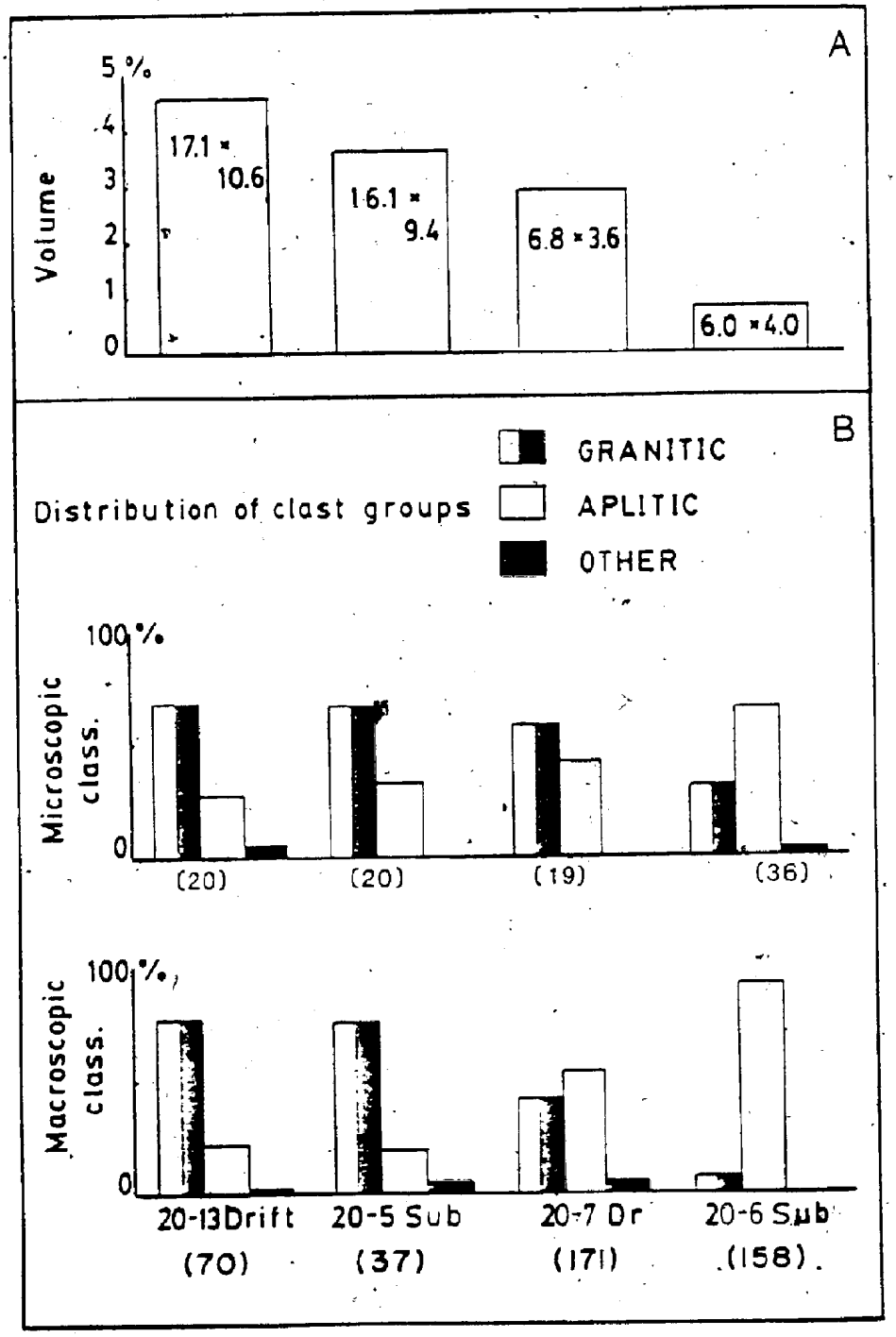
A
5 %
4
3
2
1
0
Volume
17.1 × 10.6
16.1 × 9.4
6.8 × 3.6
6.0 × 4.0
B
GRANITIC
APLITIC
OTHER
Distribution of clast groups
100 %
0
Microscopic class.
(20)
(20)
(19)
(36)
100 %
0
Macroscopic class.
20-13 Drift (70)
20-5 Sub (37)
20-7 Dr (171)
20-6 Sub (158)

of type 6 clasts (microscopic classification) and of clast types 3, 8, 9, 10, 11, and 12 (macroscopic classification). The 'granitic' group clearly predominates relative to the 'aplitic' group in 20-13 Drift and 20-5 Sublevel, whereas the 'aplitic' group constitutes the bulk of the granitoid clasts present in the 20-6 Sublevel. At 20-7 Drive, each granitoid group is present in approximately equal proportions (Fig. 4.6b).

Density is the only known mechanism active during debris flow transportation that could presumably sort the transported material. The difference in density between the sulphide clasts and all other clast lithologies probably explains their presence at the base of the debris flow sequence. The concentration of granitoid clasts with the sulphidic subunits and distribution patterns for the 'granitic' and 'aplitic' group granitoid clasts between the debris flow subunits is, therefore, considered to reflect the character of, and changes in, the source area rather than processes active during transportation.

The change in character of the granitoid clasts within one debris flow sequence (i.e. between 20-13 Drift and 20-5 Sublevel, and 20-7 Drive), and also between separate debris flow sequences (the above three locations and 20-6 Sublevel) (Figure 4.6) demonstrates an apparent change in the source of granitoid clasts from predominantly granitic to

predominantly aplitic. This change must have occurred relatively quickly, i.e., within the time needed to initiate, transport and deposit one debris flow sequence. Similarly, the pronounced change in the granitoid group population between this debris flow sequence and that exposed in 20-6 Sublevel must have taken place quickly as these flows occupy the same stratigraphic position in MacLean Extension (Fig. 4.4).

This change in granitoid clast population indicates a correlation between the 'granitic' group and the most sulphide-rich debris flow sequences. Other ore-grade debris flows that lack the sulphide-rich core are dominated by the 'aplitic' group clasts, e.g. 20-6 Sublevel. Debris flow subunits with even lower sulphide concentrations are dominated by 'aplitic' group clasts as shown by the baritic polylithic low-grade breccia-conglomerate, granitoid-bearing low-grade polylithic breccia-conglomerate, granitoid-bearing arenaceous breccia-conglomerate and baritic polylithic breccia-conglomerate exposed in 20-4 Drive and 20-7 Drive (Table 4.2). Although most granitoid clasts in the arenaceous conglomerate were too small to study in detail, 'granitic' group clasts appear to be absent or rare in this unit. Granitoid clasts are entirely absent from the baritic polylithic breccia-conglomerate subunit constituting the upper ore unit (Binney et al., 1983).

LOCATION	UNIT	Clast Groupings		
		Granitic	Aplitic	Others
★[1] 20-5 Sub (south)	granitoid-bearing ore breccia-conglomerate	28	7	2
★[2] 20-13 Drift (north)	granitoid-bearing ore breccia-conglomerate	54	15	1
★[2] 20-13 Dr (both)	polylithic breccia-conglomerate	6	28	
★[4] 20-6 Sub (south)	granitoid-bearing ore breccia-conglomerate, minor baritic polylithic breccia-conglomerate and arenaceous conglomerate (undivided)	17	141	
20-6 Sub (north)		11	249	2
★[3] 20-7 Dr (north)	granitoid-bearing arenaceous breccia-conglomerate	51	54	3
"	granitoid-bearing polylithic breccia-conglomerate	14	19	3
"	arenaceous breccia-conglomerate	6	19	2
"	baritic polylithic breccia-conglomerate		8	
☆[5] 20-1 Dr (both)	baritic low grade polylithic breccia-conglomerate		22	
☆[5] 20-4 Dr (south)	baritic polylithic breccia-conglomerate and granitoid-bearing arenaceous breccia-conglomerate (undivided)	12	137	1
" (north)		20	75	5
	TOTALS (n=1012)	219	774	19
☆[9] 20-1 Dr	siltstone breccia	5	18	7
★[1] 20-5 Sub	footwall dacitic pyroclastic	10	22	4
★[3] 20-7 Dr	ore horizon dacitic pyroclastic	5	4	
☆[7] 20-1	hangingwall dacitic pyroclastic		3	

TABLE 4.2 Abundances of the 'granitic', 'aplitic' and 'other' groups of granitoid clast types at the main study locations in MacLean Extension based on the macroscopic classification of Stewart (1983).

4.8 SUMMARY OF UNDERGROUND OBSERVATIONS

This study substantiates the observations of Thurlow (1981a) and Walker and Barbour (1981) that the granitoid clasts are the most highly rounded clasts present in the transported orebodies. They are typically the largest (average clast size) clasts present where they occur and are commonly elongate or oval in shape.

The twelve granitoid clast types originally defined macroscopically can be reduced to six on the basis of microscopic textural characteristics. Five of the granitoid clast types describe a continuum from porphyritic trondhjemite and microtrondhjemite to granophyric aplite. The fine grain size of the groundmass and range in textures are interpreted to indicate relatively rapid crystallization of a magma in environments ranging from sub-volcanic to plutonic. Type 6 clasts are not common in MacLean Extension in ore zone debris flow subunits, and are largely restricted to the siltstone breccia underlying the ore zone. Type 6 clasts are mineralogically and texturally distinct and are considered to be products of an earlier crystallized magma phase.

The granitoid clast types are reduced to 'granitic' (types 1 and 3), 'aplitic' (types 2, 4 and 5) and 'other' (type 6) groups based on average grain size and groundmass textural similarities. 'Granitic' group clasts are typically more pervasively hydrothermally altered than the 'aplitic' group clasts. The introduction of calcite, barite and quartz, with sericitization of plagioclase crystals and chloritization of the mafic phases (biotite and amphibole) are the mineralogical expressions of the hydrothermal alteration. Clasts of both groups, but especially 'aplitic' group clasts, show a secondary hematite dust on the plagioclase grains. Some 'granitic' group clasts show evidence of protoclastic textures and an apparent genetic relationship between alteration and brecciation.

The largest granitoid clasts (average clast size) are found intimately associated with the greatest concentration of sulphide mineralization, as exemplified by granitoid-bearing polylithic breccia-conglomerate adjacent to sulphide matrix ore (e.g., 20-13 Drift and 20-5 Sublevel). A similar correlation exists between the maximum volume percent of a debris flow subunit occupied by granitoid clasts and the sulphide concentration. Average size and volume percent occupied by granitoid clasts decrease with increasing distance from sulphide matrix ore (e.g., 20-7 Drive and 20-4 Drive). Other sulphide-rich

members of the lower ore unit that lack the sulphide matrix ore subunit contain a greater number of granitoid clasts. These clasts are smaller and occupy less volume than those seen in polylithic breccia-conglomerate associated with sulphide matrix ore. These size and volume changes are accompanied by a a transition from 'granitic' to 'aplitic' group clasts in polylithic breccia-conglomerate with increasing distance from sulphide matrix ore. The 'granitic' group clasts predominate where sulphide matrix ore is present, e.g., 20-13 Drift and 20-5 Sublevel. "Aplitic' group clasts predominate in the subsequent less sulphidic debris flow subunits that contain smaller and better rounded clasts. A decrease in relative degree of hydrothermal alteration exhibited by the granitoid clasts accompanies the change from 'granitic' to 'aplitic' group clasts.

Chapter Five

GEOCHEMISTRY

5.1 INTRODUCTION

5.1.1 Statement of purpose

There are three primary purposes to the geochemical investigation: 1) to qualitatively describe the chemical effects of alteration on the granitoid clasts; 2) to determine if all granitoid clasts were derived from the same source (i.e. are comagmatic); 3) to evaluate the suggestion of Thurlow (1981a,b) that Buchans Group felsic volcanic rocks, the granitoid clasts and the Feeder Granodiorite are comagmatic.

It is not the intent of this study to provide an empirical evaluation of the alteration of the granitoid clasts. Without a method to demonstrate the primary unaltered magmatic composition of the clasts, quantitative estimations of the chemical changes resulting from hydrothermal alteration are difficult if not impossible. No attempt is made to model the petrogenesis of the granitoid clasts. The distinction between the effects of partial

melting in the source region of the melt and the effects of differentiation by fractional crystallization is not made. The rocks examined are assumed to be the products of partial melting and to have originally been a liquid. The discussion focuses on geochemical changes due to fractional crystallization of this liquid.

Details of the analytical methods used in this study and estimates of the accuracy and/or precision are discussed in Appendices 1, 2 and 3. Tables of the complete analytical results are given in Appendix 5. The low major element total for some samples (e.g., KQS-82-051) is due to the abundance of barium which is reported in ppm rather than % oxide and therefore is not included in the major element total. Low totals combined with LOI values result in substantial increases in the anhydrous major element compositions, especially SiO2. The low totals should not be considered to be a reflection on the quality of the major element data (see Appendix 1).

5.1.2 Method for establishing comagmatism

Prerequisites for examining the potential comagmatism of two or more suites of igneous rocks are: 1) a simple geological setting; and 2) narrowly prescribed spatial and age limits (Wilcox, 1979). For example, a suite of rocks may be produced in the same location but at different times, and show trends typically indicative of magmatic evolution, e.g., Aden volcano, South Yemen (Hill, 1974). In this case, the granitoid clasts are spatially related and were deposited in submarine debris flows within a restricted stratigraphic unit, i.e. the Buchans River Formation (Thurlow and Swanson, 1985). Similarly, the granitoid clasts, Buchans Group volcanic rocks and the two Feeder Granodiorite bodies all occur in the Buchans area (Chapters Three and Four). Previous age determinations on Buchans Group volcanic rocks and the Feeder Granodiorite give dates of 447±18 Ma and 410±80 Ma, respectively and suggest comagmatism of these rock units (Bell and Blenkinsop, 1981). Other geochronological data for a granitoid clast and Buchans River Formation rhyolite are given in Chapter Six.

Unaltered comagmatic igneous rock suites generally display compositional diversity with much of the variation gradational (Brown, 1979). Magmas become differentiated during cooling due to either crystal sorting (i.e.,

filter-pressing, flowage differentiation, gravity crystal sorting, or fractional crystallization), liquid immiscibility or gaseous (fluid phase) transfer (Bowen, 1928; Brown, 1979). Fractional crystallization results when earlier formed crystals and remaining melt become separated before chemical equilibrium between the solid and liquid phases is attained. The result is a depletion in the melt of those components forming the crystals (Presnall, 1979). The observed diversity of igneous rocks is also due, at least in part, to incremental degrees of melting in the source region of the magma (partial melting or fusion) (Bowen, 1928; Presnall, 1979). The relative importance of these different processes, differentiation and partial melting, to explain observed chemical differences in igneous rocks is seldom equivocal (Presnall, 1979).

Although it is preferable to use aphyric or phenocryst-poor lavas to examine the chemical evolution of a magma (Bowen, 1928; Wilcox, 1979), similar patterns indicative of magmatic evolution can be seen in plutonic rocks, e.g., the Skaergaard intrusion (Wager and Brown, 1968). There is, however, some doubt as to whether the bulk plutonic rock composition represents a magmatic liquid on the liquid line of descent (Wilcox, 1979). Differential gravitational settling of different mineral species during crystallization and late-stage hydrothermal alteration

effects can produce changes in the bulk composition from that predicted by chemical evolution of the magma (Wilcox, 1979). The resultant composition is therefore not related entirely to the chemical evolution of the parent liquid. The abundances of elements that appear to be immobile during rock alteration, however, allows one to determine the chemical changes related to alteration and recognize primary geochemical patterns (Cann, 1970; Alderton et al., 1980). Plutonic rocks, although not a direct measurement of the evolution of the magma, do demonstrate changes in bulk composition that can be explained (at least partially) by magmatic evolution.

Variation diagrams are effective in illustrating the course of chemical evolution of a magma (Bowen, 1928; Wilcox, 1979) and in investigating whether the origin of the observed chemical differences in the rocks are due to fractional crystallization or partial melting (Bowen, 1928; Presnall, 1979), liquid immiscibility (Roedder, 1979), volatile transfer (Burnham, 1979) or thermo-gravitational diffusion (Shaw et al., 1976; Hildreth, 1979).

Igneous rock types are generally distinguishable by their average major element contents (e.g. Nockolds, 1954; De La Roche et al., 1980) although the calculation of means and standard deviations to do so may obscure meaningful differences in the frequency distribution of the data, e.g.,

polymodality (Ehrlich, 1984). The natural heterogeneity of rocks and analytical scatter ubiquitous to geochemical analysis prevent meaningful conclusions from single analyses. Plotted analyses of several samples of a rock population will define a 'field' on a variation diagram representative of that population. This approach permits the recognition of genetically related igneous rock suites based on pairs or sets of chemical components, e.g., SiO2 and Na2O+K2O for granitoids (White and Chappell, 1983), Ti, Zr and Y for basalts (Pearce and Cann, 1973), however the prudence of this approach has recently been questioned (Whitten et al., 1984).

Similar major element contents are generally insufficient to establish or refute comagmatism. This is understandable since the earth's crust is almost entirely composed of the major elements (Mason, 1966) as reflected by the composition of the most common rock-forming minerals (olivine, pyroxenes, amphiboles, micas, feldspars and quartz). Since igneous rock classifications (Streckeisen, 1967, 1976; Bowden et al., 1984) are commonly based on mineral abundances, rock types that were formed in different tectonic settings, by different processes and from different source rocks often have the same mineralogical proportions and are often indistinguishable solely on the basis of major element compositions (De La Roche et al., 1980).

Trace element abundances, both those that form mineral species in which they are a stoichiometric component, e.g., Zr and zircon, or those that substitute for a geochemically similar major element in one of the major rock-forming or accessory minerals (e.g., Rb, Sr, Y, Nb, Ga) can be used to constrain the possible source region and petrogentic history of a rock (e.g., Ludden et al., 1982).

The ability of a trace element to substitute for a major element is determined by the atomic size and valence state of the element and the crystal lattice structure of the host mineral. Some elements become enriched or depleted in the melt relative to the solid phases during progressive crystallization depending on the phases crystallizing and the geochemical behavior of the element(s) in question (Taylor, 1965; Hanson, 1978, 1980). The degree of compatiblity of an element in the crystallizing phases has been estimated from studies in experimental petrology (e.g., Snetzler and Philpotts, 1970) and naturally occurring rocks (e.g., Hildreth, 1979). The measure of compatability is expressed by the partition coefficient for an element (Arth, 1976). and coefficients have been determined for many elements between various mineral phases and the melt, and between the melt and a vapor phase.

The whole rock trace element concentration is not, however, simply determined by mineral proportions in igneous rocks. The mineral proportions are controlled by the major element composition and the conditions of crystallization (Hanson, 1980). Other factors that control the trace element concentration in a melt (Hanson, 1978, 1980) include: 1) the original trace element concentration in the melt that is dependent on the composition of the source rock; 2) the extent of partial melting, and the mineralogy of the residue remaining at the time of separation of the melt from the residue; 3) differentiation of the melt prior to complete crystallization; and 4) chemical interactions between rocks, melts and fluids during or subsequent to crystallization. Thus, the mineral phases present do not control the trace element composition of a crystallized melt, the complete petrogenetic history and composition of the source of the melt does (Hanson, 1980).

Trace elements that have similar geochemical behaviors during petrogenetic processes because of similar atomic radii and valence states and that are relatively incompatible in the main crystallizing phases, e.g., Zr, Y, REE and other high field strength (HFS) elements, are concentrated in the melt relative to the solid phases during crystallization (Taylor, 1965; Hanson, 1978, 1980). Their abundances can be useful indicators of the degree of

magmatic differentiation (Pearce and Cann, 1973; Winchester and Floyd, 1977; Wood et al., 1979; Palacious et al., 1979; Bailey, 1981). Trace elements have been used to 'fingerprint' the tectonic setting, and hence, source rock and petrogenetic processes involved in the formation of an igneous rock (Cann, 1970; Pearce and Cann, 1973; Jakes and White, 1972; Winchester and Floyd, 1977; Floyd and Winchester, 1978; Hanson, 1978; Palacios et al., 1979; Donnelly and Rogers, 1980; Bailey, 1981; Ludden et al., 1982; Pearce et al., 1984). The distinction between products from all tectonic settings may not be possible (e.g., Wood et al., 1979; Prestvik, 1982), however, this approach can reduce the number of possible geological settings to be considered.

The elements that have been shown to be most effective in discriminating the petrogenetic history of common felsic igneous products are K, Na, Ba, Rb, and Sr (McCarthy and Hasty, 1976; Hanson, 1978; McCarthy and Fripp, 1978; Leonova, 1979; Collins et al., 1983; Lee and Christiansen, 1983; Whelan, 1983; White and Chappell, 1983). The major volumetric crystallizing phases in a felsic (>65% SiO2) magma are hornblende, biotite, plagioclase, potassium feldspar and quartz, although the crystallization of some accessory phases may significantly affect the trace element composition of the melt (e.g., Miller and Mittlefelhdt,

1982). Calcium, potassium and sodium are the dominant cations in feldspar after alumina. Barium, rubidium and strontium can substitute for these elements during crystallization. The degree with which they substitute for the major elements during progressive crystallization is relatively well understood, and useful in interpreting the origin of fresh, unaltered felsic igneous rocks (e.g., McCarthy and Fripp, 1976; McCarthy and Hasty, 1978; Hanson, 1978). Unfortunately, these same elements are typically mobile during hydrothermal alteration (Hart et al., 1974; Condie et al., 1977; Humphris and Thompson, 1978; Gelinas et al., 1982; Ludden et al., 1982; Thompson, 1983) thereby reducing their usefulness in studies of altered igneous rocks.

Petrographic evidence of hydrothermal alteration of the granitoid clasts is substantiated by the geochemical data (Section 5.2) and reduces the potential usefulness of these elements in this study. Other elements frequently used for magmatic discrimination, such as Cr, Ni and U (Donnelly and Rogers, 1980; Bailey, 1981), were precluded from a similar use in this study because they are only present in the granitoid clasts and Feeder Granodiorite at or near the detection limits of the analytical methods used.

The HFS elements, such as Al, Zr, Ti, Y and rare earth elements (REE), appear to be relatively immobile during most secondary processes (Cann, 1970; Pearce and Cann, 1973; Hart et al., 1974; Herrmann et al., 1974; Condie et al., 1977; Humphris and Thompson, 1978; Alderton et al., 1980; Ludden et al., 1982; Dostal and Strong, 1983; Thompson, 1983; Hallberg, 1984). However (at least some of) these elements may become mobile within zones of intense hydrothermal alteration associated with massive sulphide mineralization (Roberts and Reardon, 1978; MacGeehan and MacLean, 1980; Finlow-Bates, 1980; Finlow-Bates and Stumpfl, 1981; Kalogoropoulos, 1983), copper porphyry mineralization (Taylor and Fryer, 1980, 1982) and some gold occurrences (Rosylyakova and Rosylyakova, 1975; Kerrich and Fryer, 1979; Ludden et al., 1984). In contrast to the conclusions of MacGeehan and MacLean (1980), the use of zirconium is suggested by Finlow-Bates and Stumpfl (1981) to indicate the degree of magmatic differentiation, even after the intense hydrothermal alteration associated with massive sulphide formation.

The rare earth elements (REE) have been used frequently in trace element studies because of their geochemical coherence during most petrogenetic processes (Taylor, 1965; Hanson, 1980). This is attributable to their common valence state (+3) under most geologic conditions and a regular but

slight change in ionic radii from 1.03 angstroms for La to 0.86 angstroms for Lu (Hanson,, 1980). They commonly show relatively limited mobility during many secondary processes (e.g., Herrmann et al., 1974; Condie et al., 1977; Ludden et al., 1982), although there is some evidence that they may become mobile during severe (i.e. high water to rock ratios) hydrothermal alteration (Alderton et al., 1980; ; Hanson, 1980; MacGeehan and MacLean 1980; Taylor and Fryer, 1980,1982; Chatterjee and Strong, 1984). Their mobility also appears to be related to the composition of the hydrothermal fluids (e.g., F, Cl, CO2 -bearing) (Taylor and Fryer, 1983; Ludden et al., 1984). The geochemical coherence of the REE as a group, especially during magmatic processes, and their collective relative immobility during most secondary processes suggests that the relative abundances of the REE permits the use of their relative abundances as a 'fingerprint' of the source rock and degree of magmatic differentiation.

The abundances of REE are frequently normalized to the average abundance of REE in chrondritic meteorites (Coryell et al., 1963; Hanson, 1980). This normalization reduces the effects of the Oddo-Hawkins rule of cosmic abundances, which states that even numbered elements are more abundant than adjacent odd-numbered elements, thereby permitting a simplified and standardized graphical evaluation of their

relative abundances. When normalized and plotted as a group, they define a line or REE pattern. The degree of enrichment in particular REE or part of the REE group in an igneous rock is an indication of the source material and petrogenetic process that formed the rock (Hanson, 1980). For example, the fractionation of amphibole has a different effect on the REE than the fractionation of feldspar because of slightly different partition coefficients for individual REE in these minerals (Arth, 1976; Hanson, 1980). Amphibole preferentially absorbs the middle REE and heavy REE (less so) relative to the light REE, and contributes to a postive Eu anomaly in the melt (Hanson, 1980). In contrast, the feldspars, especially potassium feldspar, preferentially allows Eu into its crystal lattice because Eu does occurs in the +2 valence state, unlike the other REE, and can substitute for Sr in this phase (Hanson, 1980). Partition coefficients are merely the best estimates at present and different estimates for any element may differ significantly (see Whelan, 1983 for a comparison of some estimates).

The clear visual evidence of hydrothermal alteration (Chapter Four) and the absence of a means to demonstrate or estimate the primary unaltered composition of the granitoid clasts require an assumption of relative immobility of the trace elements used. There are a number of alteration

studies that have shown the HFS elements to be relatively immobile in altered or metamorphosed rocks (Cann, 1970; Hart et al., 1974; Floyd and Winchester, 1978; Humphris and Thompson, 1978; Alderton et al., 1980; Finlow-Bates and Stumpfl, 1981; Ludden et al., 1982; Campbell et al., 1984) and probably a similar number that indicate some mobility for these elements (e.g., Roberts and Reardon, 1978; MacGeehan and MacLean, 1980). Despite the lack of unequivocal evidence of their 'immobility' in the granitoid clasts, emphasis has been placed on their abundances because they are generally the most 'immobile' elements except during the most intense secondary processes (Campbell et al., 1984). The HFS elements are also useful indicators of the degree of magma differentiation and the tectonic setting, and are therefore considered to be the most appropriate elements available in this study to demonstrate comagmatism. In this study, Ti, Zr, Y, V, Nb and REE are emphasized for this purpose.

The approach is similar to that used by Goldie (1979) to establish comagatism between intrusive and extrusive rocks in the Noranda area. Similar abundances of these relatively immobile, discriminatory trace elements as shown on variation diagrams are interpreted to indicate a probable common origin for the igneous rocks examined, i.e., comagmatism. Similar REE patterns on standard,

chondrite-normalized REE diagrams for different rock units are considered to also suggest a possible comagmatic origin for the rocks examined.

5.2 CHEMICAL EFFECTS OF ALTERATION

5.2.1 Alteration of the granitoid clasts

The ranges of and mean major and trace element concentrations in the six granitoid clast types (defined in Chapter Four) are very similar (Tables 5.1, 5.2). All granitoid clasts are felsic in composition, and silica-saturated with SiO2 contents greater than 70% (anhydrous). They are peraluminous ($Al_2O_3 \leq Na_2O+CaO+K_2O$) and subalkaline (as defined by Irvine and Baragar, 1971).

The greater proportion of plagioclase, biotite, amphibole and magnetite in the type 6 clasts relative to the other clast types reflects their more intermediate character (Chapter Four) and is indicated by their major element chemistry, i.e., lower SiO2, higher Al_2O_3, Fe_2O_3, CaO, MgO, TiO_2, and P_2O_5 than the other granitoid clast types (Tables 5.1, 5.2). The mean compositions of types 1 through to 5 show, in addition to increasing SiO2 values, decreasing TiO_2, Fe_2O_3, MnO, MgO and CaO (Tables 5.1, 5.2). The alkalis, sodium and potassium, do not show a regular

TABLE 5.1 Range of major and trace element contents in granitoid clasts

	Type 1 (71)	Type 2 (5)	Type 3 (12)	Type 4 (6)	Type5 (1)	Type 6 (3)
SiO2	67.8-75.4	71.9-76.4	71.5-76.8	76.1-78.1	77.30	67.4-69.4
TiO2	0.08-0.30	0.08-0.28	0.05-0.23	0.08-0.23	0.13	0.33-0.43
Al2O3	10.6-12.8	9.9-11.8	8.3-12.5	10.1-11.4	11.6	13.5-14.1
Fe2O3*	0.83-3.45	0.45-2.50	0.48-2.72	0.84-1.36	0.85	3.40-4.43
MnO	0.04-0.09	0.02-0.06	0.02-0.07	0.04-0.07	0.03	0.06-0.09
MgO	0.34-1.24	0.30-1.12	0.22-1.24	0.20-0.59	0.30	0.97-1.76
CaO	1.87-3.57	1.41-2.20	1.72-3.29	1.00-2.47	1.17	2.61-4.00
Na2O	2.86-4.68	2.79-5.60	2.62-4.34	3.04-5.80	3.93	4.18-5.31
K2O	0.90-1.79	1.70-2.84	0.39-1.66	0.20-1.37	3.08	0.53-1.38
P2O5	0-0.34	0-0.09	0.01-0.07	0-0.19	0.03	0.08-0.38
LOI	2.09-4.25	1.58-3.35	2.36-4.50	1.06-3.32	1.26	1.93-3.61
Pb	10-852	7-271	11-180	22-110	43	11-25
Th	4-16	7-19	5-17	13-18	20	7-10
U	0-6	0-4	0-5	1-5	5	0-2
Rb	15-32	3-44	9-26	4-22	39	5-24
Sr	143-530	184-446	187-888	224-274	170	235-340
Y	11-29	16-36	5-23	8-41	19	22-38
Zr	79-126	88-143	56-105	73-149	86	70-129
Nb	3-6	4-6	2-7	1-8	7	4-5
Zn	60-388	24-320	33-414	30-128	29	28-203
Cu	16-85	11-165	19-59	14-38	14	14-25
Ni	0-3	0	0	0	0	0-1
Ba	236-25455	4252-22289	2580-40746	4970-12322	3942	473-4502
V	12-59	13-60	9-61	10-26	12	59-76
Cr	0	0	0	0	0	0
Ga	6-15	8-13	2-11	8-11	7	12-13

* Total iron reported as Fe2O3

0 = measured abundance is below analytical detection limit (1 ppm)

Table 5.2 Mean (standard deviation) abundances in the granitoid clast types from MacLean Extension.

	Type 1		Type 2		Type 3		Type 4		Type 5	Type 6	
SiO_2	72.31	(2.00)	74.02	(2.18)	74.13	(1.77)	77.84	(.79)	77.3	68.17	(1.08)
TiO_2	0.18	(.06)	.19	(.08)	.13	(.05)	.15	(.06)	.13	.35	(.05)
Al_2O_3	11.78	(.80)	10.94	(.73)	10.86	(1.08)	10.70	(.49)	11.6	13.77	(.31)
Fe_2O_3	1.98	(.91)	1.51	(.76)	1.10	(.59)	1.11	(.19)	.85	3.94	(.52)
MnO	.07	(.02)	.05	(.02)	.05	(.01)	.05	(.01)	.03	.07	(.02)
MgO	.76	(.34)	.59	(.34)	.48	(.27)	.35	(.16)	.30	1.32	(.40)
CaO	2.54	(.50)	1.69	(.32)	2.44	(.51)	1.58	(.59)	1.17	3.16	(.74)
Na_2O	3.73	(.58)	4.45	(1.07)	3.72	(.51)	4.84	(1.11)	3.93	4.65	(.59)
K_2O	1.30	(.29)	0.95	(1.10)	1.18	(.32)	.53	(.47)	3.08	.93	(.43)
P_2O_5	.06	(.10)	.03	(.04)	.04	(.02)	.04	(.07)	.03	.21	(.15)
LOI	3.20	(.72)	2.53	(.68)	3.41	(.69)	2.09	(.84)	1.26	2.57	(.91)
TOTAL	97.91		96.95		97.54		98.44		99.68	99.18	
TRACE ELEMENTS (ppm)											
Pb	172	245	110	126	74	54	66	34	43	16	8
Th	12	3	12	5	12	4	16	2	20	8	2
U	2	2	1	2	1	2	3	2	5	1	1
Rb	22	5	16	17	20	5	9	8	39	14	10
Sr	304	112	310	126	403	238	244	16	170	277	56
Y	28	7	25	8	15	5	32	12	19	28	9
Zr	100	18	116	22	80	13	127	27	86	105	31
Nb	4	1	5	1	5	2	5	3	7	5	1
Zn	157	93	142	138	143	102	64	35	29	98	93
Cu	37	19	57	63	36	12	25	8	14	19	6
Ni	0	-	0	-	0	-	0	-	0	0	-
Ba	7943	7515	12455	8566	13456	11510	8055	2403	3942	1829	2314
V	38	14	30	20	33	15	17	6	12	70	9
Cr	0	-	0	-	0	-	0	-	0	0	-
Ga	10	3	10	2	8	3	9	1	7	12	1
n	11		4		12		6		1	3	

0 = measured abundance is below analytical detection limit (1 ppm)

variation between types 1 through to 5, in accord with the evidence of alkali metasomatism presented below (Fig. 5.1). Ranges indicate that types 1 and 3 (granitic group) are more variable in composition than the 'aplitic' group member (types 2, 4 and 5).

Hydrous and other volatile-bearing minerals are commonly produced during hydrothermal alteration. Secondary hydrous minerals (sericite and chlorite) and other volatile-bearing minerals (calcite and barite) are present in all granitoid clasts (Chapter Four). The presence of calcite, barite, sericite and quartz in the groundmass of the 'granitic' group clasts is ubiquitous and pervasive. The same minerals also commonly occur as veins in the 'aplitic' group clasts and replacing plagioclase phenocrysts. The abundance of these secondary minerals will presumably increase with increasing intensity or duration of alteration, therefore, loss on ignition (LOI) content can provide a qualitative measure of the intensity of alteration. The relatively high LOI values (Table 5.1) of the granitic group clasts (types 1 and 3) demonstrates their more intense hydrothermal alteration relative to the 'aplitic' group clasts. Such clear evidence of alteration suggests that the major element composition of the clasts may probably have been modified by this alteration.

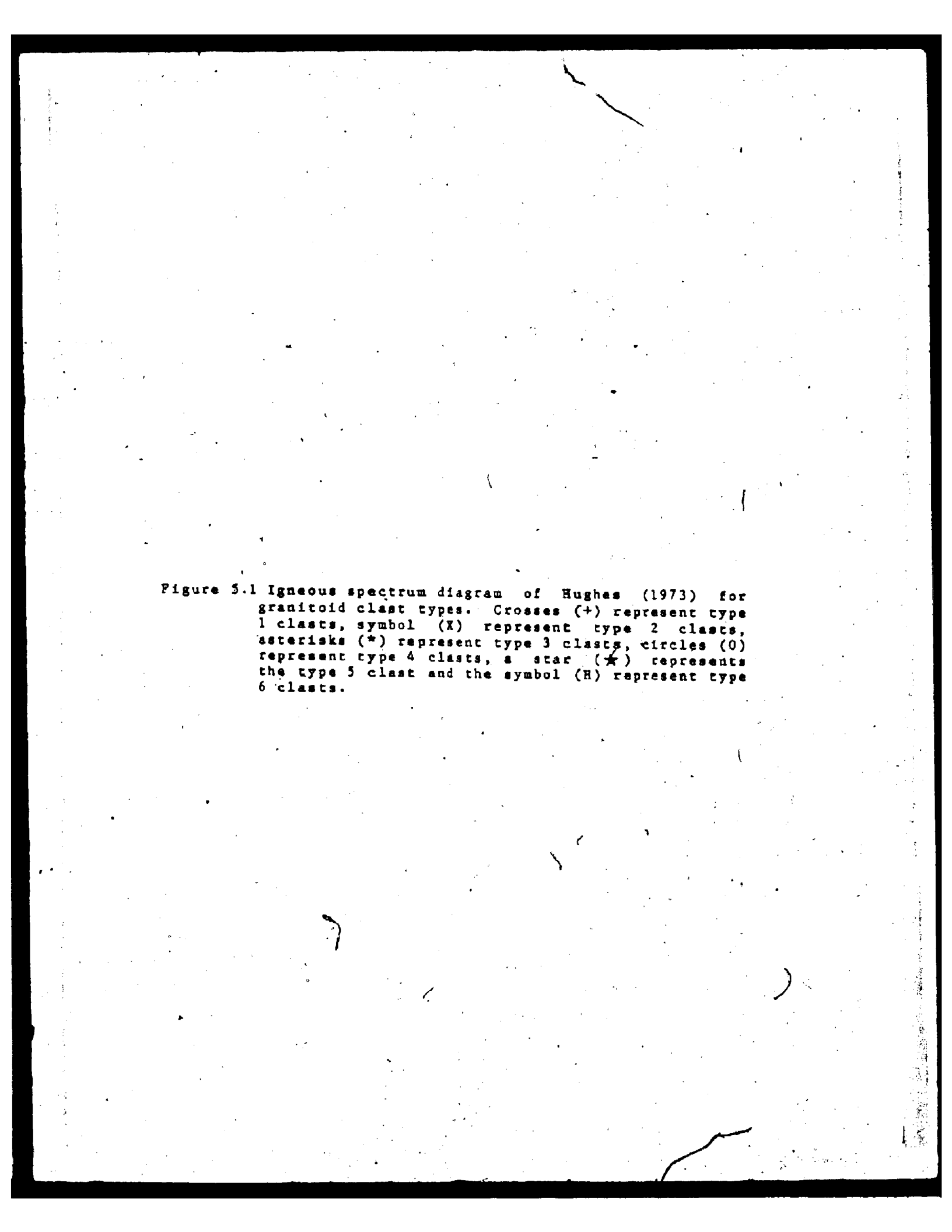

Figure 5.1 Igneous spectrum diagram of Hughes (1973) for granitoid clast types. Crosses (+) represent type 1 clasts, symbol (X) represent type 2 clasts, asterisks (*) represent type 3 clasts, circles (0) represent type 4 clasts, a star (★) represents the type 5 clast and the symbol (H) represent type 6 clasts.

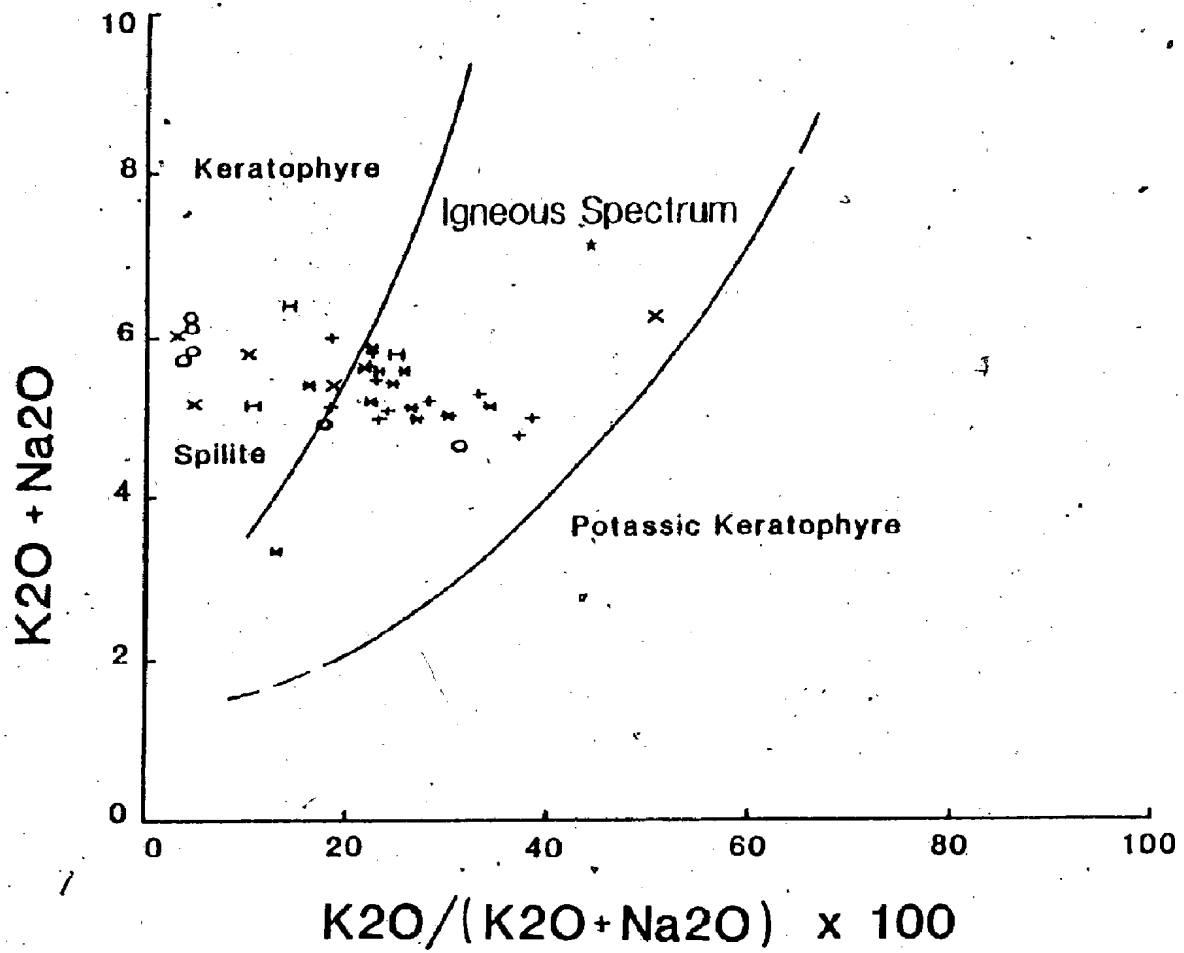
10
8
6
4
2
0
Keratophyre
Igneous Spectrum
Spilite
Potassic Keratophyre
K2O + Na2O
0
20
40
60
80
100
K2O/(K2O+Na2O) x 100

One method that can be used to test the effect of alteration on the granitoid clasts is the alkali diagram of Hughes (1973). On this diagram, unaltered common igneous rocks will plot in the 'igneous spectrum' field. Igneous rocks that plot outside this field are considered to indicate some form of alkali metasomatism and are termed spilites or keratophyres. In Figure 5.1, most clasts fall within the igneous spectrum, whereas some do not. The visually less altered 'aplitic' group clasts (types 2, 4 and 5) indicate greater alkali mobility than the more obviously and pervasively altered 'granitic' group clasts and plot in the keratophyre field (Figure 5.1). Based on mean potassium and sodium contents in the clast types that form these groups (Table 5.2), the 'aplitic' group clasts (types 2 and 4 especially) appear to have lost potassium and possibly gained sodium during this alkali metasomatism. In contrast however, the type 5 clast does not appear to have suffered a loss of potassium (Table 5.2; Figure 5.1).

The greater abundance of calcite in the 'granitic' group clasts probably accounts for their higher mean CaO values (types 1 and 3) (Table 5.2) and is expressed in the Na/K/Ca diagram (Fig. 5.2) by the shift of the 'granitic' group clasts toward the Ca apex. A shift of the 'aplitic' group clasts toward the Na apex is also apparent.

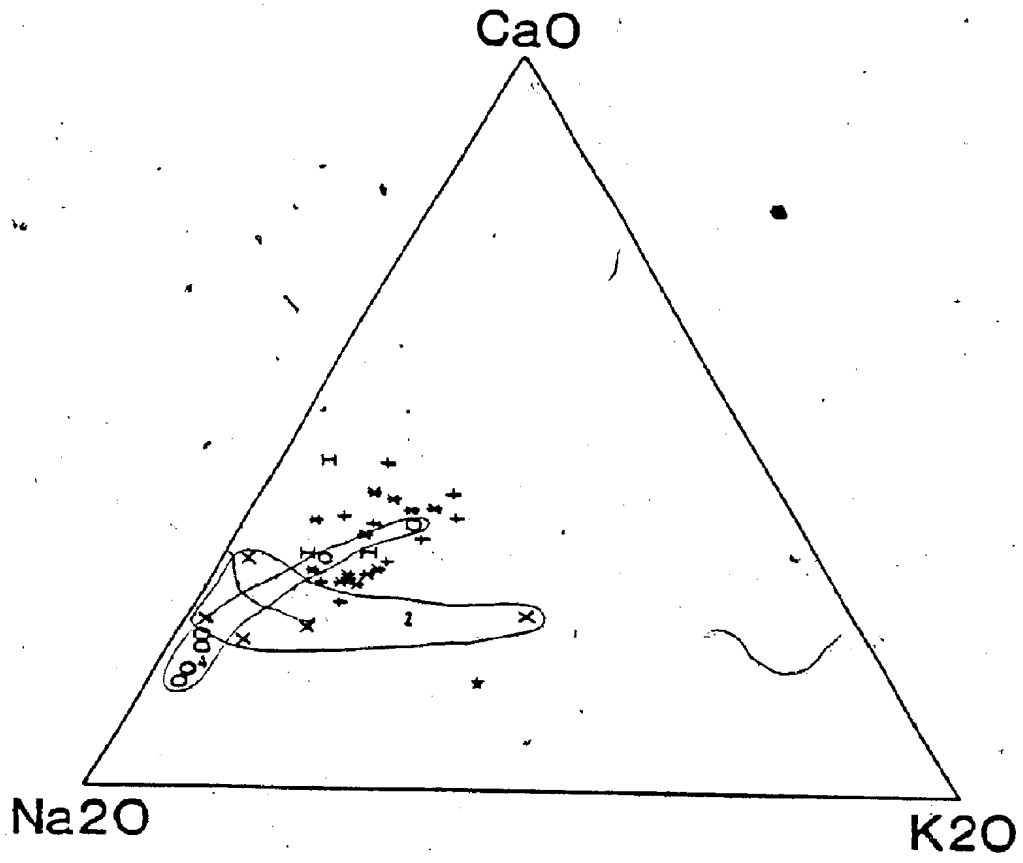

FIGURE 5.2 $Na_2O/K_2O/CaO$ diagram for granitoid clast types. Symbols as defined in Figure 5.1. Fields of type 2 and 4 (aplitic group) granitoid clasts are shown.

The barium contents are characteristically high in Buchans Group volcanic rocks (Thurlow, 1981a). This is also true for granitoid clast types 1 - 5 (Table 5.2). Secondary barite is commonly observed in these clasts partially replacing plagioclase grains and associated with quartz and calcite veins (Chapter Four). The positive correlation between Ca and Ba contents and loss-on-ignition values is evident in Fig. 5.3. The higher degree of hydrothermal alteration observed in thin sections of types 1, and 3 relative to the other clast types is clearly expressed by the higher concentration of these components. The lower Ca and Ba contents with correspondingly low LOI values indicate the weaker effect of this alteration process on the type 2, 4 and 5 clasts.

The hematite staining of plagioclase grains in the 'aplitic' group clasts may be related to the alkali metasomatism indicated by Figure 5.1. The loss of a volatile phase during rapid crystallization could remove potassium and other incompatible phases that are typically concentrated in an exsolved vapor or fluid phase. The iron-bearing nature of this phase as proposed by Stanton and Ramsay (1980) may account for the hematite stains observed.

The positive correlation between Ca and Sr (Fig. 5.4) suggests that they have been controlled by the same chemical

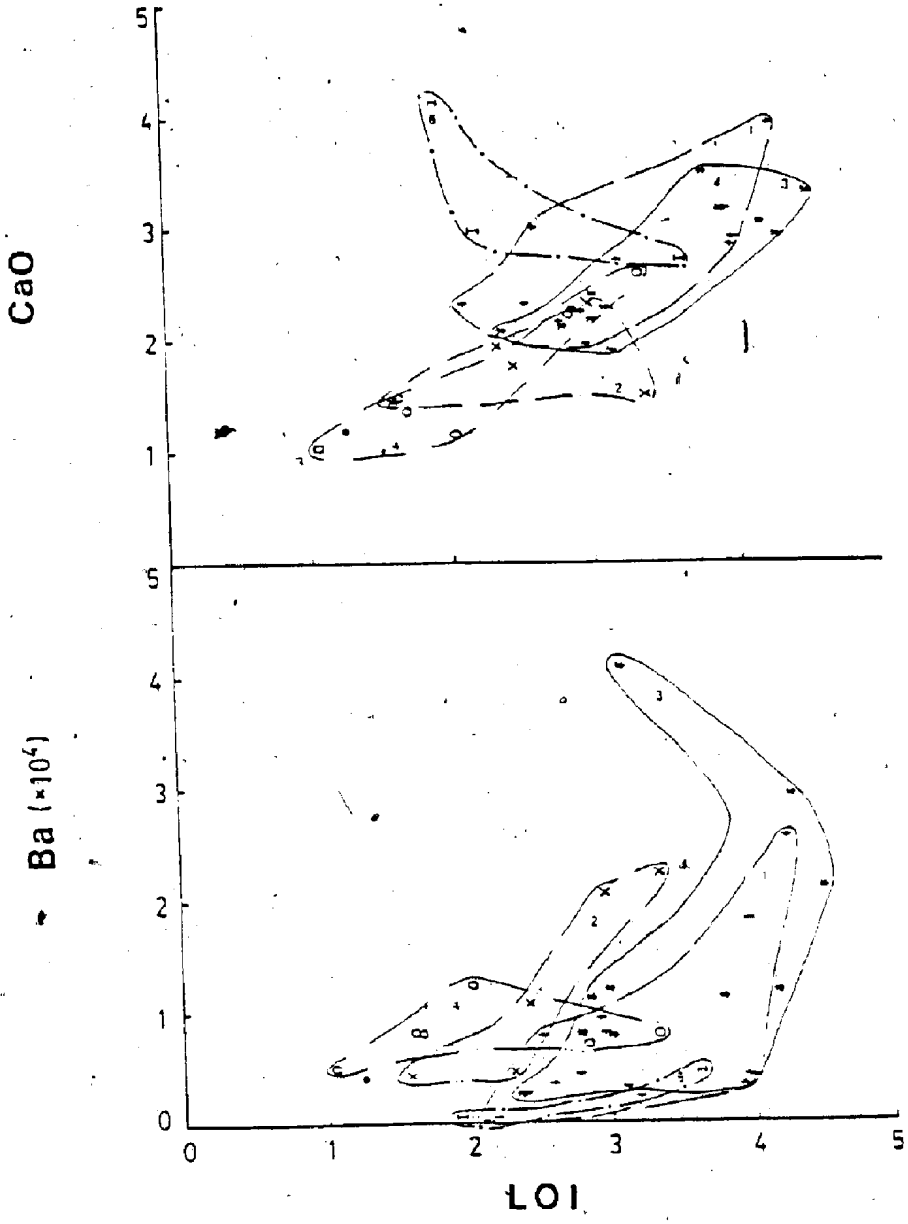

FIGURE 5.3. Loss-on-ignition (LOI, weight %) vs. Ba ($x10^4$ ppm) and CaO (weight %) variation diagrams for the granitoid clast types. Symbols as defined in Figure 5.1.

reaction (Humphris and Thompson, 1978). Although Sr can substitute for Ca in plagioclase, the positive correlation between CaO and LOI (Fig. 5.3) suggests that Sr may have substituted for Ca in the calcite crystal lattice.

The presence of secondary silica in the granitoid clasts is interpreted to have resulted from hydrothermal alteration (Chapter Four). The high-silica nature of the clasts is indicated by their high mean SiO2 abundances (Table 5.2). When SiO2 is plotted against the Agpaiitic index (Na2O+K2O/Al2O3) (Fig. 5.5), the higher SiO2 content of the clasts relative to the Feeder Granodiorite bodies is evident, and is interpreted to express silicification of the granitoid clasts. The highly variable nature of the alkali metasomatism of the granitoid clasts is demonstrated by the large scatter of the granitoid clasts in Fig. 5.5.

5.2.2 Alteration of the Feeder Granodiorite

The relative lack of alteration in the Wiley's River Intrusion and the Topsail granite observed visually is verified on the Hughes (1973) alkali diagram (Fig. 5.6). The Little Sandy Lake Intrusion shows evidence on this diagram of alkali metasomatism similar to that seen in the aplitic group (Fig. 5.1) and by the shift in the field of the Little Sandy Lake Intrusion toward the Na apex on the Na/K/Ca diagram (Fig. 5.7). The Little Sandy Lake Sequence

Figure 5.4 CaO (weight %) vs. Sr (in ppm) variation diagram. Crosses (+) represent Topsails granite (TS) samples, circles (O) represent the Wiley' River intrusion (WR) samples, asterisks (*) represent Little Sandy Lake intrusion (LS), the symbol (H) represent rhyolites from the Little Sandy Lake area, the symbol (X) represent granitoid clasts and the star (★) is the rhyolite from the Buchans River Formation in MacLean Extension used in the geochronology study.

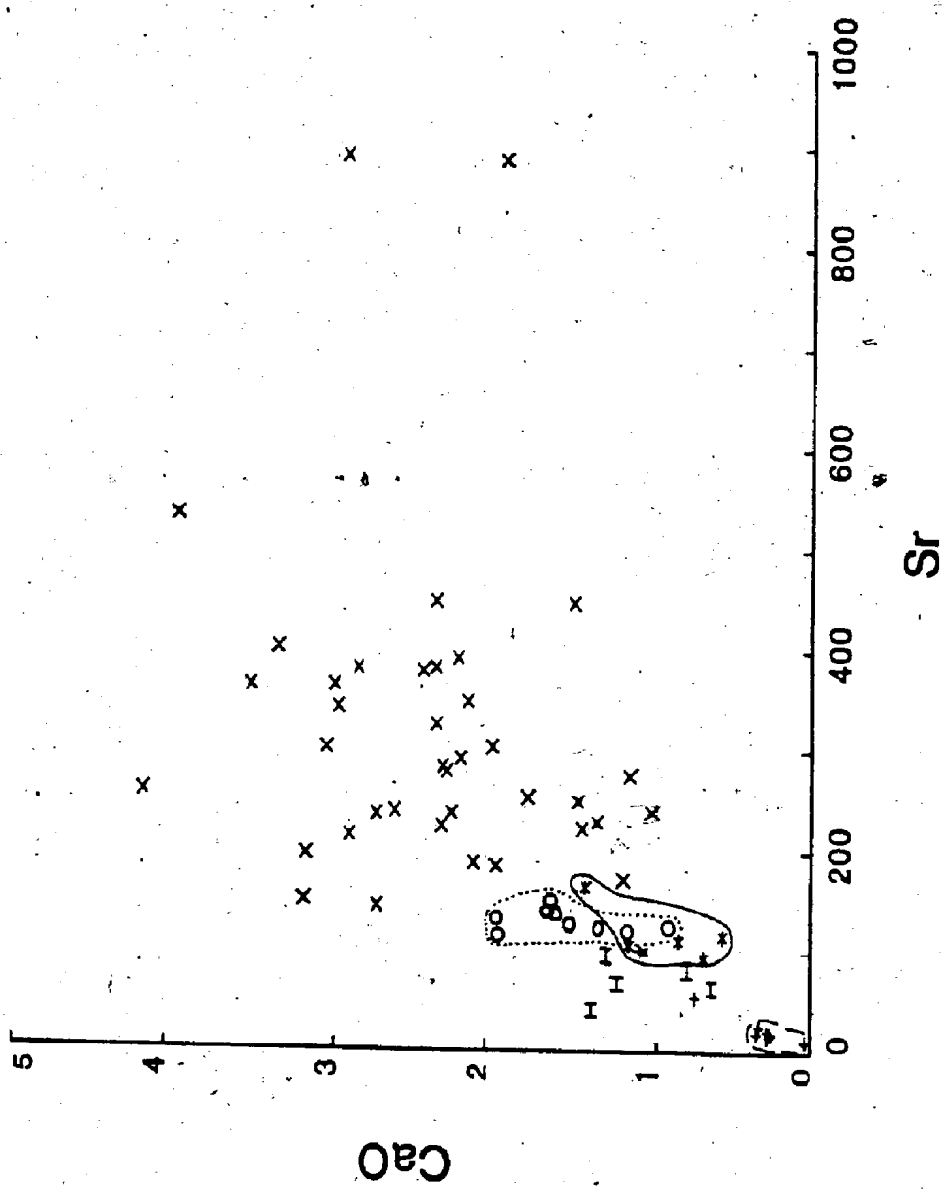
CaO
Sr
0
1
2
3
4
5
0
200
400
600
800
1000

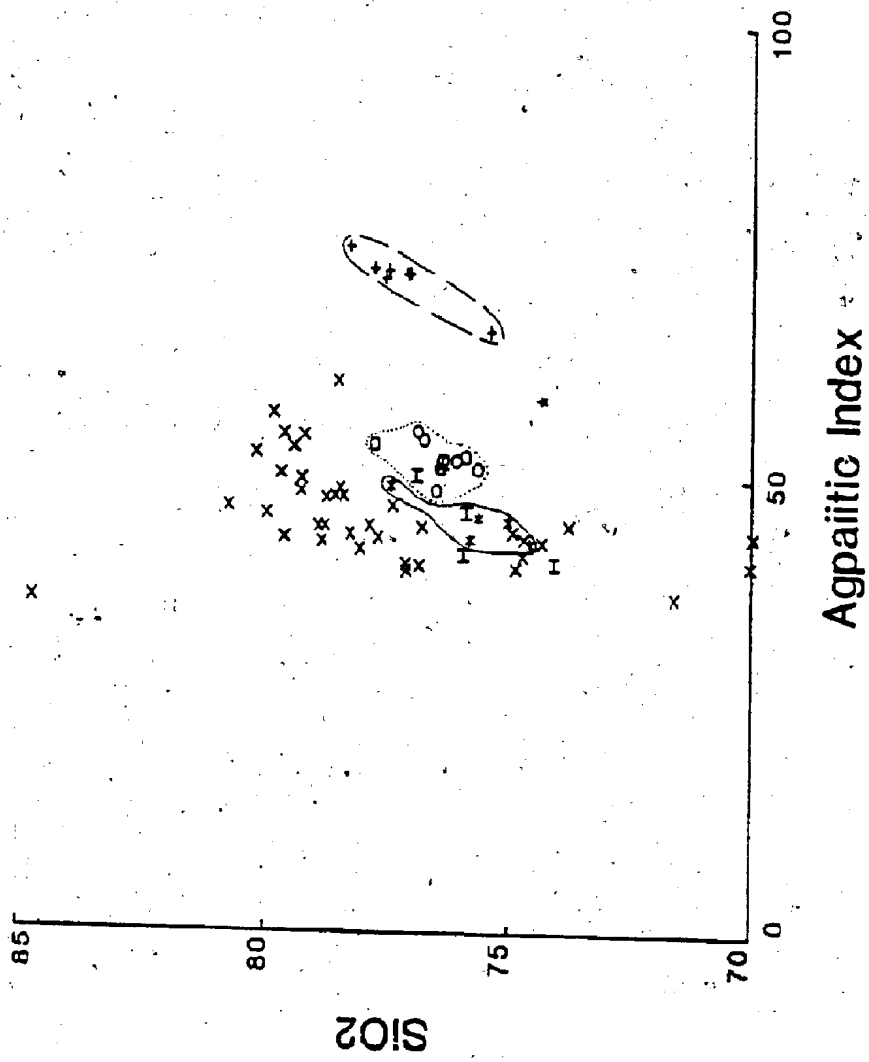

FIGURE 5.5 SiO_2 (weight %) vs. Agpaiitic Index (Na_2O+K_2O/Al_2O_3) variation diagram. Symbols as defined in Figure 5.4.

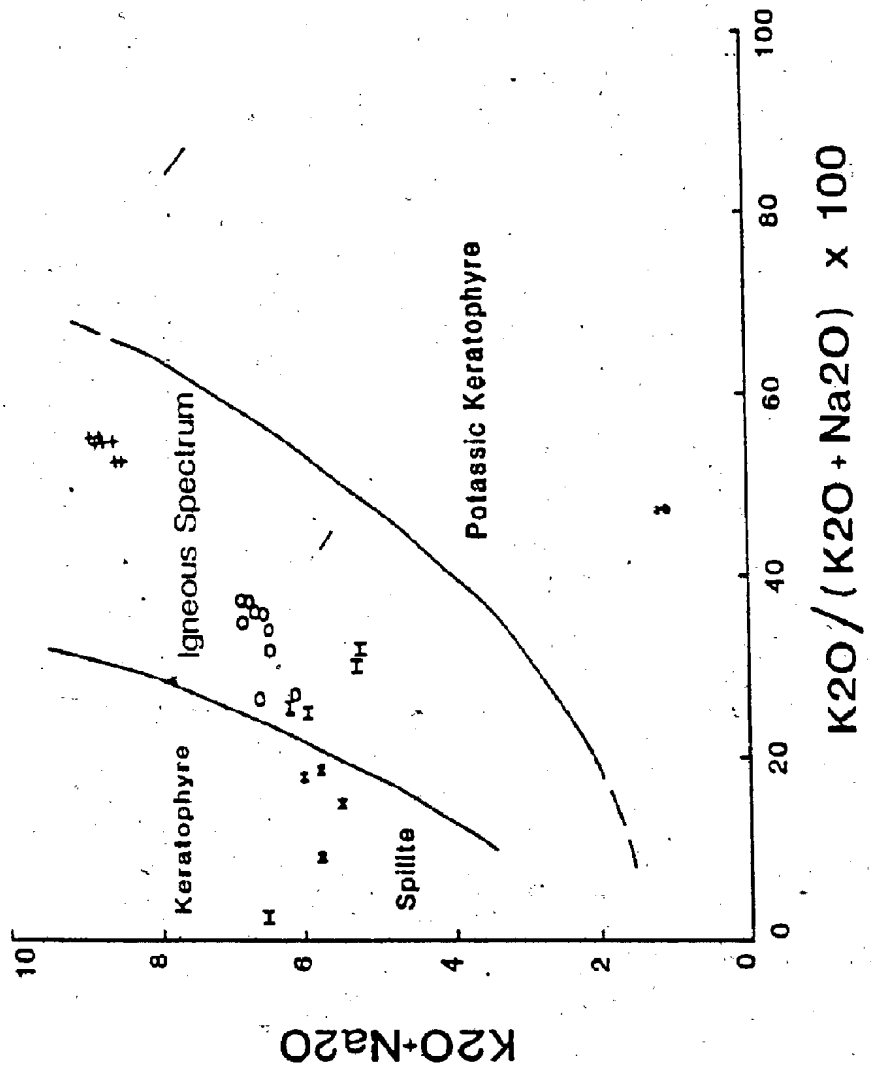

FIGURE 5.6 Igneous spectrum diagram of Hughes (1973). Symbols as defined in Figure 5.4.

rhyolitic flows do not, however, demonstrate this metasomatism suggesting that metasomatism may be due to late-stage volatile activity during or after intrusion rather than hydrothermal alteration related to submarine volcanism. The relative paucity of secondary calcite, sericite, barite and quartz in the Feeder Granodiorite bodies (Chapter Three) relative to the granitoid clasts indicates a relative absence of similar hydrothermal alteration in these bodies. This can be recognized by the lower LOI, Ca, Sr and Ba contents in these bodies (Table 5.3; Figure 5.4). Although the mafic phases in the Little Sandy Lake Intrusion are usually completely chloritized, primary and partly replaced biotite and hornblende occur in the Wiley's River Intrusion suggesting reduced fluid phase activity during or after intrusion of this body.

5.2.3 Summary of alteration effects.

Alkali metasomatism (i.e., loss of potassium) of the 'aplitic' group clasts and the Little Sandy Lake Intrusion appear to be related to the loss of a volatile fluid phase prior to final crystallization. The presence of abundant secondary minerals and whole-rock geochemical changes resulting from hydrothermal alteration reduces the usefulness of any extended discussion of major element

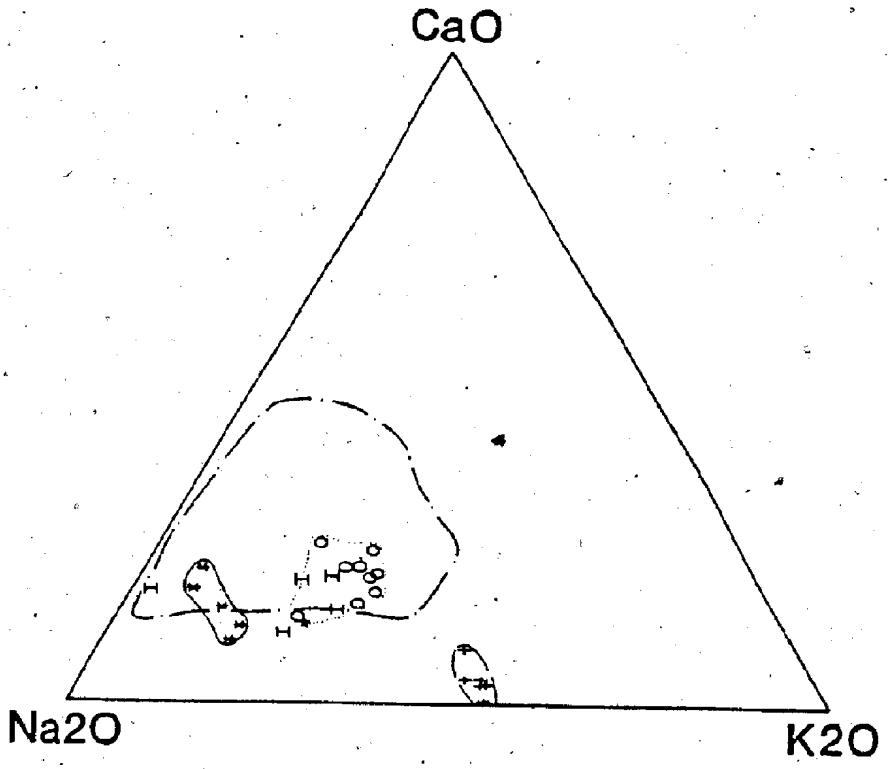

FIGURE 5.7 $Na_2O/K_2O/CaO$ diagram. Symbols as defined in Figure 5.4. The field of granitoid clasts is shown.

contents to examine comagmatism. It makes imperative the use of the 'immobile' trace elements to examine comagmatism.

5.3 Composition of the granitoid clasts

5.3.1 Trace Elements

On many of the following diagrams, one or two samples from each clast type appear to be anomolous in comparison to other samples for that population, e.g., two type 2 clasts have higher V contents than all other type 2 clasts (Fig. 5.8a) and one type 4 clast has low Y and low Zr relative to other type 4 clasts (Fig. 5.8b,c). The result is to expand the field boundaries for these types in contrast to the relatively tight clustering demonstrated by other samples of that type. The expansion of these fields due to only one or two samples should be noted by the reader.

Plots of Zr, Y, and V versus TiO2 have been constructed to determine if any significant differences or correlations between the granitoid clast types can be recognized (Fig. 5.8). Vanadium decreases with decreasing TiO2 contents (Fig. 5.8a) for all granitoid clasts suggesting a magmatic link between the clasts. The fractionation of a phase that contains both of these elements, such as ilmenite or titanomagnetite (Green, 1980; Briqueu et al., 1984) could

Figure 5.8 TiO2 (weight %) vs. trace elements (V, Y and Zr, in ppm) variation diagrams for granitoid clast types. Fields of granitoid clast type 2, 4 and 6 (after Stewart, 1984) are shown. Crosses (+) represent type 1 clasts, symbol (X) represent type 2 clasts, asterisks (*) represent type 3 clasts, circles (O) represent type 4 clasts, a star (★) represents the type 5 clast and the symbol (H) represent type 6 clasts.

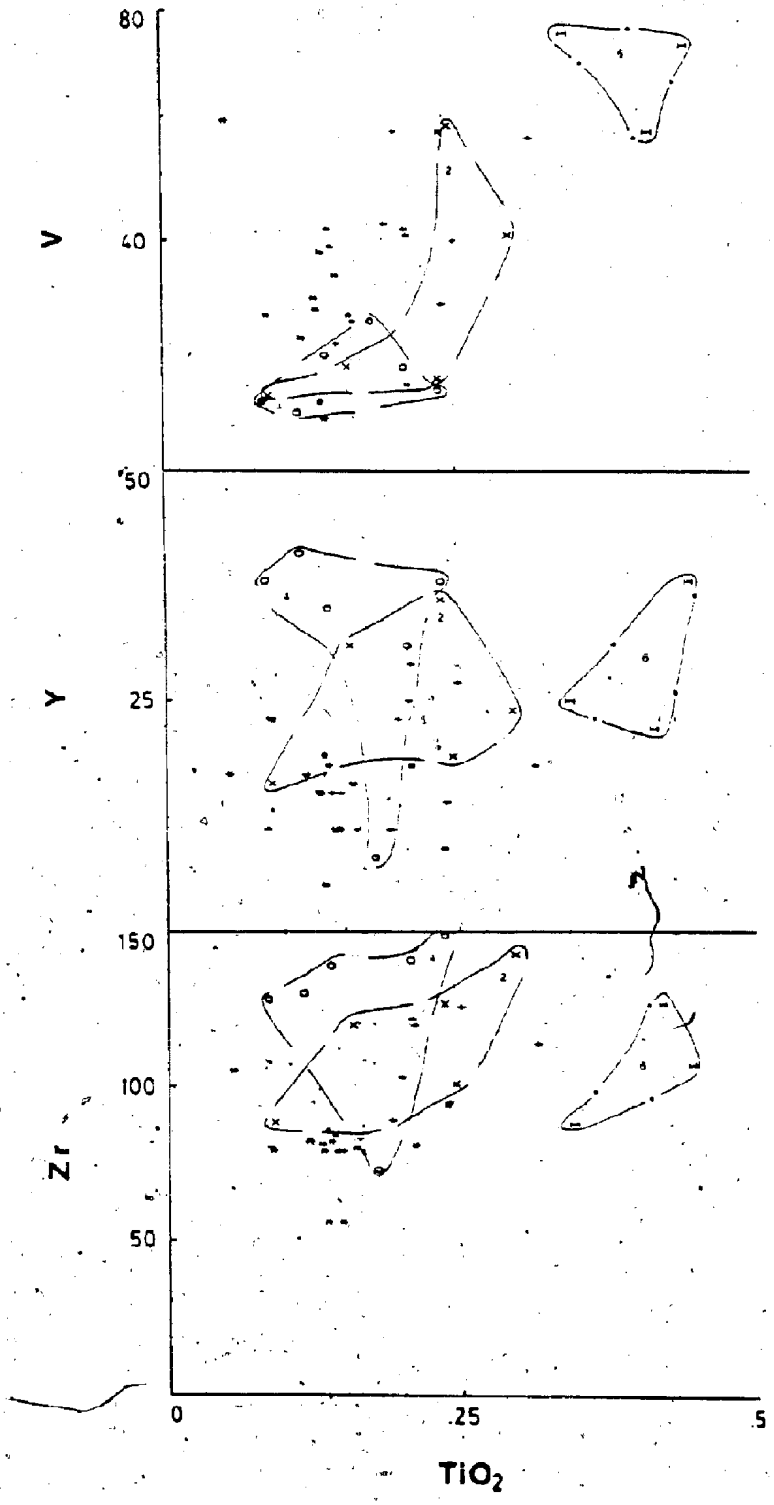
80
40
V
50
25
Y
150
100
50
Zr
0
.25
.5
TiO2

account for this correlation. The less fractionated, more intermediate character of type 6 clasts is indicated by their higher TiO_2 and V values. The slightly higher Zr and Y contents in clast types 2 and 4 (i.e. 'aplite' group) relative to most type 1 and type 3 clasts (Fig. 5.8) suggests that they may be slightly more differentiated than type 1 and type 3 clasts (i.e., the 'granitic' group). This is the typical relationship seen between comagmatic aplites and granites (e.g., Lynch and Pride, 1984). The variability in Zr and Y contents in types 1 through to 5 clasts relative to type 6 clasts, however, indicates a more ambiguous relationship. Whereas the 'aplitic' group clasts appear to have slightly higher Zr and Y contents than the type 6 clasts suggesting a slightly greater degree of differentiation, the 'granitic' group clasts have slightly lower contents of Zr and Y (Fig. 5.8b,c).

The greater abundance of Zr and Y in type 2 and 4 clasts relative to the type 1 and 3 clasts is more clearly seen in Figure 5.9 and is considered to probably indicate the greater degree of differentiation of the 'aplitic' group relative to the 'granitic' group. The lower abundances of Zr and Y in clast types 1 and 3 may be due to dilution in the more intensely altered clasts by the introduction of silica, calcium and barium or may demonstrate some mobility of these elements in the most intensely altered granitoid

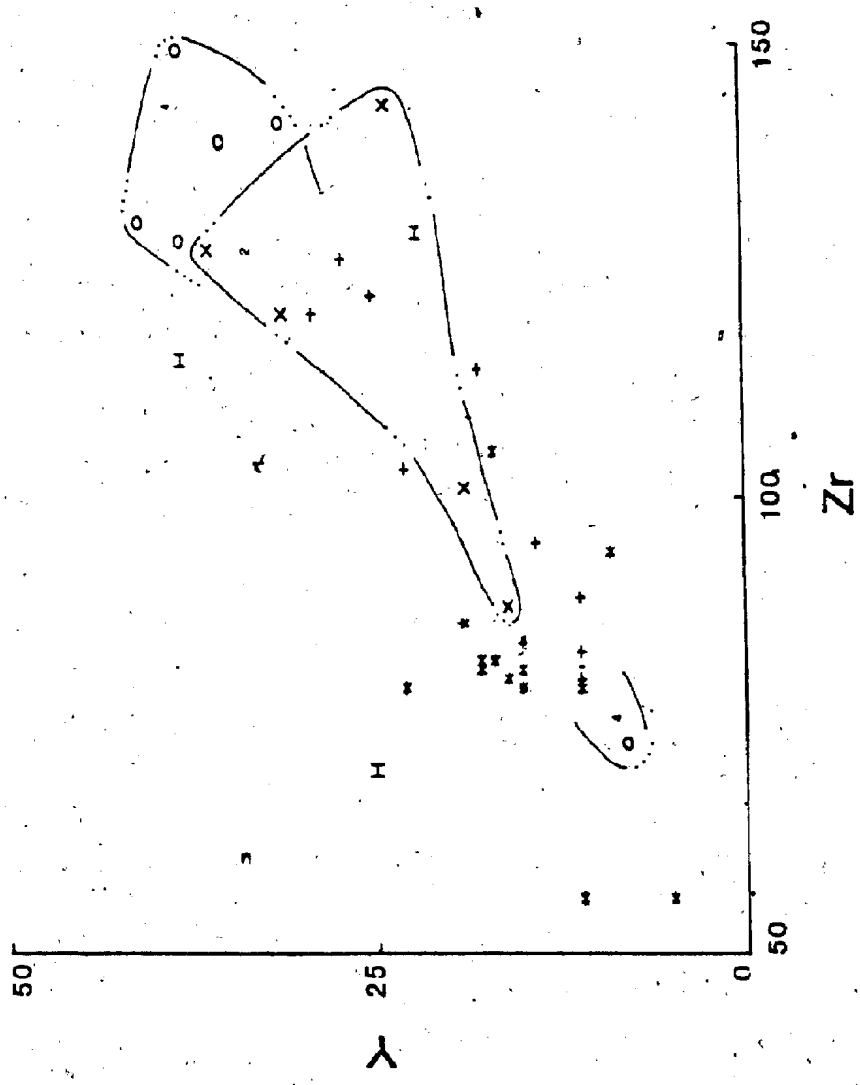

FIGURE 5.9 Zr vs. Y (in ppm) variation diagram for granitoid clast types. Symbols as defined in Fig. 5.1.

clasts.

Three supposedly immobile elements (Zr, Y, Nb) have been plotted together (Fig. 5.10) and the broad field defined by the samples along the Zr-Y join, demonstrates the variability of these elements in the granitoid clasts. The 'granitic' and 'aplitic' groups of granitoid clasts are separated on this diagram, with the 'aplitic' group (types 2 and 4) closer to the Y apex than the 'granitic' group members. The more intensely altered 'granitic' samples (types 1 and 3) are lower in mafic minerals (Chapter Four). Zircon is probably more stable under intense alteration than mafic phases, such as ilmenite, that presumably contain most of the yttrium in the sample as suggested by Finlow-Bates and Stumpfl (1981) from studies of intensely altered rocks associated with massive sulphide deposits. This implies that Y may have become mobile and lost from the most intensely altered granitoid clasts. The generally lower and more variable trace element composition of the most intensely altered granitoid clasts is probably the result of both dilution due to chemical additions during hydrothermal alteration and the limited (?) mobility of Ti, Y and Zr during this alteration. The relatively high degree of imprecision of the Ti and Y analyses because of their relatively low abundances in the granitoid clasts (Appendix 1 and 2) may also contribute to this scatter (Appendix 2).

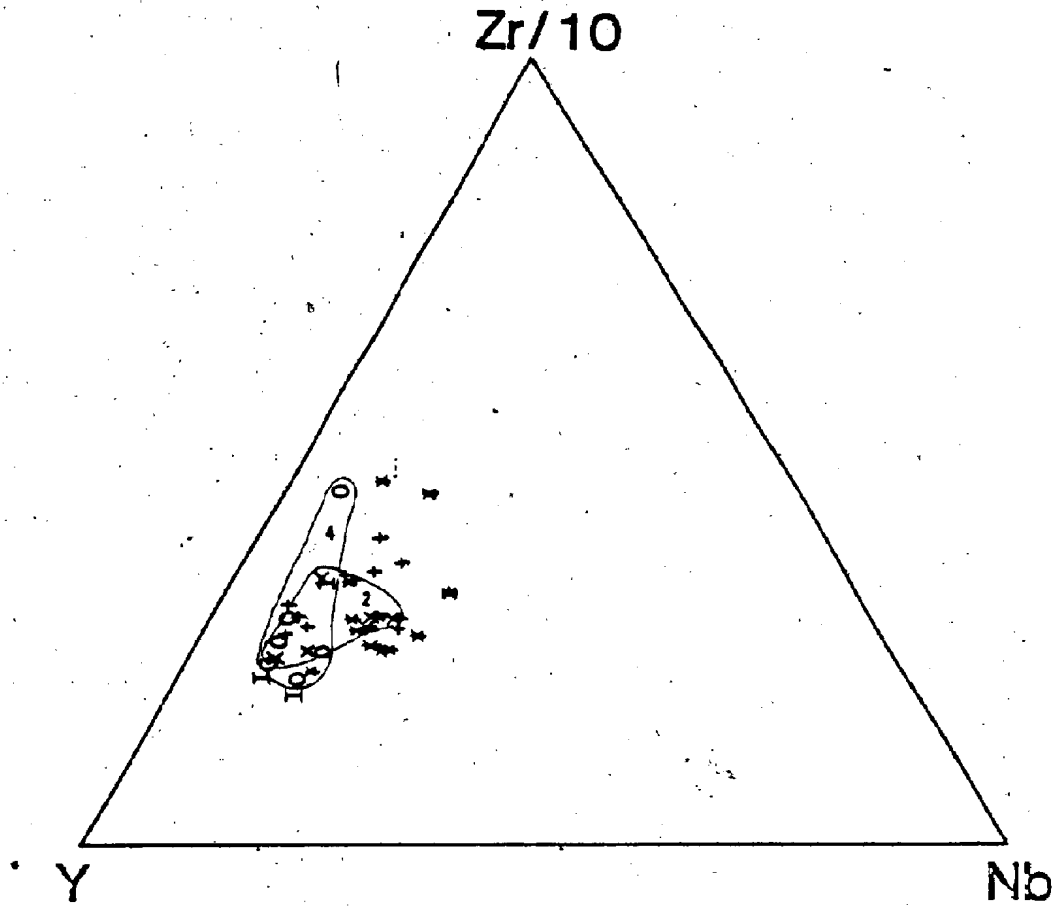

FIGURE 5.10 Zr/Y/Nb diagram for granitoid clast types. Symbols as defined in Figure 5.1. Fields of type 2 and 4 (aplitic group) granitoid clasts are shown.

A triangular plot with an element known to be mobile during many hydrothermal alteration processes (Sr) (Fig. 5.4) has also been contructed (Fig. 5.11). The higher Sr in the 'granitic' group relative to the 'aplitic' group is easily seen. Inconsistencies in the Zr and Y contents are much less evident on this figure. As discussed in Section 5.2.1, Sr appears to have been added to the clasts along with Ca during the formation of secondary calcite. This is shown by the extension of the field for the granitoid clasts toward the Sr apex (Fig. 5.11). The greater abundance of secondary calcite in the 'granitic' group clasts is reflected by the concentration of these clasts closest to the Sr apex (Fig. 5.11).

As the finest grained, most highly granophyric clasts, type 5 clasts would be expected to demonstrate a higher degree of differentiation than the other granitoid clast types and therefore, should contain the highest concentration of the incompatible elements such as Zr and Y. The relatively intermediate abundance levels of Zr and Y in the type 5 sample do not demonstrate the increase in degree of differentiation expected within the 'aplitic' group. However, one type 4 clast also shows similar relatively low or intermediate abundances of Y and Zr (Figures 5.8, 5.9). There may not be a significant or consistent increase in differentiation between type 4 and 5 clasts. More data for

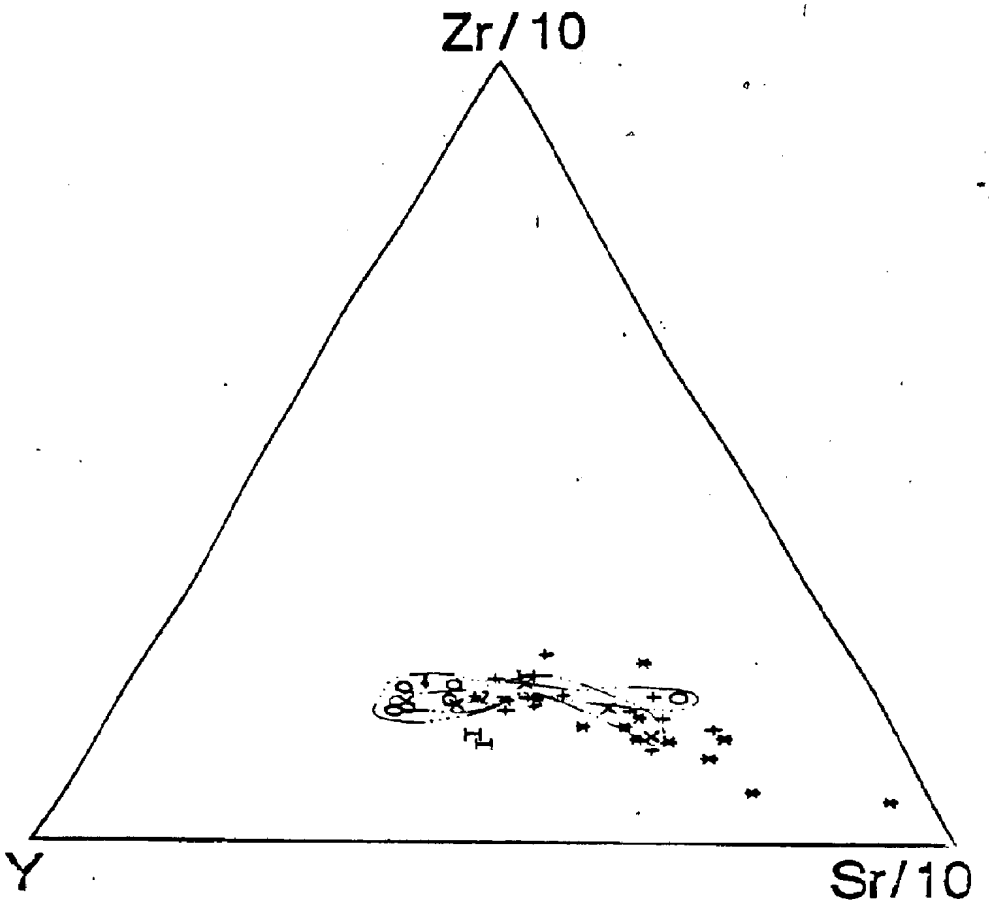

FIGURE 5.11 Zr/Y/Sr diagram for granitoid clast types. Symbols as defined in Figure 5.1. Fields of type 2 and 4 (aplitic group) granitoid clasts are shown.

type 5 clasts is required to resolve this discrepancy.

No unequivocal evidence for a genetic link between the different granitoid clasts can be demonstrated. However, the similar abundances of relatively 'immobile' incompatible trace elements (Ti, Zr, Y, Nb) that display evidence of differentiation permits their origin from a common magmatic source. With the exception of some trace element data for the only type 5 clast analysed (KQS-83-091), the geochemistry of the 'aplitic' group clasts demonstrates their slight increase in degree of differentiation from the 'granitic' group. The more intermediate character of the type 6 clasts suggested by mineralogy and major element geochemistry is also supported by the trace element data. These conclusions agree with the textural interpretation of the granitoid clasts as magmatically related products of different crystallization levels and histories (Chapter Four).

5.3.2 Rare Earth Elements

In general, rare earth elements especially those with odd atomic numbers are present in most rock types in very low concentrations (very often less than 2 ppm, for example Eu), and their absolute abundances are difficult to analyze accurately (Hanson, 1980). The XRF technique employed for

REE analysis (Appendix Four) in this study can be accurate to ± 10% or 0.1ppm (whichever is greater) (e.g., Taylor and Fryer, 1982). It is more commonly estimated to be within 10% or 1ppm (whichever is greater) (e.g., Strong, 1984) or ±10% for REE with abundances greater than 2ppm (e.g., Fryer and Edgar, 1977). Lu and Yb had an unsatifactorily low degree of reproducibility in this study and, therefore, have not been plotted. The low abundance of Eu in the granitoid clasts (1ppm except for the type 6 clast, Table 5.4) may explain the inconsistent strength and direction of the Eu anomaly in the clasts. Nevertheless, the technique can be shown to consistently reproduce the slope of the REE pattern and the relative strength of the Eu anomaly in a granitic rock standard. REE patterns produced by four replicate XRF analyses of a granite sample (MUN-1) were compared to four independently determined instrumental neutron activation analyses (INAA) from three different laboratories (Appendix Figure 3.1). REE patterns appear to be more consistently reproducible than absolute abundance levels. Only those sets of REE data that yielded similar REE patterns for duplicate samples are presented in this study (Fig. 5.12, 5.17). No REE data is available for the Little Sandy Lake Intrusion, Little Sandy Lake Sequence volcanic rocks and type 5 granitoid clasts for this reason.

Conclusions drawn from the REE data are derived mainly from the roughly similar REE patterns and abundances shown by all types of granitoid clasts (Fig. 5.12a,b). Each granitoid clast type shows evidence of moderate light REE enrichment with La contents varying between 20 and 60 times chondrite and Er contents between 3 and 10 times chondrite. The similarity in REE pattern (i.e., similar degree of light REE enrichment) and relatively similar REE abundances are interpreted to permit the conclusion that all granitoid clast types may possibly have had a common magmatic source. In addition, types 1, 2, 3 and 6 appear to lack a consistent Eu anomaly (Fig. 5.12a,b). However, a slight and relatively consistent negative Eu anomaly in the type 4 clasts is observed (Fig.5.12b) and probably indicates the removal of plagioclase during differentiation thereby depleting the melt in Eu prior to crystallization. This supports other trace element data (Section 5.3.1) that suggests that these clasts crystallized at a slightly more differentiated magmatic stage than the other granitoid clast types.

The slight changes in REE abundances within each clast type, especially type 1 and 3 clasts, may reflect the effects of dilution or mobility of the REE resulting from hydrothermal alteration (Section 5.3.1). The possible effects of hydrothermal alteration on the REE abundances and

Figure 5.12a Abundances of rare earth elements in granitoid clast types 1, 3 and 6 normalized to chondritic values of Taylor and Gorton (1977). Symbols and accompanying numbers designate the sample analysed (all numbers are KQS-82-xyz).

Figure 5.12b Abundances of rare earth elements in granitoid clast types 2 and 4 normalized to chondritic values of Taylor and Gorton (1977). Symbols and accompanying numbers designate the sample analysed (all numbers are KQS-82-xyz).

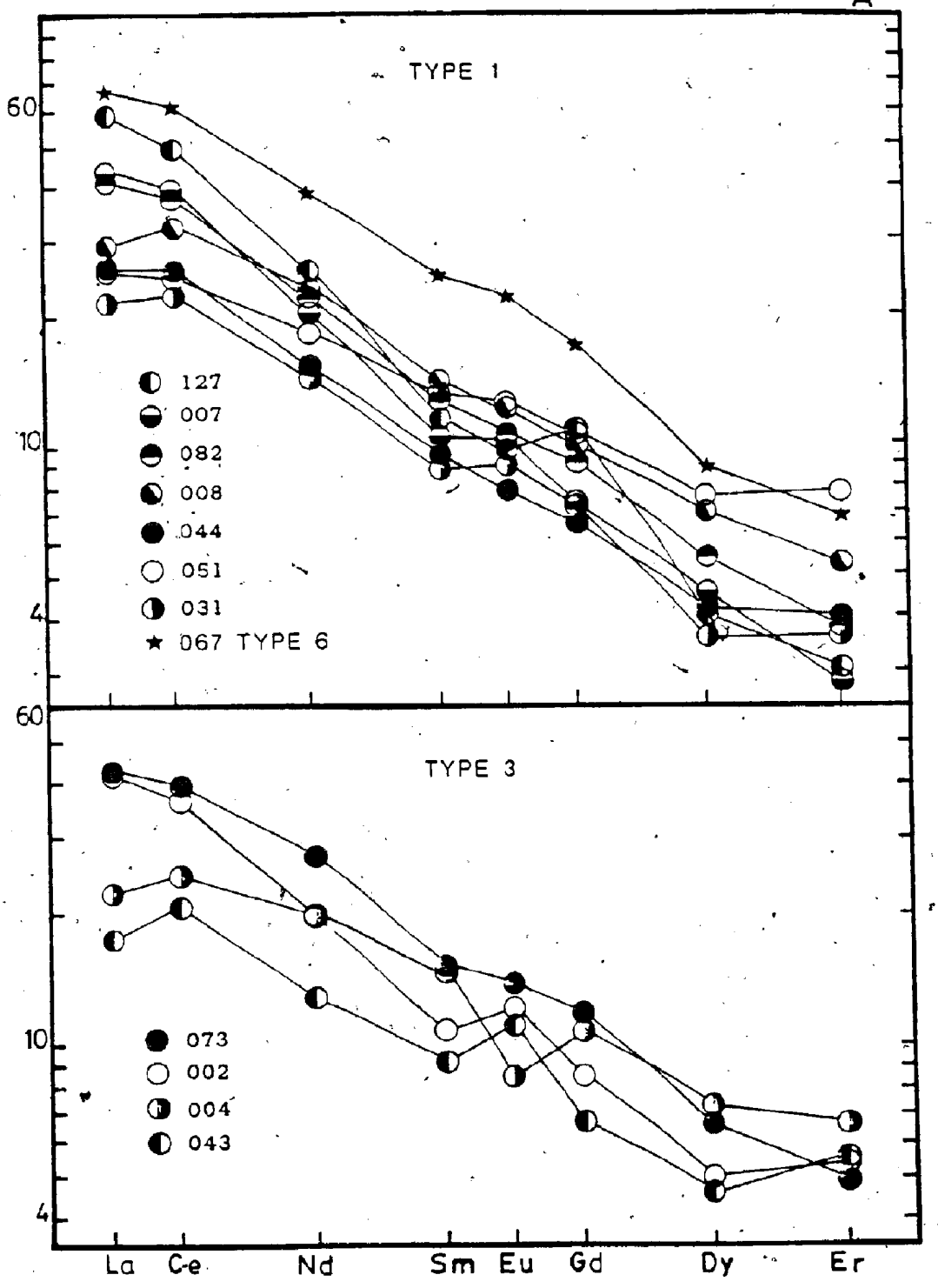
TYPE 1
60
10
4
127
007
082
008
044
051
031
067 TYPE 6
TYPE 3
60
10
4
073
002
004
043
La
Ce
Nd
Sm
Eu
Gd
Dy
Er

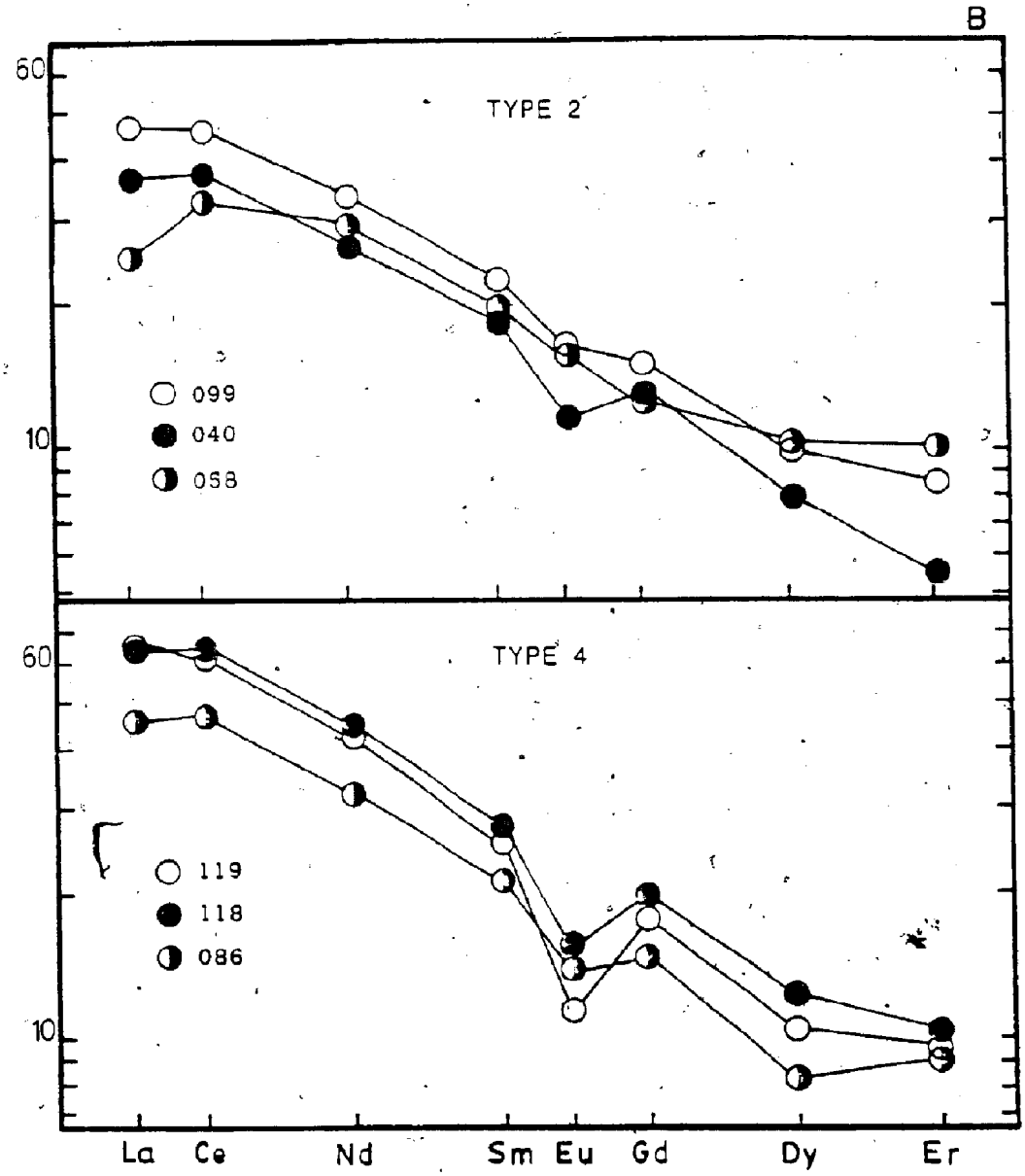
B
60
10
TYPE 2
099
040
058
60
10
TYPE 4
119
118
086
La
Ce
Nd
Sm
Eu
Gd
Dy
Er

patterns in the granitoid clasts is not clearly known because altered samples were not appropriately screened prior to analysis (Hanson, 1980).

5.4. COMAGMATISM OF THE GRANITOID CLASTS, FEEDER GRANODIORITE AND BUCHANS GROUP FELSIC FLOWS

5.4.1 Introduction

The major, trace and REE geochemistry of the granitoid clasts, the Feeder granodiorite (Wiley's River intrusion and Little Sandy Lake intrusion) and Buchans Groups felsic flows has been compared to evaluate the comagmatism of these suites proposed by Thurlow (1981a,b). The Topsails granite is younger than the Buchans Group (Bell and Blenkinsop, 1981; Taylor et al., 1980; Whalen and Currie, 1985), and can be shown to have major and trace element abundances that are different from the granitoid clasts (Stewart, 1984). Topsails-type granite data have been plotted on a number of diagrams to demonstrate the discriminatory value of the diagrams employed and does not imply that it is considered to be a possible source of the granitoid clasts.

As discussed in Section 5.1.2, comparisons of major element contents usually cannot demonstrate significant differences or similarities to demonstrate or refute comagmatism. In addition, the alteration of the granitoid clasts and the Little Sandy Lake Intrusion further diminish the usefullness of major element comparisons. Therefore, emphasis has been placed on trace element contents to investigate comagmatism. However, since all rock units do not evidence hydrothermal alteration, a brief discussion of the major element contents precedes the discussion of the results of the trace element studies.

5.4.2 Major elements

The Buchans Group flows, granitoid clasts and Feeder Granodiorite bodies have similar mean major and trace element abundances (Table 5.3). Lithogeochemical data for Buchans Group flows from Thurlow (1981a) augments that from the Buchans River Formation rhyolite in MacLean Extension used in the radiometric study and five Little Sandy Lake Sequence rhyolitic flows. Only flows with $>65\%$ SiO_2 from Thurlow (1981a) have been used to make the comparison of mean major element abundances more meaningful (Table 5.3).

Table 5.3 Mean (standard deviations) abundances in granitoid clasts, Feeder granodiorite, Buchans Group felsic flows, Little Sandy Lake area rhyolites and Topsails granite.

	Granitoid Clasts		Wiley's River Intrusion		Little Sandy Lake Intrusion		Buchans Group Flows		Little Sandy Lake Felsic Flows		Topsails Granite	
SiO_2	73.66	(2.81)	75.10	(.82)	73.48	(1.15)	71.44	(3.56)	73.86	(1.06)	76.24	(1.04)
TiO_2	.18	(.04)	.23	(.03)	.23	(.05)	.34	(.17)	.22	(.06)	.13	(.07)
Al_2O_3	11.36	(1.15)	12.09	(.24)	12.38	(.40)	13.31	(1.17)	12.36	(.25)	11.96	(.44)
Fe_2O_3	1.63	(1.02)	2.06	(.14)	3.19	(.47)	2.94	(1.57)	2.79	(.87)	1.39	(.30)
MnO	.05	(.02)	.05	(.01)	.08	(.02)	.07	(.05)	.10	(.01)	.03	(.02)
MgO	.62	(.38)	.46	(.11)	1.16	(.14)	.83	(.69)	1.35	(.68)	.11	(.07)
CaO	2.26	(.70)	1.50	(.32)	.93	(.33)	1.69	(1.00)	1.05	(.30)	.33	(.22)
Na_2O	4.07	(.84)	4.31	(.20)	4.80	(.26)	4.08	(.96)	4.42	(1.09)	3.94	(.08)
K_2O	1.11	(.63)	2.15	(.32)	.78	(.27)	2.57	(1.28)	1.26	(.62)	4.64	(.15)
P_2O_5	.06	(.08)	.05	(.02)	.08	(.02)	-	-	.09	(.05)	.03	(.02)
LOI	2.90	(.89)	.59	(.19)	1.54	(.22)	1.96	(1.02)	2.03	(.46)	.51	(.09)
TOTAL	97.90		98.90		98.65		99.23		99.53		99.31	
					TRACE ELEMENTS (ppm)							
Pb	101	(147)	13	(5)	7	(2)	nd		6	(3)	18	(5)
Th	12	(4)	11	(2)	10	(4)	nd		5	(4)	30	(2)
U	2	(12)	2	(2)	0	-	nd		0	-	8	(3)
Rb	19	(10)	54	(11)	17	(7)	45	(24)	24	(13)	152	(21)
Sr	321	(162)	129	(11)	118	(27)	155	(82)	70	(20)	24	(14)
Y	21	(10)	34	(4)	26	(8)	nd		34	(10)	84	(14)
Zr	100	(25)	126	(8)	118	(10)	130	(35)	108	(18)	189	(21)
Nb	5	(2)	5	(1)	4	(55)	8	(4)	3	(1)	35	(5)
Zn	128	(97)	21	(7)	35	(9)	nd		47	(9)	28	(9)
Cu	35	(26)	11	(7)	15	(6)	nd		15	(3)	16	(15)
Ni	0	-	0	-	0	-	nd		0	-	0	-
Ba	9708	(8748)	982	(198)	368	(181)	894	(431)	281	(192)	342	(113)
V	34	(19)	19	(3)	38	(3)	28	(23)	13	(11)	4	(4)
Cr	0	-	0	-	0	-	nd		0	-	0	-
n =	38		9		5		23		5		7	

The populations of interest, i.e., excluding the Topsails granite, are: 1) silica-over-saturated, 2) subalkaline (after Irving and Baragar, 1971), and 3) peraluminous ($Al_2O_3/CaO+Na_2O+K_2O$ .1). The granitoid clasts contain lower mean abundances of TiO_2, Fe_2O_3 and Al_2O_3 and higher CaO abundances than other rock units. All units record a K_2O/Na_2O ratio 0.5 except for the Buchans Group data from Thurlow (1981a). The lower K_2O in the granitoid clasts and the Little Sandy Lake Intrusion is attributed to loss during alkali metasomatism (Figures 5.1, 5.4).

5.4.3 Trace Elements

On variation diagrams of Rb, Y, Zr and V versus SiO_2 (Fig. 5.13, 5.14) it is demonstrated that there is an overlap of the fields defined for the Wiley's River Intrusion and the Little Sandy Lake Intrusion. The granitoid clasts show V, Y and Zr abundances similar to the Feeder Granodiorite bodies, but at slightly higher SiO_2 values which are probably due to the silicification of the clasts (Chapter Four and Section 5.2). Buchans Group felsic flows have V, Rb and Zr abundances that show considerable overlap with the fields for both Feeder Granodiorite bodies as well as approximating (albeit at slightly lower SiO_2 contents) the abundances observed in the granitoid clasts.

Figure 5.13 $iO2 (weight %) vs. Y and Zr (in ppm) variation diagrams. Fields of Buchans Group felsic flows (BV) (from Thurlow, 1981a) and granitoid clasts (GC) are shown. Crosses (+) represent Topsails granite (TS) samples, circles (0) represent the Wiley' River intrusion (WR) samples, asterisks (*) represent Little Sandy Lake intrusion (LS), the symbol (H) represent rhyolites from the Little Sandy Lake area, and the star (★) is the rhyolite from the Buchans River Formation in MacLean Extension used in the geochronology study.

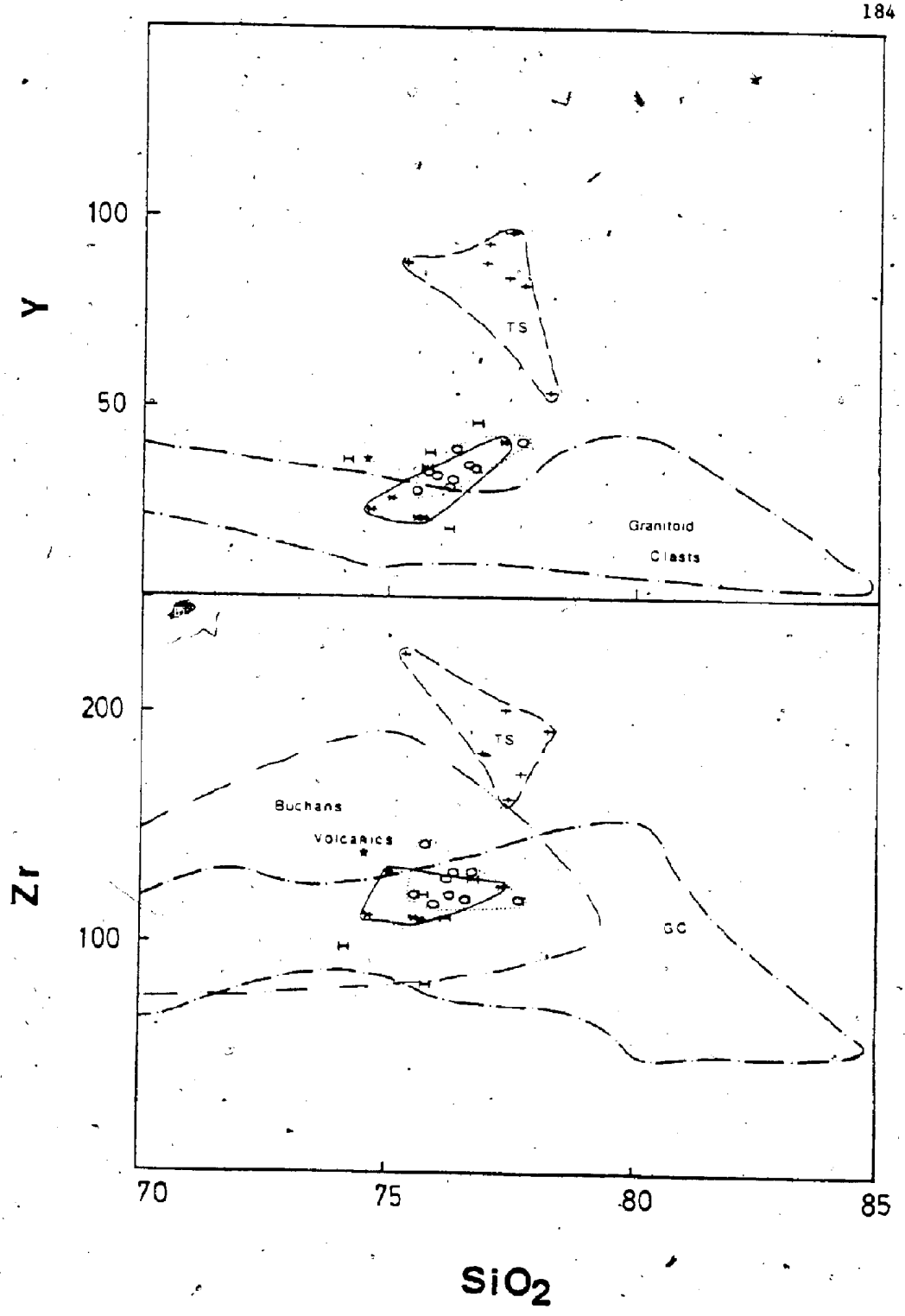
Y
100
50
TS
Granitoid
Clasts
Zr
200
100
TS
Buchans
Volcanics
GC
70
75
80
85
SiO2

Figure 5.14 SiO2 (weight %) vs. trace elements (V and Rb, in ppm) diagrams. Fields of Buchans Group felsic flows (BV) (from Thurlow, 1981a) and granitoid clasts (GC) are shown. Crosses (+) represent Topsails granite (TS) samples, circles (O) represent the Wiley' River intrusion (WR) samples, asterisks (*) represent Little Sandy Lake intrusion (LS), the symbol (H) represent rhyolites from the Little Sandy Lake area, and the star (★) is the rhyolite from the Buchans River Formation in MacLean Extension used in the geochronology study.

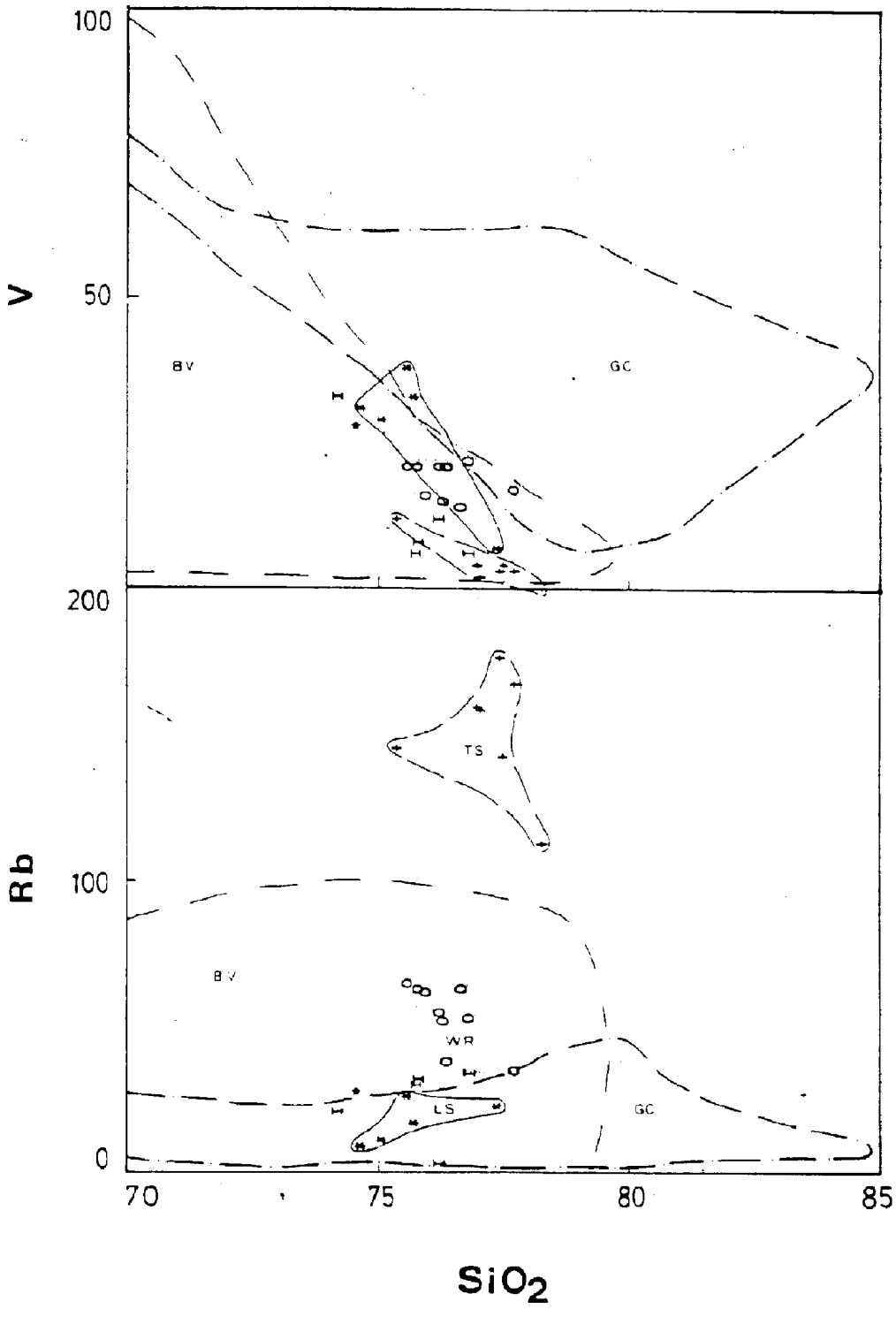
100
50
V
BV
GC
200
100
0
Rb
TS
BV
WR
LS
GC
70
75
80
85
SiO2

Data for rhyolitic flows from the Little Sandy Sequence and Buchans River Formation (KQS-82-210) obtained during this study show similar abundances to both Feeder Granodiorite bodies, the granitoid clasts and other Buchans Group felsic flows (Fig. 5.13, 5.14). The discriminatory power of these diagrams is shown by the separation of the Topsails granite from all other rock units (Fig. 5.13, 5.14).

Comparisons of paired immobile minor and trace elements (Ti, Zr, Y) show the same result (Figure 5.15a,b). The fields for the Wiley's River intrusion, Little Sandy Lake intrusion and the granitoid clasts are virtually identical, although the granitoid clasts demonstrate greater scatter and slightly lower Zr and Y values (see Section 5.3.1). The fields for the Wiley's River and Little Sandy Lake Intrusions overlap each other and fall within the larger field defined by the granitoid clasts (Fig. 5.15) as do flows from the Little Sandy Lake Sequence. The large field defined by Buchans Group felsic flows (from Thurlow, 1981a) overlaps the Feeder Granodiorite bodies completely and most samples from the granitoid clasts on the Zr vs. TiO2 plot (Fig. 5.15b).

The fields for the two Feeder Granodiorite bodies are virtually coincident when Zr and Y are plotted with Nb, Ga, and Sr on triangular diagrams (Fig. 5.16). These fields fall entirely within the larger field described by the

Figure 5.15a Zr vs. Y (both in ppm) variation diagram. Crosses (+) represent Topsails granite (TS) samples, circles (O) represent the Wiley' River intrusion (WR) samples, asterisks (*) represent Little Sandy Lake intrusion (LS), the symbol (H) represent rhyolites from the Little Sandy Lake area, the symbol (X) represent granitoid clasts and the star (★) is the rhyolite from the Buchans River Formation in MacLean Extension used in the geochronology study.

Figure 5.15b TiO2 (weight %) vs. trace elements (Y and Zr, in ppm) variation diagrams. Field of Buchans Group felsic flows (BV) (data from Thurlow, 1981a) is shown. Crosses (+) represent Topsails granite (TS) samples, circles (O) represent the Wiley' River intrusion (WR) samples, asterisks (*) represent Little Sandy Lake intrusion (LS), the symbol ^ (H) represent rhyolites from the Little Sandy Lake area, the symbol (X) represent granitoid clasts and the star (★) is the rhyolite from the Buchans River Formation in MacLean Extension used in the geochronology study.

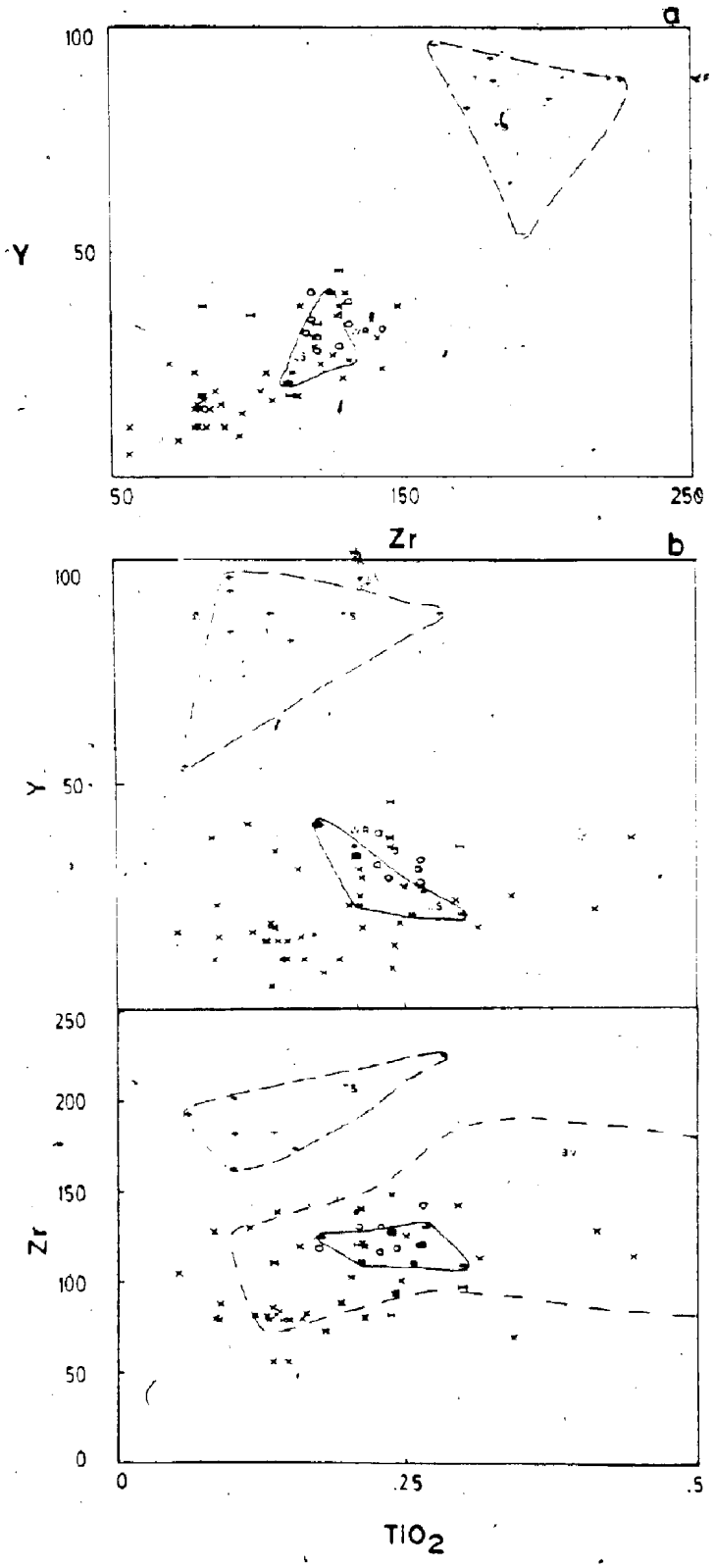
a
100
50
Y
50
150
250
Zr
b
100
50
Y
250
200
150
100
50
0
Zr
0
.25
.5
TiO2

granitoid clasts on two of these plots (Fig. 5.16a,b). The Topsails-type granite is separated on these three plots with only a slight overlap on the Zr/Y/Ga plot (Fig. 5.16b). Comparison to the Zr/Y/Nb plot of the granitoid clasts (Fig. 5.10) suggests that the Feeder Granodiorite bodies are most similar in composition to the 'aplitic' group clasts. On the Zr/Y/Sr plot, the field of the granitoid clasts extends from the fields for the Feeder Granodiorite bodies toward the Sr apex (Fig. 5.16c). The dominance of the 'aplitic' group clasts in the field for the granitoid clasts (Fig. 5.11) closest to those of the Feeder Granodiorite bodies also suggests similar compositions in these rock units (Figures 5.11, 5.16c). The addition of Sr to the 'granitic' group clasts during hydrothermal alteration is discussed in Sections 5.2 and 5.3.

Bell and Blenkinsop (1981) determined initial Sr isotopic compositions of 0.7068 and 0.7072 for the Wiley's River intrusion and the Buchans Group, repectively, in their geochronological study. No attempts were made to determine this ratio in the clasts after recognition of Sr mobility in the granitoid clasts.

The immobile trace element data show no significant differences in the primary composition of the granitoid clasts, Buchans Group felsic flows and the Feeder Granodiorite. This suggests that these rock units may have

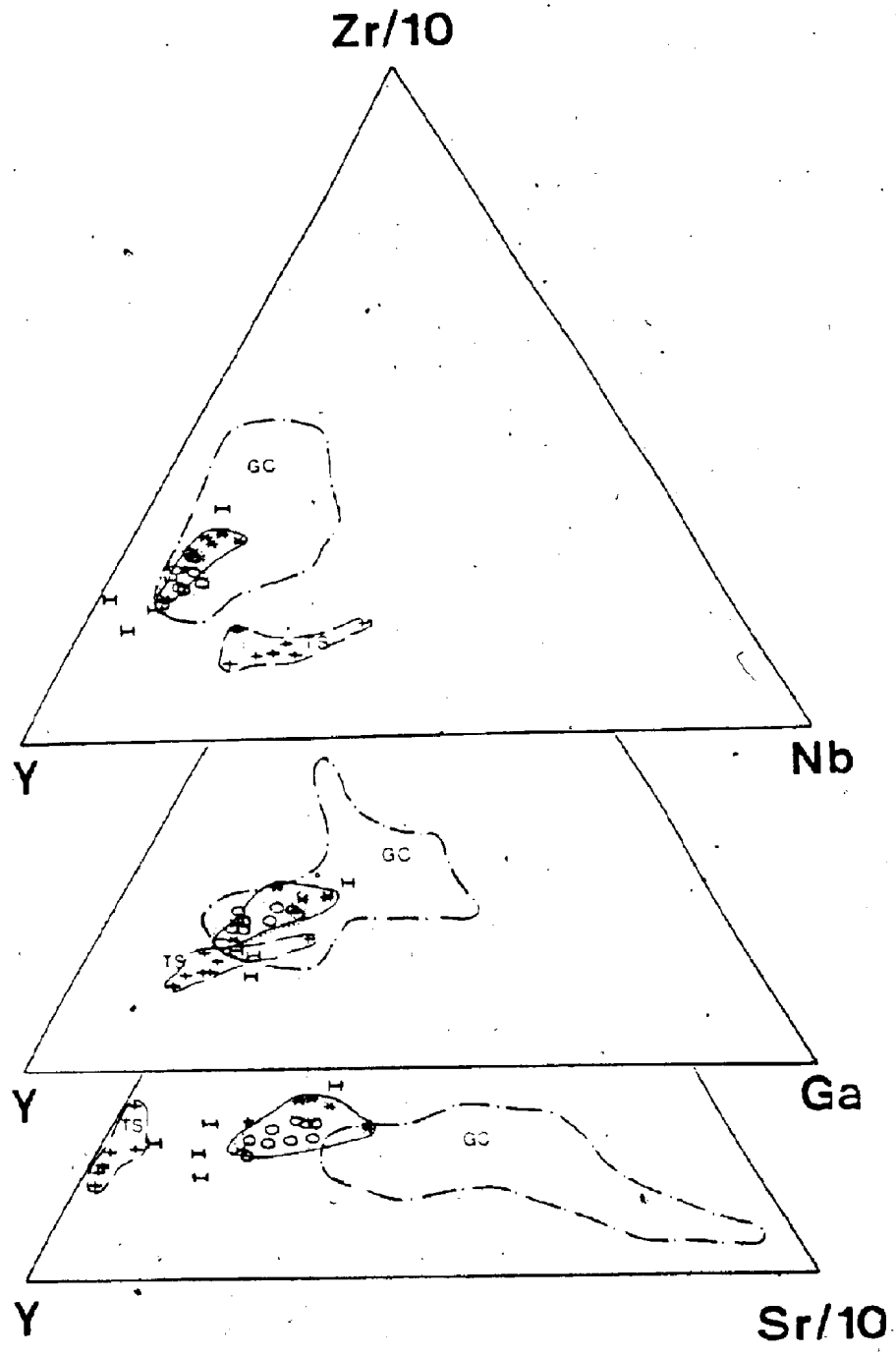

FIGURE 5.16 Triangular plots of trace elements (Zr, Y, Nb, Ga and Sr, all in ppm). Fields of granitoid clasts (GC) is shown. Symbols as defined in Figure 5.4.

had a common magmatic source.

5.4.4 Rare Earth Elements

Rare earth element patterns for the Wiley's River intrusion, felsic volcanic rocks from the Lundberg Hill Formation, and felsic volcanic rocks of the unnamed formation east of Buchans River (formerly in the Upper Buchans Subgroup) are shown in Fig. 5.17. The data for the Buchans Group felsic flows are from Strong (1984). The light REE enriched patterns for each rock unit are similar, despite the greater variability in the patterns of the Buchans Group volcanic rocks. Each unit shows similar ranges for La and Er after normalization (Figure 5.17). The consistent negative Eu anomaly of the Wiley's River intrusion indicates that it has probably been affected by plagioclase fractionation during crystallization and is therefore somewhat more differentiated than the volcanic rocks. There does not appear to be a consistent Eu anomaly in the Buchans Group flows.

Comparisons of these patterns with those for the granitoid clast types (Fig. 5.12) reveals that little recognizable difference in the degree of light REE enrichment or the range in abundance levels exists between these populations. An increasingly negative and more

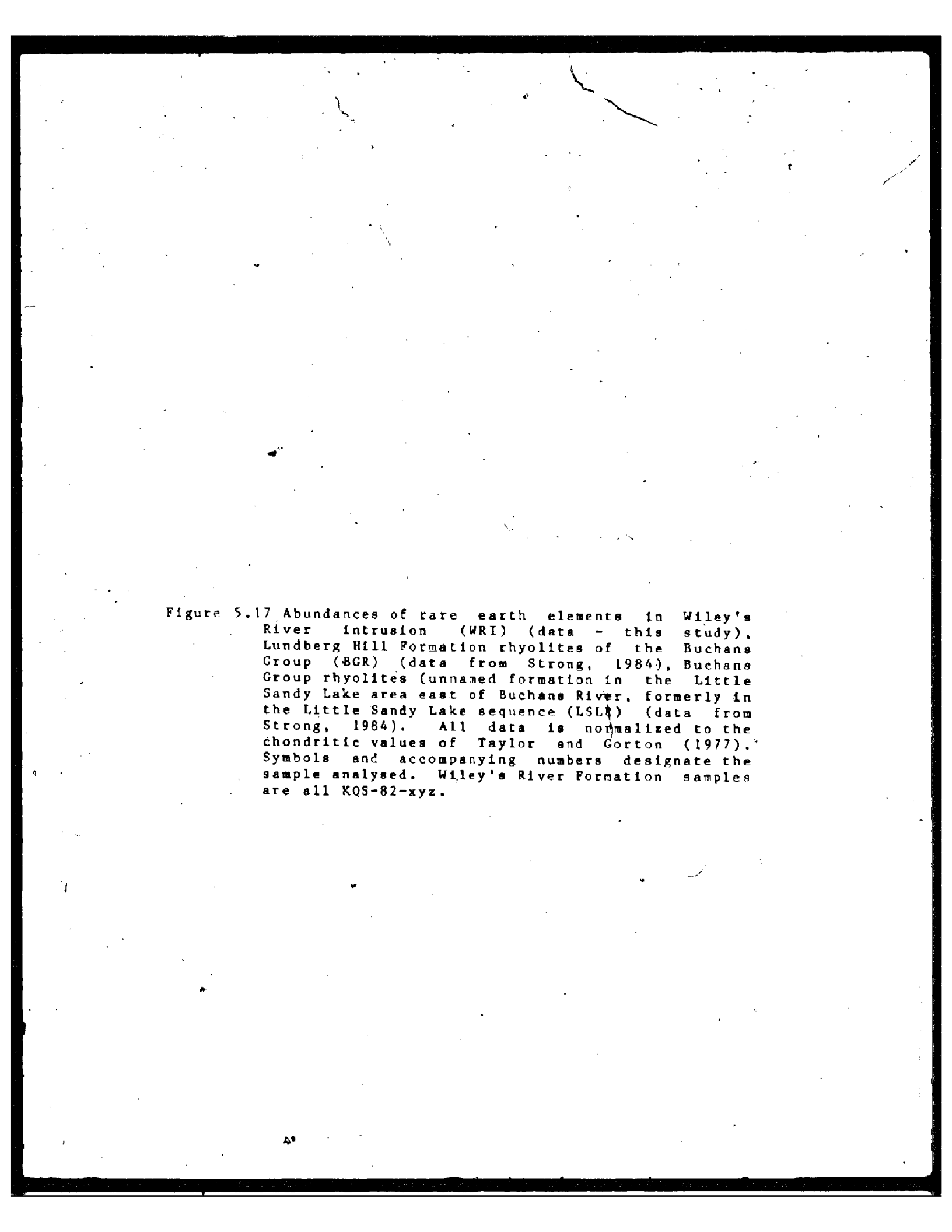

Figure 5.17 Abundances of rare earth elements in Wiley's River intrusion (WRI) (data - this study), Lundberg Hill Formation rhyolites of the Buchans Group (BGR) (data from Strong, 1984), Buchans Group rhyolites (unnamed formation in the Little Sandy Lake area east of Buchans River, formerly in the Little Sandy Lake sequence (LSL)) (data from Strong, 1984). All data is normalized to the chondritic values of Taylor and Gorton (1977). Symbols and accompanying numbers designate the sample analysed. Wiley's River Formation samples are all KQS-82-xyz.

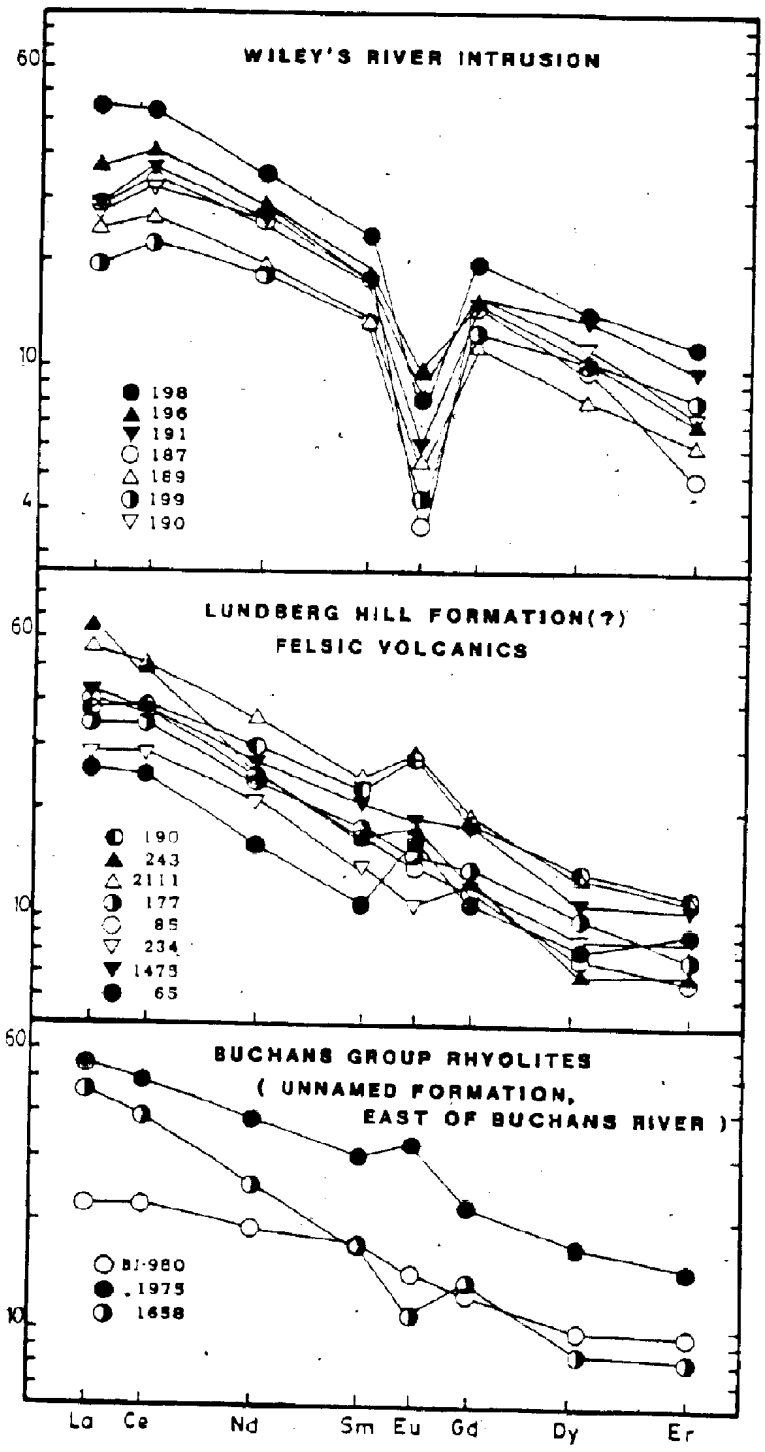
WILEY'S RIVER INTRUSION
60
10
4
198
196
191
187
189
199
190
LUNDBERG HILL FORMATION(?)
FELSIC VOLCANICS
60
10
190
243
2111
177
85
234
1473
65
BUCHANS GROUP RHYOLITES
(UNNAMED FORMATION,
EAST OF BUCHANS RIVER)
60
10
BJ-980
1975
1658
La
Ce
Nd
Sm
Eu
Gd
Dy
Er

TABLE 5.4 Rare earth element contents in granitoid clasts and Wiley's River intrusion

	TYPE 1							TYPE 3				TYPE 6
	KQS-82-007	KQS-82-008	KQS-82-031	KQS-82-044	KQS-82-051	KQS-82-082	KQS-82-127	KQS-82-002	KQS-82-004	KQS-82-043	KQS-82-073	KQS-82-067
La	13.88	9.43	6.79	8.20	8.13	13.01	18.53	12.92	7.02	5.52	13.06	20.76
Ce	31.07	26.67	16.10	20.95	20.16	30.25	39.88	29.78	19.87	16.99	32.31	49.21
Nd	12.13	13.74	8.60	9.82	11.10	13.19	15.23	11.92	11.94	7.73	16.23	23.12
Sm	2.07	2.81	1.74	1.91	2.61	2.54	2.25	2.14	2.92	1.80	3.17	4.84
Eu	0.74	0.88	0.66	0.58	0.90	0.76	0.70	0.88	0.62	0.81	1.01	1.60
Gd	1.91	2.59	1.93	1.73	2.82	2.38	2.85	2.21	2.79	1.73	3.08	4.40
Dy	1.50	2.28	1.18	1.39	2.51	1.81	1.31	1.63	2.36	1.51	2.14	2.85
Er	0.61	1.13	0.79	0.86	1.70	0.82	0.64	1.15	1.42	1.18	1.03	1.24

	TYPE 2			TYPE 4			WILEY'S RIVER INTRUSION						
	KQS-82-040	KQS-82-058	KQS-82-099	KQS-82-086	KQS-82-119	KQS-82-118	KQS-82-187	KQS-82-189	KQS-82-190	KQS-82-191	KQS-82-196	KQS-82-198	KQS-82-199
La	11.41	7.87	14.81	14.25	20.41	20.25	9.11	7.74	8.53	9.10	11.62	17.04	6.06
Ce	30.35	26.24	37.76	37.98	50.49	53.28	27.22	21.56	26.32	29.45	32.79	42.76	18.18
Nd	15.67	17.38	20.10	19.31	24.60	26.97	15.48	11.71	15.55	15.95	17.14	21.04	10.88
Sm	3.59	3.89	4.44	4.21	5.04	5.44	3.57	2.68	3.33	3.29	3.60	4.71	2.67
Eu	0.84	1.11	1.19	1.01	0.83	1.14	0.26	0.39	0.65	0.44	0.71	0.59	0.31
Gd	3.37	3.22	3.90	3.83	4.63	5.18	3.84	2.97	4.19	4.08	4.00	5.16	3.29
Dy	2.56	3.32	3.10	2.68	3.42	4.07	3.24	2.63	3.78	4.47	3.39	4.64	3.37
Er	1.17	2.15	1.81	1.92	2.06	2.26	1.05	1.30	1.57	2.10	1.50	2.49	1.75

consistent Eu anomaly can be seen by comparing the Buchans Group volcanic rocks to the 'granitic' group clasts to the 'aplitic' group clasts to the Wiley's River intrusion (Fig. 5.12, 5.17). This can be attributed to an increase in fractionation of plagioclase from the melt in the source magma chamber.

The REE data supports the previous mineralogical, textural and geochemical evidence that these rock units are probably from the same magma chamber, but they probably did not crystallize synchronously.

5.4.5 Tectonic setting

Trace element discrimination diagrams for the tectonic interpretation of granitic rocks proposed by Pearce et al. (1984) have been constructed (Figures 5.18, 5.19).

The previously identified island arc setting of the Buchans Group volcanic rocks (Strong, 1977; Thurlow, 1981a) and, the proposed comagmatism of the granitoid clasts, Buchans Group felsic volcanic rocks and the Feeder Granodiorite bodies are both supported by the results of these plots. The comagmatic rock units all plot within the volcanic arc granite (VAG) field (Figures 5.18, 5.19). The discrimination of a different magmatic source for the

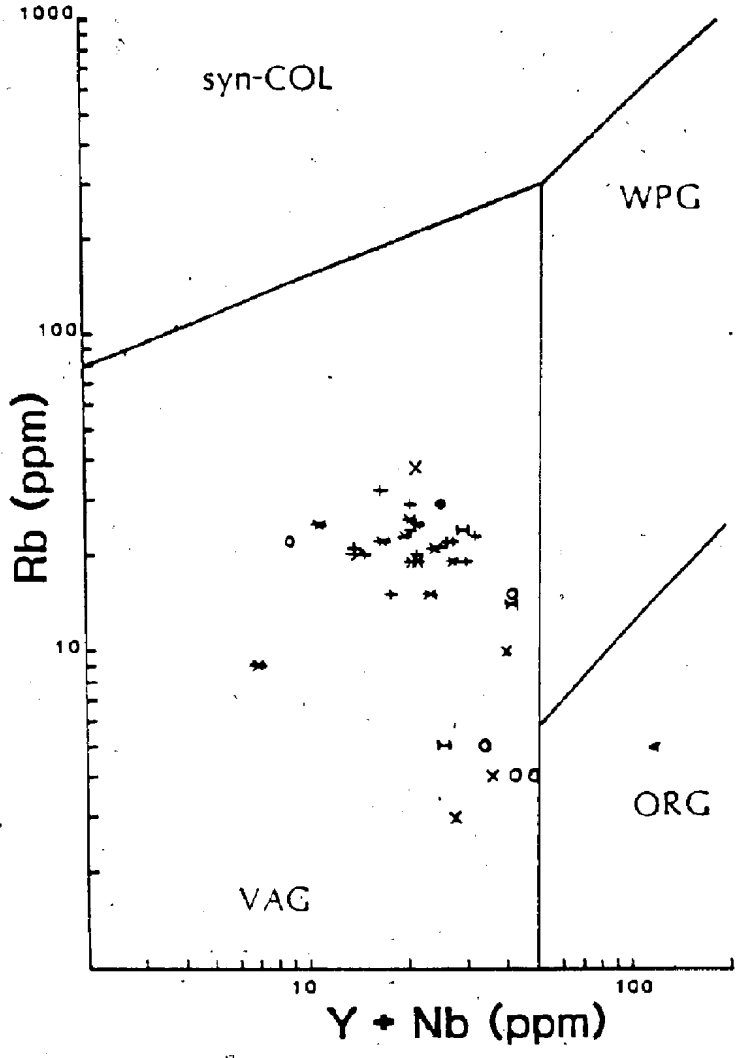

FIGURE 5.18 Tectonic discrimination diagram of Pearce et al. (1984) for the granitoid clast types. Symbols as defined in Figure 5.1. Fields for volcanic arc granites (VAG), ocean ridge granites (ORG), within plate granites (WPG) and syn-collison granites (syn-COL) are shown.

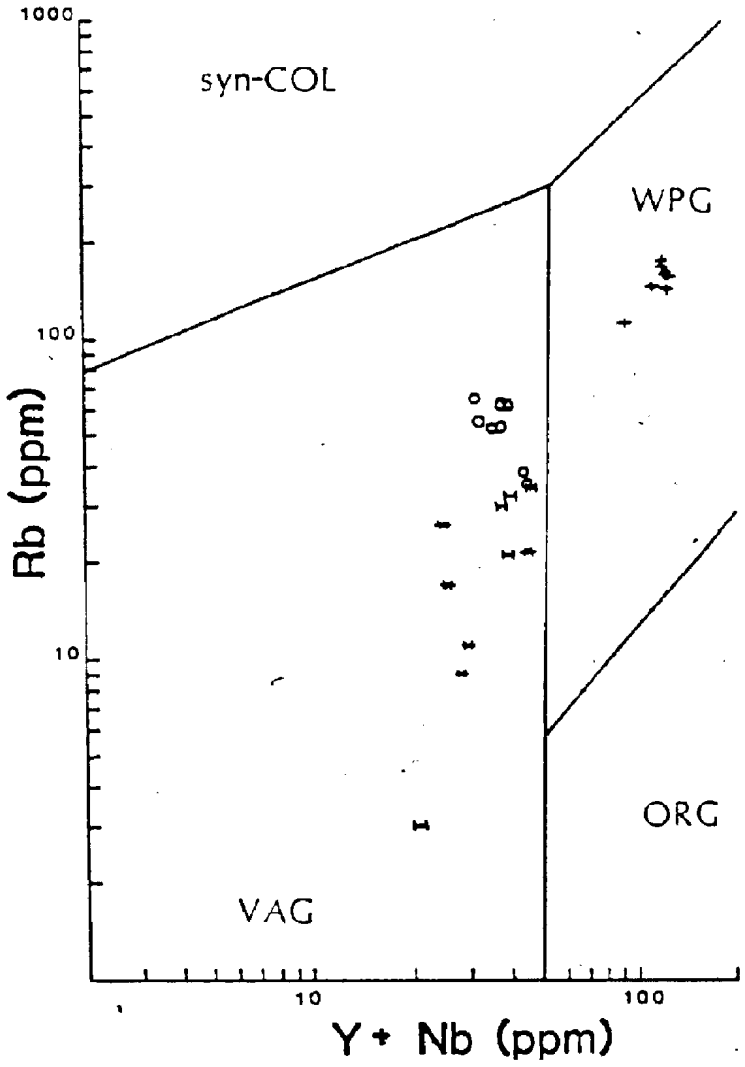

FIGURE 5.19 Tectonic discrimination diagram of Pearce et al. (1984). Symbols as defined in Figure 5.4. Fields for volcanic arc granites (VAG), ocean ridge granites (ORG), within plate granites and syn-collision granites (syn-COL) are shown.

Topsails granite is clearly demonstrated (Fig. 5.19).

The fields for the granitoid clasts and Feeder Granodiorite are not exactly coincident. However, loss of potassium during alkali metasomatism of the 'aplitic' group granitoid clasts is presumably the cause of the lower Rb contents in these clasts (Figure 5.18). The possible mobility of some HFS elements or the effects of dilution on their measured abundances (Section 5.3) probably explains the scatter shown by the granitoid clast samples parallel to the Y+Nb axis.

The loss of K and chemically similar Rb from the Little Sandy Lake Intrusion during alkali metasomatism similar to that of the 'aplitic' group clasts is shown in Figure 5.19. The slightly greater degree of differentiation of the Wiley's River Intrusion relative to the other rock units is expressed by its slight shift upward and to the right from the other samples (Pearce et al., 1984).

5.5 SUMMARY

Comparisons of major element contents of the Wiley's River intrusion, Little Sandy Lake intrusion, granitoid clasts and Buchans Group felsic flows reveal few significant differences between these populations other than those

changes attributable to hydrothermal alteration and alkali metasomatism. The effects of the observed hydrothermal alteration of some granitoid clasts (Chapter Four), i.e., the introduction of calcite, barite, quartz and volatiles, are reflected by the higher CaO, Ba, SiO2 and LOI analyses for these clasts. Sr is shown to have been introduced with Ca to form calcite during alteration. The visually less altered clasts (types 2 and 4) and the Little Sandy Lake Intrusion do, however, demonstrate evidence of K2O and Rb loss during alkali metasomatism.

Trace element abundances of those elements known to be relatively immobile in most hydrothermally altered rocks, such as Zr, Nb, Ga and Y, are very similar in the different granitoid clast types. The REE patterns and abundance levels are very similar for each granitoid clast type. The trace element data indicates that all granitoid clasts probably had a common magmatic source. Recognizable differences between the granitoid clast types are: 1) the more intermediate character of type 6 clasts; 2) the 'aplitic' group clasts generally contain slightly greater abundances of Zr and Y and lower V contents than the 'granitic' group clasts; 3) type 4 clasts of the 'aplitic' group show a weak to moderately negative Eu anomaly. These differences are considered to reflect an increase in differentiation from the type 6 clasts to the 'granitic'

group to the 'aplitic' group clasts. Although not consistent, the type 4 and 5 clasts are the more highly differentiated than type 2 clasts.

Similar major and trace element abundances in the Feeder Granodiorite bodies, Buchans Group felsic flows and the granitoid clasts are compatible with their derivation from the same magma chamber. The Wiley's River Intrusion and 'aplitic' group clasts demonstrate trace element abundances that indicate a similar mutual degree of differentiation that is slightly greater than that shown by other rock units. The REE pattern and REE abundance levels of the Wiley's River Intrusion and Buchans Group felsic flows are similar to those shown by the granitoid clast types, with the exception of a consistent moderately negative Eu anomaly in the Wiley's River Intrusion similar to that displayed by type 4 granitoid ('aplitic' group) clasts. The negative Eu anomalies are interpreted to support the greater degree of differentiation of the Wiley's River Intrusion relative to the Buchans Group felsic flows and the 'granitic' group clasts.

The granitoid clasts, Little Sandy Lake and Wiley's River Intrusions have trace element characteristics suggesting their formation in a volcanic island arc tectonic setting.

Chapter Six

GEOCHRONOLOGY

6.1 INTRODUCTION

The age of the Buchans Group has significant implications in the understanding of the volcanic stratigraphy of the Central Volcanic Belt. The distinction between 'early' and 'late' (or 'post') island arc sequences is fundamental to the present understanding of events in central Newfoundland. Each volcanic sequence shows a different style and type of volcanism and mineralization (Strong, 1977; Dean, 1978; Kean et al., 1981; Swinden and Thorpe, 1984). The age relationships between the volcanic rocks of central Newfoundland and a period of clastic sedimentation that commenced in the Middle to Late Ordovician is not clearly established. Absolute age estimates of the volcanic rocks are sparse. As host to the Buchans orebodies, the Buchans Group records the site and time of the most significant known sulphide mineralization in Newfoundland. Therefore, any data that can assist in the stratigraphic assignment of the Buchans Group is of

importance, especially in mineral exploration.

The correlation of the Buchans Group with other volcanic rocks of central Newfoundland, especially the Robert's Arm Group has been primarily based on similarities in style of volcanism and mineralization (Swanson and Brown, 1962), and the geochemical composition of the volcanic rocks (Strong, 1977). On these bases, the Buchans Group has been grouped with the Robert's Arm Group, Cottrell's Cove Group and Chanceport Group (Strong, 1977). Together, they informally form the Buchans-Robert's Arm belt. They show geological and geochemical differences from other volcanic sequences of central Newfoundland, especially the Early to Middle Ordovician island arc volcanic sequences (Strong, 1977; Swinden and Kean, 1984; Swinden and Thorpe, 1984), formerly called the 'early' island arc sequence of Dean (1978) and Kean et al. (1981). The composition of the volcanic rocks of the Buchans-Robert's Arm belt have been shown to be analogous to modern 'late' or 'post' subduction-related island arc volcanism (Strong, 1977).

Although the critical basal contacts of the Buchans Group and other volcanic rocks of the Buchans-Robert's Arm belt are often not exposed, or appear faulted, these sequences occur to the west and north of thick clastic sequences that also face west and north (Dean, 1978). Based on fossil evidence, these clastic sequences consist of an

extensive graptolitic (Caradoc) shale-chert sequence and a Late Ordovician to Early Silurian greywacke-conglomerate sequence (Bergstrom et al., 1974). Locally, the clastic rocks conformably overlie early volcanic rock sequences, such as the Victoria Lake and Lushs Bight Groups (Dean, 1978).

The Buchans Group has yielded few fossils and no paleontological dates had ever been obtained for it prior to Nowlan and Thurlow (1984). They report a conodont assemblege of Llanvirnian-Llandeilo age in carbonate clasts within debris flows. Nowlan and Thurlow (1984) interpreted the carbonate clasts be of local origin and to have been deposited penecontemporaneously with the Buchans Group volcanic rocks. This interpretation prompted Nowlan and Thurlow (1984) to suggest a Caradocian or older age for the Buchans Group in contrast to the Silurian estimate of Swanson and Brown (1962) or the Late Ordovician (post-Caradocian) to Early Silurian estimate of Dean (1978) and Kean et al. (1981). Nowlan and Thurlow also suggested the possibility that the Buchans and Victoria Lake Groups may be time-stratigraphic equivalents. From lead isotope data, Swinden and Thorpe (1984) reject this proposal as each group displays a very different source of lead for the sulphide mineralization contained in each. The geochemical data of Strong (1977) also indicates that these two groups

probably had different magmatic sources.

Rb-Sr whole rock isochron radiometric ages have been obtained from volcanic rocks of the Buchans and Robert's Arm Groups. The dates determined, 447±7 Ma for Robert's Arm Group felsic volcanic rocks (Bostock et al., 1979), and 447±18 Ma for the Buchans Group volcanic rocks (Bell and Blenkinsop, 1981), support the correlation of these two groups. However, because of the uncertainties in the absolute calibration of the Ordovician time scale (Table 6.2; see van Eysnga, 1975; McKerrow et al., 1980; Armstrong, 1978; Ross et al., 1982; Harland et al., 1982; Ross and Naeser, 1984), these dates do not unequivocally establish a pre- or post- Caradocian time of formation for either group (see Nelson and Kidd, 1979; Dean and Kean, 1980; Currie and Bostock, 1980; for discussions of the relative and absolute age of the Robert's Arm Group by Bostock et al., 1979).

The absolute age of the Buchans Group is, therefore, crucial to our understanding of events in central Newfoundland during the early Paleozoic. For this reason and to test the hypothesis that the granitoid clasts and Buchans Group felsic flows are comagmatic, U/Pb zircon age determinations have been made. A granitoid clast and a rhyolitic flow from 20-6 Sublevel and 20-6 Drive, respectively, were sampled for this purpose (Fig. 4.2).

This is the first attempt to date the Buchans Group by this method, although another U/Pb isotopic dating study of Central Volcanic Belt igneous rocks is presently in progress (G. Dunning, written comm., 1984). This study will include new isotopic data from the Buchans River Formation rhyolite dated in this study.

6.2. NEW DATA

Sample preparation, analytical techniques and method of age calculation are discussed in Appendix 4.

6.2.1 Granitoid clast (KQS-82-095)

The largest granitoid clast observed in the Buchans River Formation in the MacLean Extension area was selected for geochronological analysis. It is a type 4 clast, a pink-red member of the 'aplitic' group (Plate 6.1). It occurred within a granitoid-bearing ore breccia-conglomerate debris flow sequence in 20-6 Sublevel (Figure 4.2). Although this was the largest clast in two dimensions (40cm x 50cm) observed in MacLean Extension, it was only 15 cm thick, and yielded only approximately 25 kg of rock chips. The zircons extracted were small (<100 microns), euhedral to

Plate 6.1 Photograph of granitoid clast (KQS-82-095) used in geochronology study prior to its extraction from granitoid-bearing polylithic breccia-conglomerate, 20-6 Sublevel, MacLean mine; alteration of clast prior to its incorporation in debris flow is shown by the termination of alteration veins at clast boundary; sharp contact with underlying felsic pyroclastic unit is evident at bottom; ball-point pen for scale.

subhedral with some imperfectly or partially formed crystals (Plate 6.3b). They were found to be less abundant relative to the quantity of zircons commonly extracted from other felsic intrusive bodies (R.W. Sullivan, pers. comm, 1983).

The granitoid clast was partially altered prior to its' incorporation into the debris flow. This can be seen in Plate 6.1, as veins with associated bleaching of the clast terminate at the clast boundary. During this alteration, calcium, barium and silica were introduced to the rock (see Chapter Five) as calcite, barite and quartz, with associated colour changes, sericitization and chloritization (Chapter Four). Some granitoid clasts (fellow members of the 'aplitic' group) show evidence of alkali metasomatism (Chapter Five). Altered and unaltered material (pink-red and white-grey, respectively) were initially kept separate during zircon extraction. However, the paucity of rock sample and total extracted zircons required analysis of both groups together (Appendix Figure 4.1).

The hydrothermal alteration created an uncommon problem in zircon extraction because barite is very seldom found in igneous rocks in significant quantities. The physical characteristics typically used to separate zircon from the bulk of the rock are specific gravity and magnetic susceptibility. Zircon and barite have nearly identical specific gravities (4.68 and 4.5, respectively) and so are

concentrated together on the Wilfley shaking table and during heavy liquid separation. Final separation of zircons from the heavy mineral fraction is usually achieved by use of a Frantz isodynamic magnetic separator (see Appendix 4). Most minerals will become magnetized in an electro-magnetic field, with this occurring at differing current strengths for different minerals. As well, this procedure removes altered, damaged or inclusion-bearing zircon crystals that often become magnetized at lower current levels. However, barite and zircon are both considered to be non-magnetic as they only become magnetized in the electro-magnetic field generated by the highest current used (1.5 amps). Therefore the Frantz, although separating barite and zircon from the other heavy minerals, concentrates them together. The ratio of barite to zircon at this point was estimated to be from 1,000/1 to 10,000/1 (Plate 6.2a), greatly increasing the difficulty in hand-picking the final zircon population for isotopic analysis. As well, barite is virtually insoluble except at high temperatures (900°C) that would presumably affect the U/Pb systematics in the zircons.

However, barite and zircon differ in their relative hardness (H= 3-3.5 and H= 7.5, respectively). The sample was abraded for 35-45 minutes by the air abrasion technique of Krogh (1982) minus the pyrite. This abrasion reduced the bulk of the barite to -400 mesh and expelled it from the air

Plate 6.2a (Top) Photomicrograph of non-magnetic, heavy mineral concentrate of granitoid clast produced by conventional geochronological separation methods showing zircon (dark rimmed grain, in centre of photo) subordinate to very abundant barite (transparent grains), and occasional opaque mineral grains; -62+44 micron seive size; before abrasion; grain mounts in alcohol; medium power (x100).

Plate 6.2b (Bottom) Photomicrograph of non-magnetic, heavy mineral concentrate of rhyolite produced by conventional geochronological separation methods showing relative proportions of zircon (dark-rimmed grains) and barite (larger, transparent flakes); grain mounts in alcohol; low power (x40).

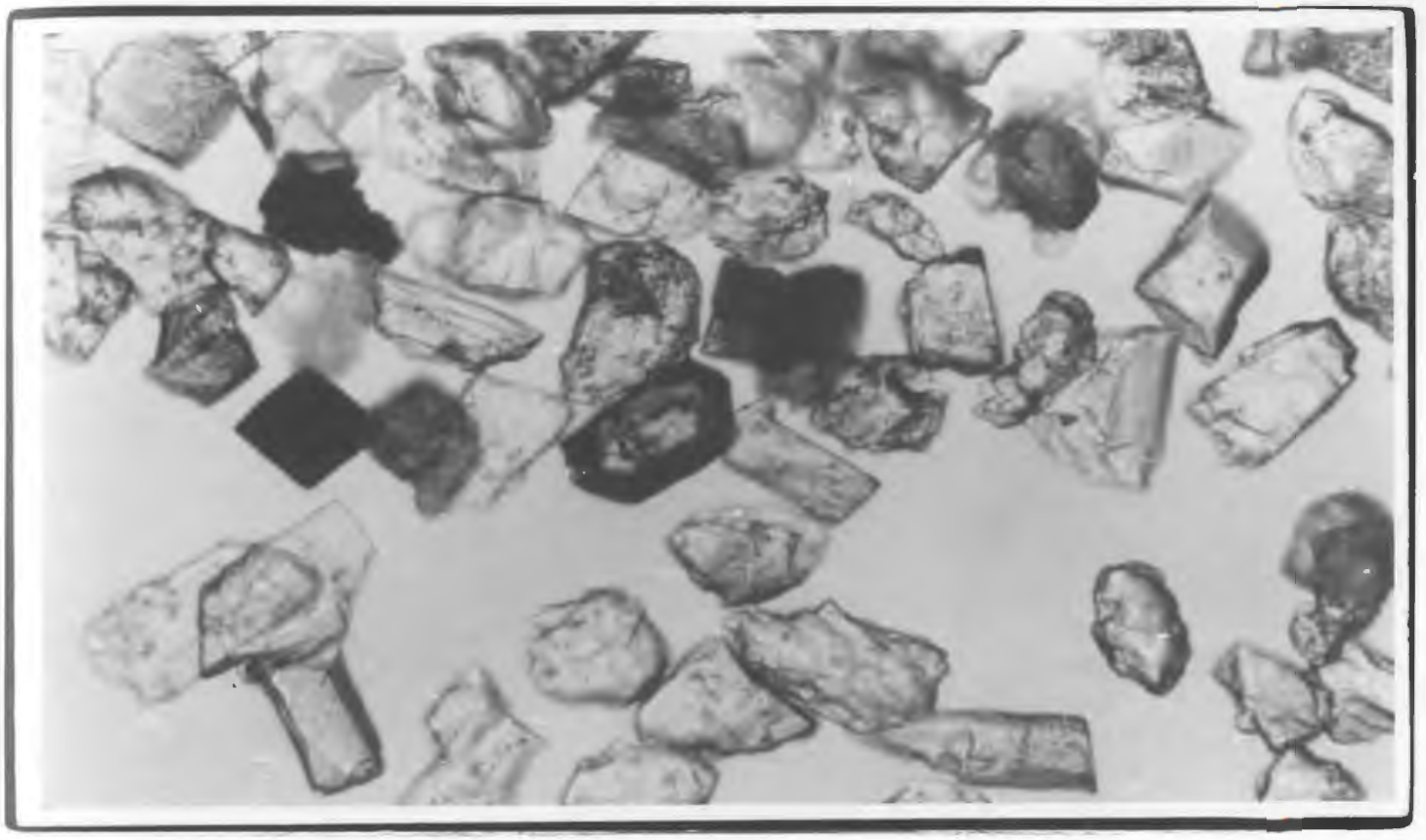

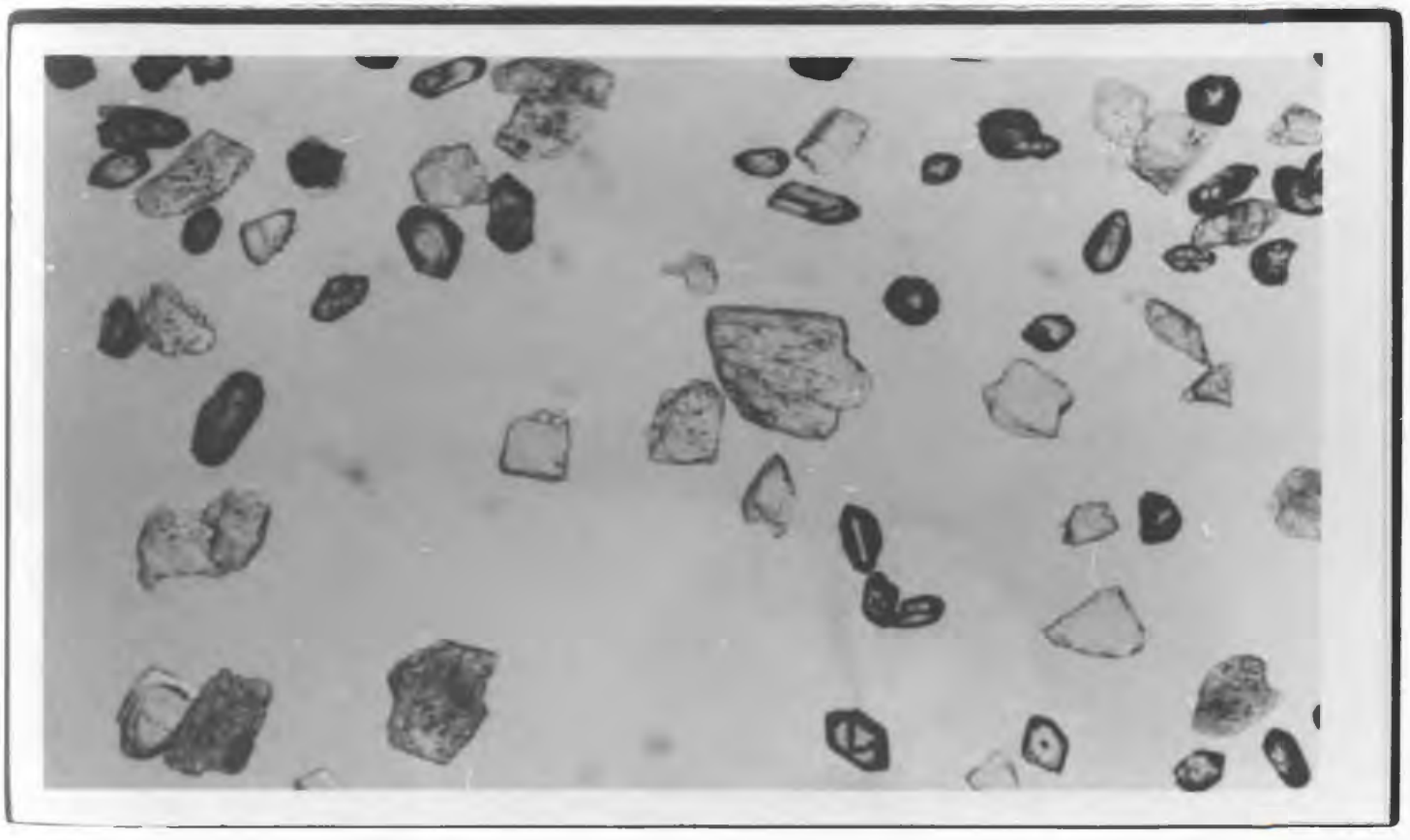

abrasion apparatus. The relatively zircon-rich population could now be conventionally separated and a final population of clear, euhedral, inclusion-free zircons (Plate 6.3b) was selected by hand-picking with a binocular microscope. During the hand-pickiing, all inclusion bearing, coloured, cracked or unusual lookiing zircons (Plate 6.3a) were excluded from the population selected for isotopic analysis.

Only one small zircon concentrate resulted from this protracted separation process (Appendix Fig 4.1). This was due to the small quantity of rock material available, the low zircon content of that material and the small average size of the contained zircons (0.074mm or smaller). The final zircon population was too light to be detectable on the 0.00001 g balance at the G.S.C. Geochronolgical Laboratory, Ottawa. Without a sample weight of the zircons analysed isotopically, measurements of the uranium and lead contents in the zircons are not possible. The measured U/Pb ratio is similar to the ratio shown by the rhyolite sample (Table 6.1), although these zircons may be richer in total uranium than the rhyolite zircons (R.W. Sullivan, written comm., 1984).

A further complication in this study was the low abundance of Pb in the zircons, i.e. less than .9 ng of Pb/aliquot. This is presumably both a reflection of their relatively young age (Paleozoic) and their source. This is

TABLE 6.1 U-Pb isotopic data

Fraction and preparation	Weight (mg)	Concentration (ppm) U	Pb	Measured $^{206}Pb/^{204}Pb$	Isotopic abundances ^{206}Pb-100 ^{204}Pb	^{207}Pb	^{208}Pb	$^{206}Pb/^{238}U$	$^{207}Pb/^{235}U$	$^{207}Pb/^{206}Pb$ (Ma)
Sample KQS-82-210 Rhyolite										
nm, -74 + 62[a]	0.50	168.6	13.57	423.3	0.0699	6.723	29.275	0.070455	0.55428	494
m2, -74 + 62[a]	0.51	123.1	10.51	493.9	0.0807	6.856	36.212	0.071158	0.55734	484
Sample KQS-82-095 Granitoid clast										
fine[b]	nd[1]	nd[1]	nd[1]	76.7	.8772	18.416	68.794	0.074556	0.57881	464

Notes: nm = non-magnetic; m2 = magnetic, +2 degrees tilt on the Frantz isodynamic separator; -74 + 62 = grain size in microns (equivalent to -200 + 325 mesh sizes); nd = not determined; a = lightly abraded to remove gangue; b = abraded to remove barite from heavy mineral concentrate

1 Weight not obtainable, measured weight was actually negative for this very small sample. U/Pb ratio = 10.52

much less than the 100 ng per cut suggested by Gebauer and Grunenfelder (1979) as necessary for routine good mass-spectrometric analysis of Pb. Even worse, the sample was contaminated with Pb by a bad batch of ion-exchange resin to produce a lead blank of 1.3 ng. Despite these problems, W.D. Loveridge (GSC, Ottawa) has obtained a concordant data point at 464 Ma for this sample (Figure 6.1). This is the same as the $^{207}Pb/^{206}Pb$ age calculated for this sample (Table 6.1).

After taking into account the uncertainty in isotopic composition from the mass-spectrometer due to the small sample size, low Pb content of the zircon, and the relatively high Pb blank, the analytical uncertainty is estimated at $\pm$40 Ma (R.W. Sullivan, written comm., 1984). This age assumes that there is no inherited lead in the zircons. No evidence of older zircon cores was observed during microscopic separation. If there is an inherited lead component, the true age could be lower than allowed by the quoted age uncertainty.

6.2.2 Rhyolite (KQS-82-210)

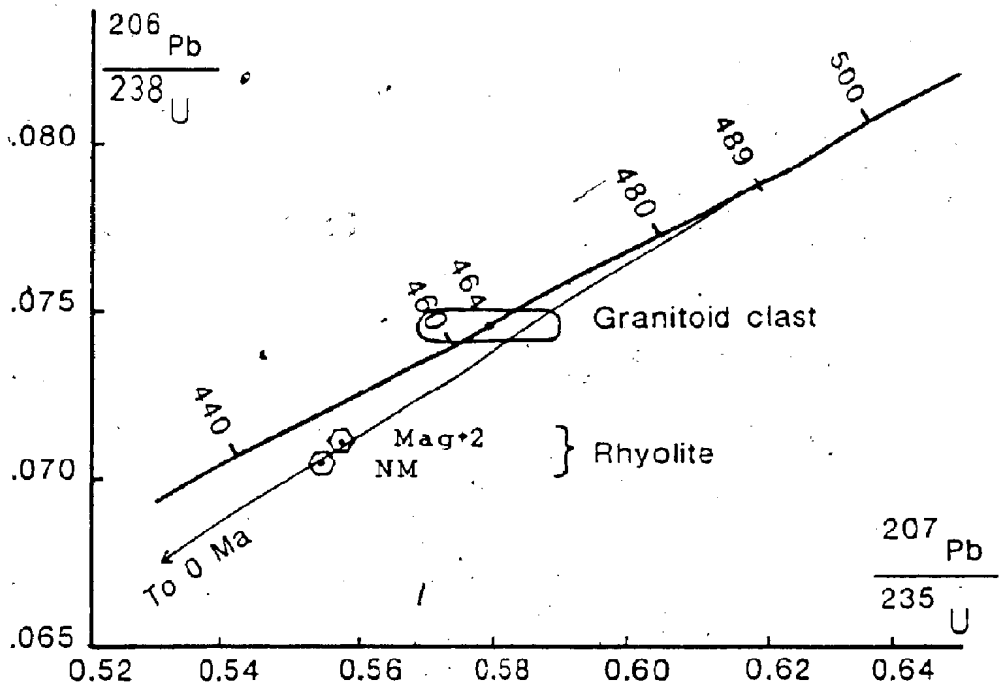

FIGURE 6.1 U/Pb concordia diagram

A maroon quartz- and feldspar-phyric rhyolite occurs within the Buchans River Formation in the MacLean Extension area (Figure 4.1). This massive unit is at least 20 m thick and is conformably overlain by a unit of dacitic pyroclastic material. The pyroclastic rocks are conformably overlain by subaqueous debris flow rocks hosting the lower ore unit of the MacLean Extension orebody (Plate 6.1). The sample location for this rhyolite in 20-6 Drive is about 30 m stratigraphically below the sample location of the granitoid clast (KQS-92-095) dated in this study (Fig. 4.1).

The extraction of zircons from this sample was less complicated than from the granitoid clast as barite was present in minimal amounts. The zircon population was typically sub- to euhedral, clear, equant in dimensions and less than 100 microns in length (Plate 6.2b). The dominant zircon population was found in the 74 to 62 micron seive size. A small amount of host rock gangue material was observed on many grains (Figure 6.4b), and was removed by abrading the sample for 10-15 minutes (Appendix Four).

The -74+62 micron size fraction was further separated on the Frantz magnetic separator into non-magnetic and magnetic fractions. The clearest, inclusion-free sub- and euhedral zircons (Plate 6.4a) were hand-picked under the binocular microscope for selection for isotopic analysis. Abrasion produced a -62+44 micron size fraction, in addition

Plate 6.3a (Top) Photomicrograph of example of inclusion-bearing, cracked zircon from granitoid clast with attached gangue material excluded from zircon population selected for isotopic analysis; grain mounts in alcohol; high power (x400).

Plate 6.3b (Bottom) Photomicrograph of zircon population selected from granitoid clast for isotopic analysis after abrasion and hand-picking; largest zircon is <74 microns; grain mounts in alcohol; low power (x40).

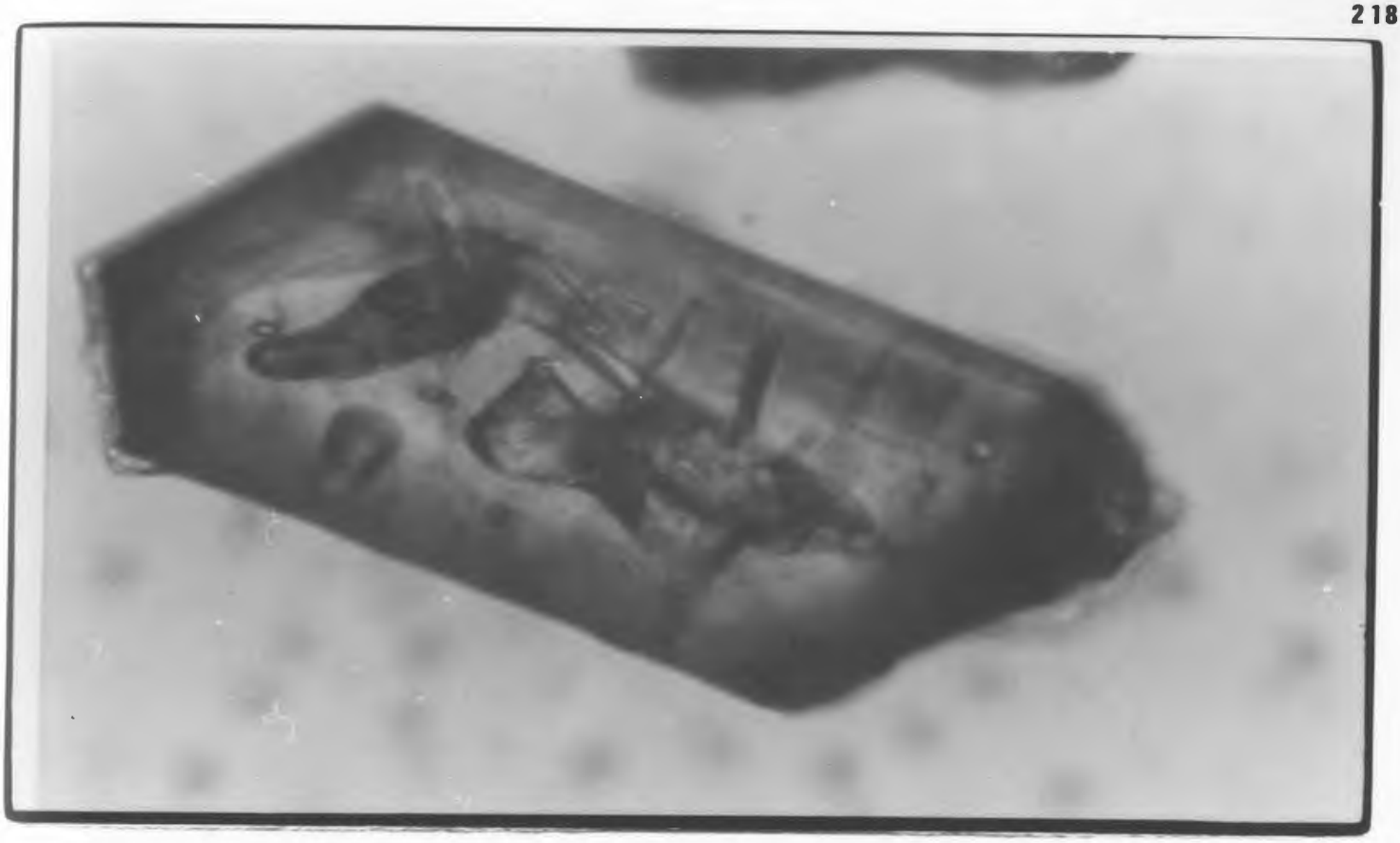

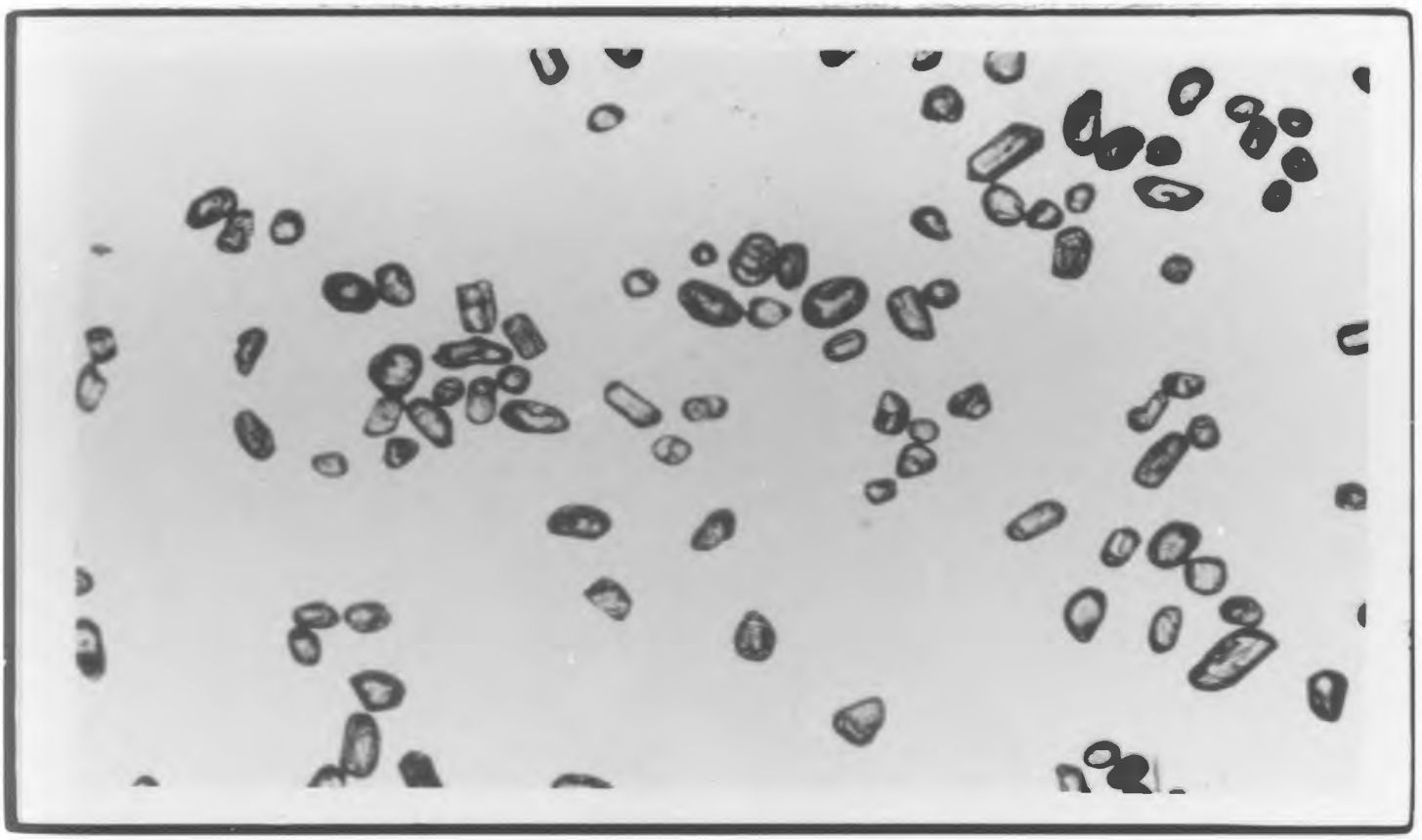

Plate 6.4a (Top) Photomicrograph of typical euhedral, clear, inclusion-free zircon selected from rhyolite for isotopic analysis; -62+44 micron seive size; lines within grain are crystal faces, not inclusions or an older core; grain mounts in alcohol; high power (x400).

Plate 6.4b (Bottom) Photomicrograph of euhedral, clear zircon from rhyolite with small amount of attached gangue material prior to abrasion; from non-magnetic, heavy mineral concentrate; grain mounts in alcohol; high power (x400).

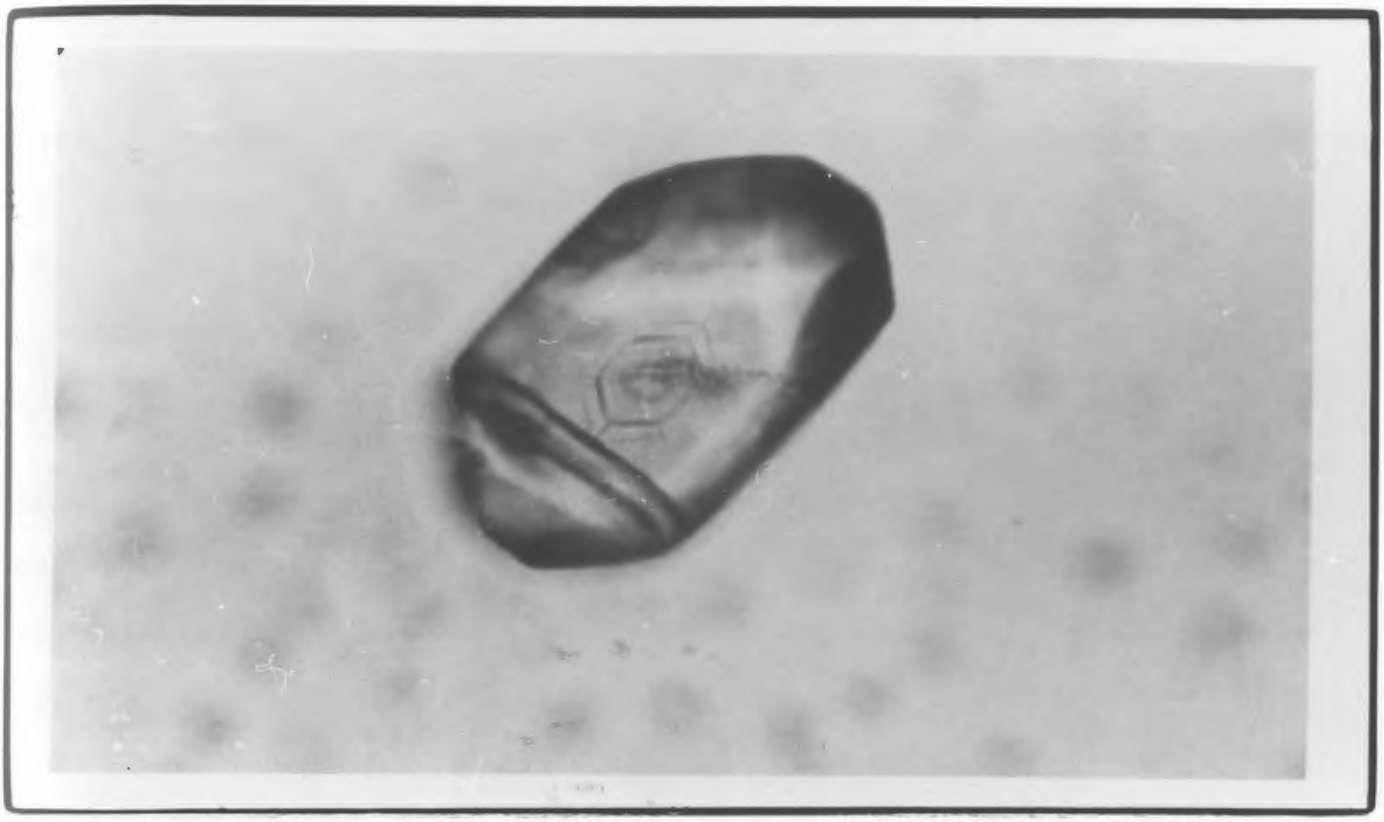

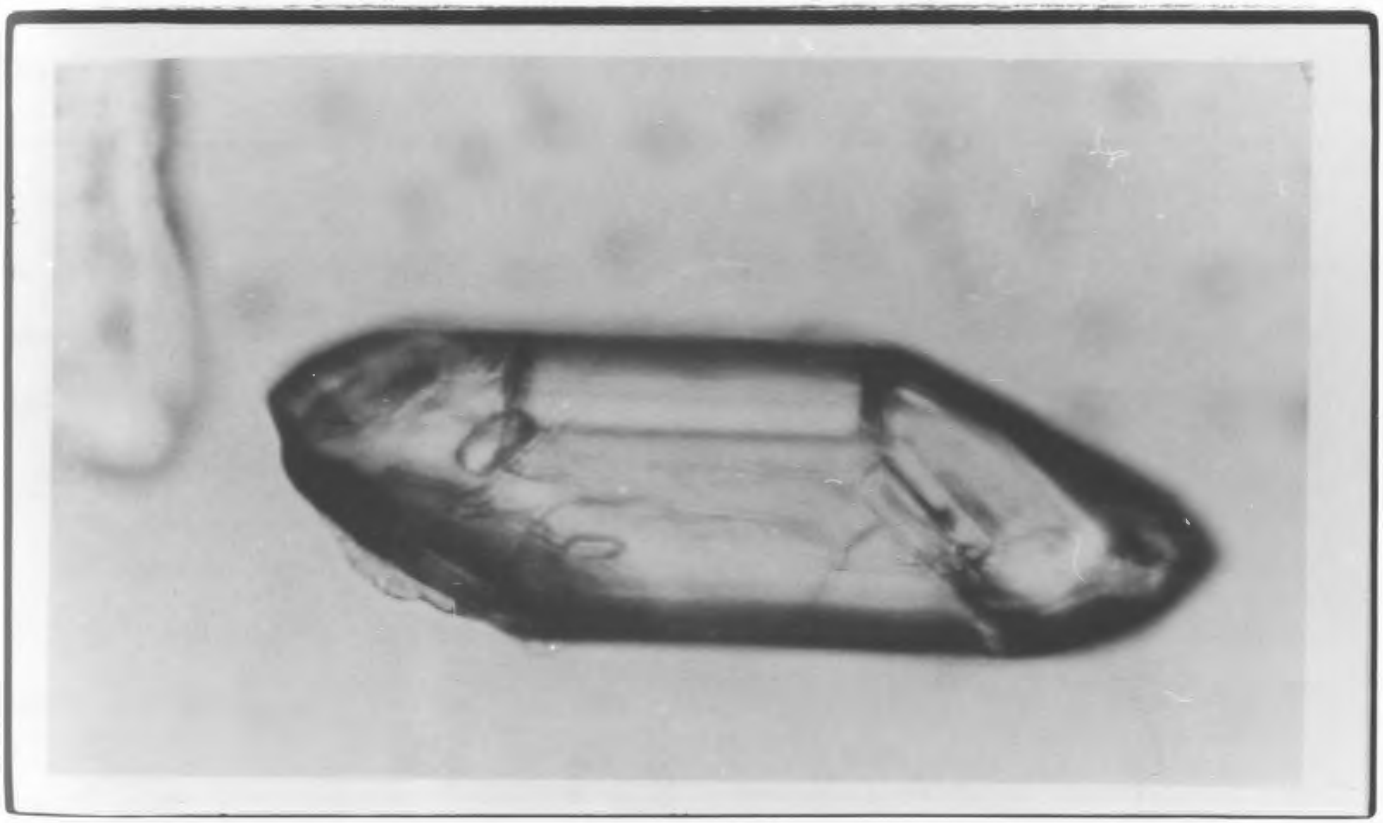

to the original size fraction (Appendix Figure 4.2). However, during analysis, this sample did not yield any reportable data due to excessively short vaporization time during the mass-spectrographic analysis (R.W. Sullivan, pers. comm., 1984).

The two isotopic data points obtained from the rhyolite zircons lie close together near the concordia curve (Figure 6.1). They define, however, a line-of-best-fit which has a negative lower intercept. The lower intercept on concordia diagrams is commonly interpreted to record a time of lead loss subsequent to the closure of the mineral system at the time of crystallization (Gebauer and Grunenfelder, 1979). A negative intercept would therefore represent a future time, which is, of course, meaningless. This intercept is probably due to the closeness of the two points used to define the line, and the fact that only two points are used to define it. For this reason, a second line-of-best-fit that passes through the origin and the two points has been drawn. This chord intersects the concordia curve at 489 Ma (Figure 6.1), which is considered to be the best estimate for the time of formation of the rhyolite.

Zircons from the two fractions of the rhyolite are very low in U (169ppm and 123ppm, Table 6.1). Therefore, radiation damage to the zircons in c.500 Ma would probably be slight. Lead loss is often attributed to the amount of

radiation damage to the zircon crystal lattice (Gebauer and Grunenfelder, 1979), which is related to the concentration of U within the zircon and the amount of time since formation. Interaction with groundwater is known to promote lead loss (Gebauer and Grunenfelder, 1979). Since the sample is from > 1 km below the earth's surface, interaction with groundwater has probably been a geologically recent event. Therefore, a 0 Ma lead loss line is physically realistic.

The date of 489 Ma is also the average of the two 207Pb/206Pb ages (Table 6.1). Since the two 207Pb/206Pb ages differ by 10 Ma, a reasonable value for the uncertainty in this age for the rhyolite is considered to be ±20 Ma (R.W. Sullivan, written comm., 1984).

As in the case of the granitoid clast sample, this age assumes that there is no inherited lead component in the zircons. If there is such a component, the true age could be lower than allowed by the quoted uncertainty limits. However, the zircons are very low in Pb (approximately 2 ng per cut, Table 6.1), suggesting that if there is an inherited component, it must be very small.

6.3 DISCUSSION OF THE ANALYTICAL RESULTS

6.3.1 Source of the granitoid clasts

It became apparent during the study that because of the paucity of both sample material and recoverable zircons from the granitoid clast only one analytical point could be produced for that sample. Rather than abandon the study, it was decided to accept a compromise. The abrasion needed to remove the excess barite would also abrade the zircons and would push the analytical point from these zircons toward, and hopefully onto, the concordia curve (Krogh, 1982). An isochron would be defined by the three rhyolite isotopic analyses. If the clast and rhyolite were comagmatic (and at worst, penecontemporaneous), the granitoid clast data point would fall on or near the isochron defined by the rhyolite zircons within the limits of analytical uncertainty. From Figure 6.1, it can be seen that this result was obtained (uncertainty bars determined by W.D. Loveridge, G.S.C.).

The granitoid clast zircon isotopic analytical point is on concordia and overlaps the isochron defined by the rhyolite sample zircons within the estimated isotopic analytical uncertainty (Figure 6.1). The radiometric dates determined for the granitoid clast (464±40 Ma) and a Buchans Group rhyolite (489±20 Ma) also overlap within the estimated

uncertainties of their age. A direct measurement of the U and Pb abundances in the clast is not possible because its weight was too small to be detectable on the equipment available. However, the calculated U/Pb ratio in the granitoid clast zircons (10.52) is similar to that shown by the rhyolite zircons (12.42 and 11.71; Table 6.1). The analytical results are interpreted to permit a comagmatic origin for the the Buchans Group and the granitoid clasts (Chapter 5).

The analyzed clast is a member of the 'aplitic' group of clasts. On the basis of the distribution patterns of the granitoid clast types (Chapter Four), and textural (Chapter Four) and geochemical (Chapter Five) considerations, this group of granitoid clasts is thought to have crystallized more rapidly and at slightly more differentiated stage than the 'granitic' group clasts. The younger age for the clast suggests that the clast may have crystallized not long before its incorporation into the host debris flow.

The 25 Ma difference in ages is greater than that envisioned by the author for the true times of crystallization of the rhyolite and the granitoid clasts. This difference probably reflects the analytical problems encountered during the study and the resulting large uncertainty estimates for these ages rather than the absolute difference in their

individual times of crystallization. The radiometric study of Dunning (in progress) will include a re-analysis of the same rhyolite and may resolve this apparent discrepancy.

6.3.2 Age of the Buchans Group

The age of 489±20 Ma for the rhyolite is clearly indicative of a pre-Caradocian age of deposition for at least some of the Buchans Group. Even with the large age uncertainty, only one recently proposed time scale for the Ordovician (Ross and Naeser, 1982; Ross et al., 1984) would permit this age to be possibly within the Caradocian (Table 6.2). This strongly mitigates against the post-Caradocian age for the Buchans Group suggested by Strong (1977), Dean (1978) and Kean et al. (1981). Depending on the time scale employed (Table 6.2), this age appears to indicate an Arenigian (van Eysinga, 1975; Ross and Naeser, 1982; Harland et al., 1982) or Llanvirnian (Armstrong, 1978; McKerrow et al., 1980) age of formation. Lead/Lead ages for the rhyolite (484 and 494 Ma) are both Llanvirnian or older, no matter which scale is used. The date of 489±20 Ma appears to be significantly older than the Rb-Sr whole rock date of 447±18 Ma for the Buchans Group by Bell and Blenkinsop (1981). However, these dates only differ by 4 Ma if one takes into account the maximum uncertainty limits in

Table 6.1 Comparison of estimates for the absolute ages (Ma.) for the base of the Silurian epoch and the base of the British paleontological stages of the Ordovician epoch.

	van Eysinga (1975)	Armstrong (1978)	McKerrow et al. (1980)	Harland et al. (1982)	Ross & Naesser (1984)
Silurian	434	446	438	438 ±12 (2)	436
Ashgill	439	455	445	448 ±12	?
Caradoc	449	465	467	458 ±16	475
Llandeilo	460	477	479	468 ±16	477
Llanvirn	471	492	489	478 ±16	487
Arenig	490	500	504	488 ±20	493
Tremadoc	500	510	519	505 ±32	515

these dates, i.e., 489-20 Ma and 447+18 Ma.

The measured age of the granitoid clast (464 Ma) can be no younger than Caradocian, regardless of the scale used. The uncertainty limits permit it to have a true age that could even be Silurian. However, Silurian dates of 420-430 Ma from the Topsails Granite (Whalen and Currie, 1985), that post-dates the deformation and thrusting of the Buchans Group (Thurlow, 1981a,b), disallows the possibility of such a young age for the granitoid clasts or the Buchans Group.

Ages of 477 and 481 Ma (Dunning, 1984) for trondhjemites associated with ophiolitic rocks of the Annieopsquotch Complex to the south of the Buchans Group may indicate that the age determined for the rhyolite is too old. As well, Dunning (1984) produced dates for a trondhjemite and gabbro of 486 and 489 Ma, respectively, from the Betts Cove Ophiolite Complex to the north of Buchans. All of these dates are estimated to be accurate within 4.0 Ma or less (op cit.) and suggest that the date determined for the rhyolite is either too old or that Buchans Group volcanism was roughly contemporaneous with magmatism associated with the formation of oceanic crust in Newfoundland as preserved in the Annieopsquotch Mountains and western Notre Dame Bay. The large age uncertainties for the date from the rhyolite make any conclusions regarding this possible discrepancy tenuous.

The dates for the granitoid clast and the rhyolite are compatible with the paleontological age (Llanvirn-Llandeilo) assigned to the Buchans Group by Nowlan and Thurlow (1984) and support their interpretation of a pre-Caradocian time of formation for the Buchans Group.

The Glover Island Formation (Knapp, 1984) on the western flank of the Topsails Igneous terrane shows many similarities to the Buchans Group (Whalen and Currie, 1985). Conodonts in the Glover Island Formation indicate an Arenigian time of deposition (Whalen and Currie, 1985). Whalen and Currie suggest that it may, therefore, be a slightly older, lithologically similar correlative to the Buchans Group. A granitoid body in the Hinds Lake pluton of the Topsails Igneous terrane has yielded a Middle Ordovician zircon age, identical to but more precise than the age for the granitoid clast determined in this study (Whelan and Currie, 1985). They suggest that the Buchans Group may be better considered affiliated with the Topsails Igneous terrane than the volcanic rocks of the Central Volcanic Belt of Newfoundland. Although inconclusive, the available isotopic data appears to support this contention.

In order to resolve this and other problems of the relative and absolute stratigraphy of central Newfoundland, accurate age determinations on the Buchans Group and other igneous rocks in the area are required. This work is

presently in progress (Dunning, pers. comm., 1984) and will include new isotopic data from the MacLean Extension rhyolite dated in this study. However, no results from this study are available at this time.

6.4 CONCLUSIONS

Only tentative conclusions may be drawn from the data due to the large degree of uncertainty in the absolute ages determined in this study. The overlap of the isotopic analysis for zircons from the granitoid clast with the isochron constructed by isotopic analyses of zircons from the rhyolite, as well as an overlap within the estimated age uncertainties for each, indicate a broadly contemporaneous time of formation for the granitoid clasts and the Buchans Group volcanic rocks (Chapter Five). The younger age for the granitoid clast relative to the rhyolite makes it impossible for the granitoids to have been eroded from a crystalline terrane older than the Buchans Group rhyolite. The fine grained aplitic and granophyric texture of some of the granitoid clasts suggests they crystallized rapidly. This may have occurred close to the time of their incorporation into the debris flow. A penecontemporaneous or contemporaneous time of origin for these clasts and the Buchans Group volcanic rocks supports the interpretation of

Nowlan and Thurlow (1984) that all clasts present in debris flows at Buchans (including the conodont-bearing carbonate clasts) were derived locally.

The age of the Buchans Group appears to be Caradocian or older based on the radiometric data. The radiometric dates from the rhyolite and especially the granitoid clast indicate, within the estimated age uncertainties, that the Buchans Group magmatism may have persisted into the Caradocian.

Chapter Seven

DISCUSSION and CONCLUSIONS

7.1 INTRODUCTION

A model to explain the presence and provenance of granitoid clasts in sediment debris flows at Buchans must be able to account for several features evidenced by these clasts. These include: 1) the greater degree of roundness of the granitoid clasts relative to other clast lithologies; 2) the maximum abundance of granitoid clasts (by volume) and the largest (average size) granitoid clasts proximal to the maximum sulphide accumulations in the debris flows deposits; 3) the range of igneous textures evident in the granitoid clasts (plutonic, aplitic-granophyric); 4) the geochemical differences and similarities between the granitoid clasts and their apparent comagmatism; 5) the changes in the composition and textural character of the granitoid clast population within and between debris flow sequences; 6) the apparent comagmatism of the granitoid clasts and Buchans Group felsic flows; 7) the hydrothermal alteration of the granitoid clasts and its variable intensity; 8) evidence of

brecciation in some granitoid clasts that appears to be related to the alteration process; and 9) the roughly coeval radiometric dates (within estimated analytical and age uncertainties) obtained for a granitoid clast and Buchans Group rhyolite, and the slightly younger age obtained for the granitoid clast relative to the underlying rhyolite unit. The model presented here attempts to explain these features in the context of existing knowledge of events at Buchans.

7.2 GENERAL DISCUSSION OF EVENTS AT BUCHANS

The in situ and transported massive sulphide orebodies at Buchans are considered to have formed in a manner analogous to the Tertiary Kuroko deposits of Japan (Thurlow, 1977, 1981a,b). Hydrothermal fluid flow during a period of dominantly explosive felsic volcanic activity resulted in the deposition of the sulphide ore bodies (Henley and Thornley, 1981). The discharge of metalliferous hydrothermal fluids at or near the sea floor/sea water interface deposited ponds of sulphide mud that, when lithified formed the in situ orebodies (Henley and Thornley, 1981). During the fluids' passage to the discharge site, the porous and fractured rocks of the Ski Hill and Buchans

River Formations (Thurlow and Swanson, 1985) were altered and mineralized (Henley and Thornley, 1981).

In situ ore deposition was preceded and possibly accompanied and terminated by volcanic and/or phreatomagmatic explosions. These explosions both brecciated the pre-existing rocks and deposited highly porous pyroclastic rocks facilitating the movement of hydrothermal fluids. This permitted the high discharge rates necessary for the geologically reasonable time spans of ore formation that are estimated at both Buchans and Kuroko to be from 500 to 5000 years (Henley and Thornley, 1981; Cathles, 1983)

The sulphide mud ponds were disrupted and fragmented while still in a plastic state (Thurlow and Swanson, 1981). Parts of this sulphide body were mechanically transported down paleo-slope in sediment debris flows, both as lithified (angular) and unlithified (wispy and plastically deformed) clasts (Thurlow, 1977, 1981b). The disruption and subsequent transportation of the sulphide mud ponds was intermittent, and occurred during episodic felsic pyroclastic volcanism (Binney et al., 1983).

The debris flows were probably initiated at or near sea level (Nowlan and Thurlow, 1984). Recent studies in the Kuroko district demonstrate the formation of the volcanic

and sedimentary rocks associated with the massive sulphide orebodies there at water depths of approximately 3500m (Guber and Merrill, 1983). Other recent studies show the theoretical possibilty of both vesicular basalts (Dudas, 1983) and felsic pyroclastic rocks forming at similar depths (Burnham, 1983). The highly amygdular nature of many Buchans Group basaltic rocks and the abundance of felsic pyroclastic rocks were used by Thurlow (1981a,b) in his original interpretation of a shallow water origin for the Buchans Group and its' orebodies. However, the amygdular basalt that was formerly assigned to the Footwall Basalt is now considered to be in the Sandy Lake Formation and to stratigraphically overlie the orebodies. Therefore, the proposed shallow marine to subaerial environment of deposition proposed for the Buchans Group and its orebodies (Thurlow, 1981b; Nowlan and Thurlow, 1984) may require reappraisal. The depth at which the volcanism occurred and the debris flows initiated is presently not known with any certainty.

The high energy event that initiated the mass sediment movement was probably due to either explosive volcanic activity, phreatomagmatic explosions or earthquakes related to either process (Thurlow and Swanson, 1981). This is in contrast to the slumping of massive sulphide orebodies at the Kosaka mine, Japan due to intrusive activity

(Hashiguchi, 1983). Explosive volcanic activity may be due, at least in part, to phreatomagmatic activity (Williams and McBirney, 1979) that is caused by meteoric or sea water coming into contact with a shallow magma chamber and explosively changing into a vapor phase (Wolfe, 1980). Phreatomagmatic explosions also occur when magmatic hydrothermal fluids cross the boiling point-depth (BPD) curve in their ascent to the discharge site (Henley and Thornley, 1981). The BPD curve marks the temperature and pressure conditions under which a super-heated fluid will explosively expand to steam and rupture the overlying rock (Burnham, 1979). The explosive volcanic activity accompanying these debris flows (Binney et al., 1983) suggests that it was this activity and possible related earthquakes that initiated the mass sediment movement at Buchans.

A heat source is thermodynamically necessary to drive a hydrothermal convection cell (Cathles, 1981, 1983). A shallow (subvolcanic), cooling igneous body is generally postulated as this source (Franklin et al., 1981). The occurrence of shallow, felsic intrusive bodies spatially associated with the massive sulphide orebodies is common in the Kuroko district (see Ishihara, 1974; Lambert and Sato, 1974; Ohmoto and Skinner, 1984) and in some Precambrian volcanogenic sulphide deposits (Campbell et al., 1981).

However, the postulated genetic control of the composition of these intrusive bodies on the formation of ore deposits (Campbell et al., 1981, 1982) does not appear valid at Buchans (Strong, 1984).

Stable isotope studies at Buchans indicate that the mineralizing fluid was composed dominantly of seawater, but with a minor component of magmatic fluids (Kowalik et al., 1981). Models for the source of the metals at Buchans indicate that the underlying volcanic rocks could not yield the known metal concentration by leaching and that there must have been some contribution of metals from a magmatic source (Sawkins and Kowalik, 1981). These data suggest that there was a magma chamber in close proximity to and probably beneath the Buchans orebodies when they were deposited.

Stanton and Ramsay (1980) suggest that the time of volatile loss in relation to the extent of differentiation in a magma system may be an important control on whether massive suphide orebodies are deposited, the size and metal composition of the orebodies, the apparent calc-alkaline composition of the related volcanic rocks and the abundance of explosive volcanic activity associated with ore deposition. Large tonnage Pb-rich ores are typically restricted to highly evolved magma systems. The apparent calc-alkaline composition of the Buchans Group, the abundance of explosive felsic volcanic rocks in the Buchans

River Formation that hosts the orebodies, the large tonnage and Pb component of the Buchans ores and the magmatic component to the mineralizing fluids and ore metals present at Buchans appear to support their hypothesis.

A volatile phase can become concentrated in the melt during progressive crystallization of a magma (Burnham, 1979). This is the result of the relative incompatibility of volatile components with respect to the main crystallizing silicate phases. When the concentration of volatiles exceeds their solubility in the melt and the confining pressure, the expulsion (exsolution) of a hydrous fluid phase from the melt can occur (Burnham, 1979). The exsolution of this fluid typically ruptures the enclosing strata and, if it occurs at shallow enough depths, may vent explosively to the surface. This is considered to be the cause of breccia pipes associated with some Kuroko (Takanouchi, 1978; Urabe et al., 1983) and copper porphyry orebodies (Sillitoe and Sawkins, 1971; Norton and Cathles, 1973).

Hydrothermal fluid flow would presumably be concentrated in any pre-existing structures in the host rocks as appears to have occurred at Buchans (Thurlow and Swanson, 1985). A periodicity in explosions may be expected as the channelways of the plumbing system became blocked due to mineral deposition in the upper levels due to changes in

the physico-chemical conditions encountered by the fluids during upward movement. Such blockages would build up fluid pressures until they exceeded lithostatic pressures and ruptured the rock thereby permitting the resumption of fluid flow. Subsequent mineral deposition may again block the channelways and the process is repeated.

The transportation of subsurface material upward by explosive hydrothermal activity in structurally controlled zones of fluid flow has been proposed as a method for the rounding and transportation of subsurface material present in some breccia pipe ore deposits (e.g., Bryant, 1968; Armbrust, 1969; Mitcham, 1974). Explosive exsolution of a fluid phase from an intrusive body is considered to be the mechanism that transported rounded and altered intrusive material occurring in intrusive breccia pipes at Cornwall, England (Allman-Ward et al., 1982). Wolfe (1980) considers explosive hydrothermal activity to be necessary to transport any subsurface material to the surface rather than the fluidization model of Reynolds (1954) invoked by Bryant, Mitcham, Allman-Ward et al. (op cit) and other workers. The presence of clasts of previously mineralized and altered volcanic rocks that were apparently brought from the stockwork zone (Thurlow and Swanson, 1981; Henley and Thornley, 1981) clearly indicates the movement of subsurface material upward to be incorporated in Buchans debris flows.

The explosive felsic volcanism associated with sulphide mineralization at Buchans is recorded the host rocks of the Buchans River Formation. This volcanic episode was succeeded by the voluminous, relatively quiescent basaltic volcanism of the overlying Sandy Lake Formation. The relationship between the felsic volcanism that produced the material for the arkose and arkosic conglomerate deposits within the Sandy Lake Formation (Section 2.6.5) to the earlier felsic volcanic centers in the Buchans area is presently unknown.

7.3 DISCUSSION OF OBSERVED FEATURES OF GRANITOID CLASTS IN MacLEAN EXTENSION

The model presented (Section 7.4) attempts to account for all the observed features of the granitoid clasts listed above (Section 7.1). The most significant of these features are considered to be: 1) the apparent comagmatism of the granitoid clasts and the Buchans Group felsic volcanic rocks; 2) the greatest concentration (by volume) of granitoid clasts proximal to the maximum sulphide concentrations in MacLean Extension orebody; 3) the occurrence of the largest, most altered and dominantly 'granitic' group granitoid clasts proximal to the maximum

sulphide concentrations in MacLean Extension.

Major, trace and rare earth element abundances in the granitoid clasts are sufficiently similar to indicate that they probably had a common magmatic source (Section 5.3). Similar trace and REE abundances suggest that the granitoid clasts and Buchans Group felsic volcanic rocks also had a common magmatic source (Section 5.4). The two bodies of Feeder Granodiorite could have been part of this same magma system, although one, the Wiley's River Intrusion, appears to have crystallized at a slightly more differentiated stage than the Buchans Group felsic volcanic rocks, the granitoid clasts or the Little Sandy Lake Intrusion (Section 5.4).

Radiometric dates of the time of crystallization of a granitoid clast and a Buchans River Formation rhyolite from MacLean Extension mine overlap within the estimated uncertainties in the dates, empirically supporting their probable comagmatic origin.

The range of igneous textures from plutonic to sub-volcanic demonstrated by the granitoid clasts has been interpreted to reflect different crystallization histories or levels for the clasts and provides the basis of the classification of granitoid clasts types and derivative groups (Chapter Four). This apparent comagmatism and the indication of progressive differentiation from the more

intermediate composition of type 6 clasts to the felsic 'granitic' group and then to the 'aplitic' group supports this interpretation (Section 5.3).

The observed distribution of the granitoid clasts is interpreted to significantly constrain the origin of the granitoid clasts. Their maximum concentration (both volume and size) with the sulphide-rich sections of the debris flow sequence has profound restrictions on their possible source area. Other than density there is no known process that would concentrate the granitoid clasts with the sulphides during transportation in the debris flow. There is probably no appreciable density difference between the granitoid clasts and other clasts lithogies to warrant their concentration in close proximity to the sections of the debris flows containing the greatest abundance of the significantly denser sulphide clasts and sulphide matrix material (sulphide matrix ore). Mixing of material within a flow during transport would presumably dilute any pre-existing concentration. No apparent concentration of other clast lithologies with the sulphide-rich zones of the debris flows is observed. This suggests that the source of the granitoid clasts and the site of the sulphide mineralization were spatially associated prior to their incorporation in the debris flows and that there has been no density sorting during flow movement.

The alteration of the granitoid clasts is similar to that typically seen in volcanic rocks associated with massive sulphide deposits including Buchans, i.e. chloritization of mafic minerals, sericitization of plagioclase, and the introduction of carbonate and silica (Franklin et al., 1981; Thurlow, 1981a; Urabe et al., 1983). The pervasively altered granitoid clasts (i.e., members of the 'granitic' group; Section 4.7), are most abundant in the earlier, more sulphide-rich sections of the debris flows, such as those seen at 20-13 Drift and 20-5 Sublevel in MacLean Extension. Several of the most intensely altered clasts were apparently brecciated prior to or accompaning the alteration (Section 4.6). These features suggest exposure of these granitoid clasts to the hydrothermal fluids responsible for the massive sulphide mineralization and the associated alteration and mineralization of the underlying volcanic rocks.

Alteration of the clasts could have possibly occurred within the debris flow during transportation or even post-transport. If so, one may expect to see clasts with more altered rims than cores. This was not observed. Alteration is generally pervasive, or occurs as veins that almost invariably are truncated at clast boundaries. In addition, the presence of alteration selvedges on some but not all sides of other lithic clasts (Thurlow, 1981a;

Thurlow and Swanson, 1981) does not support a syn- or post-transportation origin for this alteration. This latter phenomenon has been elegantly explained by Thurlow (1981a) as a result of fracturing and alteration of rocks underlying the sulphide mud pond and their subsequent fragmentation and incorporation into the debris flow. Thurlow (1981a) has suggested that the anomalous Ba contents that characterize the host rocks to the mineralization could be due to diffusion from the barium-rich orebodies. However, the typical association of barite with pervasive alteration and accompanying brecciation would appear to rule out a diffusive origin for the barite seen in the granitoid clasts.

The less pervasive or lack of alteration effects in the 'aplitic' group indicates a source that was less affected by hydrothermal fluids than the 'granitic' group clasts. The very fine grain size and abundance of granophyric textures in the 'aplitic' group clasts suggests rapid crystallization, probably at a high crustal level. The alkali metasomatism shown by 'aplitic' group clasts may be due to the loss of a late-stage volatile phase that accompanied this rapid crystallization.

The absence of sulphide matrix ore and the corresponding lower concentration of sulphides in subsequent debris flows indicates a decrease in the amount of sulphides available in the source region of the debris flows. The finer grained, aplitic, less pervasively altered and typically smaller granitoid clasts with granophyric intergrowths (i.e., the 'aplitic' group members) replace the 'granitic' group as the dominant granitoid clasts in these later, less sulphide rich debris flows (e.g., 20-6 Sublevel) (Section 4.7). A decrease in the average granitoid clast size, degree of hydrothermal alteration and volume of the debris flow occupied by granitoid clasts accompanies this change in the granitod clast population (Chapter Four). The absence of any granitoid clasts in the subeconomic, baritic upper ore unit of the MacLean Extension orebody (Binney et al., 1983; Section 4.2) further substantiates a change in the source region of the debris flows. Therefore a change in the character of the granitoid clasts from dominantly 'granitic,' altered and rounded to 'aplitic', and less altered with a decrease in average size and volume occupied by granitoid clasts accompanies the general decrease in the concentration of sulphides and increase in the barite contained in the debris flow deposits. These changes appear to indicate the disruption of the hydrothermal fluid system that deposited the sulphide minerals by the high energy event that initiated the debris

flow movement.

There is no evidence that the greater degree of rounding of the granitoid clasts relative to other clast lithologies is due to sedimentary processes. The elongate form displayed by most granitoid clasts (Plate 7.1) (Section 4.3.2), especially the spindle-shaped clasts (Plates 4.3, 4.11) are atypical of boulders and cobbles of undeformed felsic intrusive rocks that have been rounded by sedimentary processes. The irregular nature of the outer surface of a granitoid clast does not resemble that typically seen in rounded granitic boulders in sedimentary rocks (Plate 7.2).

Rounded granitoid clasts have been seen in breccia pipes in the Kuroko district (Takanouchi, 1978; Urabe et al., 1983) and economically mineralized breccia pipes in the Canadian Shield (Armbrust, 1969). Similar breccia pipes with rounded igneous material are associated with porphyry copper deposits (Bryner, 1961; Bryant, 1968; Norton and Cathles, 1973; Sillitoe and Sawkins, 1971; Carlson and Sawkins, 1980), although many of these pipes indicate the presence of chemically distinctive fluids, i.e. they are often tourmaline-bearing suggesting F- or B-rich fluids. No evidence of rounding due to the corrosive ability of the hydrothermal fluids responsible for formation of breccia pipes have been observed (cf. Sawkins, 1969). Rounding of granitoid clasts due to comminution in such pipes by the

Plate 7.1 Photograph of elongate granitoid clast in granitoid-bearing polylithic breccia-conglomerate, 20 Level, MacLean Extension.

Plate 7.2 Photograph of granitoid clast in granitoid-bearing polylithic breccia-conglomerate with irregular outer surface in contrast to smooth, rounded surface of rhyolite clast at upper right; black ore clast with wispy terminations at bottom; 20-5 Sublevel, MacLean mine; knife for scale.

expulsion of hydrous fluids from a magma system is especially well evidenced at Cornwall, England (Allman-Ward et al., 1982). The control of breccia pipe occurrences by fault structures and movement on these structures has also been proposed as a mechanism for rounding clasts contained in breccia pipes (Mitcham, 1974).

Granitoid clasts occur in the Buchans Group in many breccia flows that do not contain sulphide mineralization of any significance. However, this is generally only as rare, isolated clasts. Whether these were produced at the same time as the granitoid clasts in mineralized debris flows is unknown, partly because of uncertainties in the stratigraphic position of these units in the Buchans Group.

The extreme rounding of granitoid clasts in the Old Buchans conglomerate orebody (Thurlow and Swanson, 1981) suggests sedimentary reworking. In this deposit, not just the granitoid clasts, but all lithic clast types present are well rounded and appear to indicate a sedimentary reworking that is lacking in clasts seen in other rudaceous units at Buchans. This deposit is different from other transported orebodies at Buchans and may be evidence of a reworked debris flow deposit.

7.4 A MODEL FOR THE OCCURRENCE OF THE GRANITOID CLASTS

The model presented here is based on the preceding discussion (Section 7.3) and is shown schematically in Figure 7.1. It is based primarily on observations of granitoid clasts in MacLean Extension area but is believed to apply to other granitoid clasts associated with transported orebodies contained in the Rothermere-MacLean channel (Walker and Barbour, 1981).

Insufficient detailed observations and lack of accessibility preclude definitive statements regarding possible differences in granitoid clasts found in other transported orebodies at Buchans. The present interpretation of the restriction of all significant sulphide mineralization to a single stratigraphic level (Thurlow and Swanson, 1985) suggests that the presented model for the source of the granitoid clasts in the MacLean Extension orebody may be applicable to other transported orebodies at Buchans outside the Rothermere-MacLean channel.

Explosive felsic volcanism typifies the Buchans River Formation (Sections 2.6.4; 4.2). The deposition of the siltstone unit and the sulphide mud ponds represented by the in situ orebodies appears to record an hiatus in this volcanism (Figure 7.1a). The highly felsic composition of

the magma is shown by the composition of the clasts in the pyroclastic rocks (Thurlow, 1981a) and that of interbedded rhyolitic units. Felsic magmas are typically very viscous and may promote such an hiatus during volcanism (Williams and McBirney, 1979). The large size of the in situ orebodies at Buchans may possibly reflect the length of this hiatus in volcanism.

The rugged paleo-topography of the area is indicated by the restricted distribution of the siltstone, siltstone breccia and debris flow sequences and may have been controlled by early fault planes (Thurlow and Swanson, 1985). Correspondingly, other early fault structures may have localized the sites of in situ sulphide mineralization and related alteration. A magmatic component to the hydrothermal fluids responsible for this mineralization has been postulated by (Kowalik et al., 1981; Sawkins and Kowalik, 1981). A cooling and crystallizing magma chamber underlying the site of mineralization is the presumed source of these fluids and metals. The apparent comagmatism of all the granitoid clast types and between the granitoid clasts and Buchans Group felsic volcanic rocks indicates their origin from the magma chamber that was feeding the Buchans Group volcanic pile and that may have been responsible, at least in part, for the massive sulphide mineralization.

Figure 7.1 Idealized cross-sectional model for the genesis of the granitoid clasts associated with transported sulphide orebodies at Buchans: a) hiatus in felsic volcanism permitting; deposition of sulphide muds and siltstone unit, partial crystallization of underlying magma chamber with accompanying release of a volatile phase that fractures the intruded rock and possibly contributes fluid and metals to the hydrothermal fluids depositing the sulphide muds: b) period of felsic pyroclastic volcanism, propagation of a breccia pipe containing granitoid clasts toward the surface; c) either accompanying or preceeding another period of felsic pyroclastic activity, the breccia pipe breaches the surface in the vicinity of the sulphide mud pond, probably explosively; as a result of this explosion, accompanying volcanism or related earthquakes, debris flows are initiated that transport portions of the sulphide mud pond, ejected granitoid clasts and other entrained material downslope as debris flows. Subsequent debris flows are increasingly less sulphide- and granitoid-rich and are presumed to indicate a waning of sulphide mineralization and the explosiveness of the associated hydrothermal activity.

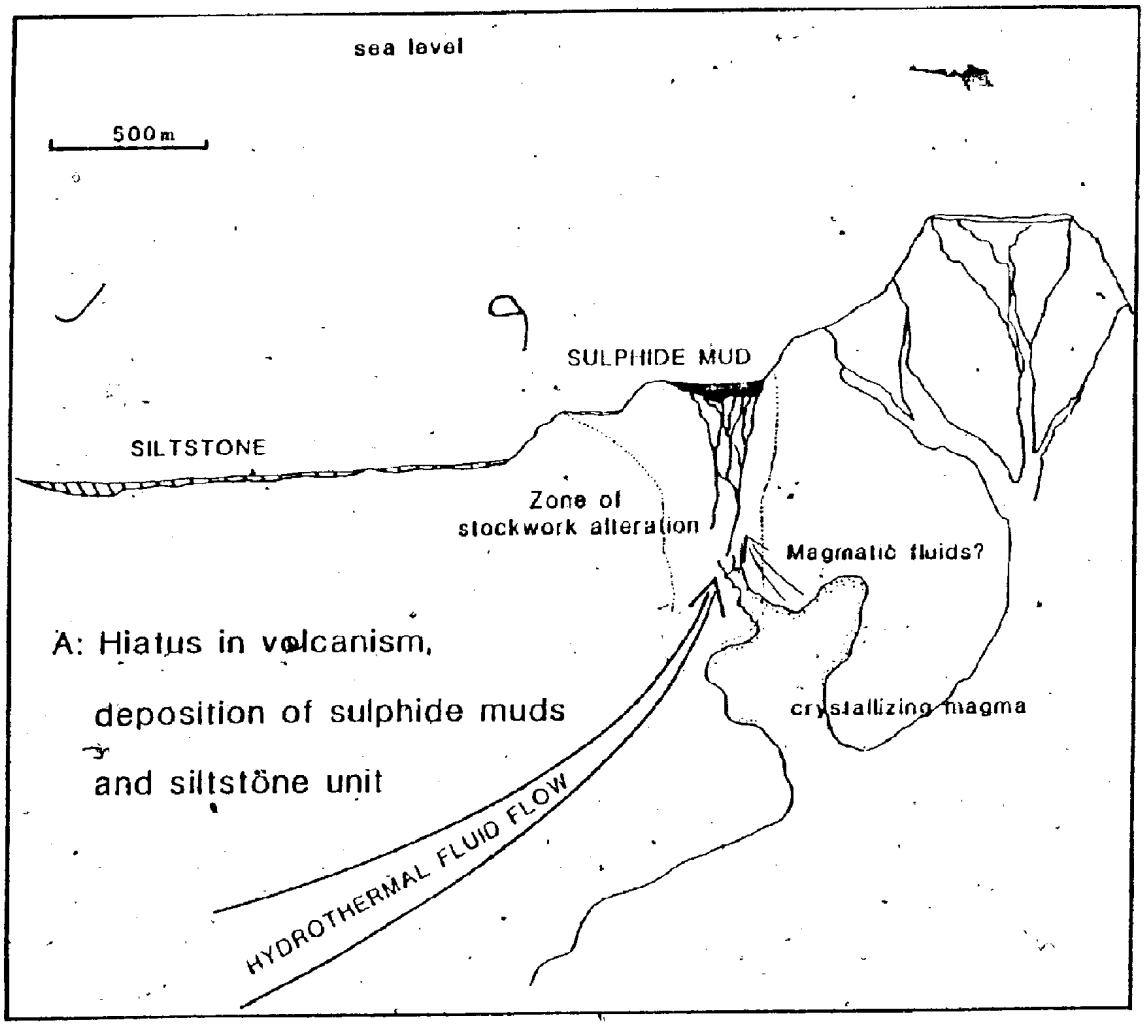
sea level
500m
SULPHIDE MUD
SILTSTONE
Zone of
stockwork alteration
Magmatic fluids?
A: Hiatus in volcanism,
deposition of sulphide muds
and siltstone unit
crystallizing magma
HYDROTHERMAL FLUID FLOW

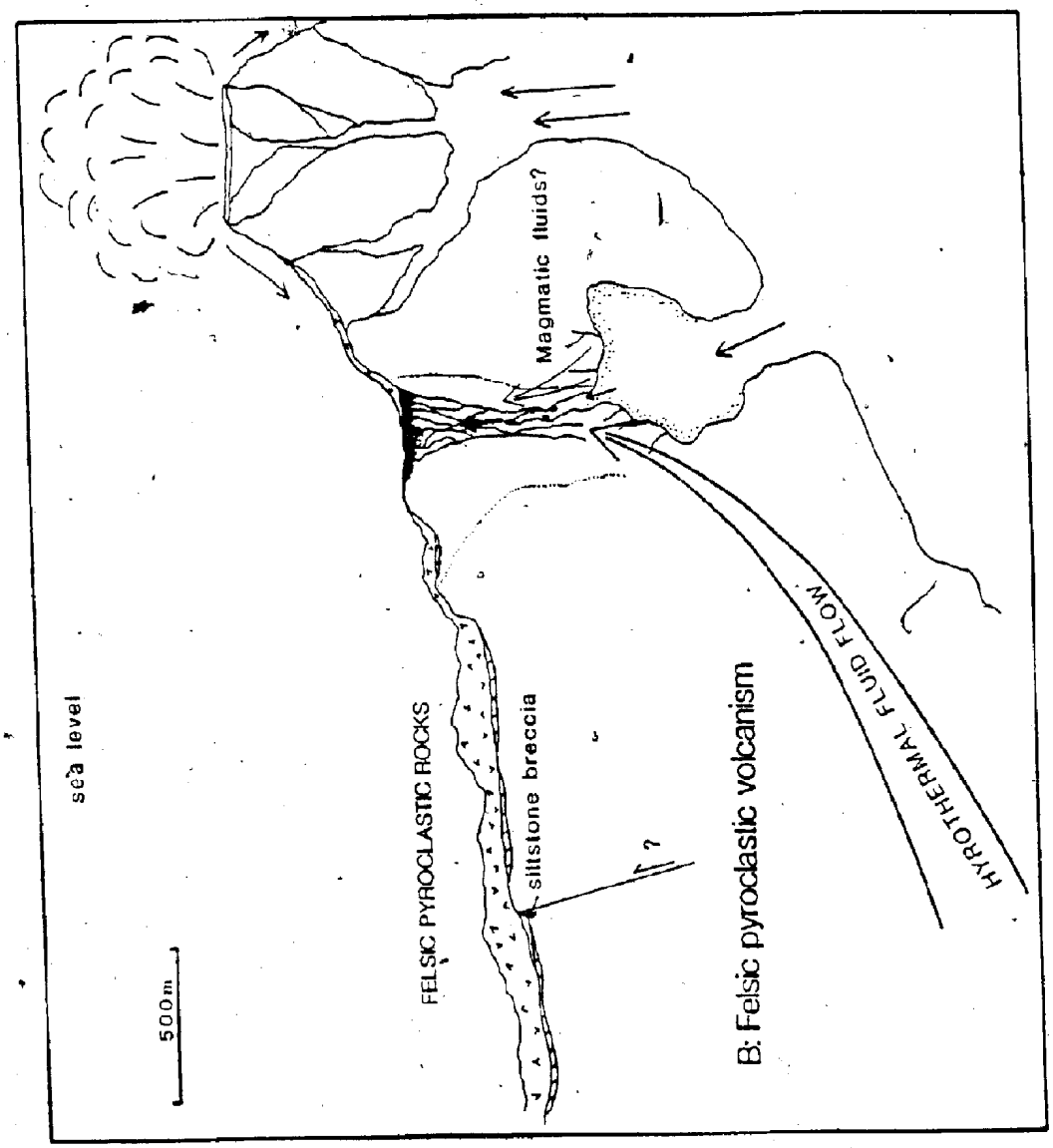

FIGURE 7.1 (continued)

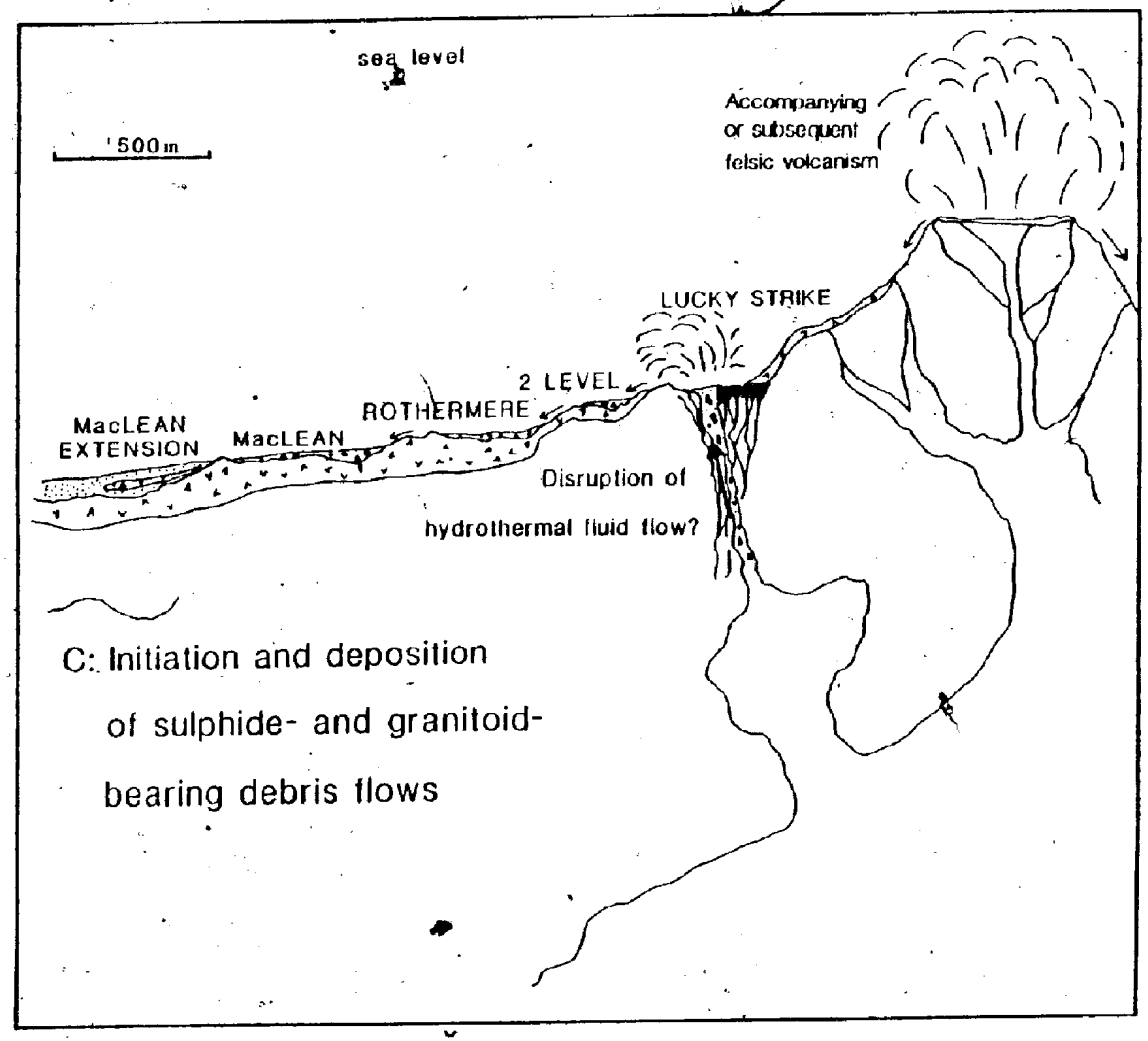

FIGURE 7.1 (continued)

The similar effects of hydrothermal alteration exhibited by the granitoid clasts to that typically seen associated with massive sulphide alteration zones suggests the exposure of the clasts to the mineralizing fluids. The loss of a volatile phase from a magma chamber is often an important determinant in the formation of orebodies (Burnham, 1979) and particularly for the formation of massive sulphide orebodies in calc-alkaline volcanic rocks (Stanton and Ramsay, 1980). The expulsion of hydrous fluids from a magma typically alters the apical sections of the intrusion until lithostatic pressure is exceeded and they can be released. The outermost crystalline parts of magma body would be altered by these exsolved fluids. As a result of the increase in pressure generated by this process, a breccia pipe began to emanate from this magma chamber. As the pipe was propagated toward the surface, intrusive material was transported from tha magma chamber (Figure 7.1b). The large density differences between the hydrothermal fluid and granitic material makes transportation by fluidization processes (Reynolds, 1954) in breccia pipes unlikely (Wolfe, 1980). Wolfe favours ballistic transport by phreatomagmatic explosions such as those produced by the expulsion of volatiles from a magma chamber. Rounding of the granitoid clasts is believed to have occurred during their transportation to the surface in the breccia pipe.

The high degree of rounding of the granitoid clasts may indicate repeated episodes of these explosions, possibly as the fracture system that localized the breccia pipe (Mitcham, 1974) was being propogated to the surface. Periodic explosive activity may be expected as continuous mineral deposition eventually blocks the fluid channelways and fluid pressures build up until they exceed the containing lithostatic pressure. Periodic movement on fault structures controlling the breccia pipe would both promote rounding by comminution in zones of constriction (Mitcham, 1974) and by the explosive periodic release of fluid pressures due to this movement.

The apparent relationship between the degree of rounding, alteration and brecciation of the granitoid clasts by hydrothermal fluids can be explained by this process of transportation. The location of this pipe is unknown but the similarities in style of hydrothermal alteration suggests it could have occurred within the zone of stockwork alteration underying the in situ orebodies.

The occurrence of the most sulphide-rich section at the base of the earliest debris flow is possibly due to density sorting during transportion but probably reflects changes in the source area for the flows. The concentration of the granitoid clasts with the sulphidic sections of the debris flow sequence is interpreted to indicate a spatial

relationship prior to their incorporation into the debris flows. Combined with the style of alteration of the clasts, and the evidence of a magmatic component to the mineralizing fluids, this is interpreted to indicate that the breccia pipe that transported the granitoid clasts breached the surface either directly underneath the sulphide mud pond or nearby.

The initiation of the mass sediment movement was apparently some high energy event (Thurlow and Swanson, 1981; Walker and Barbour, 1981; Binney et al., 1983; Binney, 1985). Whether this event was the explosive hydrothermal fluid activity that is interpreted to have transported subsurface material upward, felsic explosive volcanism or earthquakes related to either process cannot be unequivocably established. However, the decrease in sulphides and increase in barite contained in subsequent debris flows indicates that a significant disruption of the hydrothermal fluid system responsible for sulphide mineralization occurred at this time.

The presence of the most granitic (i.e., those from the greatest depth?) granitoid clasts, their high degree of alteration, large size and concentration with the sulphidic sections of the earliest debris flows possibly indicate that when the breccia pipe containing the granitoid clasts breached the surface, the resulting explosion initiated the

debris flow movement (Figure 7.1c).

The change in the character of the granitoid clasts in the later debris flows (i.e. from 'granitic' group clasts to 'aplitic' group clasts) shows a change in the source region of the granitoids during the period of debris flow movements. The more differentiated composition, finer grain size and abundant granophyric textures indicate that these clasts probably crystallized more rapidly at shallower levels than the 'granitic' group clasts. The apparently lower degree of alteration in the 'aplitic' group clasts possibly indicates a more rapid transportation history than that of the 'granitic' group clasts. These changes plus the absence of any granitoid clasts in the upper ore unit demonstrates the diminishing energy level of the explosive activity. A drop in the explosive energy may be expected after the breccia pipe breaches the surface releasing the confined hydrothermal pressures. The correlative decrease in sulphide concentration in the upper ore unit suggests that these explosions disrupted the hydrothermal fluid flow. The lack of known economic sulphide mineralization at higher stratigraphic levels indicates the possible termination of sulphide mineralization as a result of this activity. These features suggest that the explosive events that transported the granitoid clasts (and fragments of many altered and mineralized volcanic lithogies) to the surface may have also

initiated the movement of the debris flows.

No other potential source for the granitoid clasts can account for all of these features: the apparent comagmatism of the clasts and the hosting volcanic rocks; the similar ages for the volcanic rocks and granitoid clasts; the range of igneous textures present in the granitoid clasts; the variable hydrothermal alteration of the granitoid clasts and the relationship between degree of roundness, alteration and brecciation demonstrated by some granitoid clasts; and the intimate association of the largest, most altered 'granitic' group granitoid clasts with the maximum sulphide accumulations in the debris flow sequence and the subsequent increase in the proportion of the smaller, less volumetrically important and less hydrothermally altered 'aplitic' group granitoid clasts in later debris flow sequence subunits spatially removed from the sulphide-rich sections of the sequence (Table 7.1).

The main difficulty with the presented model is the absence of a known breccia pipe in the Buchans Group, especially in the vicinity of the in situ or stockwork orebodies. However, the recent recognition of the thrust duplex structures (Thurlow and Swanson, 1985) formed during a period of thrust movement of the Buchans Group and the resulting improved stratigraphic model of the Buchans Group adds to the plausibility of this model. The localization of

POTENTIAL SOURCES OF GRANITOID CLASTS / OBSERVED FEATURES OF GRANITOID CLASTS	Beach deposits derived from:		Breccia pipes located:	
	exotic crystalline terrane	upthrust block of Buchans Group magma chamber	removed from site of sulphide deposition	near site of sulphide deposition
Apparent comagmatism of all granitoid clast types	P	Y	Y	Y
Apparent comagmatism between granitoid clasts and Buchans Group felsic volcanic rocks	D	Y	Y	Y
Roughly coeval radiometric age with Buchans Group felsic volcanism	N	Y	Y	Y
Range of igneous textures (granitic to subvolcanic)	P	D	Y	Y
Greater rounding relative to other clast lithogies	P	P	Y	Y
Maximum abundance (vol) and size found with maximum sulphide concentration	N	N	N	Y
Type and variability of hydrothermal alteration	D	D	P	Y
Decrease in abundance, size and proportion of 'granitic' group clasts with increasing distance from maximum sulphide concentration (within and between debris flow sequences)	N	N	N	Y

Y = yes P = possible D = doubtful N = no

Table 7.1 Comparison of observed features of granitoid clasts in MacLean Extension with the proposed source for the clasts (right-hand column) and alternative sources (first three columns). Yes indicates that the source can explain the observed feature; possible indicates that the source can possibly explain the feature but not as conclusively as a 'yes' response; doubtful indicates that the source may explain the feature and cannot be dismissed entirely but is considered to be geologically unlikely; no indicates that the potential source can not possiby explain the observed feature.

thrust movements on bedding planes and zones of previous movement and/or alteration suggested by Thurlow and Swanson (1985) is significant. The zone of intense alteration underlying the original sites of in situ sulphide mineralization would almost certainly be one of the zones affected by the later thrusting movement. The presence of the in situ Oriental orebody at the base of the Oriental thrust block exemplifies this process (Thurlow and Swanson, 1985). The removal of the in situ orebodies from their original site of deposition by thrusting seems likely. The direction of thrusting toward the southeast (Thurlow and Swanson, 1981, 1985) suggests that the original site may have been overthrust and occurs at depth northwest of Buchans. This could explain why no evidence of breccia pipes is presently observed at Buchans.

7.5 SUMMARY AND CONCLUSIONS

Granitoid clasts found in association with the transported orebodies at Buchans are largest, and occupy the greatest volume of the host polylithic breccia-conglomerate subunit when proximal to the greatest sulphide accumulation in the sequence of debris flow deposits. The granitoid clasts are typically the most rounded clast lithology present in the debris flow deposits. They decrease in size and volume with increasing distance from the lowermost sulphide-rich sections of the debris flow sequence. They show igneous textures and compositions ranging from trondhjemite (rare) to quartz porphyritic microtrondhjemite to aplite to granophyric aplite. All granitoid clasts have been classified into six 'types' based on these textural and grain size differences. The five most abundant 'types' are reduced to 'granitic' and 'aplitic' groups based on textural similarities.

Hydrothermal fluids deposited calcite, barite and quartz, sericitized plagioclase grains, and chloritized all mafic phases present. Despite this alteration, and variable alkali metasomatism (loss of K) that is presumed due to late-stage volatile loss, all granitoid clasts appear to have a common magmatic source based on similar trace element abundances.

The 'granitic' group clasts are typically larger, occupy more volume and are more altered than 'aplitic' group clasts. The proportion of 'aplitic' group clasts to 'granitic' group clasts increases with decreasing sulphide concentration in the debris flow sequence. Similarly, the average size and volume occupied by granitoid clasts in debris flow subunits decreases with increasing distance from the sulphide-rich sections of the debris flow deposits.

All granitoid clasts appear to represent fragments of the same magma system that produced the felsic volcanic rocks of the Buchans Group. This conclusion is based on similar mineralogical and petrographic features, and similar major and trace element abundances (especially TiO_2, Zr, Y, V, Nb, Ga and REE) between granitoid clast types and the Buchans Group felsic flows. U/Pb isotopic data for an 'aplitic' group clast, although imprecise, overlaps within analytical uncertainty the isochron produced from a Buchans River Formation rhyolite. The calculated ages, 464 ± 40 Ma and 489 ± 20 Ma respectively, overlap within the estimated age uncertainties.

The granitoid clasts were altered, rounded and transported to the surface in breccia pipes by explosive volatile activity that is probably due (at least in part) to the exsolution of an aqueous phase from the source magma chamber. The explosive hydrothermal events that transported

the granitoid clasts (and fragments of previously deposited lithologies) to the surface may have initiated the movement of the debris flows when the breccia pipe breached the surface, disrupted the *in situ* sulphide mineralization process and resulted in the eventual cessation of massive sulphide deposition at Buchans.

The change in character of the granitoid clasts during the period of production of the debris flows from highly altered 'granitic' group clasts to a finer grained, smaller, and volumetrically less abundant 'aplitic' group clasts suggests that the latter originated from shallower depths and had a more rapid transportation history (i.e. less exposure to the hydrothermal fluids) than the 'granitic' group clasts.

The Feeder Granodiorite as exposed at Wiley's River is considered a high level plutonic facies of the Buchans Group, and evidence of a slightly more differentiated magma than that which produced the Buchans Group felsic volcanic rocks and granitoid clasts. The textural, mineralogical and geochemical similarities between these populations suggested by Thurlow (1981a,b) are verified. The Little Sandy Lake intrusion appears to be from the same magma system as the Wiley's River Intrusion, Buchans Group felsic flows and the granitoid clasts on the basis of textural and mineralogical similarities and major and trace element geochemistry.

The geochronological study, although relatively imprecise, suggests that the Buchans Group is Middle Ordovician (Llanvirn-Llandeilo?) in age rather than post-Caradocian as suggested by earlier workers. If true, this requires a reappraisal of the position of the Buchans Group in central Newfoundland volcanic stratigraphy.

REFERENCES

Abbey, S., 1968. Analysis of rocks and minerals by atomic absorption spectroscopy; Part 2; Determination of total iron, magnesium, calcium, sodium and potassium. Geological Survey of Canada, Paper 68-20.

Alderton, D.M.H., Pearce, J.A. and Potts, P.J., 1980. Rare earth element mobility during granite alteration: evidence from southwest England. Earth and Planetary Science Letters, v.49, p.149-165.

Allman-Ward, P., Halls, C., Rankin, A. and Bristow, C.M., 1982. An intrusive hydrothermal breccia body at Wheal Remfry in the western part of the St. Austell granite pluton, Cornwall, England; in Metallization Associated with Acid Magmatism, ed. A.M. Evans, v. 6, Wiley, Chichester, p.1-28.

Anderson, F.D., 1972. Buchans and Badger map areas, Newfoundland. Geological Survey of Canada, Paper 72-1, Part A, p.2.

Anger, C., 1963. The lead-zinc-copper deposits of Buchans, middle Newfoundland. Neues Jahrbuch fur Mineralogie, Montashefte, p.126-136.

Arculus, R.J. and Wills, K.J.A., 1980. The petrology of plutonic blocks and inclusions from the Lesser Antilles Island Arc. Journal of Petrology, v.21, p.743-799.

_____, Johnson, R.W., Chappell, B.W., McKee, C.O. and Sakai, H., 1983. Ophiolite contaminated andesites, trachybasalts and cognate inclusions of Mount Lamington, Papua New Guinea: anhydrite-amphibole bearing lavas and the 1951 cumulodome. Journal of Volcanology and Geothermal Research, v.18, p.215-247.

Armbrust, G.A., 1969. Hydrothermal alteration of a breccia pipe deposit, Tribag Mine, Batchawana Bay, Ontario. Economic Geology, v.64, p.551-563.

Armstrong, R.L., 1978. Pre-Cenozoic Phanerozoic time scale-computer file of critical dates of new and in-progress decay constant revisions; in Contributions to the Geological Time Scale, eds. G.V. Cohee, M.F. Glaessner and H.D. Hedberg; American Association of Petroleum Geologists, Studies in Geology, v.6, p.73-91.

Bailey, J.C., 1981. Geochemical criteria for a refined tectonic discrimination of orogenic andesites. Chemical Geology, v.32, p.139-154.

Barker, D.S., 1970. Compositions of granophyre, myrmekite and graphic granite. Geological Society of America Bulletin, v.81, p.3339-3350.

Barker, F., 1979. Trondhjemite: definition, environment and hypotheses of origin, in Trondhjemites, Dacites and Related Rocks, ed. F. Barker, Elsevier, Amsterdam, p.1-12.

Bell, K. and Blenkinsop, J., 1981. A geochronological study of the Buchans area, Newfoundland; in The Buchans Orebodies: Fifty Years of Geology and Mining, eds. E.A. Swanson, D.F. Strong, J.G. Thurlow; Geological Association of Canada Special Paper 22, p.91-111.

Bergstrom, S., Riva, J. and Kay, M., 1974. Significance of conodonts, graptolites and shelly faunas from the Ordovician of western and northern-central Newfoundland. Canadian Journal of Earth Sciences, v.11, p.1625-1660.

Binney, W.P., 1984. Estimation of physical parameters of MacLean Channel sulphide-bearing debris flows, Buchans, Newfoundland; in Current Research, Part A, Geological Survey of Canada, Paper 84-1A, p.495-498.

_____, Thurlow, J.G. and Swanson, E.A., 1983. The MacLean Extension orebody, Buchans, Newfoundland; in Current Research, Part A, Geological Survey of Canada, Paper 83-1A, p.313-319.

Bostock, H.H., Currie, K.L. and Wanless, R.K., 1979. The age of the Robert's Arm Group, north-central Newfoundland. Canadian Journal of Earth Sciences, v.16, p.599-606.

Bouley, B.A., 1978. Volcanic stratigraphy, stratabound sulphide deposits and relative age relations in the East Penobscot Bay area, Maine. Unpublished Ph.D. thesis, University of Western Ontario, 168p.

_____ and Hodder, R.W., 1983. Strata-bound polymetallic sulphide deposits in Siluro-Devonian volcanics at Harbourside, Maine. Economic Geology, v.79, p.1693-1702.

Bowden, P., Batchelor, R.A., Chappell, B.W., Didier, J. and Lameyre, J., 1984. Petrological, geochemical and source criteria for the classification of granitic rocks: a discussion. Physics of the Earth and Planetary Interiors, v. 35, p.1-11.

Bowen N.L., 1928. The evolution of the igneous rocks. Dover Publications, New York, 332p.

Briqueu, L., Bougault, H. and Joron, J-L., 1984. Quantification of Nb, Ta, Ti and V anomalies in magmas associated with subduction zones: petrogenetic implications. Earth and Planetary Science Letters, v.68, p.297-308.

Broecker, W.S. and Oversby, V.M., 1971. Chemical equilibria in the Earth. McGraw-Hill, New York, 318 p.

Brown, G.M., 1979. The problem of the diversity of igneous rocks; in The Evolution of Igneous Rocks, ed. H.S. Yoder, Jr., Princeton Press, p.3-14.

Bryant, D.G, 1968. Intrusive breccias associated with ore, Warren (Bisbee) Mining District, Arizona. Economic Geology, v.63, p.1-12.

Bryner, L., 1961. Breccia and pebble columns associated with epigenetic ore deposits. Economic Geology, v.56, p.488-508.

Buchans Staff, 1955. Buchans operation, Newfoundland. Canadian Institute of Mining and Metallurgy Bulletin, v.48, p.349-353.

Burnham, C.W., 1979. Hydrothermal fluids at the magmatic stage; in Geochemistry of Hydrothermal Ore Deposits, ed. H.L. Barnes. John Wiley and Sons, New York, p.71-136.

_____, 1983. Deep submarine pyroclastic eruptions. Economic Geology Monograph 5, p.142-148.

Calhoun, T.A. and Hutchison, R.W., 1981. Determination of flow direction and source of fragmental sulphides, Clementine deposit, Buchans, Newfoundland; in The Buchans Orebodies: Fifty Years of Geology and Mining, eds. E.A. Swanson, D.F. Strong and J.G. Thurlow, Geological Survey of Canada Special Paper 22, p.187-204.

Campbell, I.H., Franklin, J.M., Gorton, M.P., Hart, T.R. and Scott, S.D., 1981. The role of sub-volcanic sills in the generation of massive sulphide deposits. Economic Geology, v.76, p.2248-2253.

_____, Coad, p., Franklin, J.M., Gorton, M.P., Scott, S.D., Sowa, J. and Thurston, P.C., 1982. Rare earth elements in acid volcanics associated with Cu-Zn massive sulphide mineralization: a preliminary report. Canadian Journal of Earth Sciences, v.19, p.619-623.

_____, Lesher, C.M., Coad, P., Franklin, J.M., Gorton, M.P. and Thurston, P.C., 1984. Rare-earth element mobility in alteration pipes below massive Cu-Zn-sulphide deposits. Chemical Geology, v.45, p.181-202.

Cann, J.A., 1970. Rb, Sr, Y, Zr and Nb in some ocean floor basalt rocks. Earth and Planetary Science Letters, v.10, p.7-11.

Carlson, S.R. and Sawkins, F.J., 1980. Mineralogic and fluid inclusion studies of the Turmalina Cu-Mo bearing breccia pipe, northern Peru. Economic Geology, v.75, p.1233-1238.

Cathles, L.M., 1981. Fluid flow and genesis of hydrothermal ore deposits. Economic Geology, 75th Anniversary Volume, p.424-457.

_____, 1983. An analysis of the hydrothermal system responsible for massive sulphide deposition in the Hokuroku Basin of Japan. Economic Geology Monograph 5, p.439-487.

Chatterjee, A.K. and Strong, D.F., 1984. Rare earth and other element variations in greisens and granites associated with East Kemptville tin deposit, Nova Scotia, Canada. Transactions, Institute of Mining and Metallurgy (Section B: Applied Earth Sciences), v.93, p.59-70.

Church, W.D. and Stevens, R.K., 1971. Early Paleozoic ophiolite complexes of the Newfoundland Appalachians as mantle-oceanic crust sequences. Journal of Geophysical Research, v.76, p.1460-1466.

Cobbing, E.J. and Pitcher, W.S., 1972. The coastal batholith of central Peru. Journal of the Geological Society of London, v.128, p.421-460.

Coleman, R.G. and Donato, M.M., 1979. Oceanic plagiogranite revisited, in Trondhjemites, Dacites and Related Rocks, ed. F. Barker, Elsevier, Amsterdam, p.149-168.

Collins, W.J., Beams, S.D., White, A.J.R. and Chappell, B.J., 1982. Nature and origin of A-type granites with particular reference to southeastern Australia. Contributions to Mineralogy and Petrology, v.80, p.189-200.

Conrad, W.K. and Kay, R.W., 1984. Ultramafic and mafic inclusions from Adak island: crystallization history and implications for the nature of primary magmas and crustal evolution in the Aleutian Arc. Journal of Petrology, v.25, p.88-126.

_____, Kay, S.M. and Kay, R.W., 1983. Magma mixing in the Aleutian arc: evidence from cognate inclusion and composite xeneoliths. Journal of Volcanology and Geothermal Research, v.18, p.279-295.

Constantinou, G. and Govett, G.J.S., 1973. Geology, geochemistry and genesis of Cyprus sulphide deposits. Economic Geology, v.68, p.843-858.

Coryell, C.D., Chase, J.W. and Winchester, J.W., 1963. A procedure for the geochemical interpretation of terrestial rare-earth element abundances. Journal of Geophysical Research, v.68, p.559-566.

Coyle, M., Strong, D.F., Gibbons, D. and Lambert, E., 1985. Geology of the Springdale Group, Central Newfoundland; in Current research, Part A, Geological Survey of Canada, Paper 85-1A, p.157-163.

Currie, K.L and Bostock, H.H., 1980. The age of the Robert's Arm Group, north-central Newfoundland: reply. Canadian Journal of Earth Sciences, v.17, p.804-806.

Dahlstrom, C.D.A., 1970. Structural geology in the eastern margin of the Canadian Rocky Mountain. Bulletin of the Canadian Petroleum Geologists, v.18, p.332-406

Dean, P.L., 1977. A report on the geology and metallogeny of the Notre Dame Bay area. Department of Mines and Energy, Government of Newfoundland and Labrador, Mineral Developement Division, Report 77-10, 17p.

_____, 1978. The volcanic stratigraphy and metallogeny of the Notre Dame Bay, Newfoundland. Memorial University of Newfoundland, Geology Report No. 7, 205p.

_____ and Kean, B.F., 1980. The age of the Robert's Arm Group, north-central Newfoundland: discussion. Canadian Journal of Earth Sciences, v.17, p.800-804.

_____ and Strong, D.F., 1975. The volcanic stratigraphy, geochemistry and metallogeny of the central Newfoundland Appalachians (Abstract). Geological Association of Canada Annual Meeting, p.745-746.

DeGrace, J.R., Kean, B.F., Hsu, E. and Green, T., 1976. Geology of the Nippers Harbour map area (2E/13), Newfoundland. Newfoundland Department of Mines and Energy, Mineral Development Division, Report 76-3, 73p.

De La Roche, H., Leterrier, J., Grandclaude, P. and Marchal, M., 1980. A classification of volcanic and plutonic rocks using R1R2- diagram and major element analyses- its relationship with current nomenclature, Chemical Geology, v.29, p.183-210.

DePaolo, D.J., 1981. A neodymium and strontium isotopic study of the Mesozoic calc-alkaline granitic batholiths of the Sierra Nevada and Peninsular Ranges, California. Journal of Geophysical Research, v.86, p.10470-10488.

Donnelly, T.W. and Rogers, J.J.W., 1980. Igneous series in island arcs: the northwest Caribbean compared with world-wide island arc assemblages. Bulletin Volcanologique, v.43, p.347-382.

Dostal, J. and Strong, D.F., 1983. Trace element mobility during low-grade metamorphism and silicification of basaltic rocks from St. John, New Brunswick. Canadian Journal of Earth Sciences, v.20, p.431-435.

Dudas, F.O., 1983. The effect of volatile content on the vesiculation of submarine basalts. Economic Geology Monograph 5, p.134-141.

Dunning, G.R., 1981. The Annieopsquotch ophiolite belt, southwest Newfoundland; in Current Research, Part B, Geological Survey of Canada, Paper 81-1B, p.11-15.

_____, 1984. The geology, geochemistry, geochronology and regional setting of the Annieopsquotch Complex and related rocks of southwest Newfoundland. Unpublished Ph.D. thesis, Memorial University of Newfoundland.

_____ and Herd, R.K., 1980. The Annieopsquotch ophiolite complex, southwest Newfoundland, and its regional relationships; in Current Research, Part A, Geological Survey of Canada, Paper 80-1a, p.227-234.

_____ and Krogh, T., 1983. Tightly clustered, precise, U/Pb (zircon) ages of ophiolites from the Newfoundland Appalachians. Geological Society of America, Northeast Section, Abstracts with Programs, v.15, no. 3, p.136.

Eby, G.N., 1972. Determination of Rare-Earth, Yttrium and Scandium abundances in rocks and minerals by an ion exchange-x-ray fluorescence procedure. Analytical Chemistry, v.44, p.2137-2143.

Ehrlich, R., 1984. Curry into hominy- a common outcome of unquestioning use of statistical analysis involving means and standard deviations (abstract), Geological Society of America Annual Meeting, v.16, no.6, p.499.

Erlich, E.N., Kutyev, F.Sh., Bogoyavlenskaya, G.E., Tolskikhin, I.N., Mamyrin, B.A. and Khabarin, L.V., 1979. Cognate inclusions in basalt-andesite rock series. Bulletin Volcanologique, v.42, p.152-166.

Finlow-Bates, T., 1980. Chemical transfers in some Paleozoic submarine hydrothermal systems of volcanic association (abstract). Norges Geologiske Undersokelse, No.360, p.73.

_____ and Stumpfl, E.F., 1981. The behavior of so-called immobile elements in hydrothermally altered rocks associated with volcanogenic submarine-exhalative ore deposits. Mineralium Deposita, v.16, p.319-328.

Floyd, P.A. and Winchester, J.A., 1978. Identification and discrimination of altered and metamorphosed volcanic rocks using immobile elements. Chemical Geology, v.21, p.291-306.

Franklin, J.M., Lydon, J.W. and Sangster, D.F., 1981. Volcanic-associated massive sulphide deposits. Economic Geology, 75th Anniversary Volume, p.485-627.

Friedman, G.M., 1971. Staining; in Procedures in sedimentary petrology, ed. R.E. Carver, Wiley-Interscience, New York, p.522-527.

Fryer, B.J., 1977. Rare earth evidence in iron-formations for changing PreCambrian oxidation states. Geochimica et Cosmochimica Acta, v.41, p.361-367.

_____ and Edgar, A.D., 1977. Significance of rare earth distributions in coexisting minerals of peralkaline undersaturated rocks. Contributions to Mineralogy and Petrology, v.61, p.35-48.

Fujii, T. and Scarfe, C.M., 1982. Petrology of ultramafic nodules from West Kettle River, near Kelowna, Southern British Columbia. Contributions to Mineralogy and Petrology, v.80, p.297-306.

Gebauer, D. and Grunenfelder, M., 1979. U-Th-Pb dating of minerals; in Lectures in Isotope Geology, eds. E. Jager and J.C. Hunziker; Springer-Verlag, New York, p.105-131.

Geological Survey of Canada, 1968. Aeromagnetic map, Rainy Lake area (12 A/14). Geophysical Map 273G (revised).

George, P.W., 1937. Geology of lead-zinc-copper deposits at Buchans, Newfoundland. American Institute of Mining and Metallurgical Engineers, T.P. 816, Class 1, Mining Geology, No. 70.

Goldie, R., 1979. Consanguineous Archean intrusive and extrusive rocks, Noranda Quebec: chemical similarities and differences. PreCambrian Research, v.9. p.275-287.

Green, T.H., 1980. Island arc and continental-building magmatism- a review of petrogenetic models based on experimental petrology and geochemistry. Tectonophysics, v.63, p.367-385.

Guber, A.L. and Merrill, S.,III, 1983. Paleobathymetric significance of the foraminifera from the Hokoruku district, Japan. Economic Geology Monograph 5, p.55-70.

Hallberg, J.A., 1984. A geochemical aid to igneous rock type identification in deeply weathered terrain. Journal of Geochemical Exploration, v.20, p.1-8.

Hanson, G.N., 1978. The application of trace elements to the petrogenesis of igneous rocks of granitic composition. Earth and Planetary Science Letters, v.38, p.26-43.

_____, 1980. Rare earth elements in petrogenetic studies of igneous systems. Annual Review of Earth and Planetary Sciences, v.8, p.371-406.

Harland, W.B., Cox, A.V., Llewellyn, P.G., Picton, C.A.G., Smith, A.G., and Walters, R., 1982. A geological time scale; Cambridge University Press, Cambridge, 128p.

Harris, C., 1983. The petrology of lavas and associated plutonic inclusions of Ascension Island. Journal of Petrology, v.24, p.424-470.

Hart, S.R., Erlank, A.J. and Kable, E.J.D., 1974. Sea-floor basalt alteration: some chemical and Sr isotopic effects. Contributions to Mineralogy and Petrology, v.44, p.219-230.

Hashiguchi, H., 1983. Penecontemporaneous deformation of Kuroko ore at the Kosaka mine, Akita, Japan. Economic Geology Monograph 5, p.167-183.

Hatch, F.H., Wells, A.K. and Wells, M.K., 1972. Petrology of the igneous rocks (13th edition). Thomas Murby and Co., London, 551p.

Haworth, R.T., LeFort, J. and Miller, H.G., 1978. Geophysical evidence for an east-dipping subduction zone beneath Newfoundland. Geology, v.6, p.522-526.

Helwig, J.A. and Sarpi, E., 1969. Plutonic-pebble conglomerates, New World Island, Newfoundland and the history of eugeosynclines; in North Atlantic-Geology and Continental Drift, ed. M. Kay,; American Association of Petroleum Geologists, Memoir 12, p.408-413.

Henley, R.W. and Thornley, P., 1981. Low grade metamorphism and geothermal environment of massive sulphide ore formation, Buchans, Newfoundland; in The Buchans Orebodies: Fifty Years of Geology and Mining, eds. E.A. Swanson, D.F. Strong and J.G. Thurlow; Geological Association of Canada Special Paper 22, p.205-228.

Herrmann, A.G., Potts, M.J. and Knake, D., 1974. Geochemistry of the rare earth elements in spilites from the oceanic and continental crust. Contributions to Mineralogy and Petrology, v.44, p.1-16.

Hibbard, J., 1983. Geology of the Baie Verte Peninsula; Newfoundland Department of Mines and Energy, Mineral Developement Division, Memoir 2, 279p.

Hibbard, J. and Williams, H., 1979. Regional setting of the Dunnage Melange in the Newfoundland Appalachians. American Journal Of Science, v.279, p.993-1021.

Hildreth, E.W., 1979. The Bishop Tuff: evidence for the origin of zoned magma chambers; in Ash Flow Tuffs, eds. C.E. Chapin and W.E. Elston; Geological Society of America Special Paper 180, p.43-72.

Hill, P.G., 1974. The petrology of the Aden volcano, People's Democratic Republic of Yemen. Unpublished Ph.D. thesis, University of Edinburgh.

Hovorka, D. and Fejdi, P., 1980. Spinel peridotite xenoliths in the West Carpathian Late Cainozoic alkali basalts and their tectonic significance. Bulletin Volcanologique, v.43, p.96-106.

Hughes, C.J., 1973. Spilites, keratophyres and the igneous spectrum. Geological Magazinie, v.109, p. 513-527.

Humphris, S.E. and Thompson, G., 1978. Trace element mobility during hydrothermal alteration of oceanic basalts. Geochimica et Cosmochimica Acta, v.42, p.127-136.

Hutchinson, R.W., 1981. A synthesis and overview of Buchans geology; in The Buchans Orebodies: Fifty Years of Geology and Mining, eds. E.A. Swanson, D.F. Strong and J.G. Thurlow; Geological Association of Canada, Special Paper 22, p.325-350.

Irvine, T.N. and Baragar, W.R.A., 1971. A guide to the chemical classification of the common volcanic rocks. Canadian Journal of Earth Sciences, v.8, p.523-548.

Ishihara, S.(ed.), 1974. Geology of the Kuroko deposits. Society of Mining Geologists Special Issue No. 6, 435p.

Jackson, K.C., 1970. Textbook of Lithology. McGraw Hill, New York, 552p.

Jakes, P. and White, A.J.R., 1972. Major and trace element abundances in volcanic rocks of orogenic areas. Geological Society of America Bulletin, v.83, p.29-40.

Jenness, S.E., 1954. Geology of the Gander River Ultrabasic Belt, Newfoundland. Unpublished Ph.D. thesis, Yale University, 182p.

_____, 1958. Geology of the Gander River Ultrbasic Belt, Newfoundland, Geological Survey of Newfoundland, Report 14, 58p.

Jones, W.B., 1979. Syenite boulders associated with Kenyan trachyte volcanoes. Lithos, v.12, p.89-97.

Kajiwara, Y., 1970. Syngentic features of the Kuroko ore from the Shakanai mine; in Volcanism and Ore Genesis, ed. T. Tatsumi; University of Tokyo Press, Tokyo, p.197-206.

Kalogeropoulos, S.I., 1983. Chemistry and role of zirconium in the formation of the Tsunokakezawa No. 1 Orebody, Fukazawa Mine, Japan. Mineralium Deposita, v.18, p.535-541.

Karlstrom, K.E., 1983. Reinterpretation of Newfoundland gravity data and arguements for an allochthonous Dunnage zone. Geology, v.11, p.263-266.

Kean, B.F., 1977. Geology of the Lake Ambrose sheet, west half; in Report of Activities, Newfoundland Department of Mines and Energy, Report 77-1, p.21-25.

____, Dean P.L. and Strong, D.F., 1981. Regional geology of the central volcanic belt of Newfoundland; in The Buchans Orebodies: Fifty Years of Geology and Mining; eds. E.A. Swanson, D.F. Strong and J.G. Thurlow; Geological Association of Canada Special Paper 22, p.65-78.

____ and Strong, D.F., 1975. Geochemical evoluton of an Ordovician island arc of the central Newfoundland Appalachians. American Journal of Science, v.275, p.97-118.

Kents, P., 1964. Special breccias associated with hydrothermal developements in the Andes. Economic Geology, v.59, p.1551-1563.

Kerrich. H.R. and Fryer, B.J., 1979. Archean precious metal hydrothermal systems, Dome Mines, Abitibi Greenstone Belt. II - REE,and oxygen isotope studies. Canadian Journal od Earth Sciences, v.16, p.440-458.

Knapp, D.A., 1983. Ophiolite emplacement along the Baie Verte-Brompton line at Glover Island, western Newfoundland. Unpublished Ph.D. thesis, Memorial University of Newfoundland, 338p.

Kowalik, J., Rye, R. and Sawkins, F.J., 1981. Stable isotope study of the Buchans polymetallic sulphide deposits; in The Buchans Orebodies: Fifty Years of Geology and Mining, eds. E.A. Swanson, D.F. Strong and J.G. Thurlow;Geological Association of Canada, Special Paper 22, p.229-254.

Krogh, T.E., 1973. A low-contamination method for the hydrothermal decomposition of zircon and extraction of U and Pb for isotopic determinations. Geochimica et Cosmochimica Acta, v.37, p.485-494.

_____, 1982. Improved accuracy of U-Pb zircon ages by the creation of more concordant systems using an air-abrasion technique. Geochimica et Cosmochimica Acta, v.46, p.637-649.

Kuno, H., 1969. Mafic and ultramafic nodules in basaltic rocks of Hawaii. Geological Society of America, Memoir 115, p.189-234.

Lambert, I.B. and Sato, T., 1974. The Kuroko and associated ore deposits of Japan: a review of their features and metallogenesis. Economic Geology, v.69, p.1215-1236.

Langmhyr, F.J. and Paus, P.E., 1968. The analysis of inorganic siliceous materials by atomic absorption spectrophotometry and the hydrofluoric acid decompostion techniques, Part I: the analysis of silicate rocks. Anal. Chem. Acta, v.43, p.397-408.

Lee, D.E. and Christiansen , E.H., 1983. The granite problem as exposed in the Southern Snake Range, Nevada. Contributions to Mineralogy and Petrology, v.83, p.99-116.

Lemeyre, J. and Bowden, P., 1982. Plutonic rock type series: discrimination of various granitoid series and related rocks. Journal of Volcanology and Geothermal Research, v.14, p.169-186.

Leonova, L.L., 1979. Geochemistry of trace elements in acid volcanic rocks. Bulletin Volcanologique, v.42, p.212-218.

Lewis, J.F., 1973. Petrolgy of the ejected plutonic blocks of the Soufriere volcano, St. Vincent, West Indies. Journal of Petrology, v.14, p.81-112.

Lorenz, B.E. and Fountain, J.C., 1982. The South Lake Igneous Complex, Newfoundland: a marginal basin-island arc association. Canadian Journal of Earth Sciences, v.29, p.490-503.

Ludden, J., Gelinas, L. and Trudel., 1982. Archean metavolcanics from the Rouyn-Noranda district, Abitibi Greenstone Belt, Quebec: 2. Mobility of trace elements and petrogenetic constraints. Canadian Journal of Earth Sciences, v.19, p.2276-2287.

Lynch, G.V. and Pride, C., 1984. Evolution of a high-level, high-silica magma chamber: the Pattison pluton, Nisling Range alaskites, Yukon. Canadian Journal of Earth Sciences, v.21, p.407-414.

MacGeehan, P.J. and MacLean, W.H., 1980. An Archean sea-floor geothermal system, 'calc-alkaline' trends and massive sulphide genesis, Nature, v.286, p.767-771.

Mason, B., 1966. Principles of Geochemistry (3rd ed.). Wiley, New York, 329p.

Mattinson, J.M., 1975. Early Paleozoic ophiolite complexes of Newfoundland: isotopic ages of zircons. Geology, p.181-183.

Maxwell, J.A., 1968. Rock and minreal analysis. Interscience, New York, p.393-396.

McCarthy, T.S. and Fripp, R.E.P., 1978. The crystallization history of a granitic magma, as revealed by trace element abundances. Journal of Geology, v.88, p.211-224.

_____, and Hasty, R.A., 1976. Trace element distribution patterns and their relationship to the crystallization of granitic melts. Geochimica et Cosmsochimica Acta, v.40, p.1351-1358.

McHale, K.B. and McHale, D.E., 1984. Oil Island, an Ordovician volcanogenic sulphide prospect. Geological Association of Canada (Newfoundland Section), Annual Meeting, Programs with Abstracts, p.5.

McKerrow, W.S., Lambert, R.St.J. and Chamberlain, V.E., 1980. The Ordovician, Silurian and Devonian time scales. Earth and Planetary Science Letters, v.51, p. 1-8.

Miller, H.G. and Deutsch, E.R., 1976. New gravitational evidence for the subsurface extent of oceanic crust in north-central Newfoundland. Canadian Journal of Earth Sciences, v.13, p.459-469.

Mitcham, T., 1974. Origin of breccia pipes. Economic Geology, v.69, p.412-413.

Neary, G.N., 1981. Mining history of the Buchans area; in The Buchans Orebodies: Fifty Years of Geology and Mining, eds. E.A. Swanson, D.F. Strong and J.G. Thurlow; Geological Association of Canada Special Paper 22, p.1-64.

Nelson, K.D., 1981. Melange developement in the Bsones Point Complex, north-central Newfoundland. Canadian Journal of Earth Sciences, v.18, p.433-442.

_____ and Kidd, W.S.F., 1979. The age of the Robert's Arm Group, north-central Newfoundland: discussion. Canadian Journal of Earth Sciences, v.16, p.2068-2070.

Newhouse, W.H., 1931. Geology and ore deposits of Buchans, Newfoundland. Economic Geology, v.26, p.399-414.

Nockolds, S.R., 1954. Average chemical composition of some igneous rocks. Geological Society of America, Bulletin, v.65, p.100-1032.

Norman, R.E. and Strong, D.F., 1975. The geology and geochemistry of ophiolitic rocks exposed at Mings Bight, Newfoundland. Canadian Journal of Earth Sciences, v.12, p.777-797.

Norton, D.L. and Cathles, L.M., 1973. Breccia pipes- products of exsolved vapor from magmas. Economic Geology, v.68, p.540-546.

Nowlan, G.S. and Thurlow, J.G., 1984. Middle Ordovician conodonts from the Buchans Group, central Newfoundland, and their significance for regional stratigraphy of the Central Volcanic Belt. Canadian Journal of Earth Sciences, v.21, p.284-297.

O'Connor, J.T., 1965. A classification of quartz-rich igneous rocks based on feldspar ratios. United States Geological Survey, Professional Paper 525-b, p.79-84.

Ohmoto, H. and Skinner, B.J. (eds.), 1983. The Kuroko and related volcanogenic massive sulphide deposits. Economic Geology Monograph 5, 604p.

Osada, T., Abe, M. and Daimaru, K., 1974. Geology of the Yoshino mine, Yamagata Prefecture; in Geology of the Kuroko Deposits, ed. S. Ishihara; Society of Mining Geologists Special Issue No. 6, p.183-187.

Palacious, M.C., Guerra, S.N. and Compano, B.P., 1983. Differences in Ti, Zr, Y and P contents in calc-alkaline andesites from island arcs and continental margins (central Andes). Geologische Rundschau, v.72, p.733-738.

Palmer, A.R., 1983. The Decade of North American Geology, 1983 Geologic Time Scale. Geology, v.11, p.503-504.

Payne, J.G. and Strong, D.F., 1979. Origin of the Twillingate trondhjemite, north-central Newfoundland: partial melting at the roots of an island arc; in Trondhjemites, dacites and related rocks, ed. F. Barker; Elsevier, Amsterdam. p.489-516.

Pearce, J.A. and Cann, J.R., 1973. Tectonic setting of basic volcanic rocks using trace element analyses. Earth and Planetary Science Letters, v.19, p.290-300.

_____, Harris, N.B.W. and Tindle, A.G., 1984. Trace element discrimination diagrams for the tectonic interpretation of granitic rocks. Journal of Petrology, v.25, p.956-983.

Penrose Field Conference Participants, 1972. Ophiolites. Geotimes, v.17, p.24-25.

Pickett, J.W. and Barbour, D.M., 1984. Geology of the Skidder prospect, Buchans, Newfoundland; in Current Research, Part A, Geological Survey of Canada, Paper 84-1A, p.581-586.

Presnall, D.C., 1979. Fractional crystallization and partial fusion; in The Evolution of Igneous Rocks, ed. H.S. Yoder, Jr., Princeton Press, p.59-75.

Prestvik, T., 1982. Basic volcanic rocks and tectonic setting. A discussion of the Zr-Ti-Y discrimination diagram and its suitability for classification purposes. Lithos, v.15, p.241-247.

Relly, B.H., 1960. The geology of the Buchans mine. Unpublished Ph.D. thesis, McGill University.

Reynolds, D., 1954. Fluidization as a geological process, and its bearing on the problem of intrusive granites. American Journal of Science, v.252, p.577-613.

Roberts, R.G. and Reardon, E.J., 1978. Alteration and ore-forming processes at Mattagami Lake mine, Quebec. Canadian Journal of Earth Sciences, v.15, p.1-21.

Roedder, E., 1979. Silicate liquid immiscibilty; in The Evolution of the Igneous Rocks, ed. H.S. Yoder, Jr., Princeton University Press, Princeton, N.J., p.15-58.

_____ and Coombs, D.S., 1967. Immiscibility in granitic melts, indicated by fluid inclusions in ejected granitic blocks from Ascension Island; Journal of Petrology, v.8, p.417-451.

Rosylyakova, N.V. and Rosylyakova, N.A., 1975. Endogenic aureoles of gold deposits - Translation Precis by R.W.Boyle, Journal of Geochemical Exploration, v.6 (1976), p.383-387.

Ross, R.J, Jr. and Naeser, C.W., 1984. The Ordovician time scale- new refinements; in Aspects of the Ordovician System, ed. D.L. Burton, Paleontological Contributions from the University of Oslo, No. 295, p.5-10.

____, ____, Izett, G.A., Obradovich, J.D., Bassett, M.G., Hughes, C.P., Cocks, L.R.M., Dean, W.T., Ingham, J.K., Jenkins, C.J., Rickards, R.B., Sheldon, P.R., Toghill, P., Whittington, H.B. and Zalasiewicz, J., 1982, Fission track dating of British Ordovician and Silurian stratotypes. Geology Magazine, v.119, p.135-153.

Sawkins, F.L., 1969. Chemical brecciation; an unrecognized mechanism for breccia formation? Economic Geology, v.64, p.613-617.

Schnetzler, C.C. and Philpotts, J.A., 1970. Partition coefficients of rare-earth elements between igneous matrix material and rock forming minerals- II. Geochimica et Cosmochimica Acta, v.64, p.331-340.

Scott, S.D., 1980. Geology and structural control of Kuroko-type massive sulphide deposits; in The Continental Crust and its Mineral Depsoits, ed. D.W. Strangway, Geological Association of Canada Special Paper 20, p.705-721.

Shaw, H.R., Smith, R.L. and Hildreth, E.W., 1976. Thermogravitational mechanisms for chemical variations in zoned magma chambers. Geological Society of America, Abstracts with Programs, v.8, p.1102.

Sillitoe, R.H. and Sawkins, F.J., 1971. Geologic, mineralogic and fluid inclusion studies relating to the origin of copper-bearing tourmaline breccia pipes, Chile. Economic Geology, 66, p.1028-1041.

Snelgrove, A.K., 1928. The geology of the central mineral belt of Newfoundland. Canadian Institute of Mining and Metallurgy Bulletin, v.21, p.1057-1127.

Stanton, R.L. and Ramsay, W.R.H., 1980. Exhalative ore, volcanic loss, and the problem of the island arc calc-alkaline series; a review and an hypothesis. Norges Geologiske Undersokelse, No.360, p.9-57.

Stephens, M.B., 1982. Spilitization, volcanite composition and magmatic evolution - their bearing on massive sulphide composition and siting in some volcanic terranes. Transactions of the Institute of Mining and Metallurgy (Section B: Applied earth sciences), v.91, p.B200-B213.

_____, Swinden, H.S. and Slack, J.F., 1984. Correlation of massive sulphide deposits in the Appalachian-Caledonian orogen on the basis of paleotectonic setting. Economic Geology, v.79, p.1442-1478.

Stewart, P.W., 1983. Granitoid clasts in boulder breccias of MacLean orebody, Buchans, Newfoundland; in Current Rsearch, Part A, Geological Survey of Canada, Paper 83-1A, p.321-324.

_____, 1984. Geochemistry of granitoid clasts from MacLean Extension orebody, Buchans, Newfoundland, and implications on their possible source; in Current Research, Part A, Geological Survey of Canada, Paper 84-1A, p.462-467.

Stillman, C.J., 1984. Ordovician volcanicity; in Aspects of the Ordovician System, ed. D.L. Burton; Paleontological Contributions from the University of Oslo, no. 295, p.183-194.

Streckeisen, A.L., 1967. Classification and nomenclature of igneous rocks. Neues Jahrbuch fur Mineralogie Abhandlungen, v.107, p.144-240.

_____, 1976. To each plutonic rock its proper name. Earth Science Reviews, v.12, p.1-33.

_____, and LeMaitre, R.W., 1979. A chemical approximation to the modal QAPF classification of igneous rocks. Neues Jahrbuch fur Mineralogie Abhandlungen, v.136, p.169-206.

Strong, D.F., 1977. Volcanic regimes in the Newfoundland Appalachians; in Volcanic Regimes in Canada, eds. W.R.A. Baragar, L.C. Coleman and J.M. Hall; Geological Association of Canada Special Paper 16, p.61-90.

_____, 1980. Granitoid rocks and associated mineral deposits of eastern Canada and western Europe; in The Continental Crust and its Mineral Deposits, ed. D.W. Strangway; Geological Association of Canada Special Paper 20, p.741-769.

_____, 1984. Rare earth elements in volcanic rocks of the Buchans area, Newfoundland. Canadian Journal of Earth Sciences, v.21, p.775-780.

Swanson, E.A. and Brown, R.L., 1962. Geology of the Buchans orebodies. Canadian Institute of Mining and Metallurgy Bulletin, v.55, p.618-626.

_____, Strong, D.F. and Thurlow, J.G. (eds.), 1981. The Buchans Orebodies: Fifty Years of Geology and Mining. Geological Association of Canada Special Paper 22, 350p.

Swinden, H.S. and Kean, B.F., 1984. Volcanogenic sulphide mineralization in the Newfoundland Central Mobile Belt; in Mineral Deposits in Newfoundland - a 1984 perspective; Newfoundland Department of Mines and Energy, Mineral Developement Division, Report 84-3, p.55-77.

_____ and Thorpe, R.I., 1984. Variations in style of volcanism and massive sulphide deposition in Early to Middle Ordovician island-arc sequences of the Newfoundland Central Mobile Belt. Economic Geology, v.79, p.1596-1619.

Takahashi, T. and Suga, K., 1974. Geology and ore deposits of the Hanaoka Kuroko belt, Akita Prefecture; in Geology of the Kuroko Deposits, ed. S. Ishihara, Society of Mining Geologists Special Issue No. 6, p.101-113.

Takanouchi, S., 1978. High salinity fluid inclusions in breccias of intrusive dikes in Hokuroku Kuroko area, Japan; in International Association on the Genesis of Ore Deposits, 5th Symposium, Program with Abstracts, p.188.

Taylor, R.P. and Fryer, B.J., 1980. Multiple-stage hydrothermal alteration in porphyry copper systems in northern Turkey: the temporal interplay of potassic, propylitic and phyllic fluids; Canadian Journal of Earth Sciences, v.17, p.901-926.

_____ and _____, 1982. Rare earth element geochemistry as an aid to interpreting hydrothermal ore deposits; in Metallization Associated with Acid Magmatism, ed. A.M. Evans, Wiley and Sons, Chichester, p.357-365.

_____ and _____, 1983. Rare earth element lithogeochemistry of granitoid mineral deposits. Canadian Institute of Mining and Metallurgy, Bulletin, v.76, p.76-84.

Taylor, R.P., Strong, D.F. and Kean, B.F., 1980. The Topsails Igneous Complex: Silurian-Devonian peralkaline magmatism in western Newfoundland. Canadian Journal of Earth Sciences, v.17, p.425-439.

_____, _____ and Fryer, B.J., 1981. Volatile control of contrasting trace element behavior in peralkaline granite and volcanic rocks. Contributions to Mineralogy and Petrology, v.77, p.267-271.

Taylor, S.R., 1965. The application of trace element data to problems in petrology. Physics and Chemistry of the Earth, v.6, p.133-213.

_____ and Gorton, M.P., 1977. Geochemical application of spark source mass spectrography III. Element sensitivity, precision and accuracy. Geochimica et Cosmochimica Acta, v.41, p. 1375-1380.

Thompson, G., 1983. Basalt-seawater interactions; in Hydrothermal processes at seafloor spreading centers, eds. P.A. Rona, K. Bostrum, L. Laubier and K.L. Smith, Jr.; NATO Conference Series, IV, Marine Sciences, v.12, p.225-278.

Thornton, C.P. and Tuttle, O.F., 1960. Chemistry of igneous rocks. I: Differentiation index. American Journal of Science, v.258, p.664-684.

Thurlow, J.G., 1973. Lithogeochemical studies in the vicinity of the Buchans massive sulphide deposits, central Newfoundland. Unpublished M.Sc. thesis, Memorial University of Newfoundland, 171p.

_____, 1977. Occurrence, origin and significance of mechanicallly transported sulphide ores at Buchans, Newfoundland; in Volcanic Processes in Ore Genesis, Geological Society of London, Special Publication No. 7, p.127.

_____, 1981a. Geology, ore deposits and applied rock geochemistry of the Buchans Group, Newfoundland. Unpublished Ph.D. thesis, Memorial University of Newfoundland, 305p.

_____, 1981b. The Buchans Group: its stratigraphic and structural setting; in The Buchans Orebodies: Fifty Years of Geology and Mining, eds. E.A. Swanson, D.F. Strong and J.G. Thurlow; Geological Association of Canada Special Paper 22, p.79-90.

_____, 1984. A geological field guide to the Buchans area; in Mineral deposits of Newfoundland - a 1984 perspective; Newfoundland Department of Mines and Energy, Mineral Developement Division, Report 84-3, p.141-146.

_____ and Swanson, E.A., 1981. Geology and ore deposits of the Buchans area, central Newfoundland; in The Buchans Orebodies: Fifty Years of Geology and Mining, eds. E.A. Swanson, D.F. Strong and J.G. Thurlow; Geological Association of Canad Special Paper 22, p.113-142.

_____, and _____, 1985. Stratigraphy and structure of the Buchans Group, in Buchans Geology, Newfoundland; 1982-1984, ed. R.V. Kirkham, in preparation.

_____, _____ and Strong, D.F., 1975. Geology and lithogeochemistry of the Buchans polymetallic sulphide deposits, Newfoundland. Economic Geology, v.70, p.130-144.

Tuach, J., 1984. Geology and volcanogenic sulphide mineralization in the Robert's Arm Group on Pilley's Island, central Newfoundland; in Mineral Deposits in Newfoundland-1984 perspective. Newfoundland Department of Mines and Energy, Mineral Developement Division, Report 84-3, p.117-127.

Urabe, T., Scott, S.D. and Hattori, K., 1983. A comparison of footwall-rock alteration and geothermal systems beneath some Japanese and Canadian volcanogenic massive sulphide deposits. Economic Geology Monograph 5, p.345-364.

Upadhyay, H.D., Dewey, J.F. and Neale, E.R.W., 1971. The Betts Cove ophiolite complex, Newfoundland: Appalachian oceanic crust and mantle. Geological Association of Canada Proceedings, v.24, p.27-34.

_____ and Strong, D.F., 1973. Geological setting of the Betts Cove copper deposits, Newfoundland: an example of ophiolite mineralization. Economic Geology, v.68, p.161-167.

van Breeman, O., Davidson, A, Loveridge, W.D. and Sullivan, R.W., 1985. U-Pb zircon geochronology of Grenville tectonics, granulites and igneous precursors, Parry Sound, Ontario. Canadian Journal of Earth Sciences, in press.

van Eysinga, F.S.W., 1975. Geological time table (3rd ed.). Elsevier Scientific Publishing Company, Amsterdam.

Volynets, O.N. and Bogoyavlenskaya, G.E., 1979. Granitoid inclusions in Quatenary lavas of Kamchatka. Bulletin Volcanologique, v.42, p.242-251.

Wager, L.R. and Brown, G.M., 1968. Layered igneous rocks. Oliver and Boyd, London and Edinburgh, 588p.

Walker, P.N. and Barbour, D.M., 1981. Geology of the Buchans ore horizon breccias; in The Buchans Orebodies: Fifty Years of Geology and Mining, eds. E.A. Swanson, D.F. Strong and J.G. Thurlow: Geological Association of Canada Special Paper 22, p.161-186.

Whalen, J.B. and Currie, K.L., 1982. Volcanic and plutonic rocks in the Rainy Lake area, Newfoundland; in Curent Research, Part A, Geological Survey of Canada, Paper 82-1A, p.17-22.

_____, and _____, 1983. The Topsails igneous terrrane of western Newfoundland; in Current Research, Part A, Geological Survey of Canada, Paper 83-1A, p.15-23.

_____, and _____, 1985. The relationship of the Topsails Igneous Terrane to the Buchans Group; in Buchans Geology, Newfoundland 1982-1984, ed. R.V. Kirkham, in prep.

White, A.J.R. and Chappell, B.W., 1983. Granitoid types and their distribution in the Lachlan Fold Belt, southeastern Australia. Geological Society of America Memoir 159, p.21-34.

Whitten, E.H.T., Li, G., BornHorst, T.J., Christenson, P. and Hicks, D.L., 1984. Quantitative recognition of suites (or other natural classes) within granitoid batholiths and other igneous assembleges (abstract). Geological Society of America Annual Meeting, v.16, no. 6, p.693.

Wilcox, R.E., 1979. The liquid line of descent and variation diagrams; in The Evolution of the Igneous Rocks, ed. H.S. Yoder, Jr., Princeton University Press, Princeton, N.J., p.205-232.

Williams, H., 1967. Silurian rocks of Newfoundland. Geological Association of Canada Paper No. 4, p.93-137.

_____, 1970. Red Indian Lake (east half) Newfoundland. Geological Survey of Canada, Map No. 1196A.

_____, 1978. Tectonic-lithofacies map of the Appalachian orogen. Memorial University of Newfoundland, St. John's, Map No. 1.

_____, 1979. Appalachian orogen in Canada. Canadian Journal of Earth Sciences, v.16, p.792-807.

_____, 1984. Miogeoclines and suspect terranes of the Caledonian-Appalachian Orogen: tectonic patterns in the North Atlantic region. Canadian Journal of Earth Sciences, v.21, p.887-901.

_____, Hibbard, J.P. and Bursnall, J.T., 1977. Geological setting of asbestos-bearing ultramafic rocks along the Baie Verte Lineament, Newfoundland. Geological Survey of Canada, Paper 77-1A, p.351-359.

Williams, H. and McBirney, A.R., 1979. Volcanology. Freeman, Cooper and Co. Ltd., San Francisco, 397p.

Wilson, J.T., 1966. Did the Atlantic close and then re-open? Nature, v.211, p.676-681.

Winchester, J.A. and Floyd, P.A., 1977. Geochemical discrimination of different magma series and their differentiation products using immobile elements. Chemical Geology, v.20, p.325-343.

Wolfe, J.A., 1980. Fluidization versus phreatomagmatic explosions in breccia pipes. Economic Geology, v.75, p.1105-1109.

Wood, D.A., Joron, J-L. and Treuil, M., 1979. A re-appraisal of the use of trace elements to classify and discriminate between magma series erupted in different tectonic settings. Earth and Planetary Science Letters, v.45, p.326-336.

Appendix

Appendix 1. MAJOR ELEMENT ANALYTICAL PROCEDURES

Major element contents were determined at Memorial University of Newfoundland (G. Andrews, analyst) using a Perkin-Elmer 303 atomic absorption spectrophotometer, with the exception of P_2O_5. The techniques used have been adapted from Langmhyr and Paus (1968) and Abbey (1968). Phosphorus contents were determined by the colorimetric techniques of Maxwell (1968).

Analytical error for major elements is estimated at <5% for SiO_2, Al_2O_3, Fe_2O_3, CaO, Na_2O, and K_2O, at <8% for MnO, MgO and LOI, at 20% for TiO_2 and higher for P_2O_5. This estimate is based on the mean percent difference for each element between replicate analyses of thirteen samples. The large errors quoted for TiO_2 and P_2O_5 are considered due to the low abundances of these elements in the rocks analysed (1.0% and ~0.3%, respectively). The low totals reflect the presence of barium in abundances of up to 4%, rather than as a trace element (i.e., in ppm.).

APPENDIX TABLE 1.1 Examples of replicate major element analyses

	Clast type 1 (82-007)		Clast type 1 (82-051)		Clast type 3 (82-088)		Clast type 4 (82-095)		Little Sandy intrusion (83-130)		MacLean Ext. rhyolite (82-210)		Wiley's River intrusion (82-187)	
	1	2	1	2	1	2	1	2	1	2	1	2	1	2
SiO2	71.6	72.1	68.5	67.8	75.8	75.6	77.0	77.9	73.6	72.4	73.7	74.0	76.4	76.4
TiO2	0.20	0.18	0.18	0.18	0.13	0.12	0.11	0.10	0.25	0.26	0.20	0.33	0.17	0.22
Al2O3	12.6	12.8	10.6	10.9	11.7	11.8	11.4	11.4	12.3	12.8	13.1	12.1	12.1	12.0
Fe2O3*	2.55	2.53	2.58	2.59	0.68	0.68	1.06	1.00	3.48	3.51	2.58	2.73	1.82	1.80
MnO	0.07	0.08	0.08	0.08	0.06	0.06	0.04	0.04	0.09	0.09	0.03	0.04	0.04	0.05
MgO	1.05	0.99	1.08	1.01	0.39	0.39	0.20	0.17	1.27	1.30	0.34	0.37	0.35	0.33
CaO	1.87	1.77	3.55	3.57	1.99	1.97	1.06	0.89	0.70	0.67	1.07	1.19	0.93	0.86
Na2O	4.30	4.19	3.63	3.47	3.94	3.94	5.80	5.36	4.56	4.50	5.55	5.68	4.77	4.88
K2O	1.24	1.22	0.99	1.04	1.27	1.27	0.26	0.24	1.04	1.08	2.20	2.13	1.71	1.80
P2O5	0.06	0.08	0.15	0.05	0.01	0.02	0.01	0.05	0.08	0.00	0.12	0.07	0.05	0.10
LOI	2.96	3.01	5.39	4.25	2.36	2.38	1.06	0.98	1.52	1.62	1.12	1.10	0.55	0.47
Total	98.80	98.95	96.73	94.94	98.33	98.23	97.94	98.13	98.89	98.23	100.01	99.74	98.89	98.91

* Total iron reported as Fe2O3

Representative examples of these replicate analyses are shown in Appendix Table 1.1. Replicates were not identifiable to the analyst.

Appendix 2. TRACE ELEMENT ANALYTICAL PROCEDURES

Sample pellets consisting of 10. g (±0.05 g) of rock powder were mixed with 1.50 g (±0.05 g) of bakelite resin. This mixture was pressed into 40mm diameter pellets at 25 tons pressure and then baked at 200°C for 15 minutes to set the binder.

Sample pellets were analyzed with a Phillips 1450 X-ray fluorescence spectrometer. To reduce instrument drift between runs, a monitor saturated with trace elements was calibrated against standards, and every element ratioed to this monitor.

Precision of the XRF data (two standard deviations) is within 10% for Th, Rb, Sr, Y, Zr, Zn and Ba, within 15% for Pb and Nb, within 20% for Ga, within 25% for V, and higher for U, Cu, Ni and Cr. This is based on five replicate analyses of an internal granite standard (MUN-1). The large errors estimated for Ni and Cr are primarily due to their low abundances near the detection limits (1 ppm) of the XRF.

APPENDIX TABLE 2.1

Mean and standard deviations of five replicate analyses of granite standard (MUN-1)

	Mean	Standard Deviation	Maximum	Minimum
Pb	37.6	2.07	35	40
Th	38.6	0.89	37	39
U	8.4	3.91	4	13
Rb	264.4	4.67	258	271
Sr	123.6	0.89	123	125
Y	34.6	1.52	32	36
Zr	132.0	6.28	121	136
Nb	24.2	1.48	22	26
Zn	31.2	0.84	30	32
Cu	13.0	2.12	11	16
Ni	1.0	1.00	0	2
Ba	423.8	6.26	417	434
V	19.2	2.28	17	23
Cr	0.4	0.89	0	2
Ga	18.0	1.58	16	20

Similarly, the large uncertainties estimated for U, Cu, V, and Ga are considered more attributable to their low abundances (20 ppm, generally) in the standard than to poor analytical techniques.

The arithmetic mean, standard deviations and ranges for the five MUN-1 analyses used to estimate the precision of the XRF data are given in Appendix Table 2.1.

Appendix 3. RARE EARTH ELEMENT ANALYTICAL PROCEDURE

Rare earth element (REE) analyses were conducted for some samples at Memorial in the April and May of 1983 by the thin-film X-ray fluorescence technique of Eby (1972) as modified by Fryer (1977) and Fryer and Edgar (1977).

Depending on the trace element contents, 1.0 to 1.5 grams of sample powder was dissolved in HF and perchloric acid, then re-dissolved in HCl. Undissolved 'sediment' was removed by centrifuging and decanting the sample. The dissolved sample is added (as approximately 1N HCl) to 10 mm diameter columns containing 15 cm of ion exchange resin (Fisher-Rexyn 10-Na resin). Initially, 2N HCl is passed through the columns to remove all elements except the REE, Y

and Ba, then 6N HCl is used to remove the latter elements from the resin. After concentration of the sample by evaporation, Ba is removed by precipitation as $BaSO_4$.

The solution is then concentrated again by evaporation, re-dissolved in 1N HCl, and passed through cleaned and re-packed columns for purification. It is then concentrated by evaporation before application to specially prepared ion exchange paper discs (coins) as a very dilute HCl solution.

The coins are measured for REE by a Phillips 1450 X-ray fluorescence spectrometer. A monitor, with known REE contents was used to calibrate the instrument with standards. All elements were ratioed to this monitor to eliminate instrument drift between runs.

The relative precision of the REE analyses is shown by Appendix Figure 3.1. The range of measured REE contents from four replicate analyses of an internal granite standard (MUN-1) are shown. Accuracy can be estimated by comparison with the REE contents of MUN-1 as determined by four independent instrumental neutron activation analyses (INAA). The INAA data is used with the permission of Dr. D.F. Strong (McM1, JH, RPT) and P. O'Neil (McM2).

Appendix Figure 3.1 Comparison of chondrite-normalized rare earth element abundances in granite standard MUN-1 as determined by XRF techniques and instrumental neutron activation (INAA) techniques. Top figure shows the range of four replicate XRF analyses of MUN-1 at Memorial University in 1983. Bottom figure shows four independent INAA results for MUN-1 (McM1 and McM2 data produced at McMaster University, McM1 data courtesy of P. O'Neil, McM2 data courtesy of D.F. Strong; JH data produced by Jan Hoertgen, courtesy of D.F. Strong; RPT data produced by R.P. Taylor, courtesy of D.F. Strong).

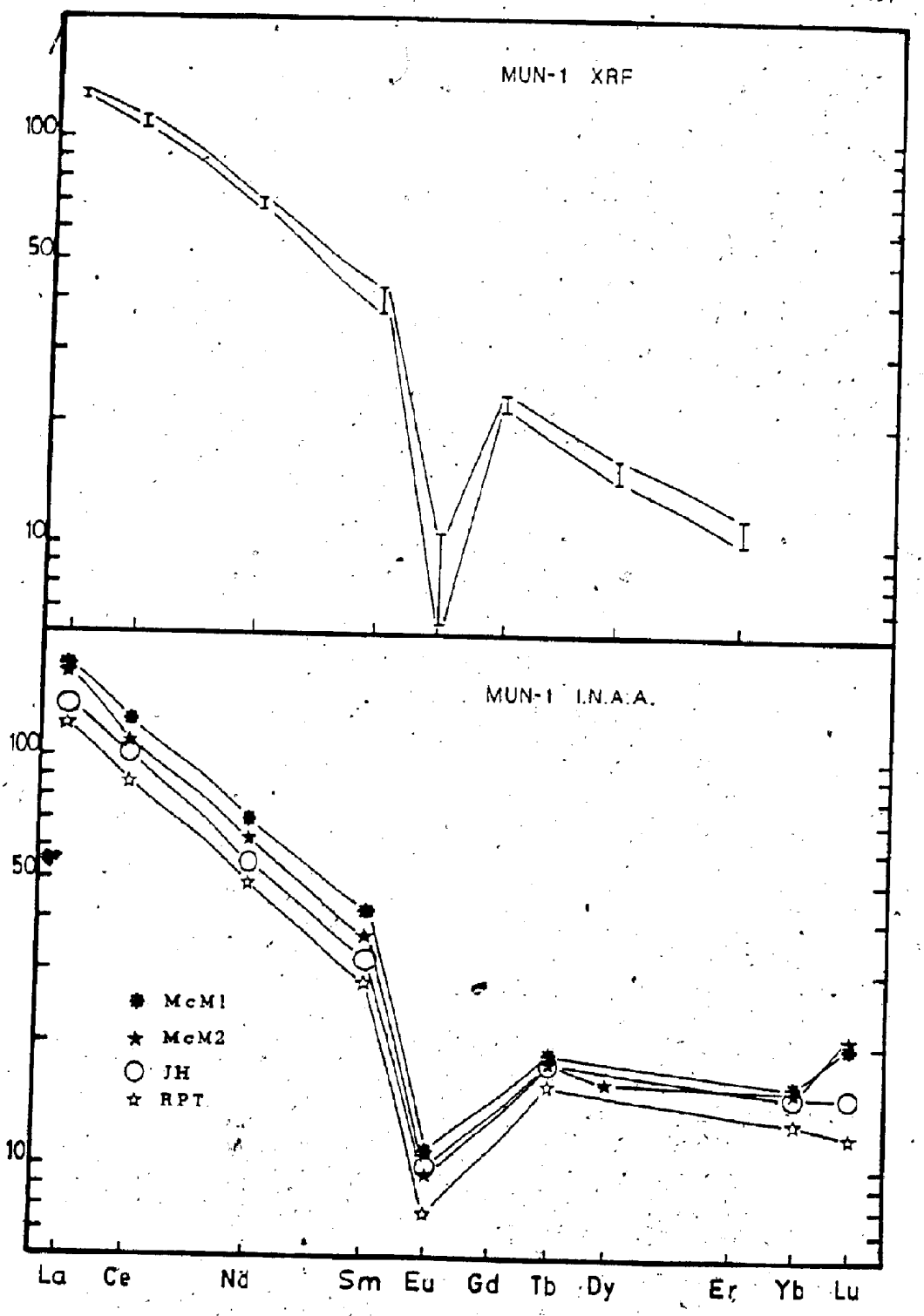
MUN-1 XRF
100
50
10
MUN-1 I.N.A.A.
100
50
10
McM1
McM2
JH
RPT
La
Ce
Nd
Sm
Eu
Gd
Tb
Dy
Er
Yb
Lu

Additional REE analyses were conducted in the fall of 1983 at Memorial University. However, because of the unsuitable reproducibility of these analyses, they have not been presented. This is the reason REE contents are lacking for some populations (e.g., Type 5 clasts; Little Sandy Lake intrusion).

Appendix 4. GEOCHRONOLOGY ANALYTICAL METHODS

The procedures used for the extraction and separation of the zircons used for isotopic analyses from the granitoid clast and rhyolite are presented as flow charts (Appendix Tables 4.1 and 4.2, respectively). Conventional procedures for crushing, seiving, Wilfley table and heavy liquid separation techniques and magnetic separation by a Frantz isodynamic separator were followed.

The proliferation of barite in the granitoid clast required additional steps before hand-picking for zircons. Air abrasion of the barite plus zircon concentrate proved to be the most effective because of the large difference in hardness between the two minerals. Abrasion reduced the bulk of the barite to -400 mesh and expelled it from the abrasion apparatus.

APPENDIX TABLE 4.1 FLOW CHART FOR GRANITOID CLAST SAMPLE KQS -82-095

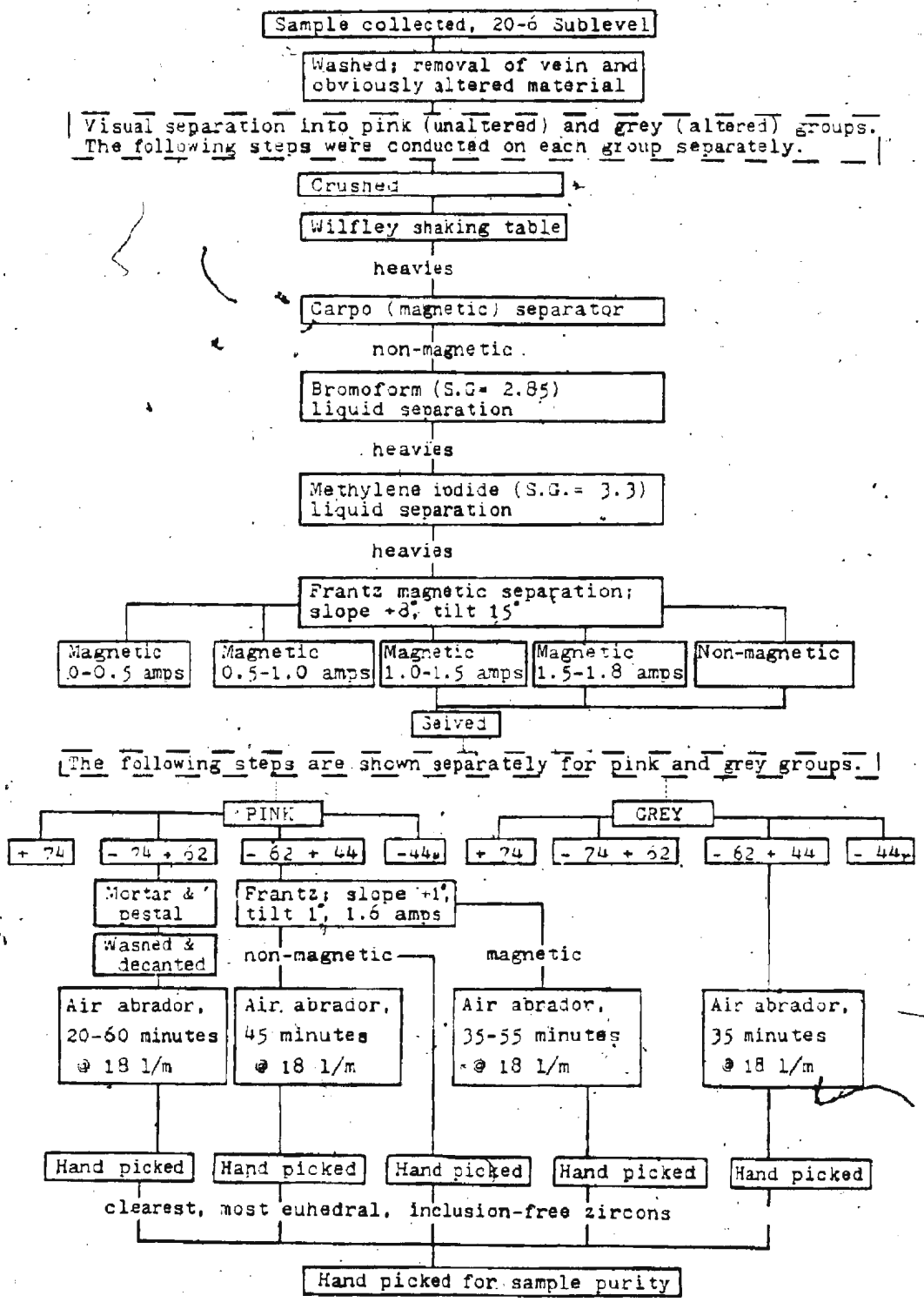

APPENDIX TABLE 4.2 FLOW CHART FOR RHYOLITE SAMPLE KQS -82-210

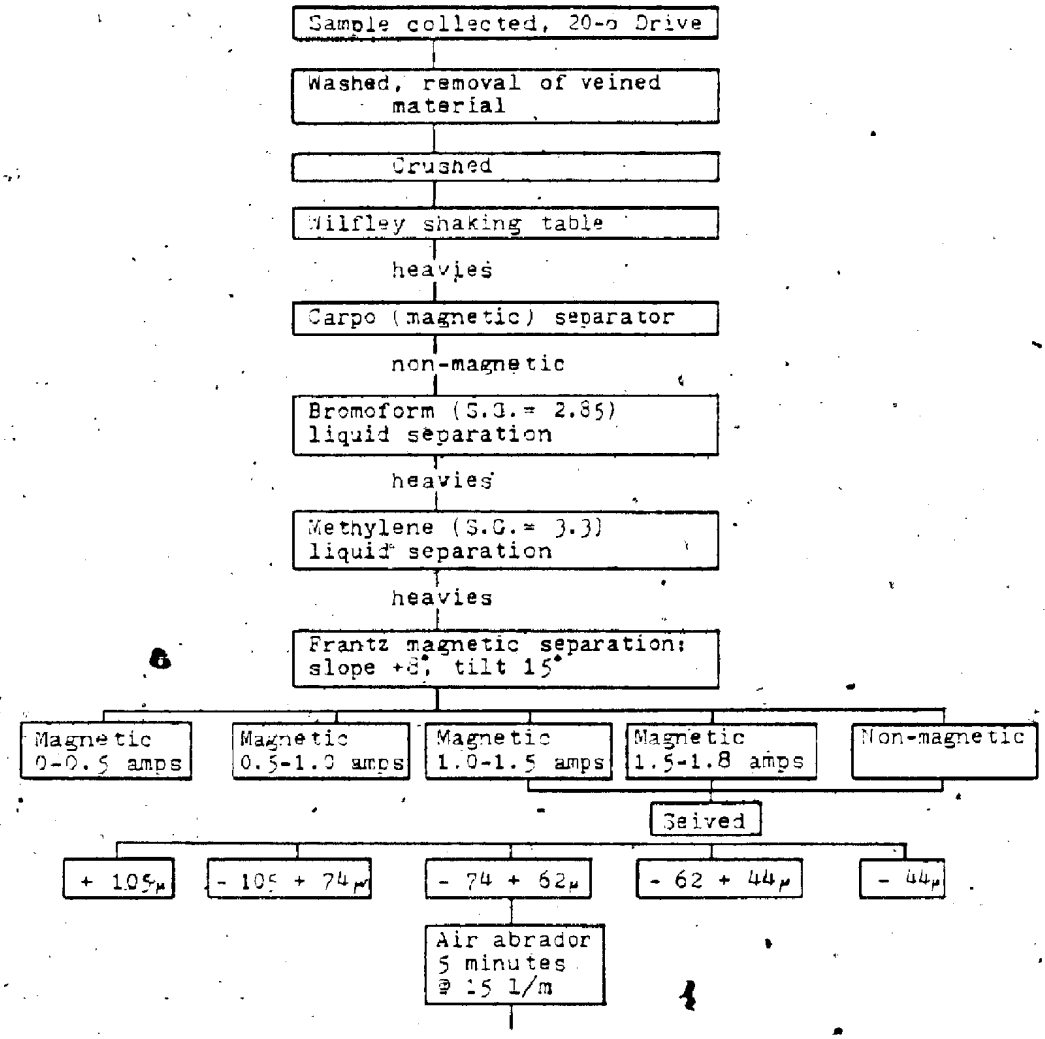

(continued)

APPENDIX FIGURE 4.2 (continued)

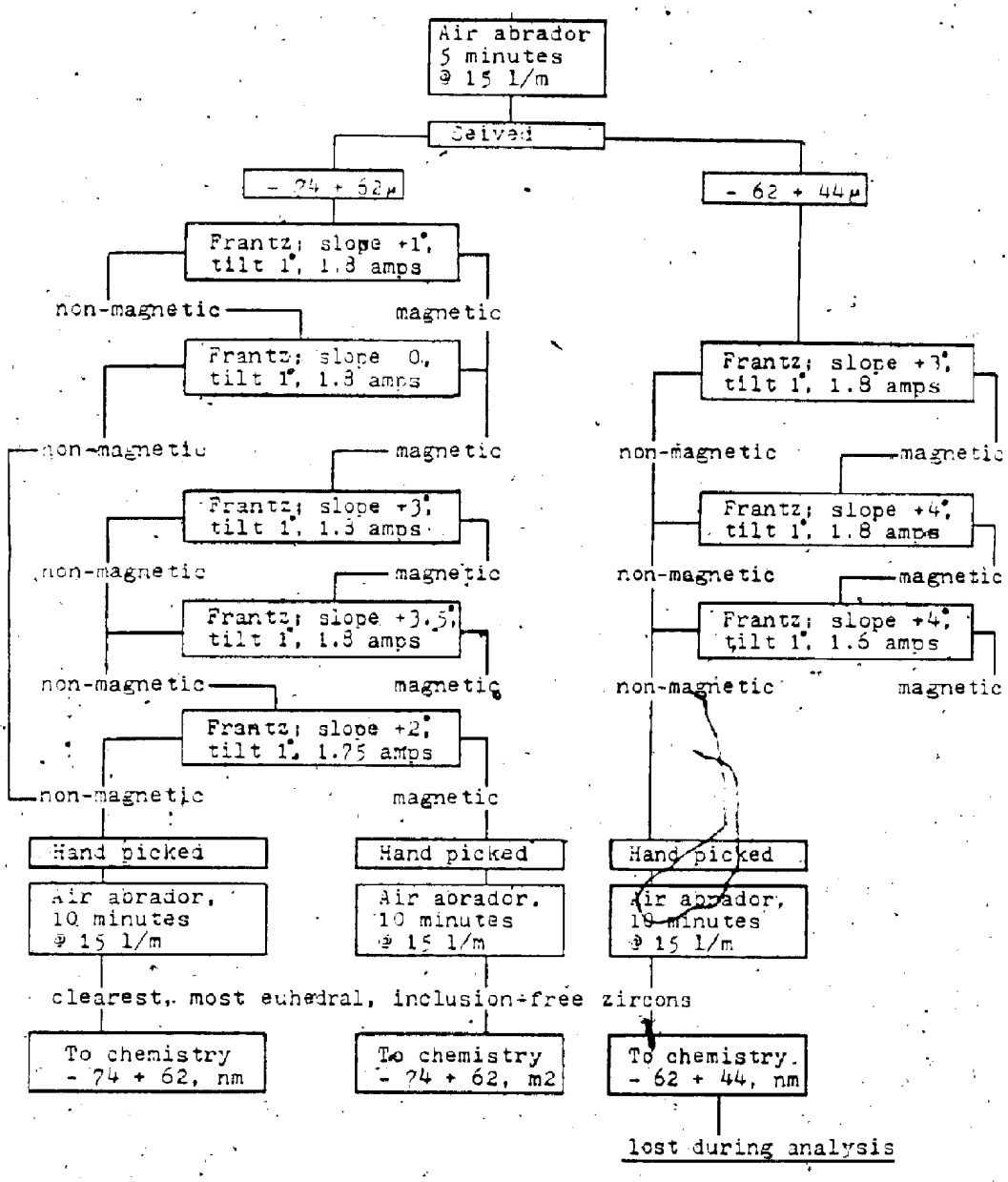

Complete details of the chemical procedures and apparatus used to determine the isotopic analyses and methods of calculation of the resulting radiometric dates at the Geochronology Lab, Geological Survey of Canada at the time of this study are given in van Breeman et al. (1985).

TYPE 1

(Granitic Group)

	82-007	82-008	82-031	82-044	82-051	82-082
SiO_2	71.60	70.60	73.70	73.20	67.80	72.30
TiO_2	.20	.30	.08	.15	.18	.13
Al_2O_3	12.60	12.80	11.90	10.60	10.90	11.80
Fe_2O_3	2.55	2.83	.83	1.03	2.59	1.65
MnO	.07	.08	.04	.05	.08	.07
MgO	1.05	.98	.35	.43	1.01	.52
CaO	1.87	2.22	2.56	2.64	3.57	2.73
Na_2O	4.30	4.68	3.35	3.59	3.47	2.89
K_2O	1.24	1.05	1.65	1.13	1.04	1.79
P_2O_5	.06	.08	.01	.02	.05	.01
LOI	2.96	2.53	3.18	3.96	4.25	3.97
TOTAL	98.50	98.15	97.65	96.80	94.94	97.86
			TRACE ELEMENTS (ppm)			
Pb	46	16	852	199	326	71
Th	13	13	13	14	11	15
U	1	2	6	2	3	0
Rb	23	20	32	20	22	29
Sr	302	380	143	378	530	213
Y	29	18	11	11	23	15
Zr	120	114	80	83	103	84
Nb	4	4	6	4	4	6
Zn	118	74	71	187	388	189
Cu	41	16	33	39	41	22
Ni	0	0	0	0	0	0
La	17	24	17	18	18	27
Ba	8033	7779	2311	18120	25455	4052
V	41	58	12	26	59	42
Ce	23	40	25	27	36	49
Cr	0	0	0	0	0	0
Ga	10	12	15	6	11	11

TYPE 1

(Granitic Group)

	82-127	83-012	83-018	83-024	83-119
SiO_2	73.90	73.20	71.70	75.40	72.00
TiO_2	.23	.18	.20	.14	.24
Al_2O_3	12.20	11.40	12.30	10.60	12.50
Fe_2O_3	1.21	1.67	3.45	1.10	2.90
MnO	.05	.04	.09	.06	.09
MgO	.56	.70	1.24	.34	1.18
CaO	2.88	2.13	2.08	3.03	2.23
Na_2O	4.03	4.16	4.07	2.86	3.60
K_2O	.90	1.18	1.20	1.68	1.40
P_2O_5	.01	.05	.07	.34	0.00
LOI	2.60	2.93	2.78	3.93	2.09
TOTAL	98.57	97.64	99.18	99.48	98.23
		TRACE ELEMENT (ppm)			
Pb	70	185	27	92	10
Th	11	9	4	16	12
U	1	4	3	2	3
Rb	15	21	22	24	19
Sr	362	277	290	149	324
Y	14	11	25	15	27
Zr	95	89	122	79	126
Nb	4	3	3	6	4
Zn	184	160	101	199	60
Cu	85	33	19	48	27
Ni	0	0	0	3	0
La	10	20	9	8	7
Ba	3507	9312	4389	4182	236
V	29	43	42	22	40
Ce	35	24	23	14	24
Cr	0	0	0	0	0
Ga	9	7	10	7	11

TYPE 3

(Granitic Group)

	82-002	82-004	82-013	82-043	82-052	82-073
SiO_2	74.20	74.20	72.80	72.90	71.50	72.80
TiO_2	.12	.05	.08	.12	.13	.15
Al_2O_3	11.10	11.40	10.30	10.70	10.90	12.10
Fe_2O_3	.94	.73	.49	1.30	1.29	1.33
Mno	.04	.03	.04	.05	.05	.05
MgO	.34	.27	.22	.51	.46	.56
CaO	2.05	2.27	2.69	2.84	3.06	3.00
Na_2O	4.15	4.31	3.94	3.27	3.48	3.21
K_2O	1.14	1.24	1.18	1.40	1.24	1.66
P_2O_5	.06	.05	.03	.07	.01	.02
LOI	3.00	3.01	4.29	4.17	4.50	3.90
TOTAL	97.14	97.56	96.06	97.33	96.62	98.78
			TRACE ELEMENTS (ppm)			
Pb	70	11	63	130	98	180
Th	11	8	14	15	14	13
U	5	0	0	3	1	0
Rb	23	19	19	25	22	26
Sr	390	377	888	300	399	195
Y	15	17	23	15	11	16
Zr	81	105	79	79	79	80
Nb	5	4	5	7	6	5
Zr	95	72	81	223	129	143
Cu	30	19	34	37	34	24
Ni	0	0	0	0	0	0
La	22	21	16	16	28	24
Ba	11913	7729	29243	11678	20949	3310
V	30	61	27	28	39	27
Ce	28	32	42	27	25	43
Cr	0	0	0	0	0	0
Ga	10	11	6	11	10	10

TYPE 3

(Granitic Group)

	83-001	83-003	83-010	83-016	83-019	83-088
SiO_2	76.70	75.70	72.30	73.90	76.80	75.80
TiO_2	.12	.20	.23	.11	.14	.13
Al_2O_3	8.30	10.70	12.50	10.20	10.40	11.70
Fe_2O_3	.48	.92	2.72	1.08	1.21	.68
MnO	.02	.04	.07	.05	.04	.06
MgO	.22	.48	1.24	.45	.56	.39
CaO	1.72	2.17	2.21	3.29	2.03	1.99
Na_2O	2.62	4.34	4.03	3.80	3.49	3.94
K_2O	.39	.83	1.38	1.09	1.28	1.27
P_2O_5	.02	.03	.06	.02	.06	.01
LOI	3.13	2.87	3.09	3.78	2.80	2.36
TOTAL	93.72	98.28	99.83	97.77	98.81	98.33
			TRACE ELEMENTS (ppm)			
Pb	49	149	28	47	38	23
Th	5	13	14	6	10	17
U	0	0	0	0	0	0
Rb	9	15	25	19	20	21
Sr	885	282	223	361	347	187
Y	5	18	9	17	11	18
Zr	56	81	94	82	56	82
Nb	2	6	2	5	3	7
Zn	75	196	169	89	414	33
Cu	59	49	30	27	55	33
Ni	0	0	0	0	0	0
La	15	10	0	10	9	6
Ba	40746	11070	3143	11130	7978	2580
V	38	15	59	23	34	9
Ce	0	17	5	6	28	16
Cr	0	0	0	0	0	0
Ga	2	8	10	7	7	9

TYPE 2

(Aplitic Group)

	82-040	82-058	82-099	83-032	83-084
SiO_2	71.90	76.10	73.80	71.90	76.40
TiO_2	.23	.15	.28	.08	.23
Al_2O_3	11.40	10.60	11.00	9.90	11.80
Fe_2O_3	2.50	1.22	1.85	.45	1.51
MnO	.06	.05	.06	.02	.05
MgO	1.12	.40	.73	.30	.41
CaO	1.41	1.69	2.20	1.74	1.41
Na_2O	4.13	5.60	4.68	2.79	5.07
K_2O	.94	.17	.23	2.84	.57
P_2O_5	.09	0.00	.04	.01	.02
LOI	3.35	2.44	2.98	2.32	1.58
TOTAL	97.13	98.42	97.85	92.35	99.05

TRACE ELEMENTS (ppm)

Pb	271	16	223	34	7
Th	12	12	9	19	7
U	2	1	0	4	0
Rb	21	4	3	44	10
Sr	445	252	446	184	221
Y	19	31	24	16	36
Zr	101	120	143	88	127
Nb	6	6	4	6	5
Zn	257	25	320	84	24
Cu	35	20	165	55	11
Ni	0	0	0	0	0
La	27	24	20	7	5
Ba	22289	10650	20489	4578	4272
V	60	18	41	13	16
Ce	13	48	17	24	22
Cr	0	0	0	0	0
Ga	12	8	13	8	10

TYPE 4

(Aplitic Group)

	82-037	82-086	82-095	82-118	82-119	83-022
SiO_2	77.50	76.10	77.00	77.20	78.10	76.10
TiO_2	.08	.13	.11	.20	.23	.17
Al_2O_3	10.10	10.70	11.40	11.00	10.80	10.20
Fe_2O_3	.84	1.26	1.06	1.15	.97	1.36
MnO	.07	.06	.04	.05	.04	.06
MgO	.49	.33	.20	.25	.24	.59
CaO	2.13	1.10	1.00	1.43	1.32	2.47
Na_2O	3.88	5.58	5.80	5.33	5.41	3.04
K_2O	.83	.26	.26	.20	.26	1.37
P_2O_5	.02	.01	.01	.03	0.00	.19
LOI	2.85	2.03	1.06	1.62	1.68	3.32
TOTAL	98.79	97.56	97.94	98.46	99.05	98.87
TRACE ELEMENTS (ppm)						
Pb	110	48	50	68	22	100
Th	16	13	18	17	15	15
U	3	3	3	1	5	5
Rb	15	4	4	5	4	22
Sr	236	274	238	248	228	238
Y	38	35	41	31	38	8
Zr	128	139	130	141	149	73
Nb	5	8	8	4	5	1
Zn	64	55	30	69	36	128
Cu	20	28	14	24	28	38
Ni	0	0	0	0	0	0
La	13	29	17	20	23	8
Ba	7001	12322	4970	8139	8041	7861
V	12	20	10	18	14	26
Ce	27	50	49	54	44	0
Cr	0	0	0	0	0	0
Ga	8	8	10	11	9	8

	TYPE 5 (Aplitic Group)	TYPE 6 (Granitoid Clast)		
	83-091	82-028	82-067	83-011
SiO_2	77.30	67.70	69.40	67.40
TiO_2	.13	.43	.40	.33
Al_2O_3	11.60	14.10	13.50	13.70
Fe_2O_3	.85	3.99	3.40	4.43
MnO	.03	.06	.06	.09
MgO	.30	1.22	.97	1.76
CaO	1.17	2.88	4.00	2.61
Na_2O	3.93	5.31	4.46	4.18
K_2O	3.08	.87	.53	1.38
P_2O_5	.03	.18	.08	.38
LOI	1.26	2.18	1.93	3.61
TOTAL	99.68	98.92	98.73	99.87
	TRACE ELEMENTS (ppm)			
Pb	43	12	11	25
Th	20	7	10	7
U	5	0	0	2
Rb	39	14	5	24
Sr	170	340	256	235
Y	19	38	22	25
Zr	86	115	129	70
Nb	7	5	4	5
Zn	29	63	28	203
Cu	14	14	17	25
Ni	0	1	0	0
La	16	5	21	0
Ba	3852	473	514	4502
V	12	74	59	76
Ce	31	32	39	17
Cr	0	0	0	0
Ga	7	12	13	12

WILEY'S RIVER INTRUSION

(Feeder Granodiorite)

	82-187	82-189	82-190	82-191	82-196
SiO_2	76.40	74.20	74.40	76.40	75.50
TiO_2	.17	.26	.26	.24	.26
Al_2O_3	12.10	12.80	12.60	12.60	12.50
Fe_2O_3	1.82	2.29	2.15	1.87	2.08
FeO	0.00	0.00	0.00	0.00	0.00
MnO	.04	.04	.05	.04	.04
MgO	.35	.49	.39	.35	.51
CaO	.93	1.50	1.58	1.34	1.62
Na_2O	4.77	4.18	4.15	4.28	4.35
K_2O	1.71	2.34	2.44	2.53	2.02
P_2O_5	.05	.05	.09	.04	.05
LOI	.55	.99	.53	.53	.49
TOTAL	98.89	99.14	98.64	100.22	99.42
TRACE ELEMENTS (ppm)					
Pb	22	7	15	15	8
Th	15	12	11	13	10
U	2	4	5	3	0
Rb	35	65	63	63	52
Sr	124	126	137	122	149
Y	41	28	33	35	31
Zr	119	121	143	119	121
Nb	5	4	5	5	5
Zn	22	9	16	21	16
Cu	25	18	15	7	5
Ni	2	0	1	0	0
La	17	18	11	15	12
Ba	1486	831	946	999	891
V	17	21	21	14	15
Ce	45	39	40	25	19
Cr	0	0	0	0	0
Ga	10	12	12	10	8

WILEY'S RIVER INTRUSION

(Feeder Granodiorite)

	82-198	82-199	82-203	83-094
SiO_2	74.70	74.70	74.90	74.70
TiO_2	.22	.22	.20	.23
Al_2O_3	12.30	12.40	12.10	12.20
Fe_2O_3	2.09	2.13	2.02	2.10
FeO	0.00	0.00	0.00	0.00
MnO	.06	.06	.05	.05
MgO	.49	.41	.46	.70
CaO	1.89	1.90	1.14	1.62
Na_2O	4.37	4.13	4.34	4.18
K_2O	2.60	2.29	2.31	2.15
P_2O_5	.08	.05	.05	.03
LOI	.67	.29	.56	.72
TOTAL	98.46	98.58	98.13	98.68
	TRACE ELEMENTS (ppm)			
Pb	16	17	10	11
Th	12	9	8	13
U	0	0	4	2
Rb	38	62	53	55
Sr	115	132	119	139
Y	39	32	34	29
Zr	131	117	131	128
Nb	6	6	4	4
Zn	31	24	27	23
Cu	7	5	6	14
Ni	0	0	0	0
La	12	7	10	10
Ba	844	897	972	970
V	21	16	22	21
Ce	23	23	20	26
Cr	0	0	0	0
Ga	10	9	12	12

LITTLE SANDY LAKE INTRUSION

(Feader Granodiorite)

	82-221	83-076	83-130	83-140	83-141
SiO_2	72.00	75.20	73.60	73.10	73.50
TiO_2	.20	.17	.25	.26	.29
Al_2O_3	13.00	11.90	12.30	12.40	12.30
Fe_2O_3	3.20	2.40	3.48	3.59	3.29
MnO	.08	.06	.09	.10	.09
MgO	.98	1.08	1.27	1.16	1.32
CaO	1.38	.57	.70	1.13	.86
Na_2O	5.05	4.79	4.56	5.08	4.52
K_2O	.50	1.04	1.04	.51	.79
P_2O_5	.10	.04	.08	.08	.08
LOI	1.68	1.79	1.52	1.21	1.49
TOTAL	98.17	99.04	98.89	98.62	98.53

TRACE ELEMENTS (ppm)

Pb	10	6	7	6	6
Th	4	11	14	12	8
U	0	0	0	5	0
Rb	9	23	26	11	17
Sr	163	115	94	106	110
Y	23	41	21	26	21
Zr	112	125	111	131	110
Nb	4	5	4	4	5
Zn	38	26	30	32	50
Cu	8	16	13	25	13
Ni	0	0	0	0	0
Ba	261	616	489	171	304
V	31	7	38	29	33
Cr	0	0	0	0	0
Ga	10	11	11	9	11

LITTLE SANDY LAKE SEQUENCE

	83-054	83-128	83-129	83-132	83-135
SiO_2	72.00	74.70	74.20	74.20	74.20
TiO_2	.29	.23	.13	.23	.20
Al_2O_3	12.60	12.00	12.30	12.30	12.60
Fe_2O_3	3.44	2.32	1.53	3.67	2.97
MnO	.05	.12	.09	.13	.09
MgO	2.39	.49	1.28	1.28	1.30
CaO	1.19	1.35	1.26	.81	.65
Na_2O	3.50	4.49	6.19	3.48	4.36
K_2O	1.53	1.53	.16	1.63	1.45
P_2O_5	.06	.05	.17	.09	.07
LOI	2.80	2.09	1.63	1.85	1.78
TOTAL	99.93	99.37	98.94	99.67	99.67
TRACE ELEMENTS (ppm)					
Pb	5	3	5	6	10
Th	5	0	5	5	11
U	0	0	0	0	3
Rb	21	34	3	32	30
Sr	69	42	96	81	64
Y	3[illegible]	46	18	38	34
Zr	9[illegible]	128	111	82	121
Nb	4	1	3	3	4
Zn	39	53	35	57	50
Cu	14	14	14	12	19
Ni	0	0	0	0	0
Ba	165	238	55	435	412
V	33	6	12	8	6
Cr	0	0	0	0	0
Ga	12	13	11	13	9

MacLean Extension

Rhyolite

82-210

SiO_2	73.70
TiO_2	.20
Al_2O_3	13.10
Fe_2O_3	2.58
MnO	.03
MgO	.34
CaO	1.07
Na_2O	5.55
K_2O	2.20
P_2O_5	.12
LOI	1.12
TOTAL	100.01

TRACE ELEMENTS (ppm)	
Pb	17
Th	12
U	1
Rb	27
Sr	100
Y	36
Zr	139
Nb	5
Zn	74
Cu	6
Ni	0
Ba	1171
V	28
Cr	0
Ga	9

VOLCANIC CLASTS

	Siltstone breccia (MacLean Ext.)		Polylithic breccia Conglomerate (MacLean Ext.)	(Little Sandy Lake area)
	82-024	82-026	82-053	83-131
SiO_2	68.00	81.80	74.10	77.10
TiO_2	.44	.25	.07	.28
Al_2O_3	17.10	9.22	10.50	10.90
Fe_2O_3	.22	1.04	1.34	2.54
FeO	0	0	0	0
MnO	.01	.02	.06	.11
MgO	.01	.56	.70	1.00
CaO	.15	1.38	2.88	1.79
Na_2O	10.12	4.10	2.32	3.91
K_2O	.08	.63	1.65	1.08
P_2O_5	.08	.24	.03	.06
LOI	.88	0.00	3.91	1.75
TOTAL	97.09	99.24	97.56	100.52
	TRACE ELEMENTS (ppm)			
Pb	14	27	46	27
Th	16	11	11	9
U	7	5	4	1
Rb	3	16	43	24
Sr	97	144	525	119
Y	44	33	20	33
Zr	159	110	82	107
Nb	5	2	6	5
Zn	0	40	87	38
Cu	28	18	16	47
Ni	0	0	0	0
La	13	3	23	0
Ba	151	379	16346	489
V	27	7	14	4
Ce	29	13	37	14
Cr	0	0	0	0
Ga	6	7	11	

TOPSAILS GRANITE

	82-171	82-193	82-195	82-204	82-206
SiO_2	74.50	75.10	76.90	77.30	76.30
TiO_2	.28	.13	.15	.10	.10
Al_2O_3	12.70	12.00	11.90	11.90	12.10
Fe_2O_3	1.90	1.22	.94	1.44	1.38
FeO	0.00	0.00	0.00	0.00	0.00
MnO	.04	.02	.02	.04	.07
MgO	.25	.11	.09	.09	.10
CaO	.77	.28	.27	.34	.26
Na_2O	3.99	3.90	3.89	4.07	3.99
K_2O	4.40	4.78	4.78	4.48	4.75
P_2O_5	.01	.06	.02	.03	.04
LOI	.61	.46	.36	.60	.45
TOTAL	99.45	98.06	99.32	100.39	99.54
TRACE ELEMENTS (ppm)					
Pb	20	14	19	10	24
Th	28	29	33	30	29
U	3	6	8	9	12
Rb	146	160	168	143	159
Sr	54	21	17	26	19
Y	88	88	82	96	93
Zr	226	183	174	163	182
Nb	27	37	40	30	35
Zn	36	33	22	12	32
Cu	16	11	9	9	7
Ni	2	0	0	0	0
La	28	18	15	22	21
Ba	528	320	271	421	299
V	12	4	3	4	2
Ce	64	49	54	42	51
Cr	0	0	0	0	0
Ga	19	20	20	17	18

TOPSAILS GRANITE

	82-229	83-103
SiO_2	76.80	76.80
TiO_2	.10	.06
Al_2O_3	11.90	11.20
Fe_2O_3	1.30	1.56
FeO	0.00	0.00
MnO	.02	.01
MgO	.08	.04
CaO	.35	.04
Na_2O	3.93	3.82
K_2O	4.72	4.60
P_2O_5	.03	0.00
LOI	.59	.49
TOTAL	99.82	98.62

TRACE ELEMENTS (ppm)

Pb	22	14
Th	33	28
U	5	12
Rb	177	113
Sr	19	11
Y	84	54
Zr	202	193
Nb	38	40
Zn	38	22
Cu	9	50
Ni	0	0
La	26	0
Ba	285	236
V	3	0
Ce	51	38
Cr	0	0
Ga	21	26

GRANITOID CLASTS IN BOULDER BRECCIAS OF MACLEAN EXTENSION OREBODY, BUCHANS, NEWFOUNDLAND[1]

Contract 1583327

Peter W. Stewart[2]
Economic Geology Division

Stewart, P.W., Granitoid clasts in boulder breccias of MacLean Extension orebody, Buchans, Newfoundland: in Current Research, Part A, Geological Survey of Canada, Paper 83-1A, p. 321-324, 1983.

Also in Current Research, ed. R.V. Gibbons, Newfoundland Department of Mines and Energy, Mineral Development Division, Report 83-1, 1983.

Abstract

Approximately fifty per cent of the Buchans massive sulphide orebodies mined to date occurred in subaqueous breccia-conglomerate beds within an Ordovician-Silurian volcanic island-arc sequence, the Buchans Group. Amongst the diverse lithic clasts in these beds are rounded, subspherical granitoid pebbles, cobbles and boulders. An intrusive body to the southwest of the mine area, the Feeder Granodiorite, is lithologically similar to some of the granitoid clasts and has been interpreted to be comagmatic with some of the Buchans Group volcanic rocks. Twelve types of granitoid clasts were recognized based on megascopic characteristics but this number will probably be reduced after laboratory investigations have been completed.

Introduction

The volcanogenic sulphide ore deposits at Buchans occur as three types: stockwork ore, in situ ore and transported ore (Thurlow, 1981a; Thurlow and Swanson, 1981). The transported ore forms a series of sulphide-bearing breccia-conglomerate beds with diverse lithic clasts, including granitoids (i.e. plutonic rocks of felsic to intermediate composition) within an Ordovician-Silurian sequence of subaqueous volcanic, volcaniclastic and sedimentary rocks. The source of these granitoid clasts has been enigmatic. An intrusive body of small surface area (approximately 1.5 km^2), the Feeder Granodiorite, outcrops 12 km southwest of Buchans. It has been interpreted to be comagmatic with Buchans Group volcanics and the possible source of the granitoid clasts (Thurlow, 1981b). A description of the central volcanic belt is given in Kean et al. (1981).

It is the intent of this study to determine the petrological character, geochemistry, and age of the granitoid clasts and of the Feeder Granodiorite and shed light on the relationship of the Feeder Granodiorite to the Buchans Group and the included granitoid clasts, and in turn on the provenance and derivation of the clasts.

Acknowledgments

The author is grateful for co-operation and help at Buchans from J.G. Thurlow, E.A. Swanson, W.P. Binney and the staff of ASARCO and Abitibi-Price.

D.F. Strong, W.H. Poole and R.V. Kirkham made many useful suggestions to improve the manuscript.

Underground Observations

The transported orebodies consist of a sequence of breccias and conglomerates which are considered to show characteristics of sediment gravity flow deposits (Walker and Barbour, 1981; Binney et al., 1983). Detailed examination of those units which are relatively rich in granitoid clasts indicates that most granitoid-rich units overlie and flank the sulphide-rich breccias. Granitoid clasts, however, are found in other units not intimately associated with the sulphide-rich breccias. These granitoid clasts are typically smaller (pebble-sized) than the typical cobble-sized granitoid clasts found with the ore. Rare granitoid clasts have been found in almost all Buchans Group formations, although nowhere in significant numbers or volume as compared to the ore horizon (J.G. Thurlow, personal communication, 1982).

The nature of the granitoid clasts varies appreciably in hand specimen. A tentative field classification based on colour, grain size, presence or absence of quartz phenocrysts and mafic mineral content indicate twelve clast types (Table 44.1).

The average granitoid clast size as determined within several exposures of granitoid-bearing (arenaceous) breccia-conglomerate (see Table 44.2) on 20 level, MacLean Extension orebody, is 6.4 by 4.1 cm. The long dimensions of granitoid clasts range from 1 cm to more than 50 cm. Where intimately associated with the transported massive sulphide ore (e.g. 20-5 sublevel, 20-13 drift), average clast size is of the order of 16.5 by 10 cm and granitoid clasts comprise approximately 4 per cent by volume. In more arenaceous units, granitoid clasts average 4.2 by 2.0 cm and constitute 1 per cent of the rock. Rare granitoid clasts have been observed in tuffaceous rocks, both overlying and underlying the ore horizon. These clasts average 7.5 by 6.0 cm and comprise much less than 1 per cent.

Granitoid clasts are subrounded to well rounded and typically subspherical, although many are oval and elongate. They are consistently better rounded than other clast types in the breccia-conglomerate units.

Surface Observations

The Feeder Granodiorite is an irregularly shaped body of approximately 1.5 km^2 occurring in upper Wiley's River area (Fig. 44.1). Along its southern and western exposures the granodiorite can be seen in contact with rocks presumed to be part of the Topsails complex (Taylor et al., 1980). At the Feeder Granodiorite-Topsails contacts, Topsails granite shows a weakly developed chilled margin against the Feeder Granodiorite. Brick-red, fine grained, equigranular dykes, macroscopically similar to the Topsails granite cut Feeder Granodiorite. The granodiorite and the Topsails granite are both cut by diabasic dykes. No exposures of the contact between Feeder Granodiorite and Buchans Group rocks were found. No definite evidence of cross-cutting relationships between diabasic and granitic dykes was observed.

---

[1] Contribution to Canada-Newfoundland co-operative mineral program 1982-1984. Project carried by Geological Survey of Canada.

[2] Department of Earth Sciences, Memorial University of Newfoundland, St. John's, Newfoundland A1B 3X5.

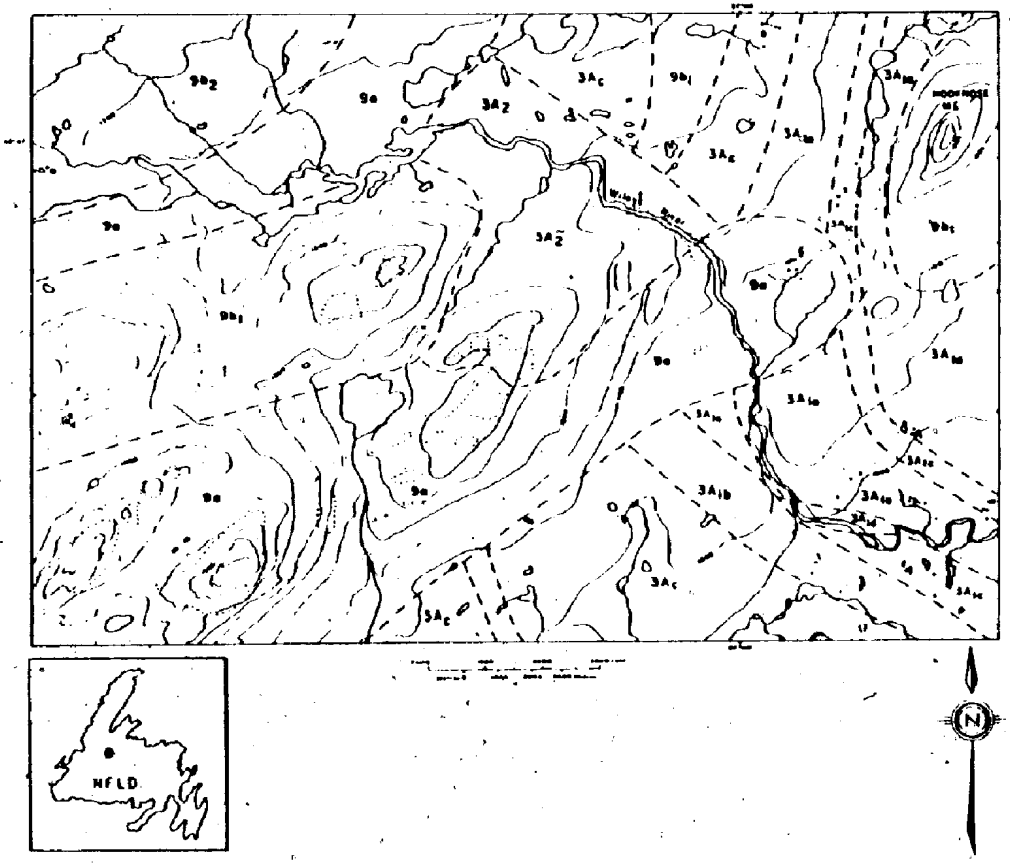

LEGEND

SILURIAN AND DEVONIAN

TOPSAILS GRANITE

9a	Alkali Feldspar granite: fine to medium grained, brick red granite
$9b_1$ | $9b_2$	Mafic Intrusives (associated with Topsails Granite): fine to coarse grained diabase ($9b_1$) and gabbro ($9b_2$)

ORDOVICIAN-SILURIAN

BUCHANS GROUP

$3A_a$ | $3A_c$	Footwall Arkose: $3A_a$, lithic arkose; $3A_c$, basaltic lava, pillow lava, pillow breccia
$3A_{1a}$ | $3A_{1b}$ / $3A_{1c}$ | $3A_{1d}$	Wiley's Prominent Quartz Sequence: Stratigraphic volcanic equivalent of 3A; characterized by quartz crystals commonly exceeding 1 cm in diameter; $3A_{1a}$, rhyolite flows and tuffs; $3A_{1b}$, dacitic pyroclastics; $3A_{1c}$, basaltic lavas, pillow lavas; $3A_{1d}$, tuffaceous siltstone.
$3A_2$	Feeder Granodiorite: whitish-brown, medium grained biotite granodiorite, with coarse grained quartz phenocrysts.

SYMBOLS

Geological boundary (defined, assumed)

Outcrop boundary (examined)

Elevations in feet above mean sea level

Approximate magnetic declination: 28° W

Formation numbers taken from and geology modified from "Geological Map of Buchans Area, Newfoundland," by Thurlow and Swanson, 1982.

Figure 44.1. Geological map of upper Wiley's River area, Buchans, Newfoundland.

The Feeder Granodiorite is a whitish brown rock, which becomes increasingly reddish toward the contact with the Toosails granite in Wiley's River area. The granodiorite is medium grained with abundant coarse grained quartz phenocrysts. Quartz crystals are generally rounded (5-10 mm average diameter), clear, locally appear as aggregates of crystals rather than true individual phenocrysts, and comprise 25-30 per cent of the rock by volume. The predominant feldspar is plagioclase, comprising 55-65 per cent of the rock, that is subhedral (locally euhedral), white and frequently darkened red-brown (by hematite). Fine grained clots of subhedral biotite crystals constitute 5 per cent. A fine grained pink-brown mineral (potash feldspar?) occurs interstitially to the quartz phenocrysts and the plagioclase (plus biotite) masses, and comprises 5 per cent of the rock.

The Toosails granite in this area is brick-red, ranges from fine- to medium-grained and is consistently equigranular. All feldspars are medium to dark red and comprise 65 per cent of the rock. Quartz crystals are clear, 1-3 mm across and form 30 per cent of the rock and biotite 5 per cent. The granite is miarolitic, especially near the contact with Feeder Granodiorite. The cavities are typically 1 mm in diameter, although near the contact they are 3-5 mm and partly filled with variable amounts of quartz,

Table 44.1

Field Classification of Granitoid Clasts

Clast type	Dominant colour, groundmass	Grain size	Phenocryst type	Mafic mineral content	Distinguishing features
1	strong-moderate brown-red	f.-m.g.	qtz. (c.g.)	variable: f.-m.g., generally distinct	colour strong brown-red; f.-m. grain size; presence of qtz. phenocrysts
2	strong-moderate brown-red	f.g.	equigranular	f.-m.g., distinct, variable	colour, strong-mod. brown-red; f. grain size; absence of qtz. phenocrysts
3	black & white with light browns, occasionally greenish or greyish	m.-c.g.	rare qtz. (c.g.)	m.-c.g.; distinct and indistinct in different clasts	coarse grain size; equigranular; spotted colour (black and white)
4	moderate-light brown (weak red)	m.g., rarely f.g.	qtz. (c.g.); rock may be m.g. & equigranular	variable; distinct & indistinct	qtz. phenocrysts; lighter red colour than type 1, otherwise the same. Includes medium grained equigranular equivalents
5	light brown-pink darkened with mafic minerals in some	f.-m.g.	equigranular	generally distinct except when very abundant & f.g.	absence of qtz. phenocrysts; same colour as type 4, or even less pink (or red)
6	variable, light green with white & light brown	f.-m.g.	qtz. (m.-c.g.) rare m.g. plag.	generally indistinct variable	presence of qtz. phenocrysts; large amount of qtz. present; absence of brown & especially red colours except in isolated crystals
7	grey-white, rarely very light brown	f.g. (rarely m.g.)	equigranular	typically indistinct, content varies from 0-20%	white and/or grey colour; commonly with pyrite
8	greenish-yellow with occasional red tinges	f.-m.g.	qtz. (m.g.)	indistinct	vague crystal boundaries, with the exception of qtz. phenocrysts; most likely a volcanic rock
9	dark-moderate greenish with specks of white (plag.), red (K-feldspar) and qtz.	f.g.	equigranular; rare m.g.	abundant, distinct, probably amphibole	dark, spotted appearance; fine grained; seen only in siltstone breccia
10	dark green with grey & light brown	f.g.	K-feldspar & plag. (m.g.) rare qtz. (smaller)	abundant (to 40%) distinct	similar to type 9 but with abundant plag. phenocrysts – only one sample seen
11	strong brown-red with white	f.-m.g.	qtz. (m.g.)	few to 5%, distinct	very abundant qtz; brown-red colour
12	variable: a mixture of whites, greens and weak browns	m.-c.g.	equigranular	unaltered, 10-15%	large grain size; equigranular; greenish plag. crystals (?)

Table 44.2

Classification – MacLean Extension Orebody
(modified after E.A. Swanson, personal communication, 1982)

Ore Horizon Sequence in MacLean Extension area	Upper Baritic Ore-Bearing member (without granitoid clasts)	Baritic unit
		Tuffaceous or breccia unit
		Baritic unit
	Felsic Pyroclastic member	Strongly lithic beds with isolated sulphide clasts; occasional polylithic breccia bed with minor granitoid clasts
	Lower Ore-Bearing member (Generally gradational from high grade at bottom to low grade arenaceous granitoid-bearing breccia-conglomerate. The top baritic bed seems distinct).	Baritic low grade polylithic ore breccia
		Granitoid-bearing breccia-conglomerate with arenaceous matrix. Beds of arenaceous wacke within unit
		Granitoid-bearing ore breccia-conglomerate; low grade with some arenaceous matrix
		Polylithic ore breccia; matrix becomes increasingly arenaceous towards top
		Mainly massive sulphide, in part streaky with minor lithic material
Intermediate Footwall Formation		Interbedded and altered mafic to felsic flows, pyroclastic rocks and volcanic breccias, related tuffaceous pyritic siltstone and wacke

specular hematite, fluorite and a silvery grey unidentified mica. At the contact, the granite shows a weakly developed graphic texture.

Summary

Granitoid clasts within the Buchans Group breccia-conglomerate beds and pyroclastic units comprise several lithologic types. Those clasts with coarse grained quartz phenocrysts (to 1 cm) in a brown-red groundmass are megascopically similar to the Feeder Granodiorite in the Wiley's River area.

The relationship of the Feeder Granodiorite to the Buchans Group remains unknown. Topsails granite has a chilled margin against the Feeder Granodiorite. Brick-red granitic dykes of presumed Topsails affiliation cut the Feeder Granodiorite. Both intrusive bodies are cut by diabasic dykes.

References

Binney, W.P., Thurlow, J.G., and Swanson, E.A.
1983: The MacLean Extension orebody, Buchans, Newfoundland: in Current Research, Part A, Geological Survey of Canada, Paper 83-1A.

Kean, B.F., Dean, P.L., and Strong, D.F.
1981: Regional geology of the central volcanic belt of Newfoundland: in The Buchans Orebodies: Fifty Years of Geology and Mining, eds. E.A. Swanson, D.F. Strong, and J.G. Thurlow; Geological Association of Canada, Special Paper 22, p. 65-78.

Taylor, R.P., Strong, D.F., and Kean, B.F.
1980: The Topsails igneous complex: Silurian-Devonian peralkaline magmatism in western Newfoundland; Canadian Journal of Earth Sciences, v. 17, p. 425-439.

Thurlow, J.G.
1981a: Geology, ore deposits and applied rock geochemistry of the Buchans Group, Newfoundland; unpublished Ph.D. thesis, Memorial University of Newfoundland, 305 p.

1981b: The Buchans Group: its stratigraphic and structural setting; in The Buchans Orebodies: Fifty Years of Geology and Mining, eds. E.A. Swanson, D.F. Strong, and J.G. Thurlow; Geological Association of Canada, Special Paper 22, p. 79-90.

Thurlow, J.G. and Swanson, E.A.
1981: Geology and ore deposits of the Buchans area, central Newfoundland; in The Buchans Orebodies: Fifty Years of Geology and Mining, eds. E.A. Swanson, D.F. Strong, and J.G. Thurlow; Geological Association of Canada, Special Paper 22, p. 113-142.

Walker, P.N. and Barbour, D.M.
1981: Geology of the Buchans ore horizon breccias; in The Buchans Orebodies: Fifty Years of Geology and Mining, eds. E.A. Swanson, D.F. Strong, and J.G. Thurlow; Geological Association of Canada, Special Paper 22, p. 161-186.

82. GEOCHEMISTRY OF GRANITOID CLASTS FROM MacLEAN EXTENSION OREBODY, BUCHANS, NEWFOUNDLAND, AND IMPLICATIONS ON THEIR POSSIBLE SOURCE[1]

Contract 1583327

Peter W. Stewart[2]
Economic Geology Division

Stewart, P.W., Geochemistry of granitoid clasts from MacLean Extension orebody, Buchans, Newfoundland, and implications on their possible source: in Current Research, Part A, Geological Survey of Canada, Paper 84-1A, p. 467-472, 1984.

Also in Current Research, Newfoundland Department of Mines and Energy, Mineral Development Division, Report 84-1A, 1984.

Abstract

Lithogeochemical analyses have been obtained on samples from the alkali feldspar phase of the Topsails granite, the Feeder Granodiorite and granitoid clasts from ore-horizon breccia-conglomerate beds in MacLean Extension area. The peraluminous Topsails granite is from an A-type (anorogenic) magma which is chemically distinct from the clasts and cannot be their source. The peraluminous Feeder Granodiorite and granitoid clasts are both from I-type (orogenic) magmas and have many geochemical similarities and some differences. The Feeder Granodiorite may be a late-stage differentiate of the source of the clasts. Variable alteration of the clasts complicates lithogeochemical interpretations. A revised petrographic classification of clasts is presented.

Résumé

Des analyses lithogéochimiques ont été effectuées sur la phase de feldspath alcalin du granite de Topsails, de la granodiorite Feeder et des fragments granitoïdes provenant d'un niveau minéralisé dans les couches de brèches et de conglomérats dans la région de la prolongation de MacLean. Le granite hyperalumineux de Topsails provient d'un magma de type A (anorogénique) qui diffère chimiquement des fragments et qui ne peut donc pas être leur source. La granodiorite Feeder et les fragments granitoïdes sont hyperalumineux et proviennent de magmas de type I (orogénique): ils pourraient avoir de nombreuses similarités et quelques différences géochimiques. La granodiorite Feeder pourrait être le produit de la différentiation tardive de la source des fragments. L'altération variée des fragments complique l'interprétation lithogéochimique. Une classification pétrographique révisée des fragments est présentée.

INTRODUCTION

The volcanogenic sulphide ore deposits at Buchans, occur as three types: stockwork ore, in situ ore and transported ore (Thurlow, 1981a; Thurlow and Swanson, 1981). These deposits are hosted by the Buchans Group of the Newfoundland Central Volcanic Belt (Kean et al., 1981), an Ordovician-Silurian sequence of subaqueous volcanic, volcaniclastic and sedimentary rocks.

The transported ore forms a series of sulphide-bearing breccia-conglomerate beds with diverse lithic clasts, including granitoids. These beds have been interpreted as deposited by debris flows (Walker and Barbour, 1981; Binney et al., 1983).

The source of the granitoid clasts has been enigmatic. Two small intrusive bodies (Wiley's River and Little Sandy intrusions) have been interpreted to be comagmatic with the Buchans Group volcanic rocks and possible sources of the granitoid clasts. They have been collectively named the Feeder Granodiorite (Thurlow, 1981a, b).

Major and trace element analyses have been carried out for twenty-one clasts collected from 20 Level of the MacLean Extension workings. Eight samples of the Wiley's River intrusion and one sample of the Little Sandy intrusion were analyzed for the same elements. Also, seven samples of the alkali feldspar phase of the Topsails granitic complex (Taylor et al., 1980; Thurlow, 1981b) from adjacent to the Buchans Group and the Wiley's Brook intrusion were analyzed for comparison.

PETROGRAPHY

Thin sections of over 150 granitoid clasts from ore horizon boulder breccia-beds have been examined. Over 90 per cent of these were from MacLean Extension orebody, with the remainder from the Oriental orebody. A revised petrographic classification of granitoid types (Table 82.1) is considered more useful than the previous field classification (Stewart, 1983). The field clast groupings of Stewart (1983) showed no geochemical coherence or petrographic distinctiveness.

Primary mineralogy of the clasts is simple and relatively consistent, i.e. quartz, plagioclase, biotite (rarely preserved, now chlorite), opaque minerals (hematite, magnetite?), apatite, zircon and sphene (rare).

Detailed petrographic examination of clasts has demonstrated that colour and mineralogical differences used in the earlier classification are primarily due to alteration. Textural differences are gradational and probably represent differences in the mode and timing of crystallization of a single magma. The clast types have been arranged to reflect these gradations, from those with the best developed crystallinity (Type 1) to the least developed (Type 5).

Type 6 clasts are texturally and mineralogically distinct. They show a weakly developed felty texture with euhedral to subhedral plagioclase laths in a groundmass of annedral plagioclase, quartz and opaque minerals. These clasts show a higher plagioclase/quartz ratio and a higher per cent of mafic and opaque minerals than the other

[1] Contribution to Canada-Newfoundland co-operative mineral program 1982-1984. Project carried by Geological Survey of Canada.

[2] Department of Earth Sciences, Memorial University of Newfoundland, St. John's Newfoundland A1B 3X5

Table 62.1. Petrographic classification of granitoid clasts

Clast type	Grain size (average/range)	Texture	Phenocrysts	Mafic mineral content	Distinguishing features
1.	medium (1 mm/0.2-3.0 mm)	seriate porphyritic	abundant qtz + feldspar; qtz typically larger (to 5 mm)	rare biotite mostly chlorite + opaques after biotite ± epidote (<5%)	relatively coarse grained, seriate texture, i.e. gradation in grain size of groundmass to phenocrysts
2.	fine (0.5 mm/0.1-2 mm)	relatively equigranular	qtz + feldspar (to 2 mm)	rare biotite; mostly chlorite + opaques after biotite + epidote (0-5 vol. %)	relatively intermediate grain size and equigranular
3.	fine to very fine (0.3 mm/0.1-0.5 mm)	hiatal porphyritic - rare micro-granophyric areas	qtz + feldspar (1-8 mm; typically in clusters (especially feldspars)	chlorite + opaques ± epidote (<5%)	hiatal porphyritic - large difference in size between phenocrysts and groundmass; abundant phenocrysts
4.	very fine (0.2 mm/0.1-0.4 mm)	equigranular	rare qtz + feldspar (to 2 mm)	chlorite + opaques ± epidote, zoisite (<5%)	equigranular, fine grain size; lack of phenocrysts; relatively minor micro-granophyric areas
5.	very fine to fine (<0.5 mm/0.1-2 mm)	variable % of well-developed micrographophyric patches	rare, mostly qtz (to 2 mm)	chlorite + opaques ± epidote (0-5%)	abundant micrographophyre; equigranular
6.	very fine (0.2 mm/0.1-0.4 mm)	equigranular euhedral to subhedral feldspars	none	very abundant, especially opaques; biotite and chlorite (to 10%)	"lath-like" texture of feldspars; abundant mafic minerals - almost exclusively restricted to siltstone breccia, under ore horizon

clast types. This type is also chemically distinct (lower SiO_2, higher TiO_2 and CaO) and primarily restricted to the siltstone breccia unit which occurs several metres stratigraphically beneath the lower ore unit in MacLean Extension area. However rare clasts of this type have been found within the lower ore unit.

Staining with sodium cobaltinitrite for potassium feldspars suggests that all feldspars are plagioclase. The alteration and lack of twinning of feldspars has precluded petrographic determination of An content, but the geochemistry suggests that they are predominantly of albitic composition.

The dusty and pitted appearance of the feldspars and the presence of secondary minerals (sericite, calcite, epidote) in the feldspar crystals suggest that they have been saussuritized. Whether this is due to hydrothermal alteration or is a product of regional metamorphism is not known. The regional metamorphism of the Buchans Group is of the prehnite-pumpellyite facies (Henley and Thornley, 1981), and the alteration may have been a product of this metamorphism.

GEOCHEMISTRY

The study was designed to assess the relationship among three sample populations: the granitoid clasts, Feeder Granodiorite (predominantly the Wiley's River intrusion) and Topsails granite. The present geochemical results are preliminary, but do suggest several points: 1) all rock types are silica-oversaturated and peraluminous; 2) the Feeder Granodiorite and the clasts are from I-type (orogenic) magmas, whereas the Topsails granite is from an A-type (anorogenic) granite; 3) trace element abundances show significant differences between the Topsails granite and the other two populations; 4) the magmatic relationship of the Feeder Granodiorite and the granitoid clasts cannot be conclusively established, or refuted with the present evidence, and 5) the clasts have undergone varying degrees of alteration, whereas the Feeder Granodiorite and the Topsails granite are comparatively unaltered. These points are examined in more detail below.

All clast samples were found to contain greater than 70% (wt.) SiO_2 (anhydrous) with some clasts exceeding 80% SiO_2. Both the Feeder Granodiorite and the Topsails granite have a more restricted silica range of about 5% SiO_2, all above 70% SiO_2.

Because of the mobility of the alkali elements during alteration, their usefulness for classification of altered rocks is suspect. As will be discussed below, the alkali distributions in the clasts were affected by alteration. For this reason, plots of Irvine and Baragar (1971) and AFM plots are not presented, but are suggestive of a calc-alkaline affinity for all populations and Strong (1977) and Thurlow (1981a) have demonstrated that the Buchans Group is calc-alkaline.

Using the granitoid classification scheme of White and Chappell (1983), the granitoid clasts and the Feeder Granodiorite crystallized from I-type magmas and the

Topsails granite from an A-type magma (Fig. 62.1). Figure 62.1b is probably a more reliable plot than Figure 62.1a which uses alkali elements. The elements Ca and especially Al are considered to be relatively immobile during alteration. High contents of highly charged cations such as Ca, Zr and Y (see Fig. 62.1b, 62.2) are considered diagnostic of A-type magmas (White and Chappell, 1983). A-type granitoid bodies in eastern Australia are associated in space and time with volcanics rocks, as is the Topsails granite (Whalen and Currie, 1983). The presence of miarolitic and granophyric textures further substantiates the designation of the Topsails granite as an A-type intrusion (White and Chappell, 1983, p. 30).

Although I-type magmas are usually subaluminous, the Feeder Granodiorite and granitoid clasts are peraluminous. This has been considered to be indicative of a minimum-temperature melt or a highly fractionated I-type melt (White and Chappell, p. 28). This allows the possibility that the Feeder Granodiorite is the more fractionated parent of the granitoid clasts, but this has not yet been demonstrated.

Plots of paired immobile elements (Fig. 62.2) have been shown to be effective in distinguishing different magma series and their tectonic settings (Pearce and Cann, 1973; Wood et al., 1979; Palacios et al., 1981). The distinction of the Topsails granite is obvious and the correlation between the clasts and the Feeder Granodiorite is suggested. Bailey (1981) proposed that Zr and Y enrichment distinguishes anorogenic andesites from orogenic andesites, which supports the anorogenic setting of the Topsails granite. The slight enrichment of the Feeder Granodiorite in Zr and Y relative to the clasts is suggestive of a late stage differentiate (Taylor, 1965).

ALTERATION

The most common expression of hydrothermal alteration is the production of hydrous minerals from the primary anhydrous minerals. Therefore, the loss on ignition (LOI) provides a qualitative means to judge the degree of alteration. Although the LOI may be a mixture of H_2O, CO_2 and possibly sulphur-bearing gases, for evaluation of the degree of alteration, LOI is considered to be mainly H_2O and CO_2.

The variable degree of alteration of the clasts is apparent from Figure 62.1. A positive correlation between both CaO and K_2O with loss on ignition is shown in Figures 62.3b, c. The feldspars are partly altered to sericite (or muscovite) and calcite, indicating that these chemical variations are probably reflecting alteration. The very high barium content of the clasts in general, and the presence of barite as secondary veins and disseminations in the clasts is also in accord with the weakly defined positive correlation between Ba and LOI in Figure 62.3d. Magnesium shows appreciable scatter around a weak positive correlation (Fig. 62.3a). Variable amounts of chlorite and magnesium in the clasts could indicate an alteration, rather than a metamorphic origin for the chlorite. Alteration is indicated mineralogically by the saussuritization of feldspars, chloritization of biotite (no other primary mafic mineral or relicts of other mafic minerals have been recognized) and introduction of barium and calcium as barite and calcite. The elevated Ba values in the clasts probably indicates that their alteration is related to the mineralizing event at Buchans (Thurlow, 1981a) or to migration of Ba from barite in the breccia-conglomerate beds during or after consolidation (op cit, p. 285). The presence of calcite ± barite veins in some samples analyzed could add to LOI scatter and mask chemical effects of rock alteration.

Ca and Sr are considered to behave similarly under many conditions (Taylor, 1963; Mason, 1966). This behavior and the contrasting dissimilar behavior of Rb and Sr are demonstrated in Figure 62.4. Sr content shows a corresponding increase with Ca content (Fig. 62.4b), whereas Rb (Fig. 62.4a) has a negative correlation (Fig. 62.4a). The increase of Ca and Sr contents in the clasts is believed due to the introduction of calcite and barite during alteration. Rubidium contents remain relatively constant in the clasts though Sr values increase. Unless Rb was uniformly depleted, which conflicts with the generally variable nature of the alteration, it was apparently unaffected by the alteration.

Figure 62.5 presents evidence which possible conflicts with Feeder Granodiorite being the parent of the clasts. If it were the parent, then it should have had a similar K_2O content, prior to the alteration of the clasts. If, as indicated in Figure 62.3c, K_2O has increased with degree of alteration (along with increasing Sr (Fig. 62.4)) then the clasts in

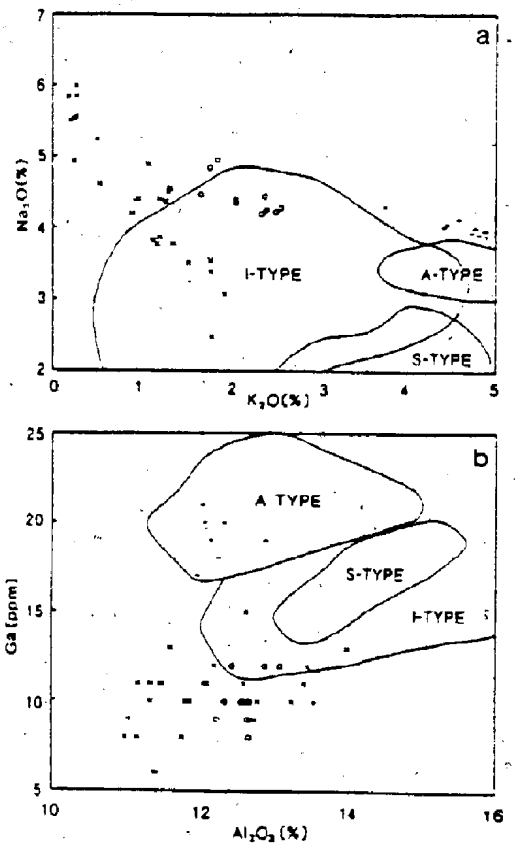

Figure 62.1. Discriminant diagram for granitoid magma series from White and Chappell (1983): a) K_2O vs Na_2O; b) Al_2O_3 vs Ga. The (x) represents a granitoid clast sample from MacLean Extension orebody, (o) represents a Feeder Granodiorite sample, the (+) represents the Topsail (alkali feldspar) granite sample, and the (*) represents the sample from the Little Sandy intrusion.

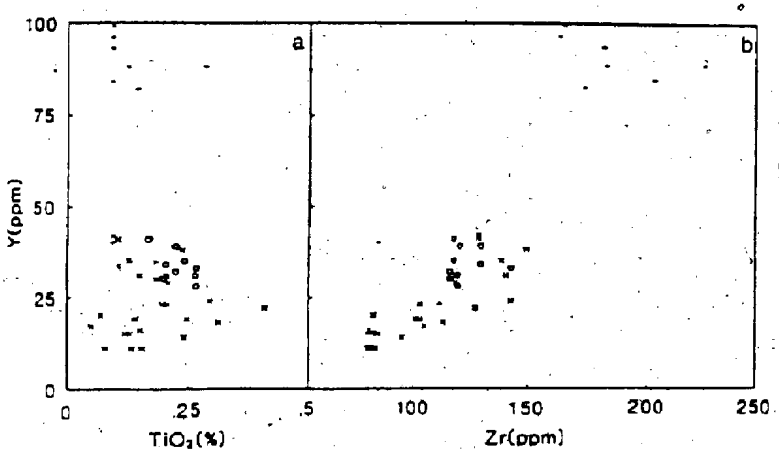

Figure 62.2

Plots of relatively immobile elements: a) TiO_2 vs Y; b) Zr vs Y, after Palacios et al., 1983. For symbols see Figure 62.1.

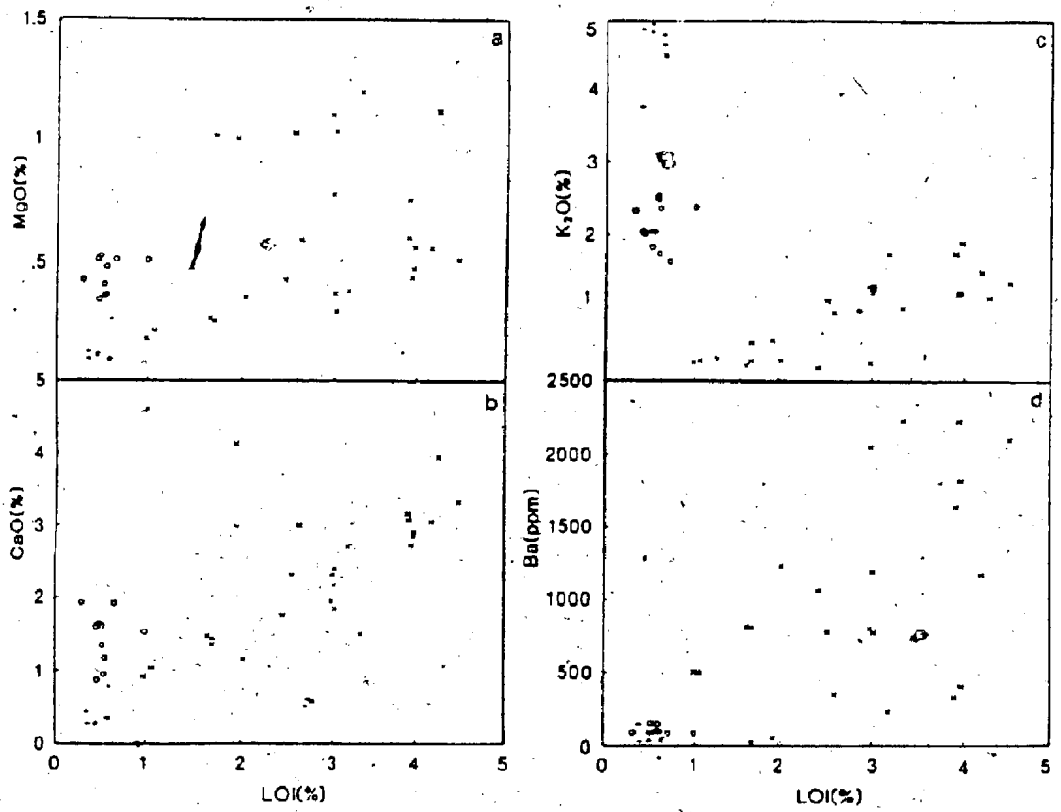

Figure 62.3. Diagrams illustrating the effects of alteration on particular elements: a) loss on ignition (LOI) vs MgO; b) LOI vs CaO; c) LOI vs K_2O; d) LOI vs Ba. For symbols see Figure 62.1.

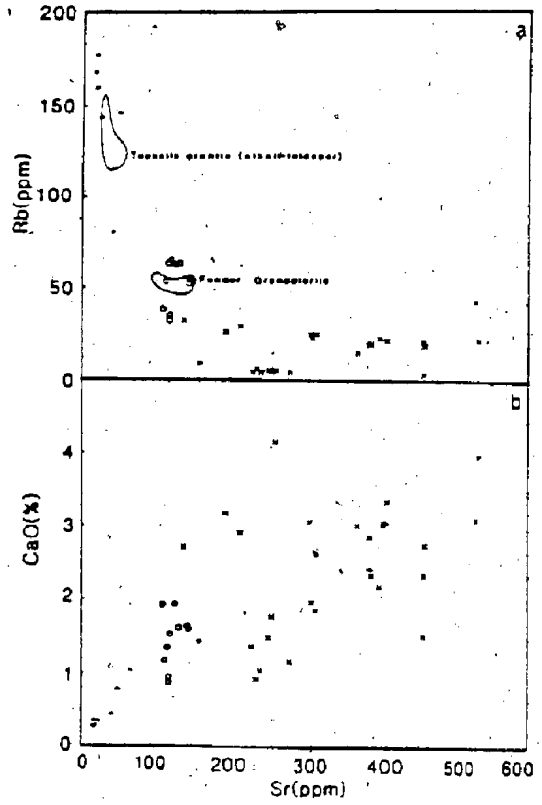

Figure 62.4. Correlation diagrams: a) Sr vs Rb. Fields after Bell and Blenkinsop, 1981; (b) Sr vs CaO. For symbols see Figure 62.1.

Figure 62.5, should plot toward the upper left part of the diagram and not the lower left part as indicated. Even if the Feeder Granodiorite is a later differentiate of the same magma and has a higher intial K_2O content, the observed trend still cannot be resolved. This underlies the difficulties in determining the changes in element contents during alteration. Work is in progress to try to resolve this problem.

The lack of apparent alteration of the Feeder Granodiorite and the Topsails granite is obvious from Figures 62.3, 62.4. The fields for the Topsails alkali feldspar phase and the Feeder Granodiorite of Bell and Blenkinsop (1981) are shown in Figure 62.4a for comparison.

One of the samples designated as a Topsails granite plots consistently outside the cluster of other Topsail samples. This is a sample of a dyke which cuts the Feeder Granodiorite and was presumed to be related to the Topsails granite, which it closely resembles megascopically. The trace element chemistry suggests that it has possibly been modified by contamination from the Feeder Granodiorite during emplacement (see Fig. 62.2a, b, especially).

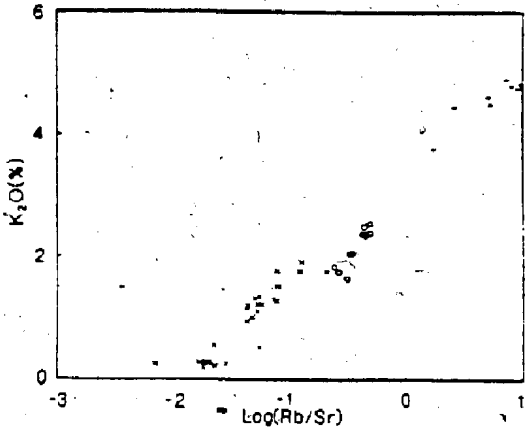

Figure 62.5. Rb/Sr expressed logarithmically vs K_2O. For symbols see Figure 62.1.

The single data point for the Little Sandy intrusion is insufficient to permit any rigorous conclusions. The data do suggest however, a closer affinity to the clasts than to the Feeder Granodiorite itself. Further analyses of samples from this body are currently in progress.

CONCLUSIONS

A few preliminary conclusions can be drawn. The Topsails granite can be clearly separated petrographically and lithochemically from the Feeder Granodiorite and granitoid clasts. This is consistent with the established geological and age relationships for the Topsails granite (Thurlow, 1981b; Whalen and Currie, 1982, 1983). As first demonstrated by Thurlow (1981a), the Feeder Granodiorite has many geochemical similarities to the clasts and may have crystallized from the magma reservoir which produced the clasts. Other element combinations suggest that the Feeder Granodiorite and clasts may be separated geochemically and may not be genetically related. Further work remains to be done before this problem can be resolved.

The Feeder Granodiorite and Topsails granite are both unaltered to weakly altered, whereas the clasts are variably altered. K_2O, CaO, MgO, Ba and Sr contents of the clasts increase erratically with increasing alteration.

ACKNOWLEDGMENTS

The author wishes to thank G. Andrew, Memorial University of Newfoundland, for the major element analyses and D. Press for assistance in the graphical presentations. The advice of J.G. Thurlow, E.A. Swanson and D.M. Barbour while in Buchans is gratefully acknowledged, and the assistance of other ASARCO and Abitibi-Price Inc. personnel in Buchans appreciated.

This study comprises a portion of the work towards a Master of Science degree at Memorial University.

Critical review of this report by R.V. Kirkham, W.H. Poole, D.F. Strong and J.G. Thurlow resulted in numerous improvements.

REFERENCES

Bailey, J.C.
1981: Geochemical criteria for a refined tectonic discrimination of orogenic andesites: Chemical Geology, v. 32, p. 139-154.

Bell, K. and Blenkinsop, J.
1981: A geochronological study of the Buchans area, Newfoundland: in The Buchans Orebodies: Fifty Years of Geology and Mining, ed. E.A. Swanson, D.F. Strong, and J.G. Thurlow: Geological Association of Canada, Special Paper 22, p. 91-111.

Binney, W.P., Thurlow, J.G., and Swanson, E.A.
1983: The MacLean Extension orebody, Buchans, Newfoundland: in Current Research, Part A, Geological Survey of Canada, Paper 83-1A, p. 313-319.

Henley, R.W. and Thornley, P.
1981: Low grade metamorphism and the geothermal environment of massive sulphide ore formation, Buchans, Newfoundland: in the Buchans Orebodies: Fifty Years of Geology and Mining, ed. E.A. Swanson, D.F. Strong and J.G. Thurlow; Geological Association of Canada, Special Paper 22, p. 205-228.

Irvine, T.N. and Baragar, W.R.A.
1971: A guide to the chemical classification of the common volcanic rocks: Canadian Journal of Earth Sciences, v. 8, p. 523-548.

Kean, B.F., Dean, P.L., and Strong, D.F.
1981: Regional geology of the central volcanic belt of Newfoundland: in The Buchans Orebodies: Fifty Years of Geology and Mining, ed. E.A. Swanson, D.F. Strong, and J.G. Thurlow: Geological Association of Canada, Special Paper 22, p. 65-78.

Mason, B.
1966: Principles of geochemistry: Wiley, New York, 3rd ed., 328 p.

Palacios, M.C., Guerra, S.N., and Campano, B.P.
1983: Difference in Ti, Zr, Y and P content in calc-alkaline andesites from island arcs and continental margin (central Andes): Geologische Rundschau, v. 72, v. 2, p. 733-738.

Pearce, J.A. and Cann, J.R.
1973: Tectonic setting of basic volcanic rocks determined using trace element analyses: Earth and Planetary Science Letters, v. 19, p. 290.

Stewart, P.W.
1983: Granitoid clasts in boulder breccias of MacLean Extension orebody, Buchans, Newfoundland: in Current Research, Part A, Geological Survey of Canada, Paper 83-1A, p. 321-324.

Strong, D.F.
1977: Volcanic regimes in the Newfoundland Appalachians: in Volcanic Regimes in Canada, ed. W.R.A. Baragar, L.C. Coleman, and J.M. Hall; Geological Association of Canada, Special Paper 18, p. 61-90.

Taylor, R.P., Strong, D.F., and Kean, B.F.
1980: The Topsails igneous complex: Silurian and Devonian peralkaline magmatism in western Newfoundland: Canadian Journal of Earth Sciences, v. 17, p. 425-439.

Taylor, S.R.
1965: The application of trace element data to problems in petrology: Physics and Chemistry of the Earth, v. 6, p. 133-213.

Thurlow, J.G.
1981a: Geology, ore deposits and applied rock geochemistry of the Buchans Group, Newfoundland: unpublished Ph.D. thesis, Memorial University of Newfoundland, 305 p.

1981b: The Buchans Group: its stratigraphic and structural setting: in The Buchans Orebodies: Fifty Years of Geology and Mining, ed. E.A. Swanson, D.F. Strong, and J.G. Thurlow; Geological Association of Canada, Special Paper 22, p. 79-90.

Thurlow, J.G. and Swanson, E.A.
1981: Geology and ore deposits of the Buchans area, central Newfoundland: in The Buchans Orebodies: Fifty Years of Geology and Mining, ed. E.A. Swanson, D.F. Strong, and J.G. Thurlow; Geological Association of Canada, Special Paper 22, p. 113-142.

Walker, P.N. and Barbour, D.M.
1981: Geology of the Buchans ore horizon breccias: in The Buchans Orebodies: Fifty Years of Geology and Mining, ed. E.A. Swanson, D.F. Strong, and J.G. Thurlow: Geological Association of Canada, Special Paper 22, p. 161-188.

Whalen, J.B. and Currie, K.L.
1982: Volcanic and plutonic rocks in the Rainy Lake area, Newfoundland: in Current Research, Part A, Geological Survey of Canada, Paper 82-1A, p. 17-22.

1983: The Topsails igneous terrane of western Newfoundland: in Current Research, Part A, Geological Survey of Canada, Paper 83-1A, p. 15-23.

White, A.J.R. and Chappell, B.W.
1983: Granitoid types and their distribution in the Lachlan Fold Belt, southeastern Australia: in Circum-Pacific Plutonic Terranes, ed. J.A. Roddick: Geological Society of America, Memoir 159, p. 21-34.

Wood, D.A., Joron, J-L., and Treuil, M.
1979: A re-appraisal of the use of trace elements to classify and discriminate between magma series erupted in different tectonic settings: Earth and Planetary Science Letters, v. 45, p. 326-336.

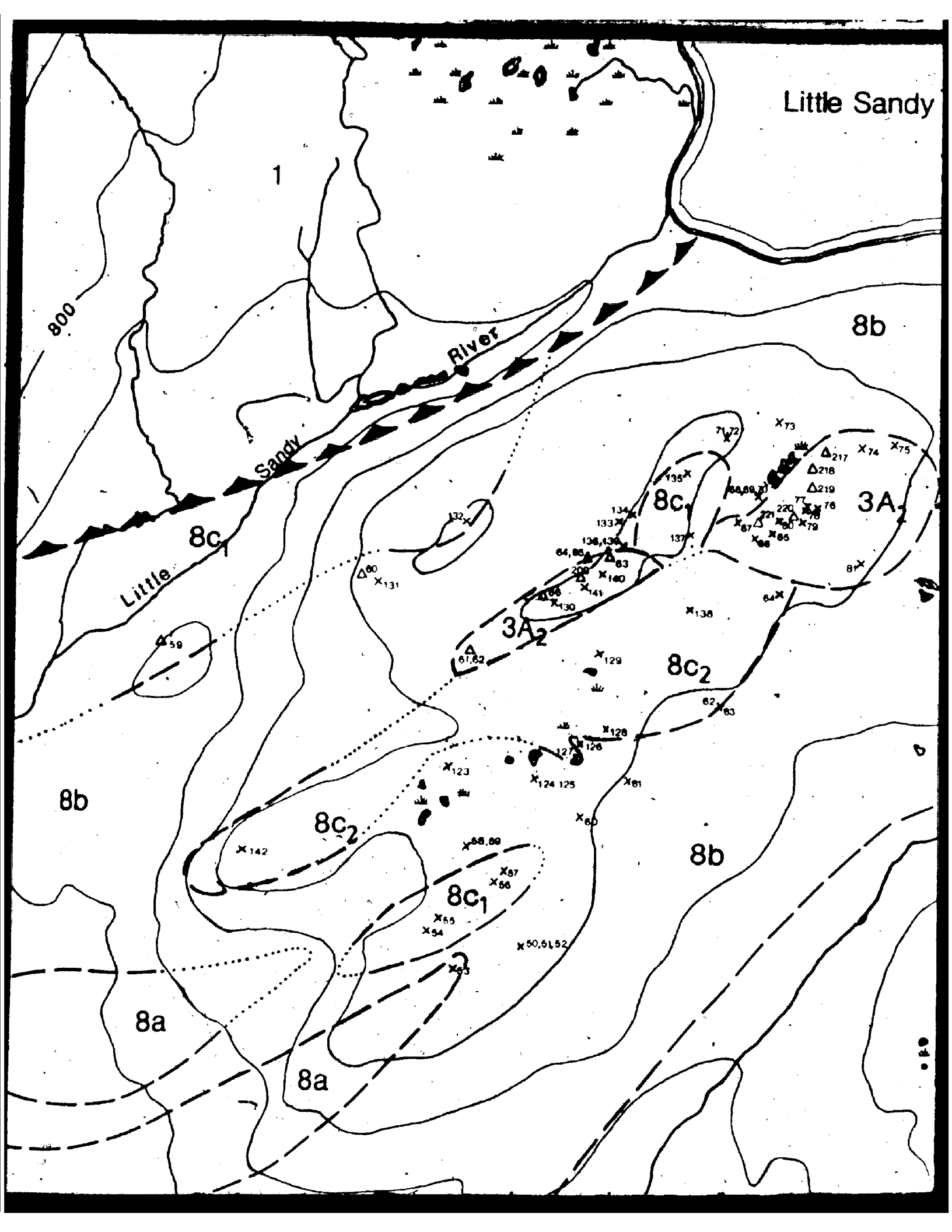
Little Sandy
1
800
8b
Sandy River
8c1
3A2
Little
8c1
3A2
8c2
8b
8c2
8b
8c1
8a
8a

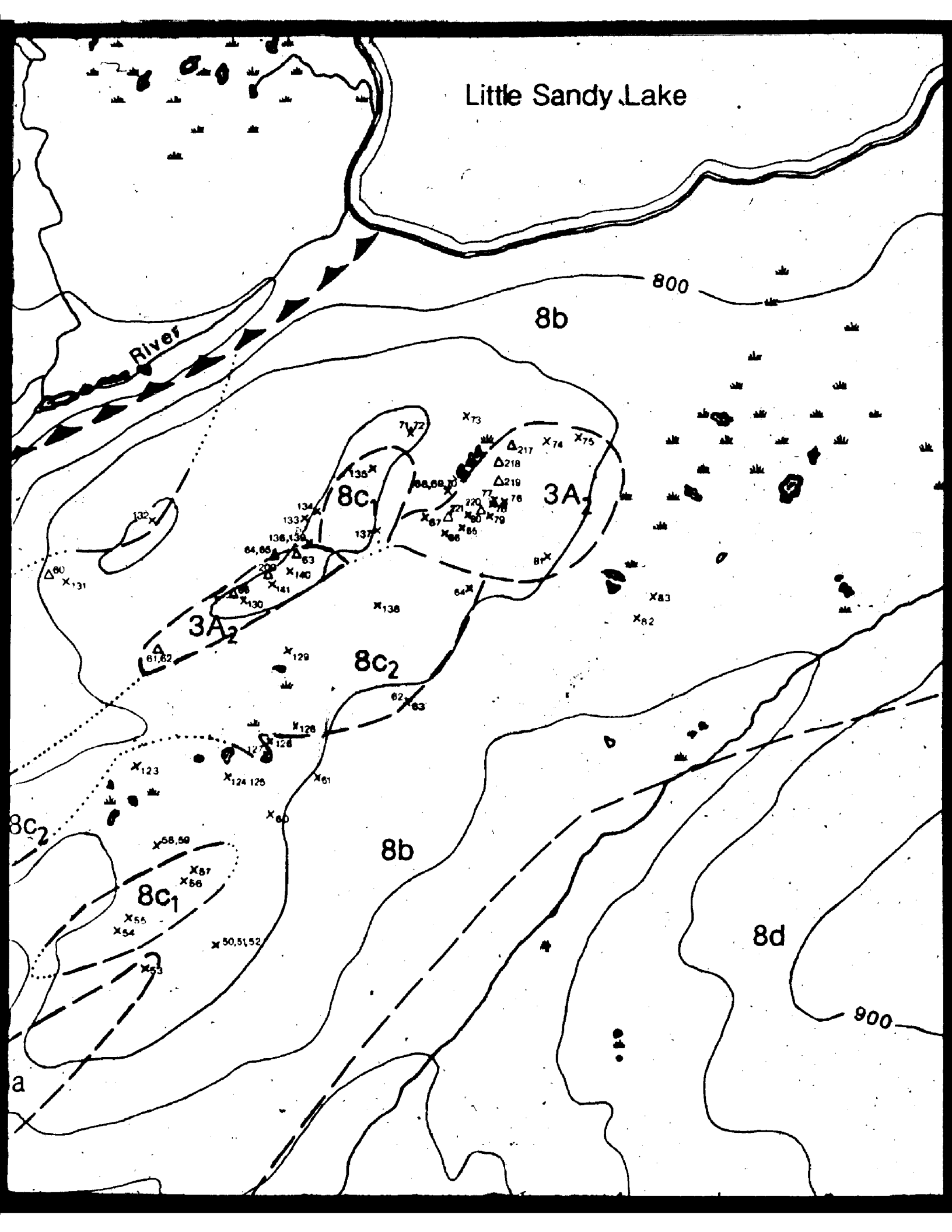
Little Sandy Lake
River
800
900
8b
8c1
8c2
3A2
8d
a

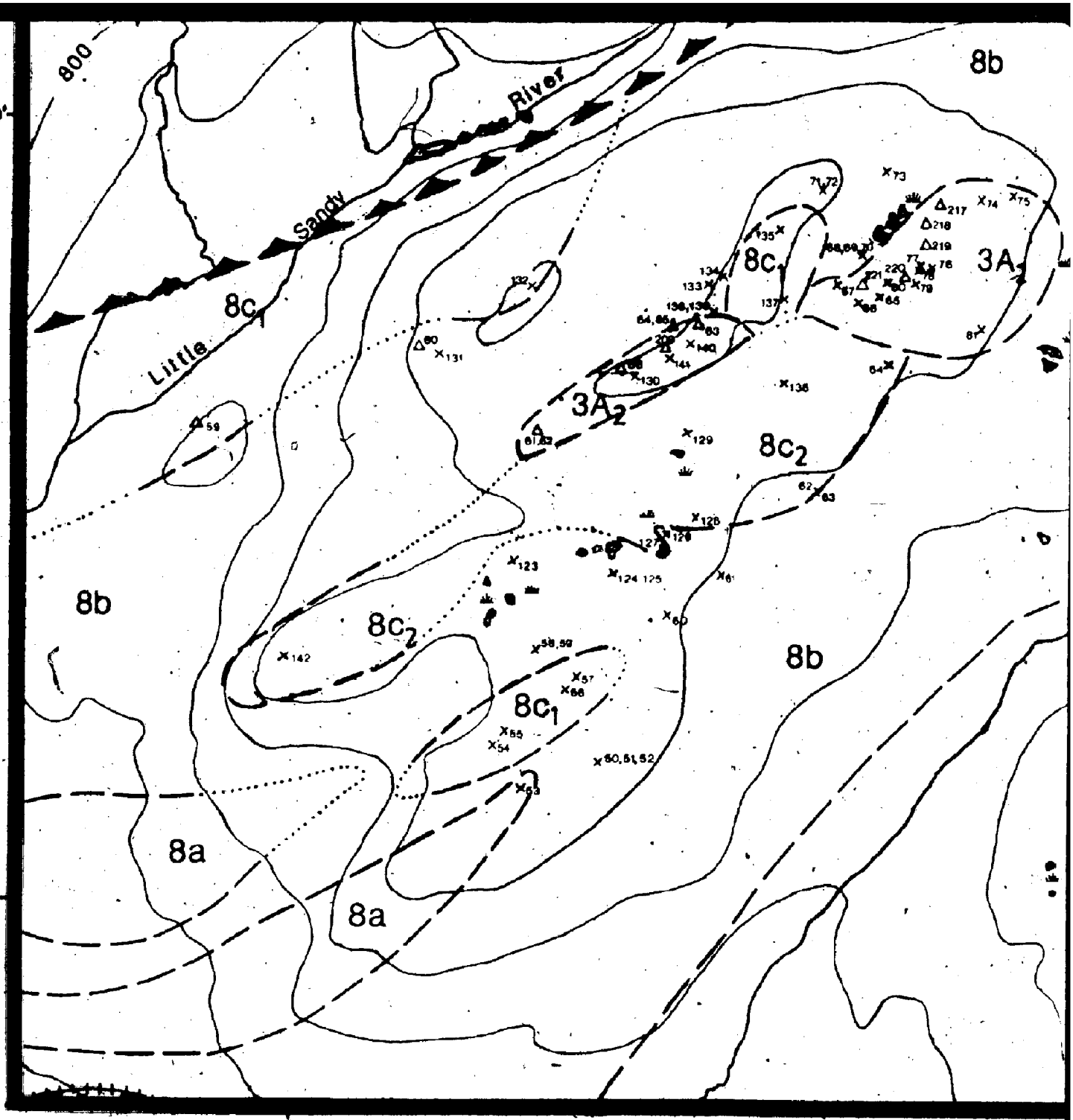

LEGEND

1000 ft

LITTLE SANDY SEQUENCE

8a	Mafic-intermediate volcanics	8b	Dacitic breccias and tuffs
8c1	Quartz-feldspar phyric rhyolite	8d	Intermediate breccias and tuffs
8c2	Aphyric rhyolite		

3 of

3A2	Feeder Granodiorite	Geological contact (a
1	Hungry Mountain Complex	

Formation numbers taken from "Geological Map of the Buchans Area" by Thurlow an

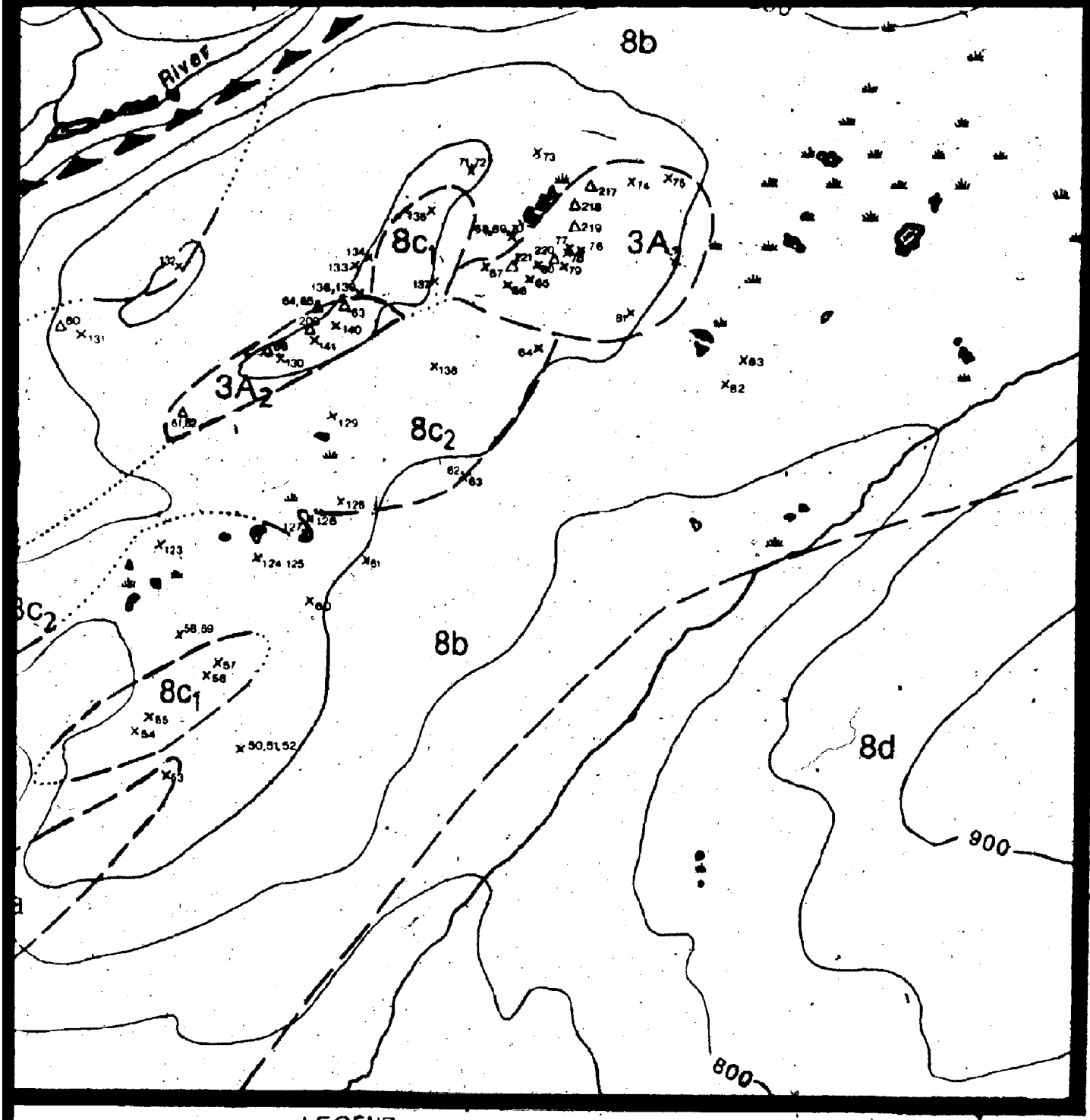

LEGEND

1000 ft 120m

E SANDY SEQUENCE

nics — 8b — Dacitic breccias and tuffs

olite — 8d — Intermediate breccias and tuffs

eeder Granodiorite

Hungry Mountain Complex

Contours are in feet above sea level

83 series samples ×

82 series samples △

Assumed thrust fault

Geological contact (approximate, assumed)

taken from "Geological Map of the Buchans Area" by Thurlow and Swanson (1981)

1 of 1

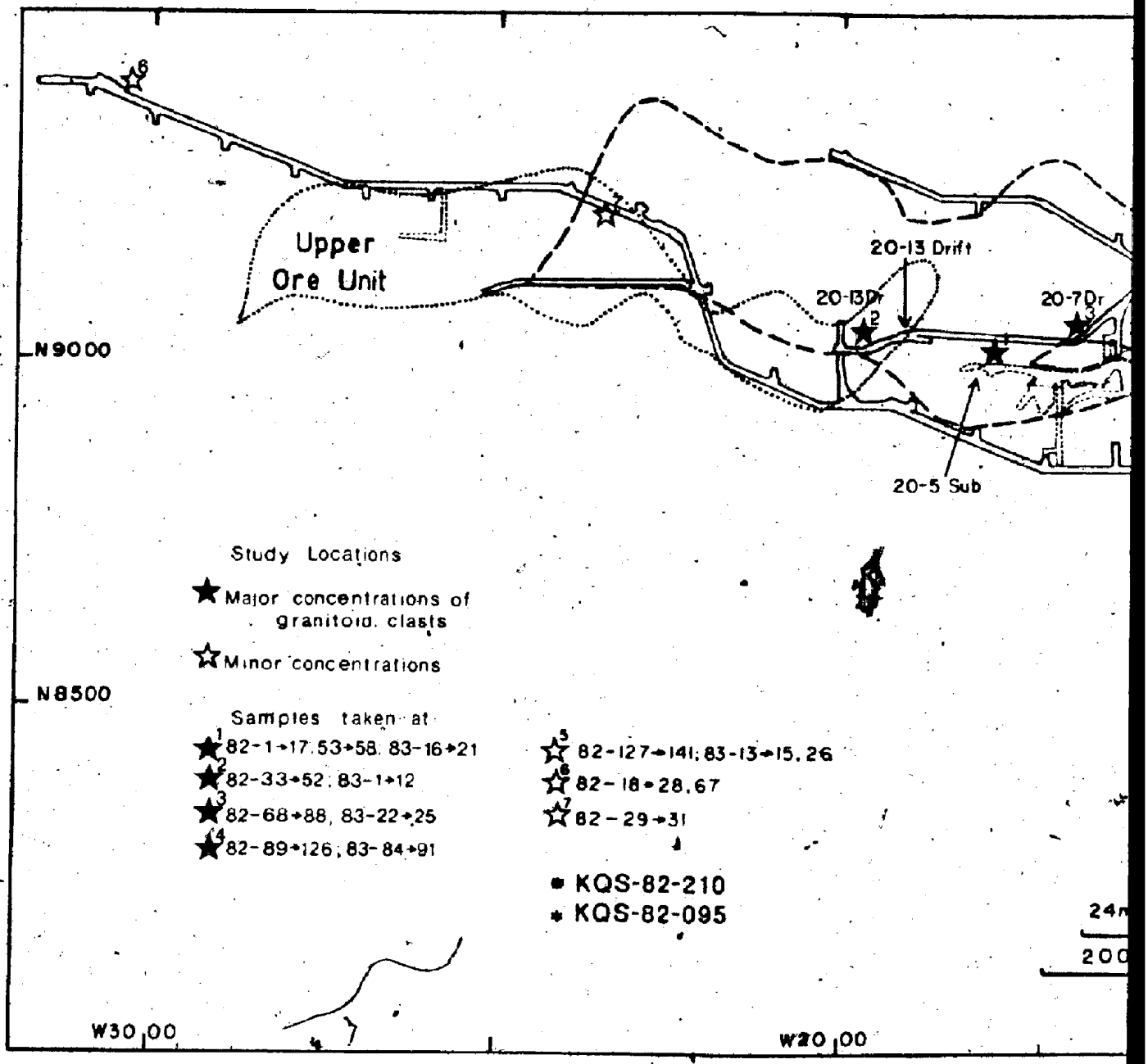
Upper
Ore Unit
20-13 Drift
20-13Dr
20-7Dr
20-5 Sub
N9000
N8500
W30 00
W20 00
Study Locations
Major concentrations of granitoid clasts
Minor concentrations
Samples taken at
1 82-1→17, 53→58, 83-16→21
2 82-33→52; 83-1→12
3 82-68→88, 83-22→25
4 82-89→126; 83-84→91
5 82-127→141; 83-13→15, 26
6 82-18→28, 67
7 82-29→31
KQS-82-210
KQS-82-095
24m
200

2 of 2

FIG. 4.2

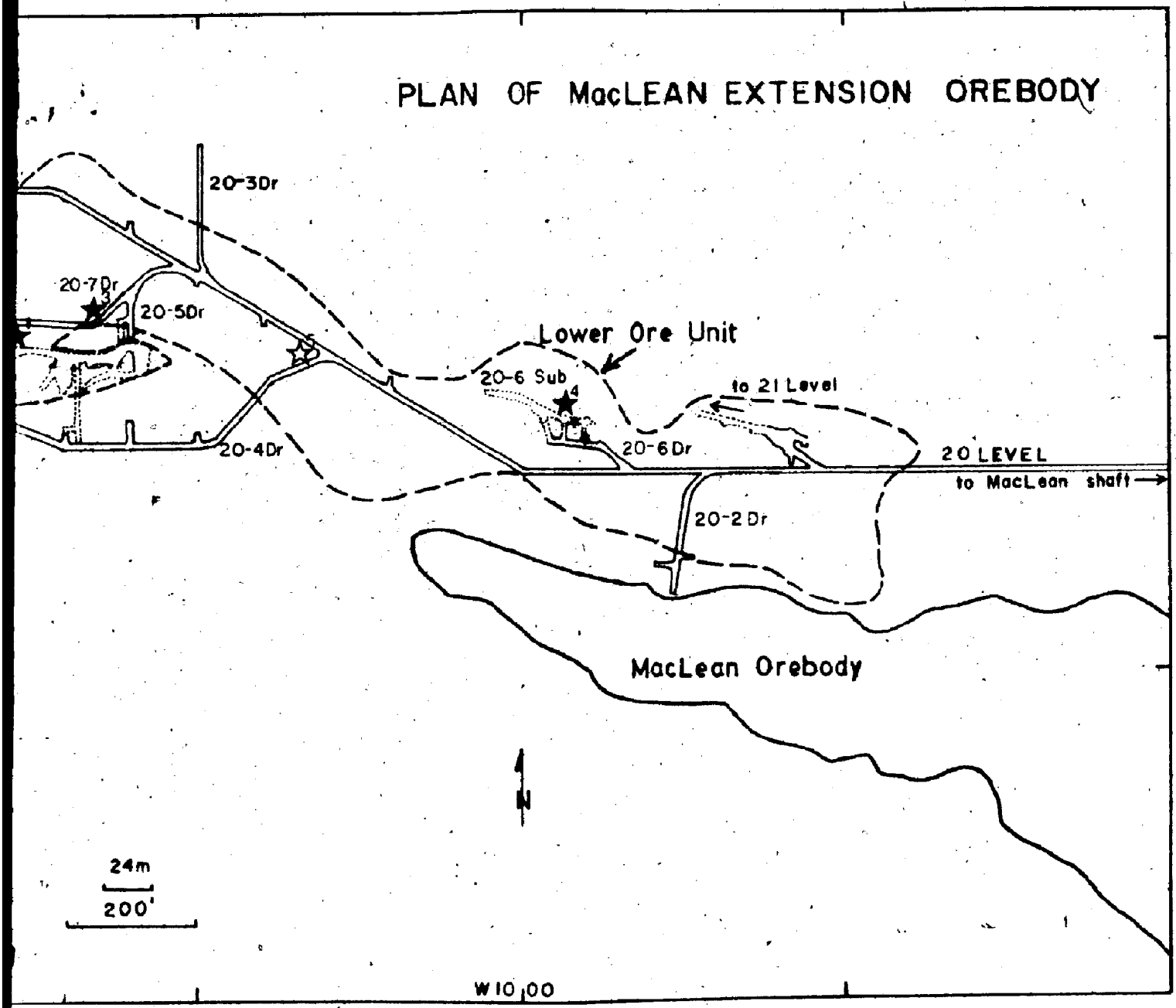
PLAN OF MacLEAN EXTENSION OREBODY
20-3Dr
20-7Dr
3
20-5Dr
Lower Ore Unit
20-6 Sub
4
to 21 Level
20-4Dr
20-6Dr
20 LEVEL
to MacLean shaft
20-2Dr
MacLean Orebody
N
24m
200'
W10,00

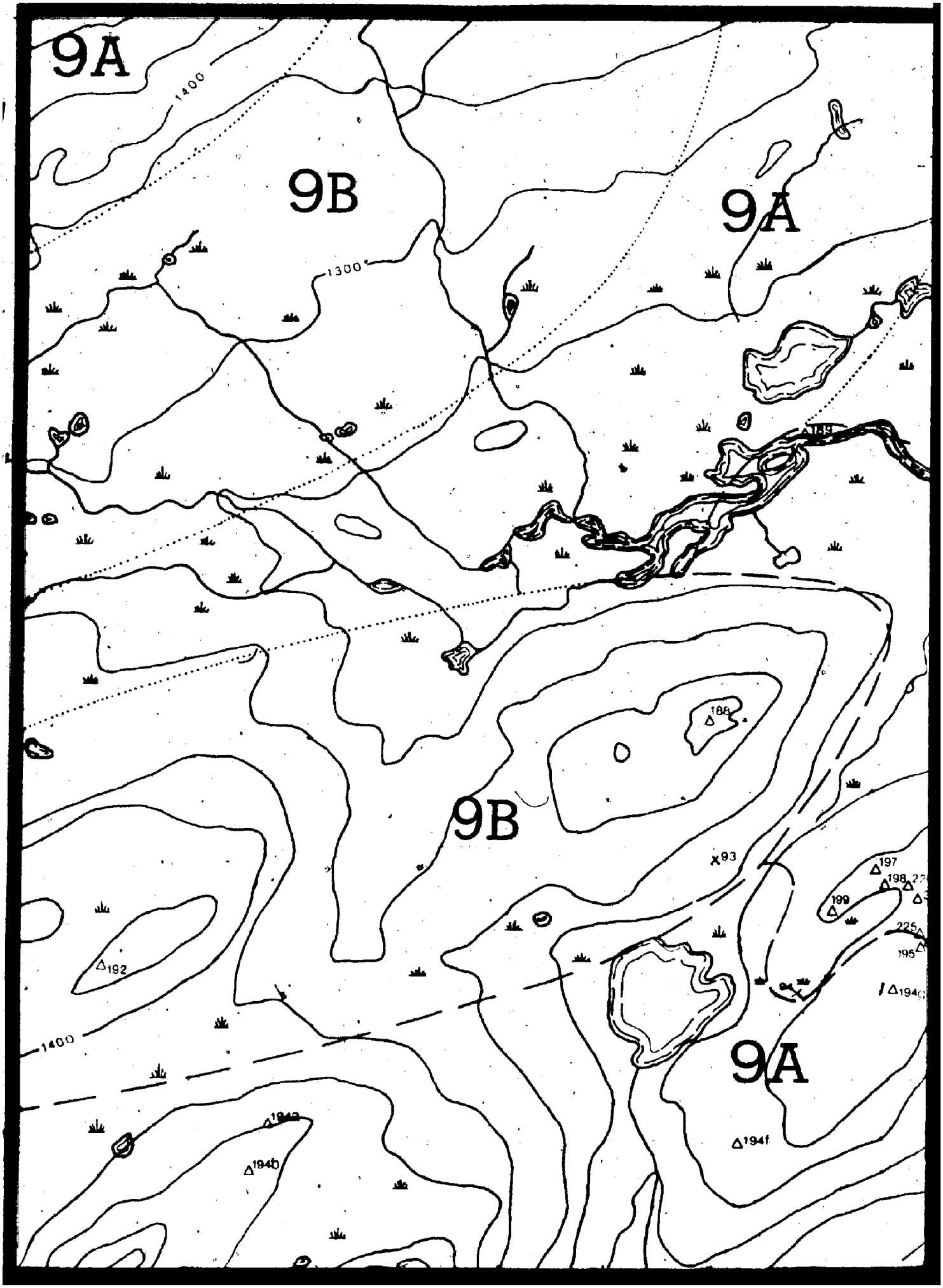
9A
1400
9B
1300
9A
189
188
9B
x93
197
198
199
225
195
192
1400
9A
194f
194b

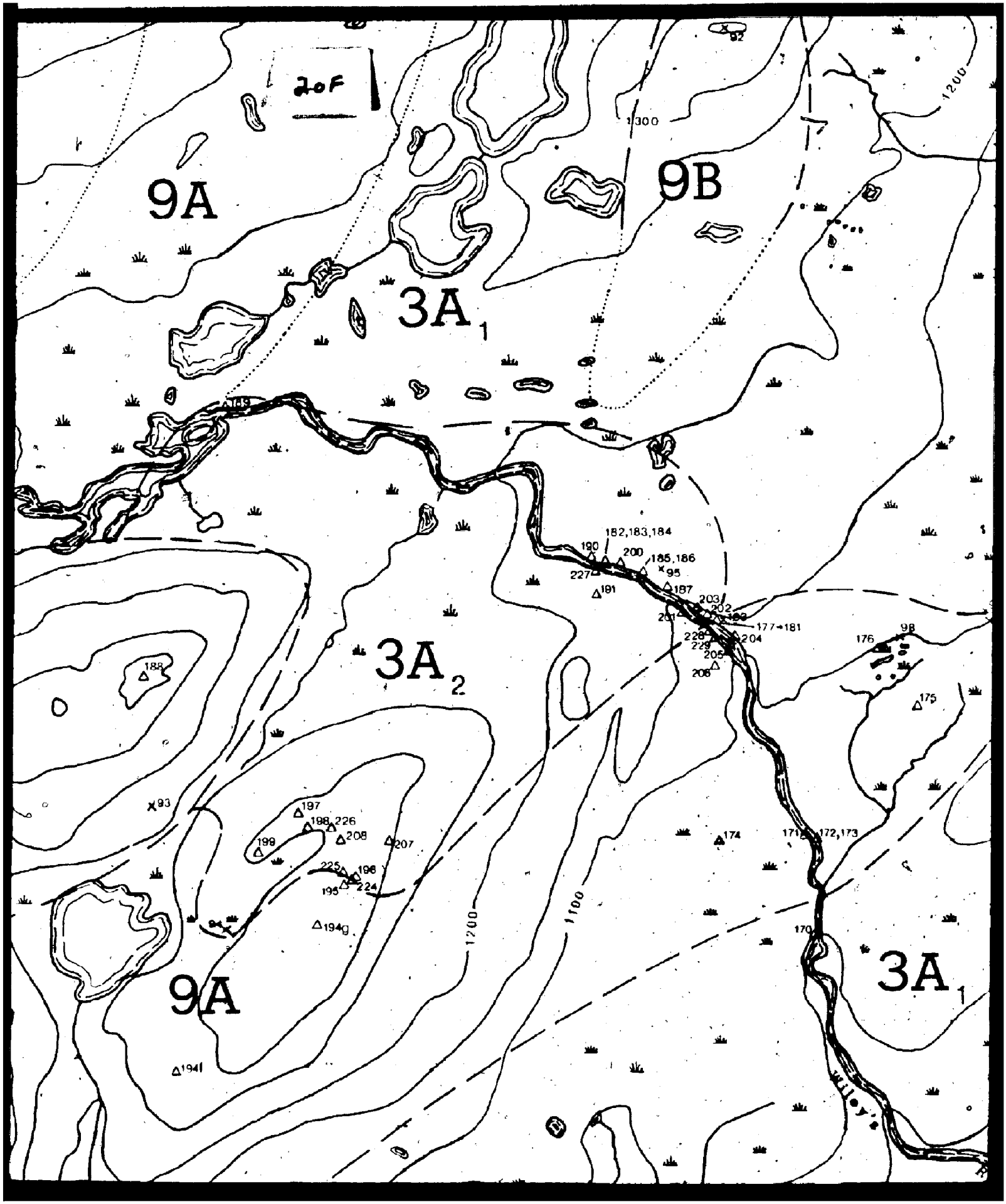
2 of
9A
9B
3A1
3A2
9A
3A1
1300
1200
1100
1200
182,183,184
190
200
185,186
95
227
191
187
203
202
177→181
204
205
206
228
229
176
98
175
188
193
197
198
226
208
207
198
225
196
195
224
194g
174
171
172,173
170
194

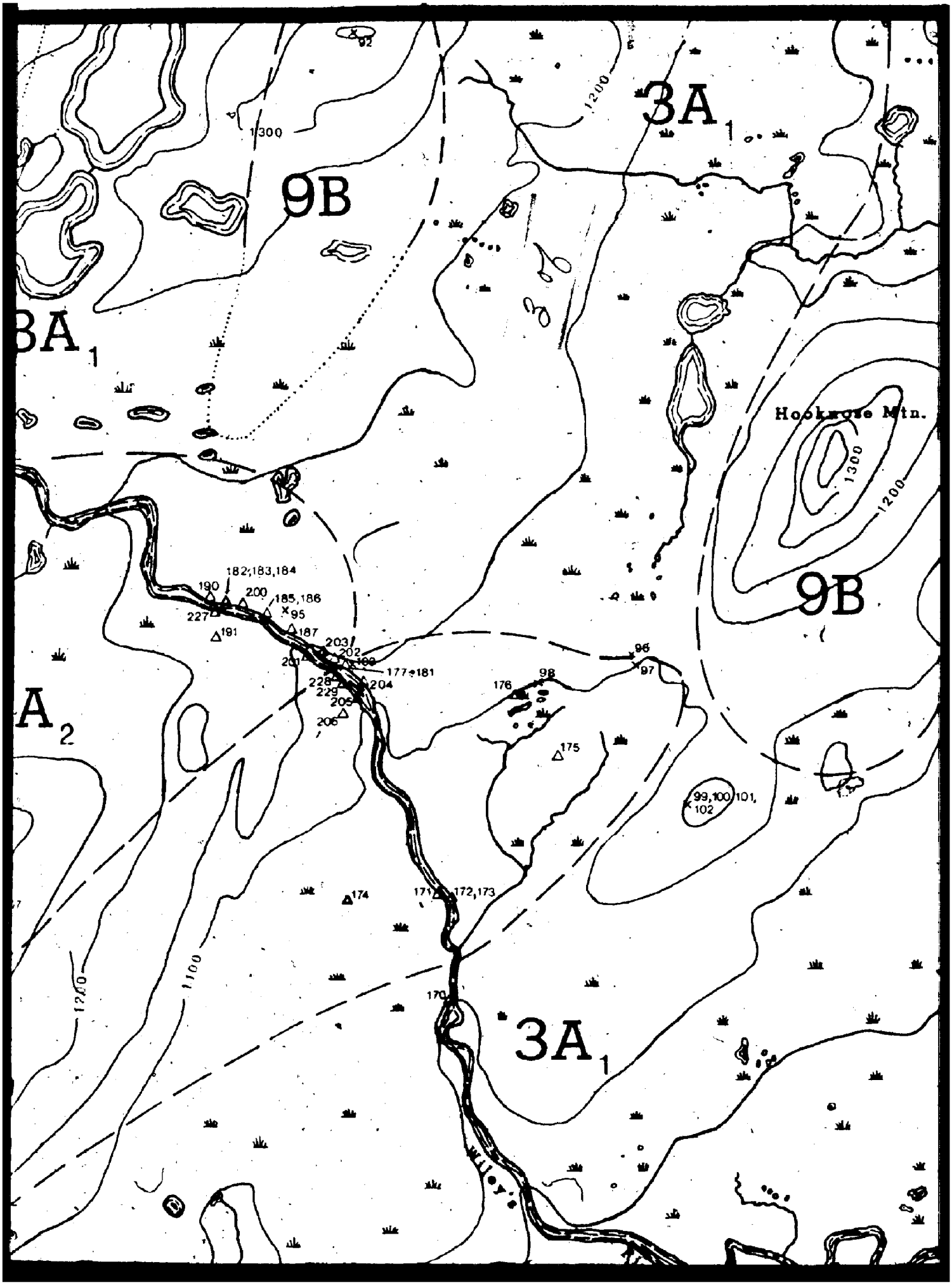
3A1
9B
3A1
1300
1200
Hookrose Mtn.
1300
1200
9B
182,183,184
190
200
185,186
227
95
191
187
203
202
201
177,181
204
228
229
205
206
96
97
98
176
175
99,100,101,
102
A2
174
171
172,173
1200
1100
170
3A1

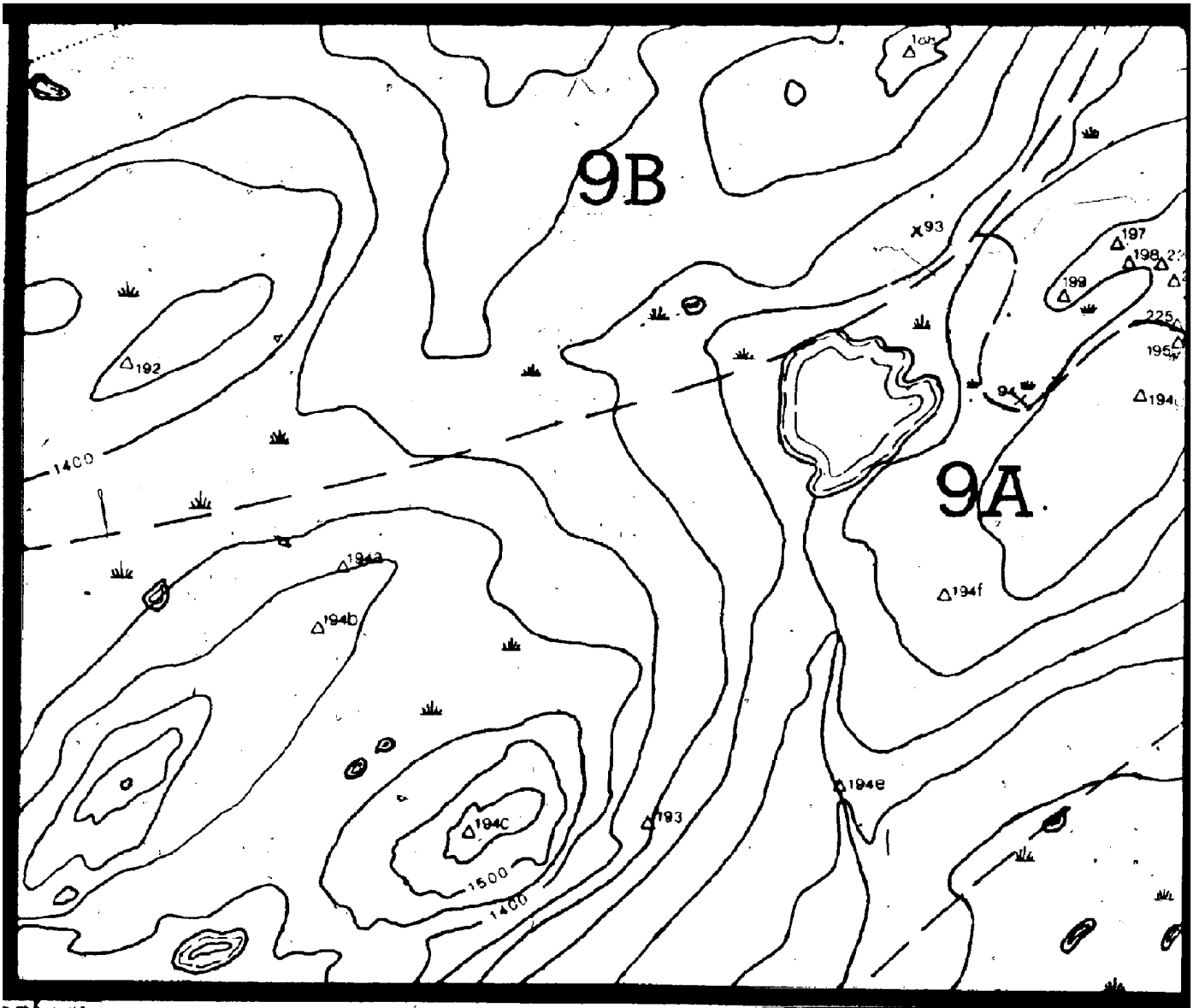

37°03'

WILEY'S RIVER

FIG

LEGEND

Topsails Granite

9A	ALKALI FELDSPAR GRANITE
9B	MAFIC INTRUSIVES

Wiley's Prominent Quartz Sequence

$3A_1$	FELSIC PYROCLASTICS WITH UNDIVIDED BASALTIC VOLCANICS
$3A_2$	Feeder Granodiorite

Formation

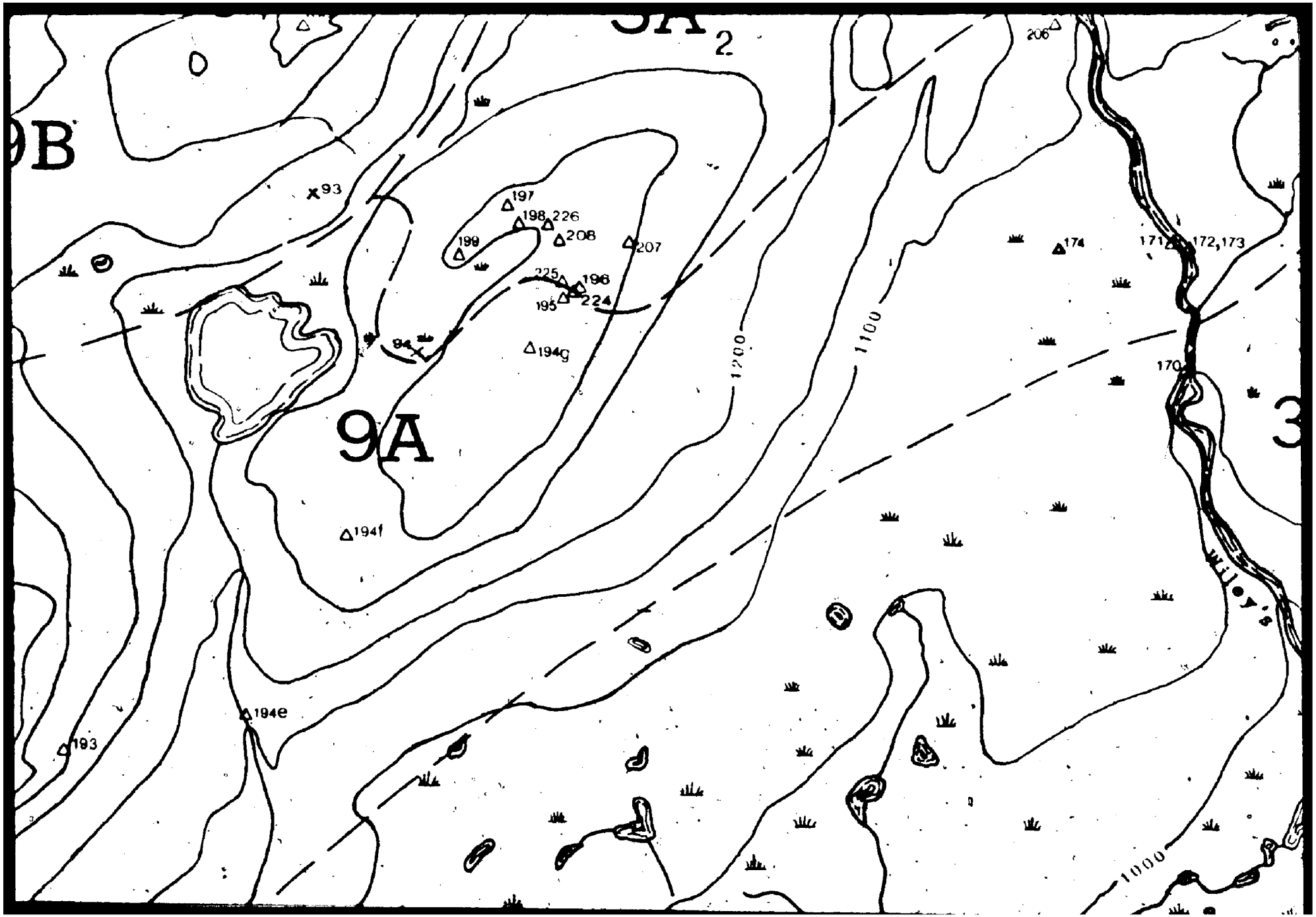
9A
9B
3A2
93
197
198
226
208
207
199
225
196
195
224
194g
1200
1100
206
174
171
172,173
170
194f
194e
193
1000

VILEY'S RIVER FIELD AREA

57°00'

FIG. 3.2

te

1000 ft

120 m

Co

ent Quartz Sequence

H. UNDIVIDED BASALTIC VOLCANICS

Geological contact (defined, ap

diorite

Formation numbers taken from "Geological Map of the Buchans Area

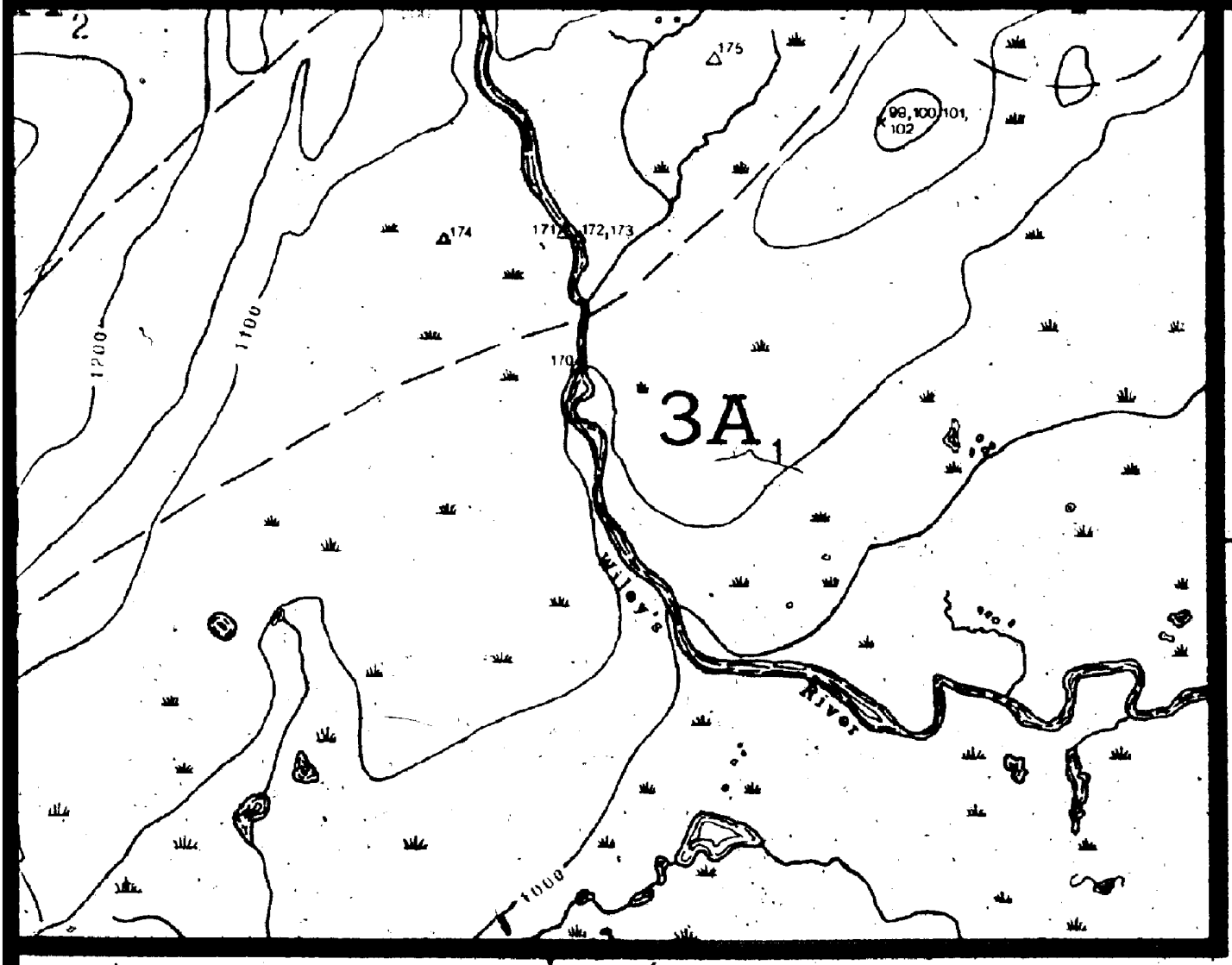

FIELD AREA

57°00'

SYMBOLS

Contours are in feet above sea level

676

83 series samples ×

82 series samples △

Geological contact (defined, approximate, assumed)

bers taken from "Geological Map of the Buchans Area" by Thurlow and Swanson (1981)

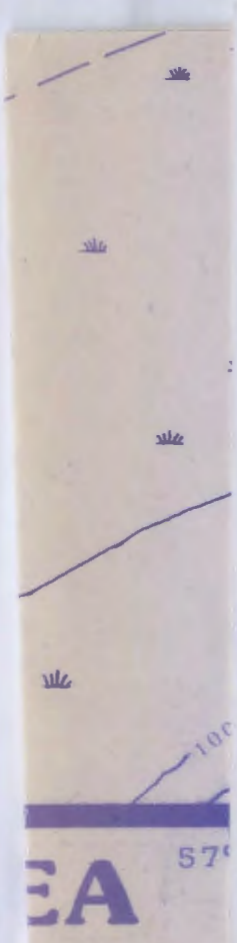

al contact (

ap of the Bu